THESIS APPROVAL

GRADUATE SCHOOL, KASETSART UNIVERSITY

Master of Science (Biochemistry)
DEGREE

Biochemistry	Biochemistry
FIELD	**DEPARTMENT**

TITLE: Protein Engineering of Betaine Aldehyde Dehydrogenases from Rice (*Oryza sativa)* for Substrate Specificity

NAME: Miss Kultida Jiamsomboon

THIS THESIS HAS BEEN ACCEPTED BY

_____ **THESIS ADVISOR**

(Mr. Nonlawat Boonyalai, Ph.D.)

_____ **THESIS CO-ADVISOR**

(Assistant Professor Prachumporn Kongsaeree, Ph.D.)

_____ **DEPARTMENT HEAD**

(Assistant Professor Kiattawee Choowongkomon, Ph.D.)

APPROVED BY THE GRADUATE SCHOOL ON _____

_____ **DEAN**

(Associate Professor Gunjana Theeragool, D.Agr)

Copyright by Kasetsart University All rights reserved

THESIS

PROTEIN ENGINEERING OF BETAINE ALDEHYDE DEHYDROGENASE FROM RICE (*Oryza sativa)* FOR SUBSTRATE SPECIFICITY

KULTIDA JIAMSOMBOON

A Thesis Submitted in Partial Fulfillment of
the Requirements for the Degree of
Master of Science (Biochemistry)
Graduate School, Kasetsart University
2012

Copyright by Kasetsart University All rights reserved

Kultida Jiamsomboon 2012: Protein Engineering of Betaine Aldehyde Dehydrogenases from Rice (*Oryza sativa)* for Substrate Specificity. Master of Science (Biochemistry), Major Field: Biochemistry, Department of Biochemistry. Thesis Advisor: Mr. Nonlawat Boonyalai, Ph.D. 151 pages.

Fragrance rice (*Oryza sativa)* contains two isoforms of BADH, named OsBADH1 and OsBADH2. OsBADH1 is implicated in acetaldehyde oxidation in rice plant peroxisomes, while the non-functional OsBADH2 is believed to be involved in the accumulation of 2-acetyl-1-pyrroline, the major compound of aroma in fragrance rice. In the present study, site-directed mutagenesis, molecular docking and molecular dynamics simulation studies were used to investigate the substrate specificity towards betaine aldehyde (Bet-ald) and γ-aminobutyraldehyde (GAB-ald). Consistent with our previous study, kinetics data indicated that the enzymes catalyze GAB-ald better than Bet-ald, and the OsBADH1 W172F and OsBADH2 W170F mutants displayed a higher catalytic efficiency towards GAB-ald than Bet-ald. Molecular docking analysis and molecular dynamics simulations for the first time provided models for aldehyde substrate-bound complexes of OsBADHs. The amino acid residues, E262, L263, C296 and W461 of OsBADH1 and E260, L261, C294 and W459 of OsBADH2 located within 5 Å of the OsBADH active site mainly interacted with GAB-ald forming strong hydrogen bonds in both OsBADH isoforms. Residues W163, N164, Q294, C296 and F397 of OsBADH1-Bet-ald and Y163, M167, W170, E260, S295 and C453 of OsBADH2-Bet-ald formed the main interaction sites while E260 of OsBADH2 showed an interaction energy of -14.21 kcal/mol. Unconserved A290 in OsBADH1 and W288 in OsBADH2 appeared to be important for substrate recognition similar to that observed in amino aldehyde dehydrogenase from *Pisum sativum* (PsAMADH). Overall, the results here help to explain how two homologous rice BADHs recognize the aldehyde substrate differently, which is a key property to their biological roles.

_____ _____ ___ / ____ / ____

Student's signature Thesis Advisor's signature

Copyright by Kasetsart University All rights reserved

ACKNOWLEDGEMENTS

I would like to gratefully thank and express my sincere appreciation to my thesis advisor Dr. Nonlawat Boonyalai for his advice, valuable guidance and encouragement throughout thesis process and my time as a M.S student.

I would sincerely like to thank my thesis committee, Assistant Professor Dr. Prachumporn Kongsaeree for her valuable comments and suggestions for completely writing this thesis.

This research was financially support by the Center of Excellence for Innovation in Chemistry (PERCH-CIC), Commission on Higher Education, the Ministry of Education, and Kasetsart University Research and Development Institute (v-t(d)43.54).

I would like to show my gratitude to National Nanotechnology Center (NANOTEC) for generously providing Discovery Studio 2.5 programs and the National Electronics and Computer Technology Center (NECTEC) for providing the computational resource.

Furthermore, I gratefully thank Dr. Witcha Treesuwan from Institute of Food Research and Product Development and Ms. Poonsap Na Nakorn from Interdisplinary Graduated Program in Genetic Engineering at Kasetsart University for their time to help and suggest me on the computational part.

Finally, I deeply appreciate my parents, my sister and my friends for their encouragements, belief, understanding and supports given to me in completing this project.

Kultida Jiamsomboon

February 2012

Copyright by Kasetsart University All rights reserved

TABLE OF CONTENTS

Page

TABLE OF CONTENTS	i
LIST OF TABLES	ii
LIST OF FIGURES	iv
LIST OF ABBREVIATIONS	vii
INTRODUCTION	1
OBJECTIVE	4
LITERATURE REVIEW	5
MATERIALS AND METHODS	59
Materials	59
Methods	62
RESULTS AND DISCUSSIONS	73
CONCLUSION	110
LITERATURE CITED	112
APPENDICES	122
Appendix A Pairwise alignment of DNA sequencing results of the OsBADH1 and OsBADH2	123
Appendix B Fluorescence binding studies	129
Appendix C Enzymatic characterization	134
CURRICULUM VITAE	139

Copyright by Kasetsart University All rights reserved

LIST OF TABLES

Table		Page
1	Summary of ALDH genes	6
2	The presence of the *ALDH* gene families in the major eukaryotic taxa	9
3	The eukaryotic *ALDH* gene families of ALDH enzyme in various organism	10
4	The *ALDH* gene families identified in various organisms	38
5	The rice ALDH protein superfamily: revised nomenclature	39
6	Amino acid sequence identity and similarity between OsBADHs and other BADHs	51
7	Chemical reagents that used for this work	59
8	List of analytical equipments	61
9	Primer sequences for site-directed mutagenesis	62
10	PCR condition for site-directed mutagenesis	63
11	Primer sequences for screening the mutant plasmid	65
12	PCR condition for colony PCR screening of mutant plasmid	65
13	List of restriction enzymes	66
14	Dissociation constant (K_d) of NAD^+ and OsBADHs	83
15	Kinetic parameters for wild type and mutant OsBADH1 with Bet-ald and GAB-ald	84
16	Kinetic parameters for wild type and mutant OsBADH2 with Bet-ald and GAB-ald	84
17	Kinetic parameters for wild type OsBADHs with acetaldehyde	86
18	The lowest binding energy of wild-type and mutant OsBADHs from docking	90
19	The binding free energy of four trajectories from OsBADH1-Bet-ald, OsBADH1-GAB-ald, OsBADH2-Bet-ald and OsBADH2-GAB-ald systems	97

Copyright by Kasetsart University All rights reserved

LIST OF TABLES (Continued)

Table		Page
20	Amino acid residues within 5 Å radius of OsBADH1-substrate complexes	102
21	Amino acid residues within 5 Å radius of OsBADH2-substrate complexes	102
22	The interaction energy of amino acid residues within 5 Å radius of OsBADH-substrate complexes	103

Copyright by Kasetsart University All rights reserved

LIST OF FIGURES

Figure		Page
1	Conversion of an aldehyde to a carboxylic acid by aldehyde dehydrogenase	5
2	The example of the name of *ALDH* gene	8
3	The structure of bovine ALDH2 tetramer	12
4	The structure of one monomer of bovine ALDH2	14
5	Active site structure of ALDH2 showing the position of the nicotinamide ring	15
6	Interactions between enzyme and NAD^+ of ALDH2	16
7	The chemical mechanism of ALDH reaction catalysis	17
8	The catalytic triad of bovine ALDH2	19
9	The different conformation of nicotinamide moiety in ALDH2	20
10	Interactions of different conformation of NAD^+ with surrounding residues of ALDH2	21
11	Proposed interactions of thiohemiacetal transition state and an acyl-enzyme intermediate	22
12	Steric clashes between the oxidized nicotinamide and the catalytic cysteine in the “resting” conformation	24
13	Conformations of the catalytic aspartic and cysteine residue in ALDH active sites	25
14	Mechanism for the proposed proton relay system in PaBADH	27
15	Chemical structure of 2-acetyl-1-pyrroline	29
16	Structure of the fragrance gene (*fgr*) of rice chromosome 8	30
17	The pathway of OsBADH2-dependent 2AP synthesis in rice	31
18	The correlation between OsBADH2 and 2AP of OsBADH2-dependent 2AP synthesis	32
19	The pathway of OsBADH2-independent 2AP synthesis in rice	33
20	Chemical structure of γ-aminobutyric acid (GABA)	34

Copyright by Kasetsart University All rights reserved

LIST OF FIGURES (Continued)

Figure		Page
21	The GABA shunt metabolic pathway and its regulation in plants	35
22	The pathway of acetaldehyde in rice under submerged conditions and following re-aeration	42
23	The pathway of the conversion of choline to glycine betaine	43
24	The oxidation of acetaldehyde in rice peroxisome	45
25	Structures of various osmoprotectants found in plants	46
26	Pathway leading to the biosynthesis of glycine betaine in different species	47
27	The structures of one monomer of BADH from cod liver	50
28	Amino acid sequence alignment of OsBADHs and other BADHs using ClustalW2	52
29	The substrate channel of PsAMADH1	54
30	The structures of the basic aldehydes	55
31	Thermodynamic cycle of a complex formation	57
32	Equations for calculation of binding free energy	57
33	PCR products obtained from site-directed mutagenesis	74
34	PCR screening of OsBADH1 mutants	74
35	PCR screening of OsBADH2 mutants	75
36	Restriction enzyme analysis of OsBADH1 mutants	76
37	Restriction enzyme analysis of OsBADH2 mutants	76
38	Pairwise alignment of partial DNA sequencing of wild-type and mutant of OsBADH1 using ClustalW2	77
39	Pairwise alignment of partial DNA sequencing of wild-type and mutant of OsBADH2 using ClustalW2	77
40	Expression analysis of OsBADH1 wild-type and mutants	78
41	Expression analysis of OsBADH2 wild-type and mutants	78
42	SDS-PAGE analysis of OsBADH1 purification	79
43	SDS-PAGE analysis of OsBADH2 purification	80

Copyright by Kasetsart University All rights reserved

LIST OF FIGURES (Continued)

Figure		Page
44	Structure of OsBADH1 and OsBADH2	81
45	Ramachadran plot of OsBADH1 model	89
46	Superposition of OsBADH complexes from docking and PsAMADH1	90
47	Molecular docking analysis of OsBADH1 complex	92
48	Molecular docking analysis of OsBADH2 complex	93
49	RMSD of OsBADH complexes	95
50	Active site of OsBADH-ligand complexes from MD simulations	99
51	The decomposition of binding free energy between ligand aldehyde and amino acid residues within 5 Å radius of OsBADH active site	104
52	ALDH active sites	107
53	The conformations of active site residue in OsBADH-substrate complexes from MD simulations compared to PaBADH (2WME) and ALDH2 (1O02)	108

Appendix Figure

B1	Fluorescence spectra of OsBADH1 upon the addition of NAD^+	130
B2	Fluorescence spectra of OsBADH2 upon the addition of NAD^+	131
B3	Binding isotherm of OsBADH1 in the presence of 5 mM NAD^+	132
B4	Binding isotherm of OsBADH2 in the presence of 5 mM NAD^+	133
C1	Effect of Betaine aldehyde (Bet-Ald) on the rate of aldehyde oxidation by OsBADH1	135
C2	Effect of γ-aminobutyraldehyde (GAB-Ald) on the rate of aldehyde oxidation by OsBADH1	136
C3	Effect of Betaine aldehyde (Bet-Ald) on the rate of aldehyde oxidation by OsBADH2	137
C4	Effect of γ-aminobutyraldehyde (GAB-Ald) on the rate of aldehyde oxidation by OsBADH2	138

Copyright by Kasetsart University All rights reserved

LIST OF ABBREVIATIONS

2AP	=	2-acetyl-1-pyrroline
Ala (A)	=	alanine
ALDH	=	aldehyde dehydrogenase
AMADH	=	amino aldehyde dehydrogenase
PsAMADH1	=	amino aldehyde dehydrogenase 1 from *Pisum sativum*
PsAMADH2	=	amino aldehyde dehydrogenase 2 from *Pisum sativum*
Å	=	angstrom
Asn (N)	=	asparagine
Bet-ald	=	betaine aldehyde
BADH	=	betaine aldehyde dehydrogenase
codBADH	=	betaine aldehyde dehydrogenase from cod liver
eBADH	=	betaine aldehyde dehydrogenase from *Escherichia coli*
OsBADH1	=	betaine aldehyde dehydrogenase 1 from *Oryza sativa*
OsBADH2	=	betaine aldehyde dehydrogenase 2 from *Oryza sativa*
Cys (C)	=	cysteine
Da	=	Dalton
E. coli	=	*Escherichia coli*
GAB-ald	=	γ-aminobutyraldehyde
GHz	=	gigahertz
Gln (Q)	=	glutamine
Glu (E)	=	glutamate
HBH-AMADH	=	high BADH homology aminoaldehyde dehydrogenase
IPTG	=	Isopropyl β-D-1-thiogalactopyranoside
kDa	=	kilodalton
k_{cat}	=	catalytic activity
k_{cat} /K_m	=	catalytic efficiency
K_d	=	dissociation constant
K_m	=	Michaelis constant
Leu (L)	=	leucine
MD	=	molecular dynamics simulation

Copyright by Kasetsart University All rights reserved

LIST OF ABBREVIATIONS (Continued)

µl	=	microliter
µM	=	micromolar
MM/GBSA	=	Molecular Mechanics-Generalized Born Surface Area
MM/PBSA	=	Molecular Mechanics/Poisson Boltzmann Surface Area
NAD^+	=	nicotinamide adenine dinucleotide
OD	=	optical density
PDB	=	Protein Data Bank
Phe (F)	=	phenylalanine
P. sativum	=	*Pisum sativum*
P. aeruginosa	=	*Pseudomonas aeruginosa*
RMSD	=	root mean square deviation
Ser (S)	=	serine
Trp (W)	=	tryptophan
Tyr (Y)	=	tyrosine

Copyright by Kasetsart University All rights reserved

PROTEIN ENGINEERING OF BETAINE ALDEHYDE DEHYDROGENASE FROM RICE (*Oryza sativa)* FOR SUBSTRATE SPECIFICITY

INTRODUCTION

Aldehyde dehydrogenases (ALDHs) (E.C. 1.2.1.3) are a superfamily of $NAD(P)^+$-dependent enzymes which metabolize many biologically important intermediate aldehydes (Liu *et al*., 1997). These aldehyde compounds are ubiquitous in nature and quite toxic to cells. Thus, the regulation of the level of aldehyde intermediates must be carefully controlled. ALDHs catalyze the irreversible oxidation of aldehyde to their corresponding carboxylic acid. Some ALDHs can catalyze a very limited range of substrates, whereas others recognize a broad range of substrates. ALDH enzymes require either NAD^+ or $NADP^+$ as a cofactor (Yoshida *et al*., 1998), and the classification of ALDH members is determined by their aldehyde substrates such as alcohol dehydrogenases, lactaldehyde dehydrogenases and aminoaldehyde dehydrogenases. Aminoaldehyde dehydrogenases (AMADHs, EC 1.2.1.19) belong to the aldehyde dehydrogenase 9 family (ALDH9) (Perozich *et al*., 1999) and are $NAD(P)^+$-dependent enzymes which can catalyze the oxidation of a broad range of ω-aminoaldehydes to the corresponding ω-amino acids. The ω-aminoaldehydes are obtained from the oxidation of polyamines such as spermine (Spm), spermidine (Spd) and putrescine (Put), which are oxidized by amine oxidases (Moschou *et al*., 2008). AMADH from *Pisum sativum* is an example of a plant AMADH that exhibits broad aminoaldehydes substrate specificity (Šebela *et al*., 2000; Tylichová *et al*., 2010). Besides AMADHs, plant betaine aldehyde dehydrogenases (BADHs, EC 1.2.1.8) also oxidize a wide range of ω-aminoaldehyde substrates in addition to its natural substrate, betaine aldehyde (Bet-ald) (Fujiwara *et al*., 2008; Bradbury *et al*., 2008; Mitsuya *et al*., 2009). BADH enzymes generally catalyze the last step in the synthesis of the osmoprotectant glycine betaine from choline (Weigel *et al*., 1986). Thus, BADHs can be classified into two subfamilies. The first group is those with high specificity for, and activity toward the substrate Bet-ald (true BADH), while the second group an exhibits broad affinity for a range of aminoaldehydes (high BADH homology

Copyright by Kasetsart University All rights reserved

aminoaldehyde dehydrogenase (HBH-AMADH)) (Fitzgerald *et al*., 2009). BADHs from rice have been previously shown to be an HBH-AMADH since they showed only moderate to low activity towards Bet-ald but high activity for aminoaldehydes (Bradbury *et al*., 2008; Mitsuya *et al*., 2009; Wongpanya *et al*., 2011). Therefore, BADHs from rice can also be considered AMADHs (Fitzgerald *et al*., 2009).

At present, five crystal structures of BADHs and two crystal structures of plant AMADHs are available in the Protein Data Bank (PDB): BADH from cod liver in apoenzyme form and in complex with NAD^+ (PDB codes 1A4S and 1BPW, respectively) (Johansson *et al*., 1998), BADH from *Escherichia coli* in apoenzyme form and in complex with NADH and Bet-ald (PDB codes 1WND and 1WNB, respectively) (Gruez *et al*., 2004), BADH from *P. aeruginosa* (PaBADH) in complex with $NADP^+$ and glycerol (PDB code 2VE5) (González-Segura *et al*., 2009), and two AMADH isoforms from *Pisum sativum* (PsAMADH1 and PsAMADH2) in complex with NAD^+ and glycerol (PDB codes 3IWK and 3IWJ, respectively) (Tylichová *et al*., 2010). Most of the known structures of BADH are in tetrameric form, except for the plant AMADH that is dimeric. Each subunit of BADH comprises a coenzyme binding domain, an oligomerization domain and a catalytic domain. The catalytic triad of BADH from *P. sativum* contains C294, N162 and E260 that are conserved in BADH from different species (Johansson *et al*., 1998; Gruez *et al*., 2004; González-Segura *et al*., 2009). In the catalytic cycle of BADH, the catalytic cysteine attacks the aldehyde substrate forming a thiohemiacetal intermediate whereas the glutamate, which is involved in the proton relay system, has been proposed to be the general base in the catalysis. The asparagine on the other hand has been implicated in stabilizing the thiohemiacetal intermediate forming the oxyanion hole (González-Segura *et al*., 2009).

Two BADH homologues in rice (*Oryza sativa*), *OsBADH1* and *OsBADH2*, are encoded on chromosome four and chromosome eight, respectively (Bradbury *et al*., 2005), and share 75% amino acid sequence identity. It has been speculated that OsBADH1 is localized in rice plant peroxisome (Mitsuya *et al*., 2009) since its deduced amino acid sequence contains a Ser-Lys-Leu (SKL) motif at the C-terminus. The subcellular localization of OsBADH2 in young panicles of rice plants by fluorescein-conjugated secondary antibody indicated that an OsBADH2 signal was

Copyright by Kasetsart University. All rights reserved

only found in the cytoplasm and not in the nucleus (Chen *et al*., 2008). Moreover, the eight-base-pair deletion in exon 7 of the *OsBADH* gene results in a truncated non-functional OsBADH2, and the partial loss of OsBADH2 function is proposed to account for the accumulation of 2-acetyl-1-pyrroline (2AP), the major compound of aroma in fragrance rice (Bradbury *et al*., 2005; Bradbury *et al*., 2008). Both OsBADHs have shown a broad aminoaldehyde substrate specificity (Bradbury *et al*., 2008; Mitsuya *et al*., 2009), and the enzymatic characterization of both OsBADHs showed that the enzymes can oxidize C3 and C4 aminoaldehydes or medium-chain aldehyde such as γ-aminobutyraldehyde (GAB-ald), 3-aminopropionaldehyde (AP-ald), 4-*N*-trimethylaminobutyraldehyde (TMAB-ald) and 3-*N*-trimethylaminopropionaldehyde (TMAP-ald) better than Bet-ald. Recently, it was reported that OsBADH2_Y420, containing a Y420 insertion similar to BADH2.8 from Myanmar fragrance rice, exhibited less catalytic efficiency toward γ-aminobutyraldehyde (GAB-ald) but not for Bet-ald compared to the wild-type enzyme (Wongpanya *et al*., 2011). This mutant may bring about the accumulation of GAB-ald/Δ^1-pyrroline, which is subsequently converted to 2-acetyl-1-pyrroline (2AP), the major compound of aroma in fragrance rice.

Although both OsBADHs are highly similar in amino acid sequence, their functions might be different. Therefore, it is of interest to elucidate and understand the substrate specificity of both OsBADHs. First, site-directed mutagenesis of amino acids involved in catalysis and substrate recognition was carried out. Cofactor NAD^+ binding to each enzyme was investigated to evaluate changes in enzyme conformation upon binding. The substrate specificity of the enzymes towards Bet-ald and GAB-ald was also investigated. In addition to biochemical experiments, molecular docking and molecular dynamics simulation were carried out to gain better understanding factors determining substrate specificity and catalysis.

Copyright by Kasetsart University. All rights reserved

OBJECTIVE

To elucidate and understand the important amino acid residues in the substrate binding pocket of OsBADH1 and OsBADH2 using site-directed mutagenesis, enzyme kinetics, molecular docking and molecular dynamics simulations.

Copyright by Kasetsart University All rights reserved

LITERATURE REVIEW

1. General feature of aldehyde dehydrogenases

Aldehyde compounds are found in living cells as physiologically derived intermediates or by-products of other compounds in several metabolic pathways including amino acid, lipid, protein and carbohydrate metabolism (Jimenez-Lopez *et al*., 2010; Kotchoni *et al*., 2010). These aldehyde compounds are ubiquitous in nature and quite toxic to cells. The highly reactive aldehydes can easily be attacked by cellular nucleophiles because of the electrophillicity of their carbonyl group. However, excess aldehydes can cause deleterious effects on organisms, metabolisms and damages to cells and tissues. The removal of aldehydes and their intermediates is essential for cellular survival (Gao and Han, 2009). Therefore, the regulation of the level of aldehydes in cells must be carefully controlled to assure normal development and growth processes, which are important for the maintenance of healthy living cells. Enzymes involved in the function of detoxification of aldehydes are called aldehyde dehydrogenases (E.C. 1.2.1.3, ALDH).

Aldehyde dehydrogenases (ALDHs) catalyze the irreversible oxidation of a wide range of toxic aldehydes to their non-toxic corresponding carboxylic acids (Liu *et al*., 1997) (Figure 1). ALDHs are found in both prokaryotes and eukaryotes. These enzymes are very diverse in that either NAD^+ or $NADP^+$ can be used as a cofactor (Yoshida *et al*., 1998).

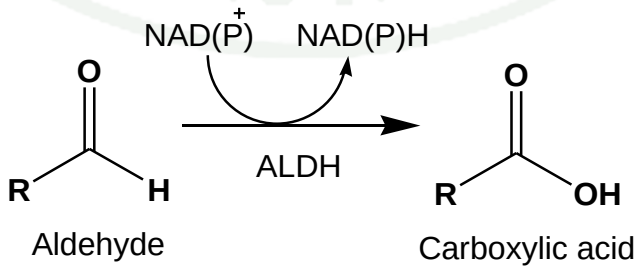

Figure 1 Conversion of an aldehyde to a carboxylic acid by aldehyde dehydrogenase

Copyright by Kasetsart University All rights reserved

ALDHs are the group of enzymes that play a role relevant in the detoxification processes. ALDHs catalyze the oxidation of wide spectrum of both aliphatic and aromatic aldehydes. Some ALDHs can catalyze a very limited range of substrates, whereas others recognize a broad range of substrates. ALDHs also exist in various subcellular compartments including cytosol, mitochondria, plastids, microsomes and peroxisomes. Additionally, ALDHs can be divided into various subfamilies with different functions comprising detoxification, intermediary metabolism, osmotic protection and NADPH generation (Perozich *et al*., 1999).

1.1 Classification of aldehyde dehydrogenase

In 2002, over 550 genes encoding ALDH proteins were identified across all species, 32 of which are found in arhaea, 351 in eubacteria, and 172 in eukaryota (Table 1) (Sophos and Vasiliou, 2003).

Table 1 Summary of ALDH genes

Superkidom	**Taxon**	**Number of genes**	**Total**
Archaea			32
	Crenarchaeota	12	
	Euryarchaeota	20	
Eubacteria			351
	Aquificales	2	
	Cyanobacteria	5	
	Firmicutes	113	
	Fusobacteria	2	
	Proteobacteria	216	
	Spirochaetales	1	
	Thermotogales	1	
	Thermus/Deinococcus group	11	

Copyright by Kasetsart University All rights reserved

Table 1 (Continued)

Superkidom	Taxon	Number of genes	Total
Eukaryota			172
	Diplomonadida	1	
	Euglenozoa	2	
	Entamoebidae	2	
	Fungi	32	
	Metazoa	90	
	Viridiplantae	45	

Source: Sophos and Vasiliou (2003)

There are many *ALDH* genes encoding ALDH protein such as *aldA, putA* and *YdcW* in *Escherichia coli* while in *Pseudomonas aeruginosa,* there are *betB, astD* and *gabD*. The number of *ALDH* genes per species varies in archaeal, eubacterial and eukaryotic organisms. It is noteworthy that some eubacterial species have more *ALDH* genes than eukaryotic organisms. It can be ascribed that the bacteria can survive in various environments, and utilize wide variety of substrates for nutrition. The nomenclature of *ALDH* genes based on sequence similarity has been updated and developed for eukaryotic *ALDH* gene (Sophos and Vasiliou, 2003). Taking a human ALDH8A1 as an example for the nomenclature (Figure 2), the name of each aldehyde dehydrogenase gene starts with ALDH, which is the root symbol of *ALDH* gene family; the arabic number represents the family and the first letter represents the gene's subfamily whereas the final number indicates an individual gene within the subfamily. Additionally, the ALDH superfamily is divided into "family" and "subfamily" based on the percent amino acid identity of each protein as compared with the others. The ALDH protein in one family is defined as having more than 40% amino acid similarity, while the sequences having more than 60% identical are considered belonging to the same subfamily. Using this definition, the eukaryotic *ALDH* genes can be classified into 20 families in the major eukaryotic taxa (Table 2) (Sophos and Vasiliou, 2003). The details of all eukaryotic ALDH families were determined as shown in Table 3 (Sophos and Vasiliou, 2003).

Copyright by Kasetsart University All rights reserved

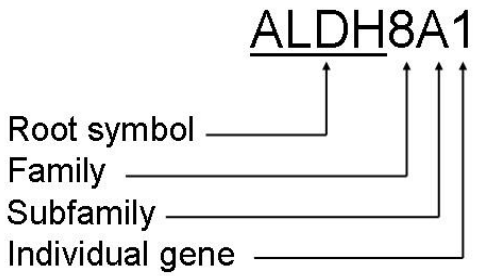

Figure 2 The example of the name of *ALDH* gene

Additionally, the ALDH superfamily can also be categorized on the basis of their substrate specificity such as (1) semialdehyde dehydrogenases, including hydroxymuconic semialdehyde dehydrogenase (E.C. 1.2.1.32), succinate semialdehyde dehydrogenase, glutamate semialdehyde dehydrogenase (E.C. 1.2.1.41), 2-amino-adipate-6-semialdehyde dehydrogenase (E.C. 1.2.1.31) and metylmalonate-semialdehyde dehydrogenase (E.C. 1.2.1.27), (2) non-specific ALDHs (E.C. 1.2.1.3), (3) betaine dehydrogenases (E.C. 1.2.1.8), (4) non-phosphorylating glyceraldehyde 3-phosphate dehydrogenases (E.C. 1.2.1.9), (5) phenylacetaldehyde dehydrogenases (E.C. 1.2.1.39), (6) lactaldehyde dehydrogenases (E.C. 1.2.1.22) and (7) ALDH-like proteins (Sophos and Vasiliou, 2003). The ALDH-like proteins contain either complete or nearly complete ALDH sequences, such as 10-formyltetrahydrofolate dehydrogenase (E.C. 1.5.1.6), Δ^1-pyrroline-5-carboxylate dehydrogenase (E.C.1.5.1.12) and Δ^1-pyrroline-5-carboxylate synthase containing γ-glutamyl phosphate reductase (E.C. 1.2.1.41). The non-specific ALDHs can react with a wide range of aliphatic and aromatic substrates.

Copyright by Kasetsart University All rights reserved

Table 2 The presence of the *ALDH* gene families in the major eukaryotic taxa

Taxa	families																			
	1	2	3	4	5	6	7	8	9	10	11	12	13	14	15	16	17	18	19	20
Diplomonadida	-	-	-	-	-	-	-	-	-	-	-	-	-	-	-	-	-	-	-	+
Entamoebidae	-	-	-	-	-	-	-	-	-	-	-	-	*	-	-	-	-	-	-	+
Euglenozoa	+	-	-	+	-	-	-	-	-	-	-	-	-	-	-	-	-	-	-	-
Fungi	+	-	-	+	+	-	-	-	-	+	-	-	-	*	*	*	-	+	-	-
Human	+	+	+	+	+	+	+	+	+	-	-	-	-	-	-	-	-	+	-	-
Metazoa	+	+	+	+	+	+	+	+	+	-	-	-	-	-	-	-	*	+	-	-
Viridiplantae	-	+	+	-	+	+	+	-	-	+	*	*	-	-	-	-	-	+	*	-

The (-) denotes absence; (+), presence; (*), present only in one taxon.

Source: Sophos and Vasiliou (2003)

Copyright by Kasetsart University All rights reserved

Table 3 The eukaryotic *ALDH* gene families of ALDH enzyme in various organism

Family	ALDH enzyme	Organism
1	class 1 ALDHs (ALDH1), 10-formyl-tetrahydrofolate dehydrogenase, indole-3-acetaldehyde dehydrogenase	animals, fungi
2	class 2 ALDHs (ALDH2)	mammalian, plants
3	class 3 ALDHs (ALDH3)	mammals, fish, insects, plants
4	Δ^1-pyrroline-5-carboxylate dehydrogenase	fungi, plants, animals
5	succinate semialdehyde dehydrogenases	fungi, plants, animals
6	methylmalonate semi-aldehyde dehydrogenase	animals, plants.
7	antiquitin proteins	plants, fish, mammals
8	a newly-characterized human ALDH that metabolizes retinaldehyde	Human
9	γ-aminobutyraldehyde dehydrogenases	mammals, fish
10	betaine aldehyde dehydrogenases	plants, yeast
11	NADP-dependent glyceraldehyde-3-phosphate dehydrogenase	plants
12	plant ALDHs which unknown functions	plants
13	protozoan ALDH	mammalian
14	yeast ALDH proteins which unknown functions	yeasts
15	yeast ALDH proteins which unknown functions	yeasts
16	yeast ALDH proteins which unknown functions	yeasts
17	*Drosophila melanogaster* ALDH gene which unknown functions	*Drosophila melanogaster*

Copyright by Kasetsart University All rights reserved

Table 3 (Continued)

Family	ALDH enzyme	Organism
18	glutamyl-γ-semialdehyde dehydrogenases	fungi, plants, animals
19	γ-glutamyl phosphate reductase	plants
20	multi-domain protein	Diplomonadida, Entamoebidae

Source: Sophos and Vasiliou (2003)

Traditionally, the non-specific mammalian ALDHs containing only three groups, namely class 1, 2 and 3 ALDHs from eukaryotic family 1, 2 and 3 (ALDH1, ALDH2 and ALDH3, respectively) have received most attention because they are involved in metabolism of acetaldehyde and detoxification of dietary aldehydes, lipid peroxidation products and anti-cancer drugs, whereas other ALDH families with diverse metabolic roles remain unattended (Perozich *et al*., 1999; Kotchoni and Bartels, 2003). ALDH1 has been isolated from mammalian cytoplasm (Moore *et al*., 1998), while ALDH2 contains the mitochondrial ALDHs isolated from various species such as the liver of human, beef and sheep (Steinmetz *et al*., 1997; Kotchoni and Bartels, 2003; Perez-Miller and Hurley, 2003). ALDH3 is a cytosolic enzyme relating with the oxidation of aromatic aldehydes and fatty aldehydes (medium-chain aliphatic aldehydes) and is associated with carcinogenesis (Muzio *et al*., 2001).

1.2 The structure of aldehyde dehydrogenase

Since the first crystal structure of human ALDH3 was available on Protein Data Bank (PDB entry 1AD3) (Liu *et al*., 1997), several structures of ALDHs have been solved, including the sheep ALDH1 (PDB entry 1BXS) (Moore *et al*., 1998), bovine ALDH2 (PDB entries 1AG8 and 1A4Z) (Steinmetz *et al*., 1997), human ALDH2 (PDB entries 1O00, 1O02) (Perez-Miller and Hurley, 2003), cod betaine aldehyde dehydrogenase (codBADH) (PDB entry 1BPW) (Johansson *et al*., 1998), *E.*

Copyright by Kasetsart University All rights reserved

coli YdcW betaine aldehyde dehydrogenase (eBADH) (PDB entry 1WNB) (Gruez *et al*., 2004), betaine aldehyde dehydrogenase from *Pseudomonas aeruginosa* (PaBADH) (PDB entry 2WME) (González-Segura *et al*., 2009) and amino aldehyde dehydrogenase (AMADH) from *P. sativum* (PsAMADH1 and PsAMADH2) (PDB entries 3IWK and 3IWJ, respectively) (Tylichová *et al*., 2010). The structures of ALDH1 and ALDH2 (cytosolic and mitochondrial, respectively) are tetrameric, whereas ALDH3 is dimeric. The structure of mitochondrial aldehyde dehydrogenase (ALDH2) from bovine liver, which shares 95% amino acid sequence identity with the human isozyme, has been solved to 2.65 Å in its apo form, and to 2.75 Å in a binary complex with NAD^+ by X-ray crystallography (PDB entries 1AG8 and 1A4Z, respectively) (Steinmetz *et al*., 1997). This enzyme catalyzes the oxidation of acetaldehyde to acetate during ethanol metabolism. The tetrameric structure of bovine ALDH2 complex with NAD^+ is shown in Figure 3 (PDB entry 1A4Z).

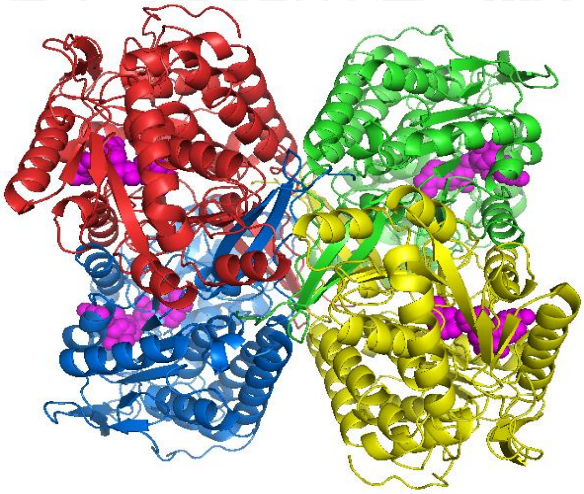

Figure 3 The structure of bovine ALDH2 tetramer. Individual subunits are colored differently. The positions of the bound NAD^+ is shown in sphere (magenta).

The active form of mitochondrial bovine ALDH2 is tetrameric with the four subunits in asymmetric unit and individual subunits comprise 8–500 amino acids. Each subunit within the tetramer is composed of three distinct domains: coenzyme binding domain (nucleotide binding domains), catalytic domain (substrate binding

Copyright by Kasetsart University All rights reserved

domain) and oligomerization domain (Figure 4A). The oligomerization domain is composed of a small three-stranded antiparallel β-sheet domain involving in subunit interactions in this tetrameric enzyme. The coenzyme binding domain includes residues 8–139 and 159–270, the catalytic domain comprises residues 271–485, and the oligomerization domain is composed of residues 140–158 and 486–495. Therefore, most dehydrogenases using NAD^+ or $NADP^+$ as a cofactor contain a conserved protein domain called the Rossmann type fold. This structural motif is found in the NAD^+-binding site of many dehydrogenases (Liu *et al*., 1997; Steinmetz *et al*., 1997; Johansson *et al*., 1998; Perez-Miller and Hurley, 2003). The coenzyme binding domain and the catalytic domain exhibit Rossmann type fold, which typically consists of α/β domains (Figure 4B). The α/β Rossmann type fold of the two large domains contains a five-stranded and four-helices. A topology diagram of an individual subunit of bovine ALDH2 is indicated in Figure 4C. The coenzyme binding domain includes strands 1 to 4, strands 7 to 11, helices A to G and helix N. The catalytic domain includes strands 12 to 18 and helices H to M. The oligomerization domain is composed of strands 5, 6 and 19. Dimer formation of ALDH2 involves contacts between the αG helices (residues 247–260) of two subunits and residues in the β18 strand (residues 450–454) of one subunit interacting with residues in the β19 strand (residues 486–495) in the other subunit. The tetramer is formed by antiparallel β-stranded interactions between β5 strands (residues 141–144) in two equivalent dimers (Steinmetz *et al*., 1997). The active site of the bovine ALDH2 enzyme lies at the base of a hydrophobic tunnel 12 Å from the surface of the enzyme. The entrance to the substrate binding site is located on the face opposite from where coenzyme binds at the position near the tetramer interface. The hydride ion from the conversion of NAD^+ to NADH, is added to either the front (the A side) or the back (the B side) of the planar nicotinamide ring. The base of the substrate-binding pocket can be divided into two halves using the position of the nicotinamide ring, the A-side and B-side convention (Steinmetz *et al*., 1997). On the A-side of the nicotinamide ring is a cluster of three cysteine residues, 301–303, and on the B-side of the nicotinamide ring are the side chains of T244, E268 and E476 (Figure 5).

Copyright by Kasetsart University All rights reserved

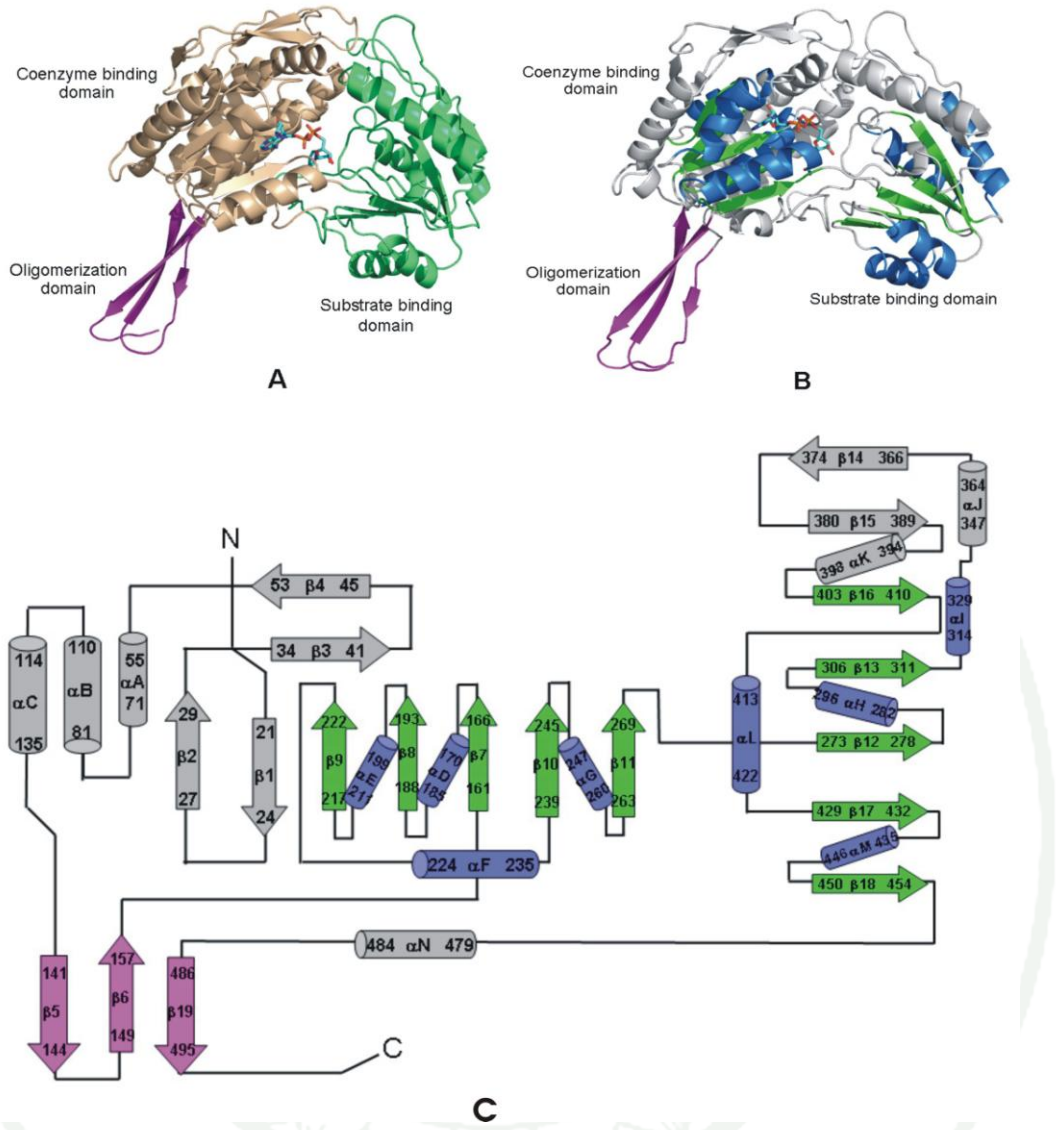

Figure 4 The structure of one monomer of bovine ALDH2. (A) Three domains of ALDH2 (B) The Rossmann type fold of ALDH2 (C) A topology diagram of an individual subunit of ALDH2. The α helices and β strands in Rossmann type fold are colored in blue and green, respectively, whereas the remaining polypeptide chain is colored in gray. The oligomerization domain is colored in purple and the bound NAD^+ is shown in stick and colored by atoms (carbon, cyan).

Source: Steinmetz *et al*. (1997)

Copyright by Kasetsart University All rights reserved

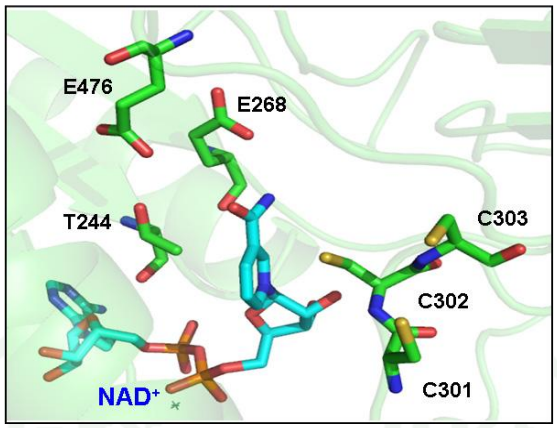

Figure 5 Active site structure of ALDH2 showing the position of the nicotinamide ring. The amino acids in the A-side (C301, C302 and C303) and the B-side (T244, E268 and E476) of the nicotinamide ring are depicted in stick representation and colored by atoms (carbon, green). The NAD^+ is shown in stick and colored by atoms (carbon, cyan).

One coenzyme molecule is bound in each of the monomer of ALDH2. The adenine ring is bound between the αF and αG helices of the nucleotide binding fold in the ALDH2 subunit structure. Both the adenine ring and the adenosine phosphate interact strongly with the αG helix. The van der Waals interaction contacts are formed between the adenine ring and G225, P226, V249, L252 and I165 (Steinmetz *et al*., 1997). None of hydrogen bonds are formed between the protein and the adenine ring of the cofactor molecule. The adenosine ribose makes the hydrogen bonds between the oxygens, O2B and O3B with the main chain O and the side chain NZ of K192, respectively (Figure 6). Moreover, the oxygen O2B forms hydrogen bond with the side chain OE1 of E195, while oxygen O3B forms hydrogen bond with the main chain O of I166. The phosphates of NAD^+ are found near the αD helix rather than near the αA helix. The adenosine phosphate makes two hydrogen bonds between the oxygen O1A and either the side chain OG or the main chain N of S246. Both the main chain N and the side chain NE1 of W168 make hydrogen bond to the nicotinamide phosphate, O2N and O1N, respectively. The nicotinamide ribose is stabilized by two hydrogen bonds between the oxygens O2D or O3D and the side chain OE1 of E399 and by van der Waals contacts with the side chain of F401.

Copyright by Kasetsart University All rights reserved

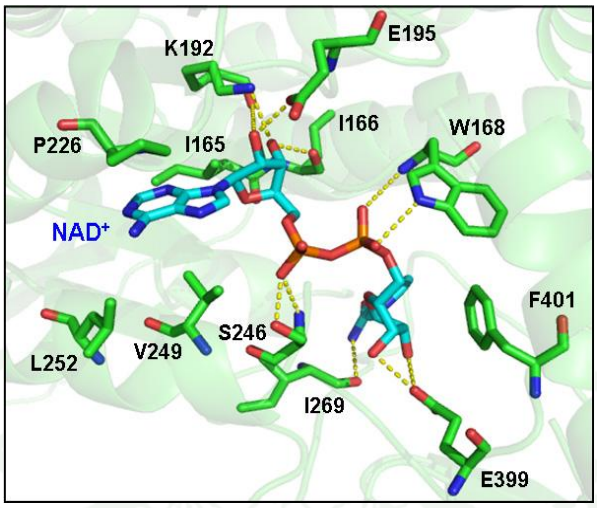

Figure 6 Interactions between enzyme and NAD^+ of ALDH2. The amino acids are depicted in stick representation and colored by atoms (carbon, green). The NAD^+ is shown in stick and colored by atoms (carbon, cyan). The yellow dashed lines indicate potential hydrogen bond interactions less than 3.3 Å.

Source: Steinmetz *et al*. (1997)

Additionally, the nicotinamide ring is held in position by a single hydrogen bond between the carboxamide nitrogen N7N of NAD^+ and the main chain O of I269, and also by van der Waals contacts with the side chains of N169, T244 and C302. The dimensions of substrate binding site of ALDH2 are lined with aromatic and aliphatic amino acids (12 × 6 × 7 Å) (Steinmetz *et al*., 1997).

1.3 Mechanism of aldehyde dehydroganse

The accepted model for human ALDH2 (PDB entry 1O02) catalysis is an irreversible ordered sequential mechanism, in which NAD^+ binds prior to aldehyde (Perez-Miller and Hurley, 2003). The covalent and general base catalysis are important for ALDH to catalyze the irreversible $NAD(P)^+$-dependent oxidation from aldehydes to acids. The overall chemical mechanism of the reaction catalyzed by ALDH can be separated into three main steps including thiohemiacetal formation, hydride transfer and deacylation, and the catalytic triad residues involved in the

Copyright by Kasetsart University All rights reserved

catalysis are C302, E268 and N169 (ALDH2 numbering) (Figure 7) (Muñoz-Clares *et al*., 2011). Firstly, in the thiohemiacetal formation step, the active thiol group of the catalytic cysteine, C302, of ALDH nucleophilically attacks the trigonal carbonyl carbon of aldehyde; a tetrahedral hemithioacetal intermediate covalently bound to the enzyme is generated. Secondly, the hemithioacetal intermediate transfers the hydride ion to the C4 position of the nicotinamide ring of $NAD(P)^+$ (oxidation), producing a thioester intermediate and $NAD(P)^+$ (reduction) or NAD(P)H.

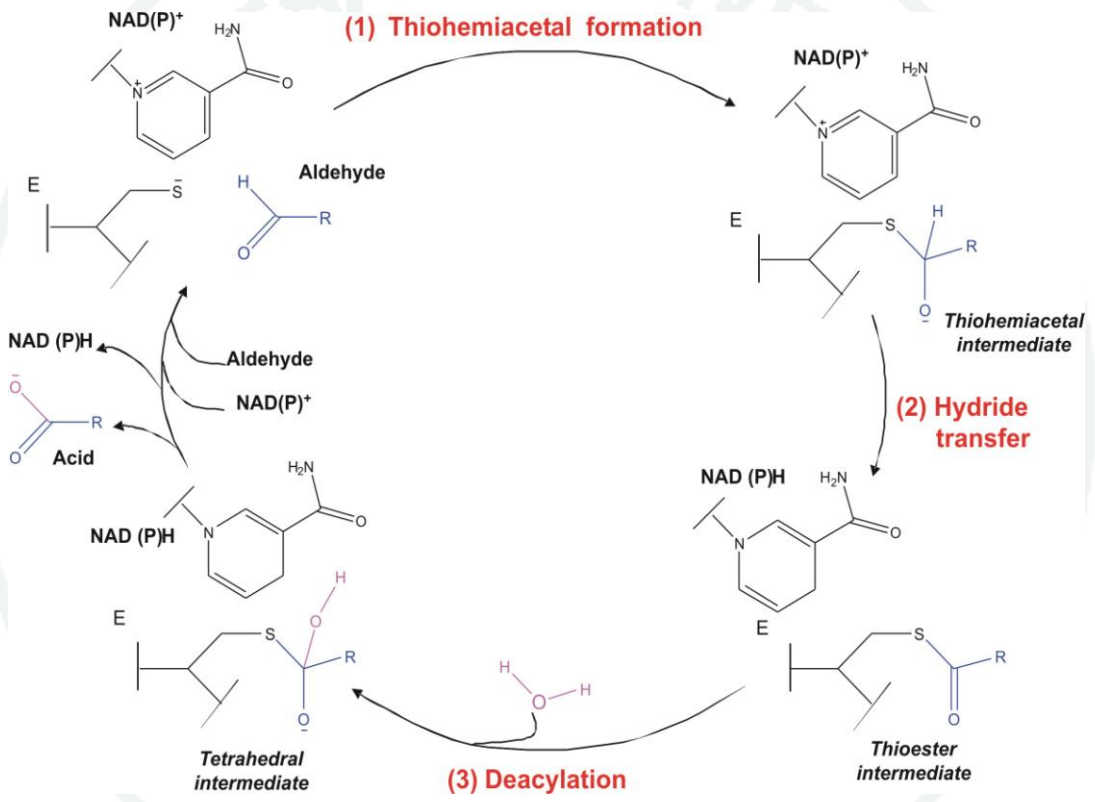

Figure 7 The chemical mechanism of ALDH reaction catalysis

Source: Muñoz-Clares *et al*. (2011)

In deacylation which is the rate-limiting step, the catalytic glutamate, E268 acting as the general base, activates the hydrolytic water to hydrolyze the thioester intermediate by nucleophilic attack. The tetrahedral intermediate is formed and releases the acid product of the reaction prior to NADH dissociation, following the regeneration of the free thiolate. Therefore, the chemical mechanism of the

Copyright by Kasetsart University All rights reserved

ALDHs involves two nucleophilic attacks: one in the thiohemiacetal formation step, carried out by the thiol group of the catalytic cysteine, and the other in the deacylation step, carried out by a water molecule (Muñoz-Clares *et al*., 2010). Both nucleophiles require to be "activated", i.e., deprotonated, for ALDH to be active at physiological pH. Therefore, E268 is essential for abstracting the proton from the thiol group of C302, as well as functioning as the general base to activate the hydrolytic water for the hydrolysis of thioester intermediate.

Three residues, C302, E268 and N169 are strictly conserved among the ALDH proteins with dehydrogenase activity (Perozich *et al*., 1999). The side chain nitrogen of N169 and the main chain nitrogen of C302 are positioned both to stabilize the oxyanion in the thiohemiacetal transition state covalently bound to the enzyme, and to orient the thiohemiacetal for optimal hydride transfer to the C4 atom of the NAD^+ (Steinmetz *et al*., 1997). The catalytic triad of bovine ALDH2 is shown with NAD^+ (PDB entry 1A4Z) (Figure 8). The position of E268 is 6.7 Å away from C302 and 3.0 Å from the carboxamide group on the nicotinamide ring of NAD^+ (Steinmetz *et al*., 1997). In this position, E268 seems unable to function in deacylation because this residue is sterically excluded from performing deacylation by the position of the nicotinamide ring. It is possible that either the nicotinamide ring or the catalytic residues positioned differently during those steps of the catalytic cycle. However, the conformational flexibility of the nicotinamide half of the cofactor and of the catalytic cysteine and glutamate residues have been proposed previously (Steinmetz *et al*., 1997; Perez-Miller and Hurley, 2003; Muñoz-Clares *et al*., 2011).

Copyright by Kasetsart University All rights reserved

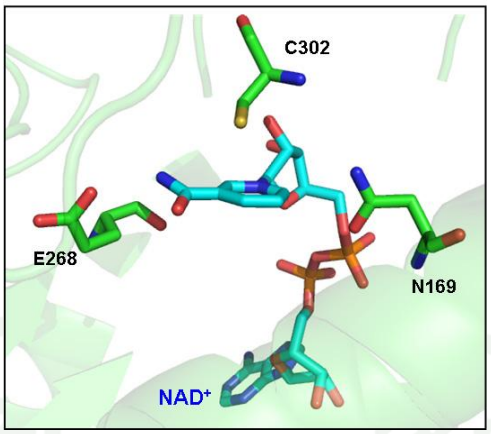

Figure 8 The catalytic triad of bovine ALDH2. The amino acids are depicted in stick representation and colored by atoms (carbon, green). The NAD^+ is shown in stick and colored by atoms (carbon, cyan).

1.4 Conformation flexibility of coenzyme and the catalytic residues in ALDH

Crystal structures of many enzymes in ALDH superfamily determined in the presence of bound $NAD(P)^+$ have exhibited conformational flexibility for the half of the nicotinamide cofactor (Steinmetz *et al*., 1997; Perez-Miller and Hurley, 2003). The movement of the nicotinamide ring in the active site of ALDHs is required for the correct positioning of the catalytic residues and the hydrolytic water during the course of the reaction (Steinmetz *et al*., 1997; Moore *et al*., 1998). The nicotinamide moiety of the coenzyme can adopt two positions, named the "hydride transfer" and the "hydrolysis" conformations (Steinmetz *et al*., 1997; Perez-Miller and Hurley, 2003) according to the catalytic step to which they have been associated. The "hydride transfer" conformation (~3.5 Å from the catalytic residue cysteine), which allows the hydride to transfer from the thiohemiacetal to the C4 of the nicotinamide ring, is adopted by $NAD(P)^+$. On the other hand, in the "hydrolysis" conformation, the nicotinamide ring moves away from the position that it occupies in the "hydride transfer" conformation, leaving some spaces for the hydrolytic water molecule to come in so that the deacylation step can take place. This conformation is then adopted by NADH. The nicotinamide ring in the "hydrolysis" conformation is positioned out of the active site by rotations about the pyrophosphate bonds. This isomerization is necessary to the enzyme catalysis in that the reduced nicotinamide ring must be

Copyright by Kasetsart University All rights reserved

displaced for the deacylating water to be properly positioned and activated by E268 for the completion of the reaction (Perez-Miller and Hurley, 2003). The difference conformation of nicotinamide ring has been observed in the crystal structure of human ALDH2 in complex with both the oxidized and reduced coenzyme, NAD^+ and NADH (PDB entries 1O00 and 1O02, respectively) (Figure 9) (Perez-Miller and Hurley, 2003).

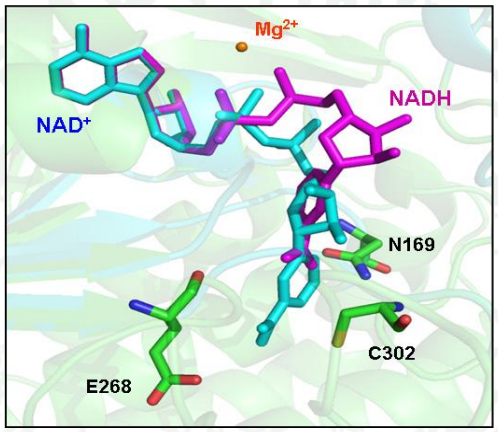

Figure 9 The different conformation of nicotinamide moiety in ALDH2. The amino acids are depicted in stick representation and colored by atoms (carbon, green). The NAD^+ and NADH are shown in stick, cyan and magenta, respectively. Mg^{2+} is also shown in sphere (orange).

The interaction of both conformations with surrounding amino acid residues of ALDH2 has been proposed (Figure 10) (Perez-Miller and Hurley, 2003). Both conformations have hydrogen bonds between adenosine ribose and I166, K192 and E195, and between adenosine phosphate and S246. In "hydride transfer" conformation, the oxygen O2A of phosphate group (PA) is directly coordinated to Mg^{2+} while the coordination between Mg^{2+} and the oxygen O1N of the other phosphate group (PN) is formed via a water molecule (Figure 10A). Both O1N and O2N of phosphate group (PN) make hydrogen bonds with the side chain NE1 of W168. The NH_2 of the carboxamide group is within 3 Å of the carbonyl oxygen of L269. The nicotinamide ribose oxygens make two hydrogen bonds with the side chain OE1 and OE2 of E399. The nicotinamide ring is sandwiched between the side chain of C302 and CG2 of T244, each ~3.4 Å from the ring. In "hydrolysis" conformation,

Copyright by Kasetsart University All rights reserved

both oxygens O2A and O1N of phosphate group (PA and PN, respectively) are directly coordinated to Mg^{2+} and only oxygen O2N is within hydrogen bonding distance of the side chain NE1 of W168 (Figure 10B). The ribose oxygens O3D and O2D make hydrogen bond with the side chains OE1 of Q349 and the side chain OE1 of E399, respectively. The carboxamide nitrogen N7N forms hydrogen bonds with the carbonyl oxygens of L269 and G245, and the oxygen O7N of the carboxamide group is within 3 Å of the side chain ND2 of N169. A magnesium ion (Mg^{2+}) coordinated to the pyrophosphate group of the cofactor in ALDH2 crystal structures permits the phosphates of NAD^+ to orient in multiple positions while the cofactor is bound. The nicotinamide ribose in "hydrolysis" conformation is shifted by ~3.5 Å toward the surface and rotated nearly 80° compared to "hydride transfer" conformation (Perez-Miller and Hurley, 2003).

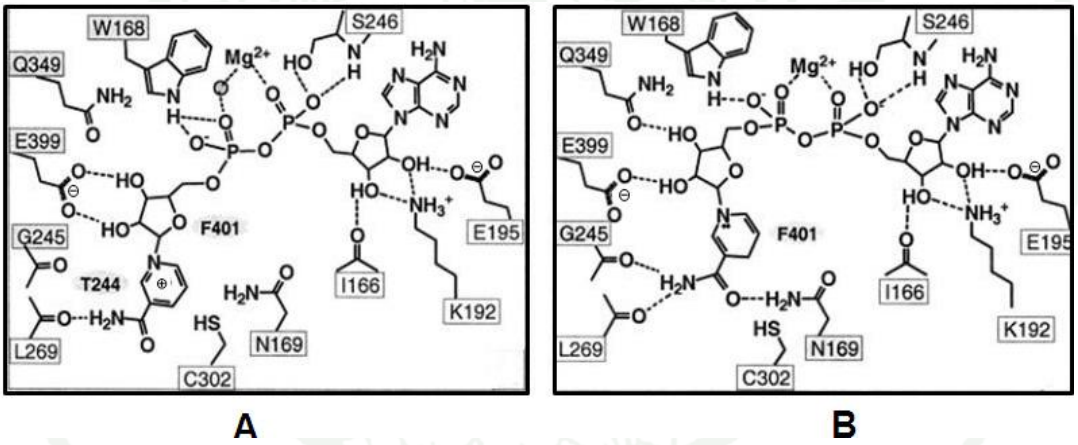

Figure 10 Interactions of different conformation of NAD^+ with surrounding residues of ALDH2. (A) the "hydride transfer" conformation (B) the "hydrolysis" conformation. The hydrogen bonds are shown with dashed lines for contacts between 2.5 and 3.2 Å in length.

Source: Perez-Miller and Hurley (2003)

For the nicotinamide ring in "hydrolysis" conformation, it is shifted about ~4 Å and rotated ~30° which occupies the former position of the ribose. In this conformation, the nicotinamide ring is also sandwiched between the backbone of

Copyright by Kasetsart University All rights reserved

G245 and the side chain of F401 (Figure 10B). However, the different conformation indicates that the "hydrolysis" conformation is favorable for NADH and the "hydride transfer" conformation is favorable for NAD^+ (Perez-Miller and Hurley, 2003). The isomerization of the coenzyme is a significant and necessary feature of catalysis (Steinmetz *et al*., 1997; Moore *et al*., 1998; Perez-Miller and Hurley, 2003). The interactions of thiohemiacetal transition state and thioester intermediate have been proposed (Perez-Miller and Hurley, 2003). The substrate (*N*,*N*-dimethylamino)-cinnamaldehyde (DACA) has been fit in the substrate tunnel of ALDH2 (PDB entry 1O01) (Figure 11) (Perez-Miller and Hurley, 2003).

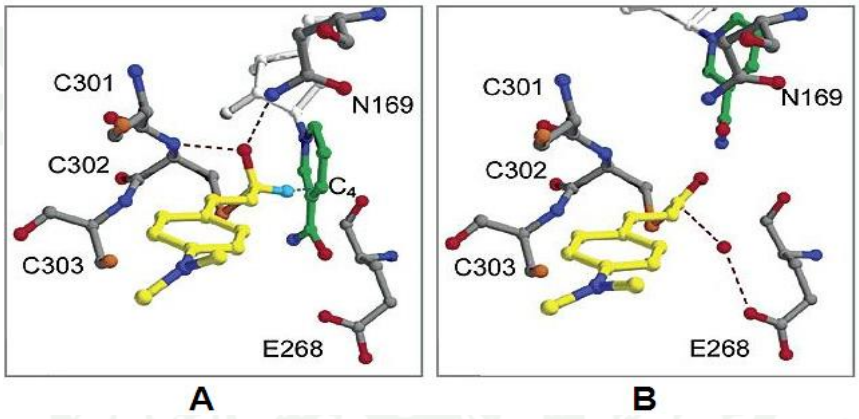

Figure 11 Proposed interactions of thiohemiacetal transition state and an acyl-enzyme intermediate. (A) the "hydride transfer" conformation of the cofactor with a predicted thiohemiacetal transition state (B) the "hydrolysis" conformation of the cofactor with a thioester intermediate intermediate. The amino acids are depicted in stick representation and colored by atoms (carbon, gray). The substrate DACA (yellow), the hydride (cyan) and nicotinamide ring (green) are shown in stick.

Source: Perez-Miller and Hurley (2003)

It was found that in thiohemiacetal transition state, NAD^+ exists in "hydride transfer" conformation. The oxyanion is stabilized by the side chain of N169 and the main chain of C302. The hydride is then transferred to C4 of the nicotinamide ring (Figure 11A). In thioester intermediate, NADH exists in "hydrolysis"

Copyright by Kasetsart University All rights reserved

conformation. E268 activates the water molecule which can then attack on the intermediate bound to release the product (Figure 11B). The oxidized cofactor, $NAD(P)^+$, binds in the conformation that leads to the oxidation of the aldehyde substrate (the "hydride transfer" conformation), whereas the reduced cofactor, NAD(P)H, binds in another conformation that allow the deacylation step (the "hydrolysis" conformations) to take place (Muñoz-Clares *et al*., 2011). According to the thiohemiacetal transition state, the hydride can be transferred from the aldehyde to $NAD(P)^+$. The thiohemiacetal intermediate is an oxyanion which is stabilized in the ''oxyanion hole" by hydrogen bond formation with the side chain of asparagine residue (N169 in ALDH2) and the main chain of the catalytic cysteine (C302 in ALDH2). Several the crystal structures of different ALDHs from various organisms have been solved in the apo and holo forms which are in complex with $NAD(P)^+$, NAD(P)H or aldehydes (Steinmetz *et al*., 1997; Johansson *et al*., 1998; Perez-Miller and Hurley, 2003; Gruez *et al*., 2004). It is interesting to note that the catalytic C302 and the catalytic E268 undergo conformational change upon binding of the coenzyme. Therefore, the dynamic component of the enzyme is crucial for the catalysis of ALDH enzymes.

The catalytic C302 residue can adopt two main conformations: the "resting" conformation in which the cysteine residue is far from the carbonyl carbon of the bound aldehyde (González-Segura *et al*., 2009) and the "attacking" conformation in which the cysteine residue is close to the carbonyl carbon of the bound aldehyde to perform the nucleophilic attack (Perez-Miller and Hurley, 2003). The thiol group of C302 residue in the "attacking" conformation is in the appropriate position to perform the nucleophilic attack on the aldehyde substrate whereas the "resting" conformation is not (Muñoz-Clares *et al*., 2010). Additionally, the thiolate form in the "attacking" conformation can be stabilized by the proximity of the positive charge of the oxidized nicotinamide whereas the position of the side chain of the catalytic cysteine in the "resting" conformation clashes with the nicotinamide ring of $NAD(P)^+$. Figure 12 shows the superimposition of the catalytic residues from PaBADH (PDB entry 2WME) and the nicotinamide ribose and nicotinamide ring from bovine ALDH2 (PDB entry 1A4Z) (Muñoz-Clares *et al*., 2010).

Copyright by Kasetsart University All rights reserved

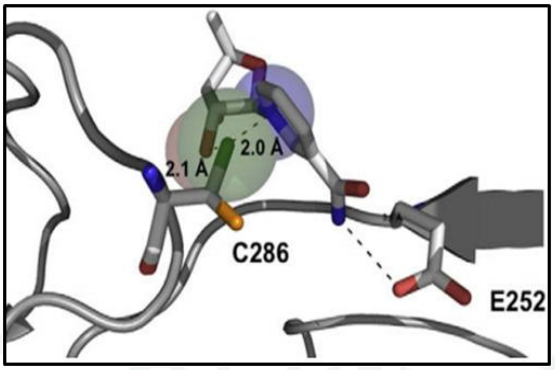

Figure 12 Steric clashes between the oxidized nicotinamide and the catalytic cysteine in the "resting" conformation. The red, blue and green semitransparent spheres represent the van der Waals surface of the nicotinamide ribose O2D, nicotinamide ring N1N, and the cysteine SG in the "resting" conformation, respectively.

Source: Muñoz-Clares *et al*. (2010)

Having looked at the catalytic C302, the possible conformation of E268 is next examined. There are three possible conformations of the catalytic residue E268: the "inside" conformation in which the E268 residue is pointed toward the catalytic C302 residue for the activation of the nucleophilic attack, since its carboxyl group is close to the thiol (Gruez *et al*., 2004; Perez-Miller and Hurley, 2003), the "intermediate" conformation in which the catalytic E268 residue is positioned at 7–8 Å from the catalytic cysteine and suited for the activation of the hydrolytic water molecule (Liu *et al*., 1997; Perez-Miller and Hurley, 2003; González-Segura *et al*., 2009) and the "outside" conformation in which the catalytic E268 releases the proton that is previously taken from either the catalytic C302 or a hydrolytic water involved in the proton relay mechanism (Perez-Miller and Hurley, 2003; González-Segura *et al*., 2009). The "inside" conformation is proposed to be incompatible with the bound oxidized cofactor (Moore *et al*., 1998) whereas the "intermediate" conformation is compatible with the oxidized cofactor (Steinmetz *et al*., 1997; González-Segura *et al*., 2009). The distinct conformations of coenzyme and both catalytic residues from PaBADH (PDB entry 2WME) (González-Segura *et al*., 2009) and ALDH2 (PDB entry 1O02) (Perez-Miller and Hurley, 2003) are displayed (Figure 13).

Copyright by Kasetsart University All rights reserved

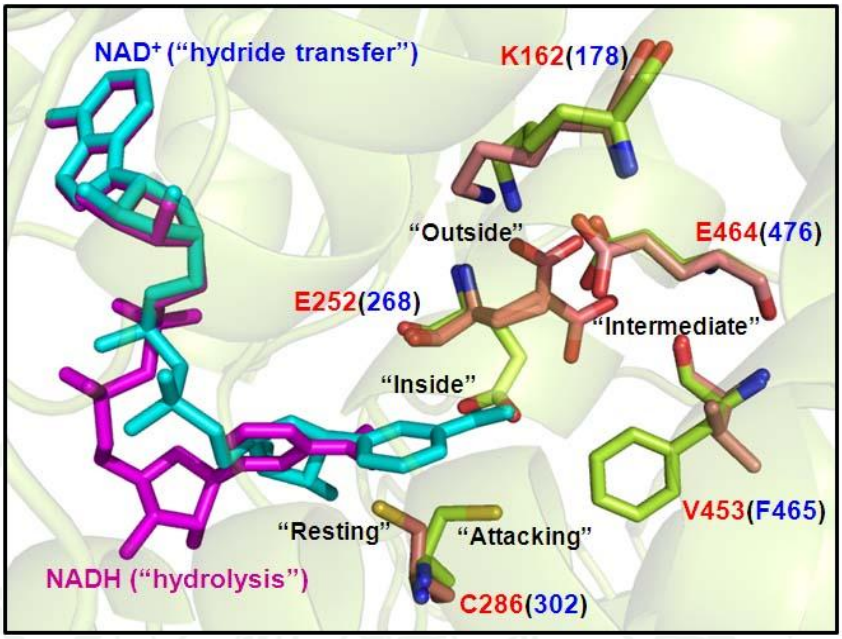

Figure 13 Conformations of the catalytic aspartic and cysteine residue in ALDH active sites. The distinct conformations of the catalytic cysteine ("resting" and "attacking") and catalytic glutamate ("inside", "intermediate" and "outside") are displayed. The amino acid residues correspond to PaBADH (2WME) are shown in red and those of ALDH2 (1O02) are shown in blue within parenthesis. The amino acid residues are shown in stick and colored by atoms (PaBADH carbon: salmon pink, and ALDH2 carbon: lemon green). The NAD^+ and NADH are shown in stick, cyan and magenta, respectively.

The catalytic cysteine (C286) in PaBADH is in the "resting" conformation and the catalytic glutamate (E252) is found in both "outside" and "intermediate" conformations whereas in ALDH2 the catalytic cysteine (C302) is found in the "attacking" conformation and the catalytic glutamate (E268) is in the "inside" conformation. It is important to note that the nicotinamide ring of the oxidized cofactors, $NAD(P)^+$ in "hydride transfer" conformation crashes the side chain glutamate in the "inside" conformation. Additionally, three amino acid residues, namely E476, F465 and K178 (ALDH2 numbering) surrounding the catalytic glutamate have some roles in the proton relay mechanism.

Copyright by Kasetsart University All rights reserved

1.5 The proton relay mechanism in ALDH

The proton relay mechanism is important for ALDH because the catalytic glutamate would release the proton that was previously abstracted from either the catalytic C302 or a hydrolytic water. This mechanism has been proposed in PaBADH (Figure 14) (González-Segura *et al*., 2009). The residues K162, E252, C286, E464 and V453 in PaBADH are equivalent to K178, E268, C302, E476 and F465 in ALDH2, respectively. According to the Figure 14, in the step (1) the deprotonated E252 existing in the "intermediate" conformation abstracts a proton from the hydrolytic water (or from the catalytic cysteine, not shown in this Figure). In the step (2), the protonated E252 is stabilized by hydrogen bonding to the main chain carbonyl oxygen of V453. Then in step (3), E252 moves to the "outside" conformation and forms a hydrogen bond with E464 allowing the proton transfer. Finally in step (4), when the protonated E464 loses the proton to a water molecule, E252 moves back to the "intermediate" conformation (or to the "inside" conformation, if the nicotinamide ring of the nucleotide is not bound). The efficient transfer of the proton from E252 to E464 is achieved when E252 is in the "outside" conformation. E464 can transfer the proton to a water molecule, which is hydrogen bonded connecting to the water channel. When the proton is transferred from E464 to the bulk water, the electrostatic repulsion between the deprotonated E252 and the deprotonated E464 would expel the former toward the "inside" and "intermediate" positions, where it can deprotonate the catalytic cysteine and the hydrolytic water molecule, respectively (González-Segura *et al*., 2009).

Copyright by Kasetsart University All rights reserved

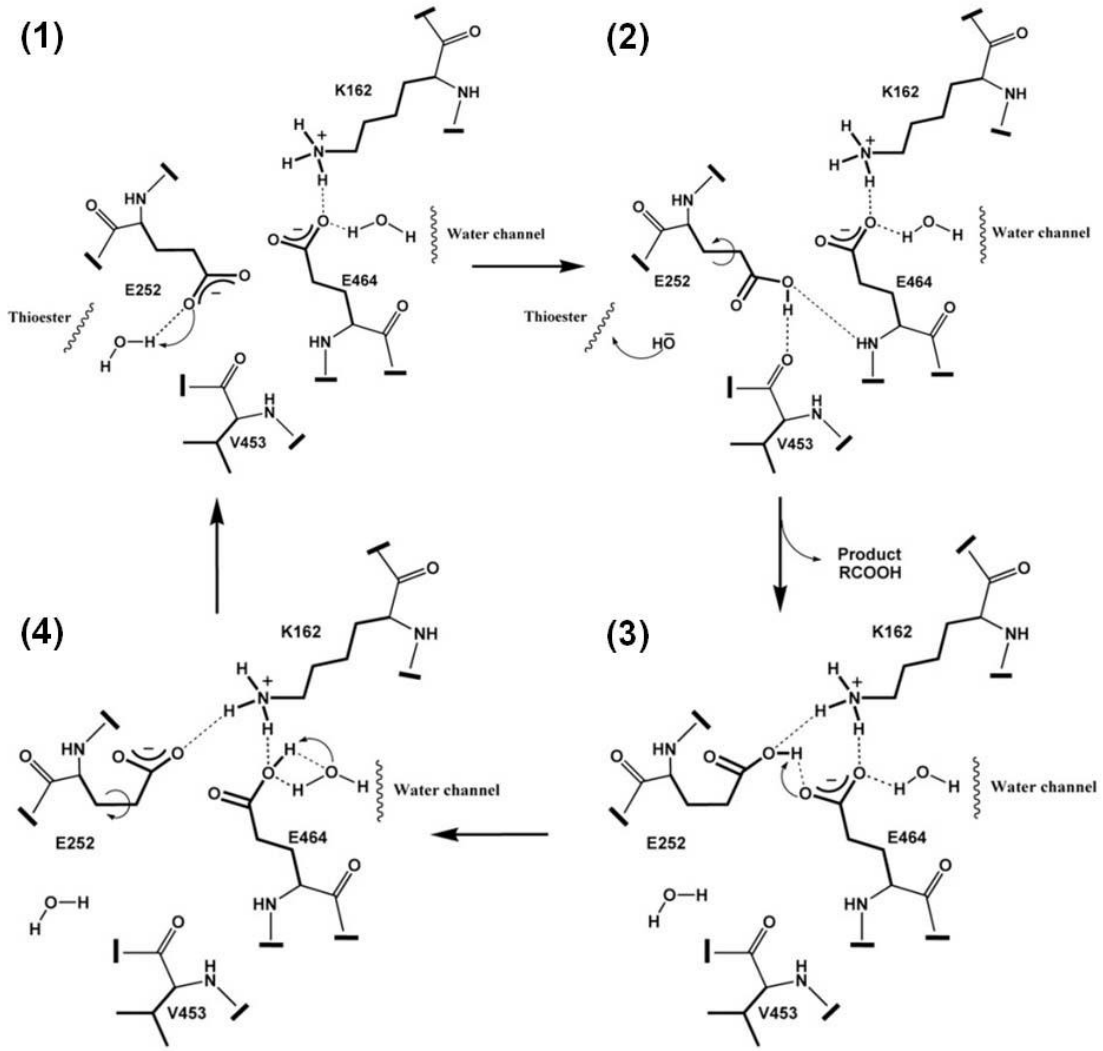

Figure 14 Mechanism for the proposed proton relay system in PaBADH

Source: González-Segura *et al*. (2009)

Copyright by Kasetsart University All rights reserved

2. Aldehyde dehydrogenase in plant

A small number of plant ALDHs in different species have been functionally characterized such as rice (*Oryza sativa*), soybean (*Glycine max*), *Arabidopsis thaliana* and pea (*Pisum sativum*) (Gao and Han, 2009; Arikit *et al*., 2010; Kirch *et al*., 2004; Šebela *et al*., 2000) as well as ALDH in human and mammal (Yoshida *et al*., 1998; Moore *et al*., 1998; Perez-Miller and Hurley, 2003). The plant ALDHs play crucial roles in development, growth and stress responses which improve the plant osmotic stress tolerance (Kotchoni and Bartels, 2003; Kotchoni *et al*., 2010). So far, the studies of plant *ALDH* genes have shown that these genes have been induced under stress conditions such as high salinity conditions or water deficit (Kotchoni and Bartels, 2003; Gao and Han, 2009). Water stress is recognized as water deficit, which leads to drought and desiccation. Additionally, the level of metabolic aldehydes and their intermediates must be strictly regulated for detoxifying the cell during stress conditions. Some of the ALDHs are related to osmotic stress tolerance, dehydration and salt stress tolerance (Kotchoni and Bartels, 2003; Kirch *et al*., 2004). The adaptation and response of plants to stress conditions are highly variable and very complex. The main enzymatic functions of ALDHs have been recognized in two ways: 1) the increased accumulation of osmolytes such as glycine betaine and 2) the detoxification of aldehydes (Kotchoni and Bartels, 2003). Until now, ALDHs in rice (*Oryza sativa*) have been investigated (Gao and Han, 2009; Tsuji *et al*., 2003; Mitsuya *et al*., 2009).

2.1 Rice (*Oryza sativa*)

Rice (*Oryza sativa*) is an important food and an excellent model crop plant for studying monocots, second to *Arabidopsis* (Kotchoni *et al*., 2010). Fragrant rice has been very popular and famous among consumers in many countries; it has been sold at a premium price in local and export markets because of their distinct aroma. Three fragrant accessions have been identified from the distinct genetic subpopulations of rice: 1) Group V such as “Basmati” and “Sadri” varieties, 2) indica such as “Jasmine” varieties and 3) tropical japonica (Kovacha *et al*., 2009). Two popular major types of fragrant rice in market have been known including the basmati

Copyright by Kasetsart University All rights reserved

rice from India and Pakistan and the jasmine rice or Thai hom Mali (Khao Dawk Mali 105) from Thailand. Fragrant rice, *Oryza sativa*, has the smallest cereal genome comprising 430 Mb across 12 chromosomes as compared to the significantly large genome sizes of sorghum, maize, barley, and wheat (about 750, 3000, 5000, and 16000 Mb, respectively) (Tyagi *et al*., 2004). Many volatile compounds have been detected in fragrant rice, but the major compound of the aroma is always mentioned as 2-acetyl-1-pyrroline (2AP) (Figure 15) (Buttery *et al*., 1983).

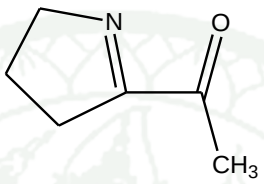

Figure 15 Chemical structure of 2-acetyl-1-pyrroline

2AP is also a potent flavor component found in both basmati and jasmine rice. 2AP can be found in all parts of fragrant rice varieties except the roots (Buttery *et al*., 1983). It was reported that the amount of 2AP in older leaves rice is less than young ones whereas the tips of rice leaves contain more 2AP compared to the base of leaves (Lorieux *et al*., 1996). Additionally, the fragrant rice and non-fragrant rice is not identified by the presence or absence of 2AP, but by the concentration of 2AP. The study of the volatile components of aromatic and non-aromatic rice varieties demonstrated that 2AP occurs in aromatic rice varieties at higher levels whereas in non-aromatic rice varieties at lower levels (Buttery *et al*., 1983). The concentration of 2AP in fragrant rice grain is 100 times higher than non-fragrant rice (Widjaja *et al*., 1996). The main difference between fragrant rice and non-fragrant rice is that non-fragrant rice contains more n-hexanal, n-heptanal, (E)-2- heptanal, 6-methyl-5-hepten-2-one, 1-octen-3-ol, n-nonanal, 2-pentylfuran, 4-vinylguaiacol and 4-vinylphenol than the fragrant rice (Widjaja *et al*., 1996). Therefore, the concentration of 2AP in combination with the concentration of these compounds has been used to determine the quality of the fragrance rice. So far, the two pathways of 2AP biosynthesis in rice have been proposed: OsBADH2-dependent 2AP synthesis (Bradbury *et al*., 2008) and OsBADH2-independent 2AP synthesis (Huang *et al*., 2008).

Copyright by Kasetsart University All rights reserved

2.1.1 OsBADH2-dependent 2AP synthesis

The fragrance in rice is associated with the presence of 2AP. Genetic analysis showed that the recessive *fgr* allele on chromosome 8 of rice has been linked to rice fragrance while the dominant *Fgr* allele is associated with lack of fragrance (Bradbury *et al*., 2005; Sakthivel *et al*., 2009). The structure of the fragrance gene (*fgr*) of rice chromosome 8 is shown (Figure 16) (Bradbury *et al*., 2005). The *fgr* gene in rice corresponds to the gene encoding betaine aldehyde dehydrogenase 2, OsBADH2. The genetic causing rice fragrance is the loss of function of OsBADH2 corresponded with the recessive nature of the trait (Bradbury *et al*., 2005). The study showed that an eight base pair deletion (5′-GATTAGGC-3′) starting at position 734 in exon 7 of OsBADH2 leads to the generation of a premature stop codon that would, if translated, produce a truncated non-functional protein (Bradbury *et al*., 2005; Chen *et al*., 2008).

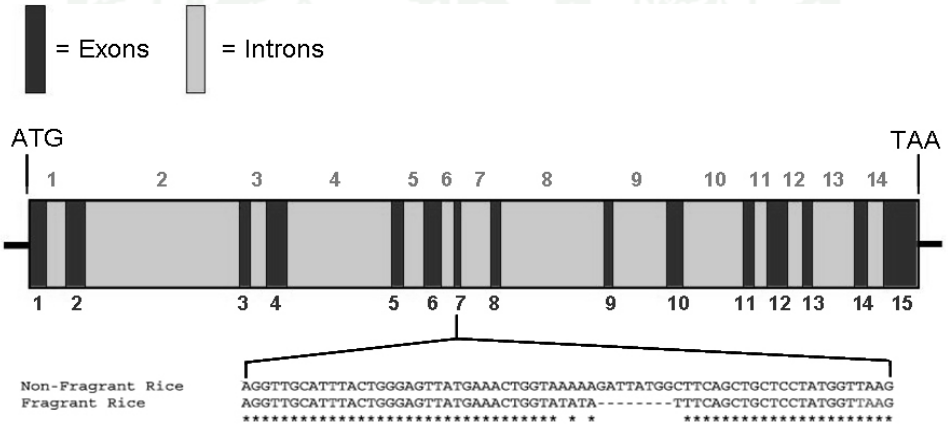

Figure 16 Structure of the fragrance gene (*fgr*) of rice chromosome 8

Source: Bradbury *et al*. (2005)

The eight base pair deletion in exon 7 encodes truncated OsBADH2 lacking 252 C-terminal residues. The missing C-terminal amino acids cover the entire substrate binding domain and partial oligomerization domains, thus generating the truncated nonfunctional OsBADH2 (Chen *et al*., 2008). Therefore, the OsBADH2-dependent 2AP synthesis has been proposed (Bradbury *et al*., 2008). The

Copyright by Kasetsart University All rights reserved

formation of 2AP can be derived from either proline or ornithine to potential substrates (in boxed) of 2AP via Δ^1-pyrroline (Figure 17).

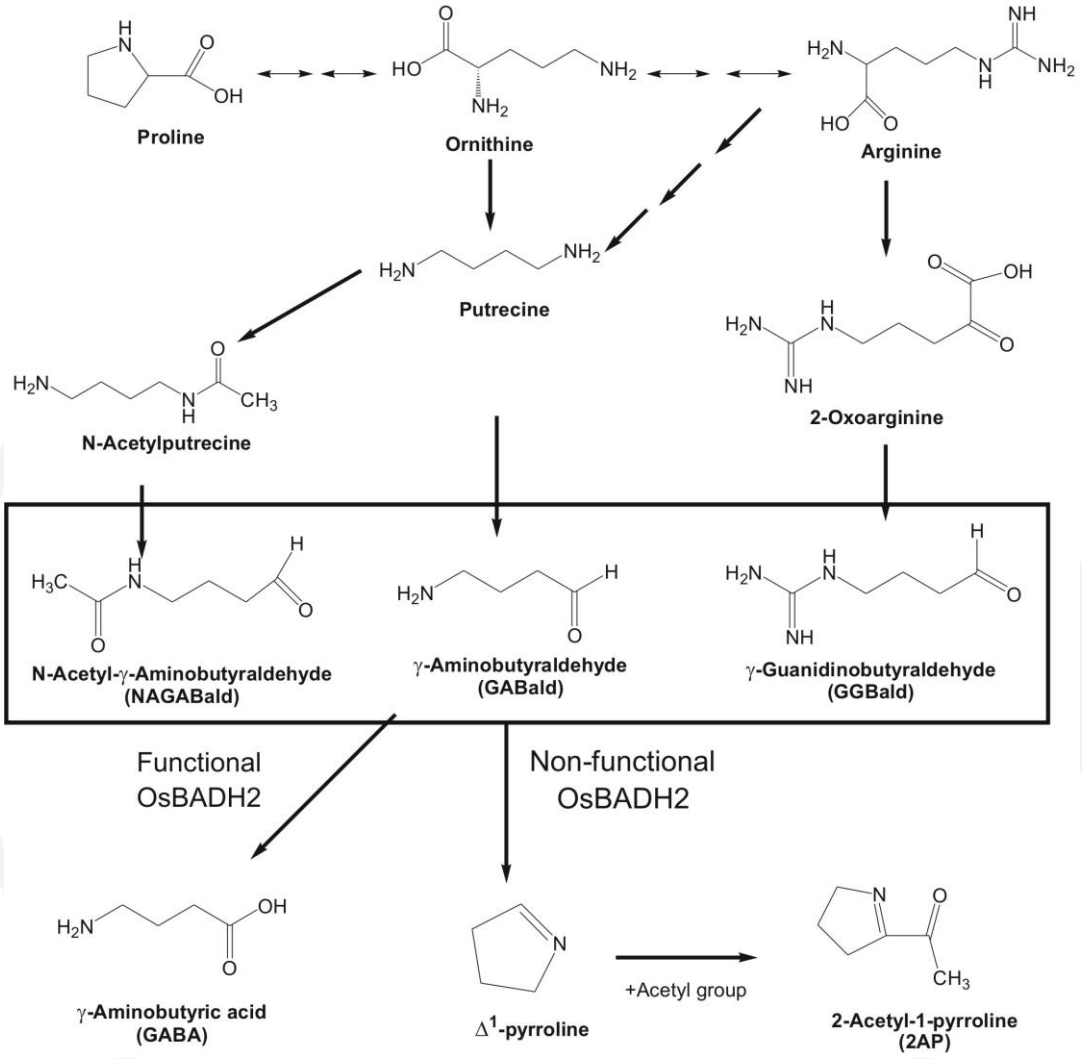

Figure 17 The pathway of OsBADH2-dependent 2AP synthesis in rice

Source: Bradbury *et al*. (2008)

Proline can be catabolized from putrecine into γ-aminobutyraldehyde (GAB-ald). Putrecine is also found at high levels in growing tissues which are rapidly dividing and is catabolized to GAB-ald by diamine oxidases or DAO (Kakkar *et al*., 2000). The influence of pH on structural form of GAB-ald has also been found that at pH 10, GAB-ald almost spontaneously cyclises to form Δ^1-

Copyright by Kasetsart University All rights reserved

pyrroline (Struve and Christophersen, 2003). The nitrogen source in the pyrroline ring of proline becomes the nitrogen in the pyrroline ring of 2AP in rice (Yoshihashi *et al*., 2002). If OsBADH2 is present and functional, it is able to convert GAB-ald to γ-aminobutyric acid (GABA). However, if OsBADH2 is absent or non-functional, GAB-ald is acetylated to form 2AP. The absence of OsBADH2 causes an accumulation of GAB-ald leading to higher 2AP production. The relation between OsBADH2 and 2AP synthesis in rice is concluded and shown in Figure 18 (Sakthivel *et al*., 2009). The 2AP synthesis is dependent on the function of OsBADH2. When OsBADH2 is non-functional, it can convert γ-aminobutyraldehyde (GAB-ald) into Δ^1-pyrroline and 2AP. Then, 2AP is accumulated in fragrant varieties (Figure 18A). However, if OsBADH2 is functional, it can convert GAB-ald into GABA. Then none of 2AP is accumulated in non-fragrant varieties (Figure 18B).

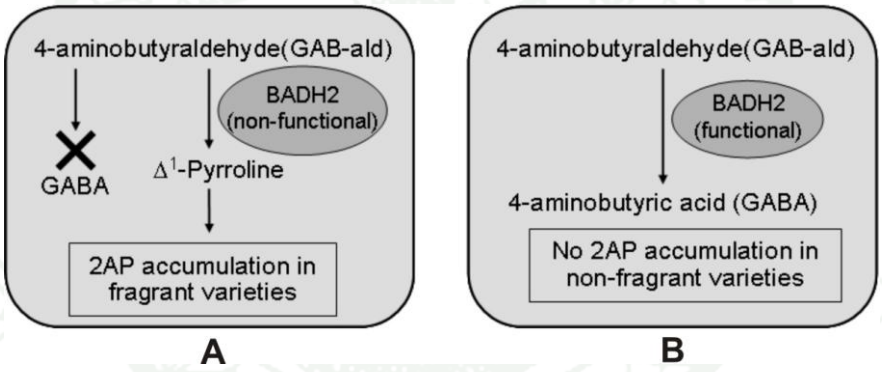

Figure 18 The correlation between OsBADH2 and 2AP of OsBADH2-dependent 2AP synthesis. (A) fragrant rice varieties (B) non-fragrant rice varieties.

Source: Sakthivel *et al*. (2009)

2.1.2 OsBADH2-independent 2AP synthesis

In higher plants, ornithine, proline, and glutamate can be converted to Δ^1-pyrroline-5-carboxylic acid via three different enzymes including ornithine aminotransferase (OAT), proline dehydrogenase (PRODH), and Δ^1-pyrroline-5-carboxylic acid synthetase (P5CS), respectively (Moschou *et al*., 2008). Δ^1-pyrroline-

Copyright by Kasetsart University All rights reserved

5-carboxylic acid usually reacts directly with methylglyoxal to form 2AP (Figure 19) (Huang *et al*., 2008). However, there is no direct involvement of OsBADH2 in this pathway. In aromatic rice Tainung 71 and 72, the increasing amounts of Δ^1- pyrroline-5-carboxylic acid have positive correlations with increases in the enzyme activities of both P5CS and OAT (Huang *et al*., 2008). In rice, glutamate is converted by P5CS to glutamyl γ-semialdehyde (GSA) which then cyclizes spontaneously to form Δ^1-pyrroline-5-carboxylic acid. Δ^1-pyrroline-5-carboxylic acid is synthesized through transamination of ornithine catalyzed by OAT. This compound can also be reduced into proline by P5C reductase. Methylglyoxal then reacts with 1-pyrroline leading to the formation of 2AP in the fragrant variety. Thus, Δ^1-pyrroline-5-carboxylic acid and methylglyoxal are important precursors for 2AP synthesis in rice.

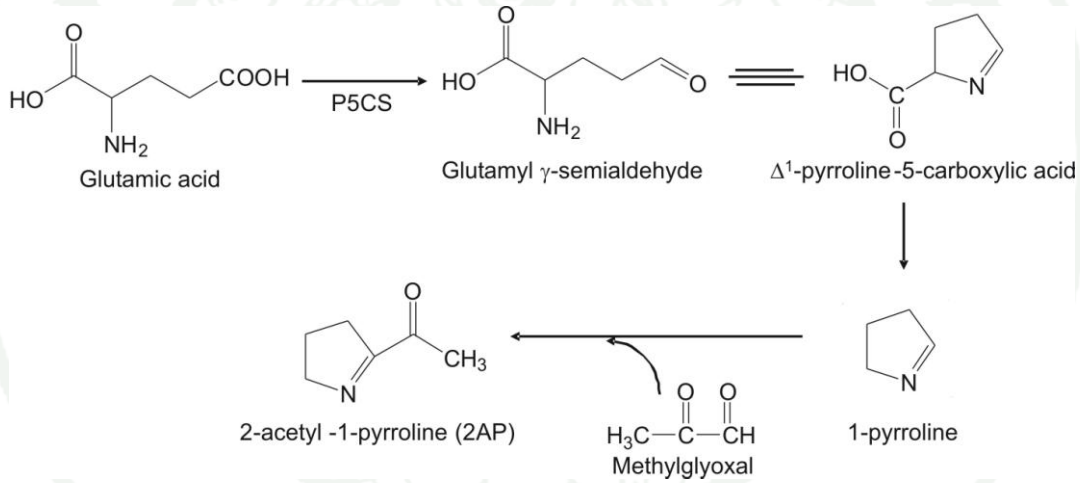

Figure 19 The pathway of OsBADH2-independent 2AP synthesis in rice

Source: Huang *et al*. (2008)

2.2 γ-aminobutyric acid (GABA)

GABA is a four carbon non-protein amino acid which is commonly presented in living organisms (Figure 20). GABA functions as a major inhibitory neurotransmitter in the mammalian central nervous system (CNS). GABA and its receptors are found in a wide range of organisms, from prokaryotes to vertebrates. It plays a role in regulating neuronal excitability throughout the nervous system. GABA

Copyright by Kasetsart University All rights reserved

is also detected in the peripheral nervous system (PNS), endocrine and several nonneural tissues (Erdo and Wolff, 1990). GABA is produced from enzyme glutamate decarboxylase (EC 4.1.1.15) or GAD that catalyzes the conversion of L-glutamate into GABA and carbon dioxide.

Figure 20 Chemical structure of γ-aminobutyric acid (GABA)

Moreover, there are two GABA receptors in CNS. First, $GABA_A$ receptor is ligand-gated chloride channel and can be detected in both vertebrates and invertebrates. Second, $GABA_B$ receptor is potassium or calcium channel coupling via GTP binding proteins. Therefore, GABA can depress the ganglionic action potentials and inhibit acetylcholine release induced by stimulation. The drugs which target $GABA_A$ receptor have been used for many years such as barbiturates and benzodiazepines. These compounds bind to the $GABA_A$ receptor and increase GABA-gated chloride conductance. Moreover, several drugs have been used for targeting in $GABA_A$ and $GABA_B$ receptors in various diseases (Foster and Kemp, 2006). For instance, SGS-742 has $GABA_B$ as a target involving in Alzheimer disease, ELB-139 has $GABA_A$ as a target implicating in Schizophrenia. Triazolam (Halcion™) and Eszopiclone (Lunesta™) have $GABA_A$ as a target involving in Insomnia. γ-vinyl GABA (Vigabatrin™) can inhibit GABA-T that implicates in epilepsy. These drugs are also used to facilitate the state of CNS depression to induce sleep, muscle relaxation and anaesthesia. Consequently, GABA analogues can act as agonists of GABA receptors which create relaxing and anti-anxiety used in medical treatments such as insomnia, clinical depression, alcoholism, and athletic performance. Subsequently, researches on GABA in vertebrates focus mainly on its role as a signaling molecule, particularly in neurotransmitter. However, in plants and animals, GABA is mainly metabolized via a short pathway called the GABA shunt, because it bypasses two steps of the tricarboxylic acid (TCA) cycle (Figure 21) (Bouché and Fromm, 2004).

Copyright by Kasetsart University All rights reserved

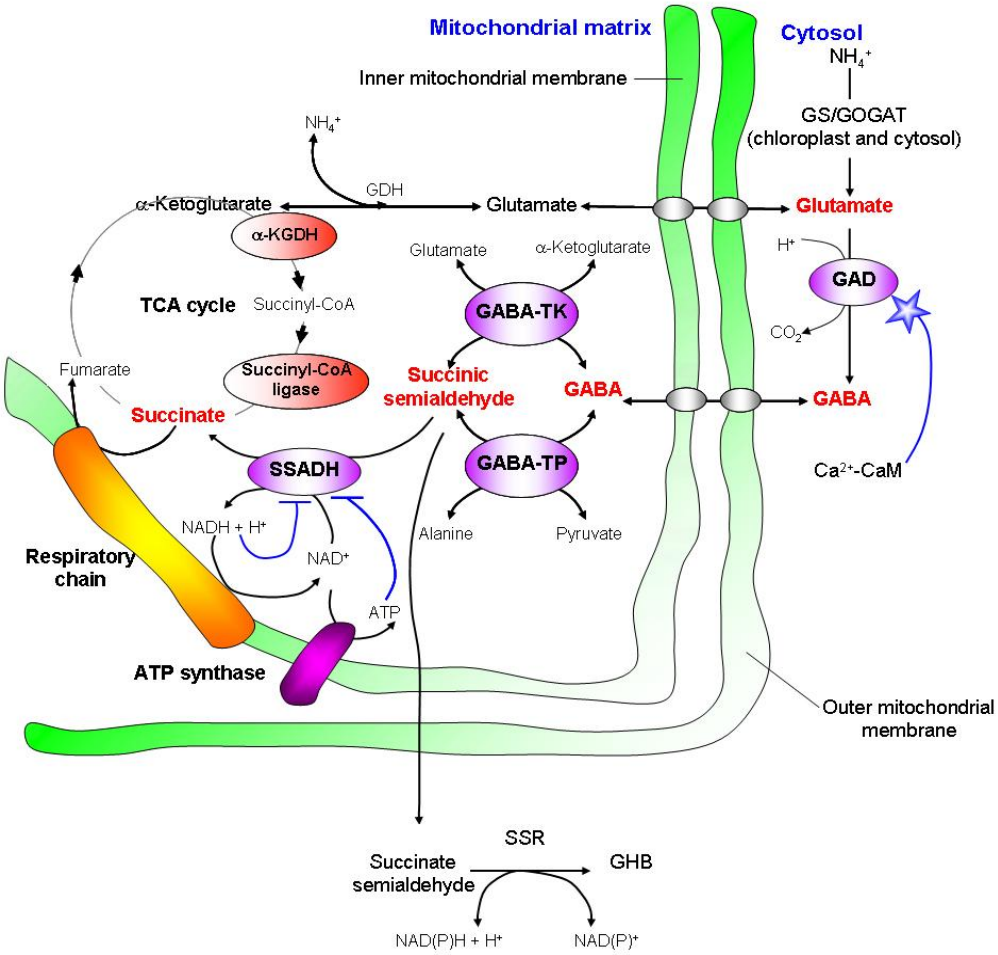

Figure 21 The GABA shunt metabolic pathway and its regulation in plants

Source: Bouché and Fromm (2004)

According to the GABA shunt metabolic pathway, the glutamine-synthetase/glutamate-synthase (GS/GOGAT) cycle is a nitrogen assimilation pathway of glutamate and amino acids in plants. Both enzymes are found in chloroplast and cytosol. The glutamate dehydrogenase (GDH) is believed to function in glutamate catabolism. The GABA shunt is composed of three enzymes (purple in Figure 21), the cytosolic enzyme glutamate decarboxylase (GAD), the mitochondrial enzymes GABA transaminase (GABA-T) and succinic semialdehyde dehydrogenase (SSADH). GAD is a cytosolic enzyme which catalyses the irreversible decarboxylation of glutamate to produce GABA, regulated by the Ca^{2+}-calmodulin (Ca^{2+}-CaM) (blue)

Copyright by Kasetsart University All rights reserved

complex. Subsequently, GABA is transported into the mitochondria, where it is converted into succinic semialdehyde by GABA transaminase using either α-ketoglutarate (by GABA-TK) or pyruvate (by GABA-TP) as amino acid acceptors. Then succinic semialdehyde is reduced by succinic semialdehyde dehydrogenase (SSADH) to form succinate, which is a substrate for the TCA cycle. Both ATP and NADH can inhibit the activity of the SSADH enzyme (blue in Figure 21). The succinyl-CoA ligase and the α-ketoglutarate dehydrogenase (α-KGDH) are two enzymes of the TCA cycle bypassed by the GABA shunt pathway. Succinic semialdehyde can also be reduced to γ-hydroxybutyric acid (GHB) using succinic semialdehyde reductase (SSR) localized in the cytosol in animal cells and plants. The GABA shunt has been associated with various physiological responses including nitrogen metabolism, regulation of cytosolic pH, detoxification of reactive oxygen radicals, osmoregulation and intracellular signal transduction (Bouché and Fromm, 2004; Kinnersley and Turano, 2000). The degradation of GABA in GABA shunt also limits the accumulation of reactive oxygen intermediates under oxidative stress conditions that also inhibit the enzymes of TCA cycle (Figure 21) (Bouché and Fromm, 2004). Additionally, GABA in plants can acting as a signaling molecule, and its important roles include the protection against oxidative stress, defense against insects and nematode, response to different stress, and contribution to the C:N balance (Shelp *et al*., 1999; Kinnersley and Turano, 2000; Coleman *et al*., 2001; Bouché and Fromm, 2004).

2.3 The classification of aldehyde dehydrogenases in rice

The ALDH family in rice consists of diverse and several enzyme families. Several methods for classification of ALDH family have been proposed but none of them can be used and held for so long. Since ALDHs have been found to exist in multiple forms which differ in either physical or functional properties and identified in almost several organisms. However, since the rice genome-sequencing project has been completed, it has paved the way for gene discovery and functional gene analysis using the rice gene data. The ALDH family in various organisms has been identified and classified (Table 4) (Jimenez-Lopez *et al*., 2010). The ALDH family of seven

Copyright by Kasetsart University All rights reserved

organisms has been observed including *Zea mays*, *Oryza sativa*, *Physcomitrella patens*, *Arabidopsis thaliana*, *Chlamydomonas reinhardtii*, Human and Fungi. The ALDH sequences of *O. sativa* are more closely related to *Z. mays*, *A. thaliana*, *P. patens* than *C. reinhardtii*, Human and Fungi, based on the phylogenetic analysis (Jimenez-Lopez *et al*., 2010). The identification of *ALDH* gene superfamily is dependent on ALDH active sites, ALDH conserved motifs and ALDH defined family criteria previously reported from *Arabidopsis ALDH* gene family (Kirch *et al*., 2004) as database search queries. According to the ALDH family criteria, proteins containing more than 40% amino acid similarity are classified in one family whereas those sharing more than 60% identical are composed to the same subfamily (Kirch *et al*., 2004).

The identification of 24 unique ALDH families has revealed a member of ten ALDH protein families in rice (ALDH2, ALDH3, ALDH5, ALDH6, ALDH7, ALDH10, ALDH11, ALDH12, ALDH18 and ALDH22) (Jimenez-Lopez *et al*., 2010). The rice ALDHs (ALDH2, ALDH3, ALDH5, ALDH6, ALDH7, ALDH10, ALDH11 and ALDH12) shares the common core of the plant ALDH families with *Z. mays*, *A. thaliana* and *P. patens*. Only ALDH22 is found in *Z. mays*, *O. sativa* and *A. thaliana* while ADLH21 and ADLH23 are found only in *P. patens*. Moreover, the gene of *O. sativa*, *Z. mays*, *A. thaliana* and *P. patens* encodes for ALDH2, ALDH3, ALDH5, ALDH6 and ALDH7, which are present in a wide variety of plants (Kirch *et al*., 2004; Kotchoni *et al*., 2010; Jimenez-Lopez *et al*., 2010).

Copyright by Kasetsart University. All rights reserved

Table 4 The *ALDH* gene families identified in various organisms

Organism	ALDH family																							
	1	2	3	4	5	6	7	8	9	10	11	12	13	14	15	16	17	18	19	20	21	22	23	24
Z.mays	-	+	+	-	+	+	+	-	-	+	+	+	-	-	-	-	-	+	-	-	-	+	-	-
O.sativa	-	+	+	-	+	+	+	-	-	+	+	+	-	-	-	-	-	+	-	-	-	+	-	-
P.patens	-	+	+	-	+	+	+	-	-	+	+	+	-	-	-	-	-	-	-	-	+	-	+	-
A.thaliana	-	+	+	-	+	+	+	-	-	+	+	+	-	-	-	-	-	-	-	-	-	+	-	-
C.reinhardtii	-	+	-	-	+	+	-	-	-	+	+	+	-	-	-	-	-	-	-	-	-	-	-	+
Human	+	+	+	+	+	+	+	+	+	-	-	-	-	-	-	-	-	+	-	-	-	-	-	-
Fungi	+	-	-	+	+	-	-	-	-	+	-	-	-	+	+	+	-	+	-	-	-	-	-	-

Presence (+) or absence (-) of *ALDH* gene family in each organism.

Source: Jimenez-Lopez *et al*. (2010)

Copyright by Kasetsart University All rights reserved

Recently, the revised nomenclature of ALDH protein subfamily in rice has been proposed according to the sequence similarity to previously characterized ALDH genes (Table 5) (Gao and Han, 2009; Kotchoni *et al*., 2010). Ten rice ALDH families have been established by multiple *ALDH* gene members (ALDH2: 5 genes; ALDH3: 5 genes; ALDH10: 2 genes; ALDH12: 2 genes; ALDH18: 2 genes). The remaining five families (ALDH5; ALDH6; ALDH7; ALDH11 and ALDH22) are represented by single *ALDH* gene. The rice *ALDH* gene superfamily is the most extensive with 21 genes compared to 14 genes in *A. thaliana* (Kirch *et al*., 2004) and 24 genes in *Z. mays* (Jimenez-Lopez *et al*., 2010). Table 5 also displays the rice ALDH family, gene locus, molecular function, localization and molecular weight of each gene. In each gene, the position of gene locus in different chromosomes is indicated; for instance, the gene locus of OsALDH2B1 is Os06g15990, which is located on chromosome 6. The molecular function of each ALDH family is different, varied and diverse.

Table 5 The rice ALDH protein superfamily: revised nomenclature

ALDH Family	Revised Annotation	Gene Locus	Molecular Function	Subcellular Localization	M.W. (kDa)
Family 2	OsALDH2B1	Os06g15990	ALDH	Mitochondrion	59.3
	OsALDH2B2	Os06g39230	ALDH	Cytosol	56.4
	OsALDH2B5	Os02g49720	ALDH	Mitochondrion	58.9
	OsALDH2C1	Os01g40870	ALDH	Cytosol	54.2
	OsALDH2C4	Os01g40860	ALDH (NAD)	Cytosol	54.2
Family 3	OsALDH3B1	Os04g45720	Variable substrate ALDH	-	54.3
	OsALDH3E1	Os02g43194	ALDH [NAD(P)$^+$]	Chloroplast	54.5
	OsALDH3E2	Os02g43280	Variable substrate ALDH	Chloroplast	54.6
	OsALDH3H1	Os12g07810	ALDH [NAD(P)$^+$]	endoplasmic reticulum	52.4
	OsALDH3H2	Os11g08300	Variable substrate ALDH	-	52.5
Family 5	OsALDH5F1	Os02g07760	SSADH, NAD or NADH as acceptor	Mitochondrion	56.1
Family 6	OsALDH6B2	Os07g09060	Methylmalonate semi-aldehyde dehydrogenase	Mitochondrion	57.2

Copyright by Kasetsart University All rights reserved

Table 5 (Continued)

ALDH Family	Revised Annotation	Gene Locus	Molecular Function	Subcellular Localization	M.W. (kDa)
Family 7	OsALDH7B6	Os09g26880	Antiquitin	-	54.5
Family 10	OsALDH10A5	Os04g39020	BADH	-	54.6
	OsALDH10A8	Os08g32870	BADH	Chloroplast, plastids	54.7
Family 11	OsALDH11A3	Os08g34210	NADP-dependent glyceraldehyde-3-phosphate dehydrogenase	Cytoplasm	53.4
Family 12	OsALDH12A1	Os05g45960	P5CDH	Mitochondrion	60.5
	OsALDH12B1	Os12g40440	P5CDH	Mitochondrion	91.0
Family 18	OsALDH18B1	Os05g38150	P5CS	-	77.7
	OsALDH18B2	Os01g62900	P5CS	-	79.5
Family 22	OsALDH22A1	Os07g48920	ALDH (NAD)	Secretory pathway	66.0

The (-) denotes no information.

Source: Gao and Han (2009) and Kotchoni *et al*. (2010)

Betaine aldehyde dehydrogenase 2 (OsBADH2) involving in OsBADH2-dependent 2AP synthesis in rice is classified in ALDH family 10 which is OsALDH10A8 located on chromosome 8 while its homologue, betaine aldehyde dehydrogenase 1 (OsBADH1), is OsALDH10A5 located on chromosome 4. The Δ^1-pyrroline-5-carboxylic acid synthetase (P5CS) implicating in OsBADH2-independent 2AP synthesis in rice is classified in ALDH family 18 (OsALDH18B1 and OsALDH18B2). To date, most of the study plant *ALDH* genes are shown to be induced under high salinity or water deficit conditions, suggesting possible roles of these genes in improving the plant osmotic stress tolerance (Kotchoni and Bartels, 2003; Tsuji *et al*., 2003; Gao and Han, 2009; Mitsuya *et al*., 2009).

Copyright by Kasetsart University All rights reserved

2.4 The study of aldehyde dehydrogenases in rice

The different four organs of rice including young leaf, young root, stem and panicle were examined by quantitative RT-PCR to detect the expression of *ALDH* genes (Gao and Han, 2009). It has been indicated that the different ALDH family was found in the different organs. For instance, OsALDH2B2, OsALDH3B1 and OsALDH18B2 were mainly expressed in stem and panicle. OsALDH2C4, OsALDH10A5 and OsALDH10A8 were expressed at high levels in young root and panicle. OsALDH3E1 and OsALDH3H2 were highly expressed in young leaf and OsALDH3E2 was barely expressed in young root. These results indicated that the expression of duplicated *ALDH* genes showed high and distinct tissue specificities for their expression patterns (Gao and Han, 2009). The microarray data of expression profiles of *ALDH* genes also revealed that the multiple member *ALDH* genes families showed the different expression in diverse tissues (Gao and Han, 2009). For example, OsALDH2B5 was slightly expressed in stigma, shoot and root whereas OsALDH2B1 was expressed at high level in most tissues, especially in shoot. The expression of OsALDH3E1 can only be detected in shoot, OsALDH3B1 was highly expressed in stigma and ovary, and OsALDH3E2 was expressed at high level in several tissues. The expression of rice *ALDH* genes was regulated by abiotic stresses (Kotchoni and Bartels, 2003; Gao and Han, 2009). The ALDH proteins are also related to development and response to environmental changes for plant adaptation (Kotchoni and Bartels, 2003). The responses of rice *ALDH* genes to drought and high salinity stresses were examined (Gao and Han, 2009). The different *ALDH* genes were either down-regulated or up-regulated in the different stress condition. For instance, OsALDH2B5, OsALDH3H2, OsALDH7B6, OsALDH10A5 and OsALDH18B1 were up-regulated by both drought and high salinity stresses while OsALDH11A3 and OsALDH22A1 were highly down-regulated by drought stress. OsALDH5F1 and OsALDH12A1 were only induced by drought stress, while OsALDH18B2 was only up-regulated by high salinity stress (Gao and Han, 2009). It is noteworthy that the *ALDH* genes encoding OsBADH2 (OsALDH10A8) and P5CS (OsALDH18B1 and OsALDH18B2) involving in 2AP biosynthesis were highly up-regulated by either drought or high salinity stresses, indicating a possible role of them in rice plant adaptation. However, these rice *ALDH* genes play crucial roles for improving rice

Copyright by Kasetsart University All rights reserved

tolerance to abiotic stresses such as osmotic stress, dehydration and salt stress (Kotchoni and Bartels, 2003). ALDH also plays an important role in metabolism of acetaldehyde in rice under submerged condition and following re-aeration (Figure 22) (Tsuji *et al*., 2003). Under submerged conditions, the anaerobic condition, pyruvate that is produced from glycolysis can be converted to acetaldehyde by pyruvate decarboxylase (PDC). At the same time, acetaldehyde is converted to ethanol by alcohol dehydrogenase (ADH) called ethanolic fermentation and to acetate by ALDH. When the submerged plants are transferred to aerobic conditions (re-aeration), the accumulated ethanol is rapidly oxidized to acetaldehyde by the reverse reaction of ADH and the peroxidation of ethanol and H_2O_2 to acetaldehyde and H_2O by catalase (CAT). Then acetaldehyde is oxidized to acetate by ALDH in mitochondria.

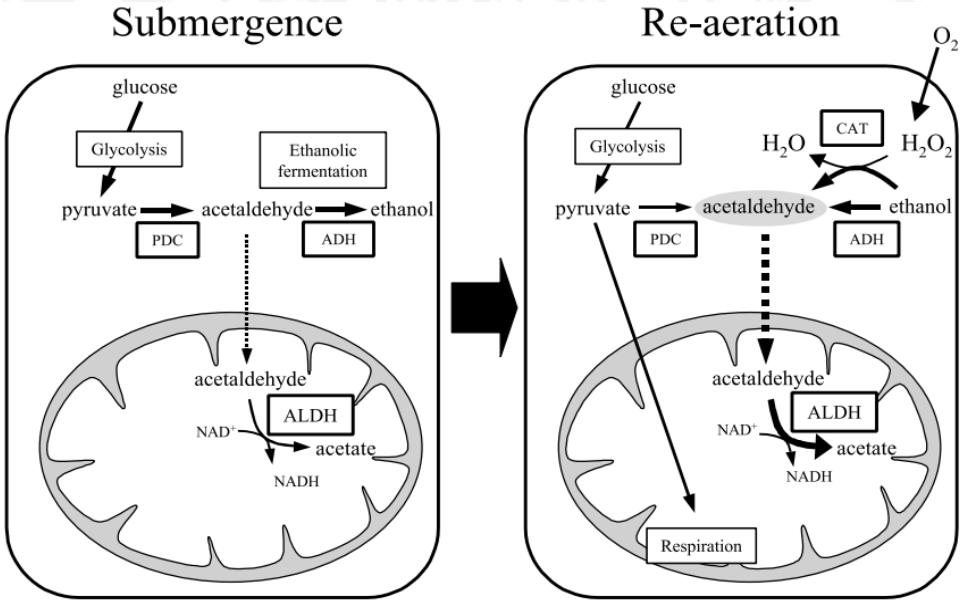

Figure 22 The pathway of acetaldehyde in rice under submerged conditions and following re-aeration.

Source: Tsuji *et al*. (2003)

Copyright by Kasetsart University All rights reserved

3. Betaine aldehyde dehydrogenase

Betaine aldehyde dehydrogenase (E.C. 1.2.1.8; BADH) is an important enzyme that catalyzes the last step in the synthesis of the osmoprotectant glycine betaine from choline (Figure 23) (Fitzgerald *et al*., 2009). Choline is converted into betaine aldehyde (Bet-ald) by choline monooxygenase (E.C. 1.14.15.7; CMO). In the second step, betaine aldehyde is converted into glycine betaine by BADH using NAD^+ as a cofactor (Weigel *et al*., 1986). Glycine betaine is a potent compatible solute produced by higher plants and bacteria under various abiotic stresses. Additionally, BADHs from various species have been studied and characterized such as in *Escherichia coli* (Boyd *et al*., 1991), *Pseudomonas aeruginosa* (Velasco-García *et al*., 1999), *Xanthomonas translucens* (Mori *et al*., 1992), barley (*Hordeum vulgare*) (Ishitani *et al*., 1995; Fujiwara *et al*., 2008) and rice (*Oryza sativa*) (Mitsuya *et al*., 2009). The reaction catalyzed by BADH involves in the choline catabolic pathway in bacteria that are able to grow in choline or choline precursors as their only carbon, nitrogen and energy sources such as the human pathogen *Pseudomonas aeruginosa* (González-Segura *et al*., 2009). The inhibition of this enzyme from *P. aeruginosa* (PaBADH) would not only block or diminish the choline catabolism but lead to the accumulation of betaine aldehyde which is a highly toxic to cell (Sage *et al*., 1997). Additionally, BADH can be considered as a suitable target for antibiotic drug design, which is the resistance for *P. aeruginosa* (González-Segura *et al*., 2009).

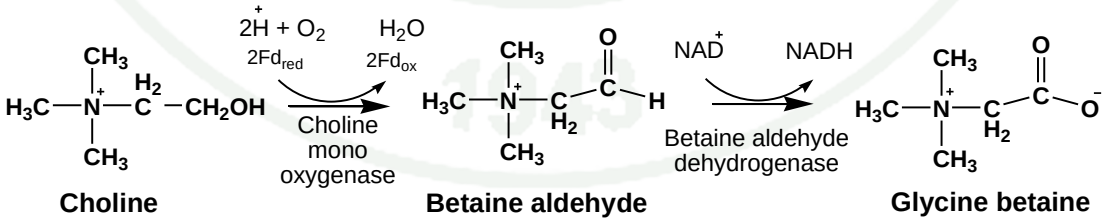

Figure 23 The pathway of the conversion of choline to glycine betaine

Source: Fitzgerald *et al*. (2009)

Copyright by Kasetsart University All rights reserved

3.1 Betaine aldehyde dehydrogenase in rice

Two BADH homologues have found in several plants such as barley (BBD1 and BBD2), *P. sativum* (PsAMADH1 and PsAMADH2) and rice (*O. sativa*) (OsBADH1 and OsBADH2). Two BADHs in barley have shown different expression pattern (Ishitani *et al*., 1995). The BBD1 transcript is mainly expressed in roots, while the BBD2 transcript is more abundant in leaves than roots. BBD1 and BBD2 are localized in peroxisome and cytosol, respectively (Ishitani *et al*., 1995). Rice also contains two expressing homologues of the *BADH* gene, namely *OsBADH1* and *OsBADH2* (Nakamura *et al*., 1997). *OsBADH1* and *OsBADH2* genes are encoded on chromosome four and chromosome eight, respectively (Bradbury *et al*., 2005) and shares 75% amino acid sequence identity. OsBADH1 and OsBADH2 belong to family 10 of the large family of aldehyde dehydrogenase (Sophos and Vasiliou, 2003; Gao and Han, 2009; Kotchoni *et al*., 2010). The deduced amino acid sequence of OsBADH1 and OsBADH2 contains serine-lysine-leucine (SKL) motif at the C-terminus, which is the consensus peroxisomal targeting sequence 1 in plants, animals, and yeasts (Wolins and Donaldson, 1997).

OsBADH1 can oxidize acetaldehyde in rice plant peroxisomes (Mitsuya *et al*., 2009). In comparison, OsBADH1 can catalyze the oxidation of acetaldehyde efficiently compared to OsBADH2. The subcellular localization of OsBADH1 protein has been monitored using GFP-OsBADH1. The result showed the localization of OsBADH1 into peroxisome. Thus, OsBADH1 possibly functions in oxidizing acetaldehyde, which is converted from ethanol by catalase (CAT) during the conversion of H_2O_2 to H_2O in peroxisome (Figure 24) (Mitsuya *et al*., 2009). For rice OsBADH2, it has been reported that the loss in function of this enzyme may be involved in the accumulation of 2AP (Bradbury *et al*., 2008).

Copyright by Kasetsart University All rights reserved

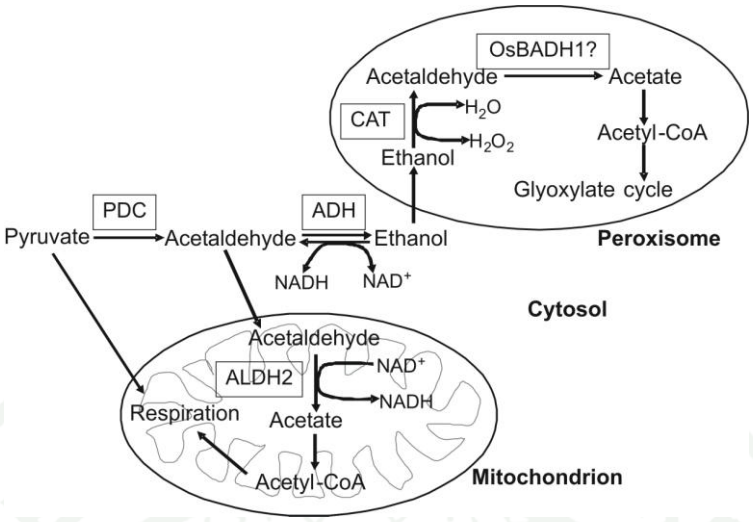

Figure 24 The oxidation of acetaldehyde in rice peroxisome

Source: Mitsuya *et al*. (2009)

3.2 Glycine betaine

Glycine betaine (GB), a quaternary ammonium compound, is an osmoprotectant and the compatible organic solute, protecting cellular components from dehydration injury. The compound produced by animals, microorganisms and plants raises the osmotic potential of the cytoplasm without disturbing metabolism or any toxic effect and stabilizes protein and membrane structure against denaturing effects of environmental stress such as high salinity, drought, UV radiation and extreme temperature (Ashraf and Foolad, 2007). The structures of osmoprotectant compounds in plants can be separated into three groups including amino acids (e.g. proline), onium compounds (e.g. glycine betaine, dimethylsulfoniopropionate), and polyols/sugars (e.g. mannitol, sorbitol, trehalose) (Figure 25) (Nuccio *et al*., 1999).

Copyright by Kasetsart University All rights reserved

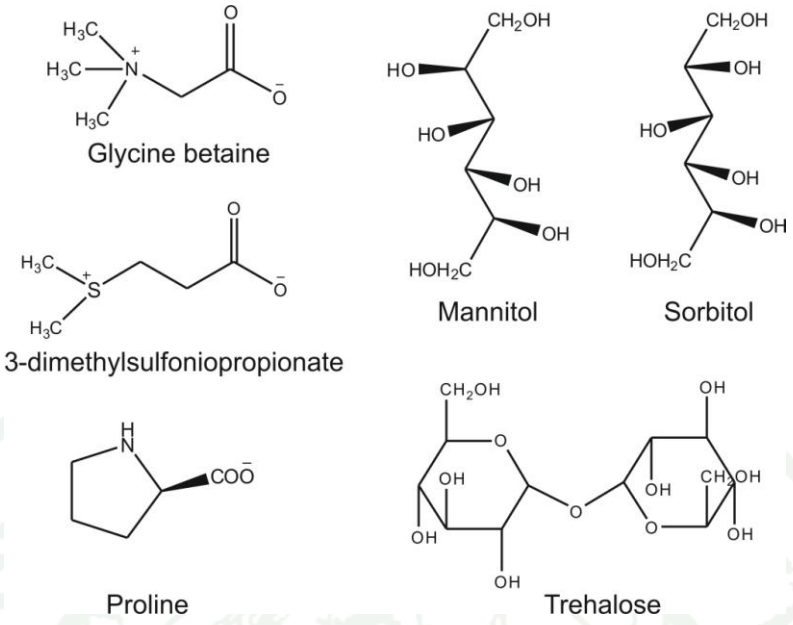

Figure 25 Structures of various osmoprotectants found in plants

Source: Nuccio *et al*. (1999)

Glycine betaine has three main functions: first the most effective osmoprotectant accumulated by both prokaryotic and eukaryotic organisms to manage with osmotic stress (Ashraf and Foolad, 2007); second a methyl donor for methionine synthesis (Muntz *et al*., 1950); and third a metabolic intermediate in the catabolism of choline and choline precursors in some bacteria such as the human pathogen *P. aeruginosa* (Velasco-García *et al*., 2006). In most organisms, the biosynthesis of glycine betaine is synthesized via the two-step oxidation of choline to betaine aldehyde (Figure 26) (Sakamoto and Murata, 2000). In higher plants, glycine betaine is synthesized via choline monooxygenase (CMO), a ferredoxin-dependent protein, and BADH. In mammalian cells and in organisms such as *E. coli*, glycine betaine is synthesized involving choline dehydrogenase (E.C. 1.1.99.1; CDH), a membrane-bound oxygen-dependent enzyme, and BADH. In soil bacterium *Arthrobacter globiformis*, glycine betaine is directly catalyzed from choline to glycine betaine by choline oxidase (E.C. 1.1.3.17; COD). Glycine betaine naturally accumulates in many crop plants such as sugar beet (*Beta vulgaris*), spinach (*Spinacia oleracea*), wheat (*Triticum aestivum*), and sorghum (*Sorghum bicolor*), which can be called "glycine

Copyright by Kasetsart University All rights reserved

betaine accumulator". However, some plant species, such as rice (*Oryza sativa*), mustard (*Brassica* spp.), arabidopsis (*Arabidopsis thaliana*) and tobacco (*Nicotiana tabacum*), naturally do not produce glycine betaine under stress or non-stress conditions. Therefore these plants are called "non glycine betaine accumulator" (Sakamoto and Murata, 2000; Ashraf and Foolad, 2007; Fitzgerald *et al*., 2009). Genes encoding BADH have been introduced to some non glycine betaine accumulator species for the production of glycine betaine to increased abiotic stress tolerance (Holmström *et al*., 1994). However, rice does not accumulate glycine betaine because it encodes non-functional choline monooxygenase (CMO) leading to the absence of Bet-ald (Fitzgerald *et al*., 2009). As the result, transgenic rice plants only showed increase in glycine betaine when exogenous Bet-ald was applied (Nakamura *et al*., 1997).

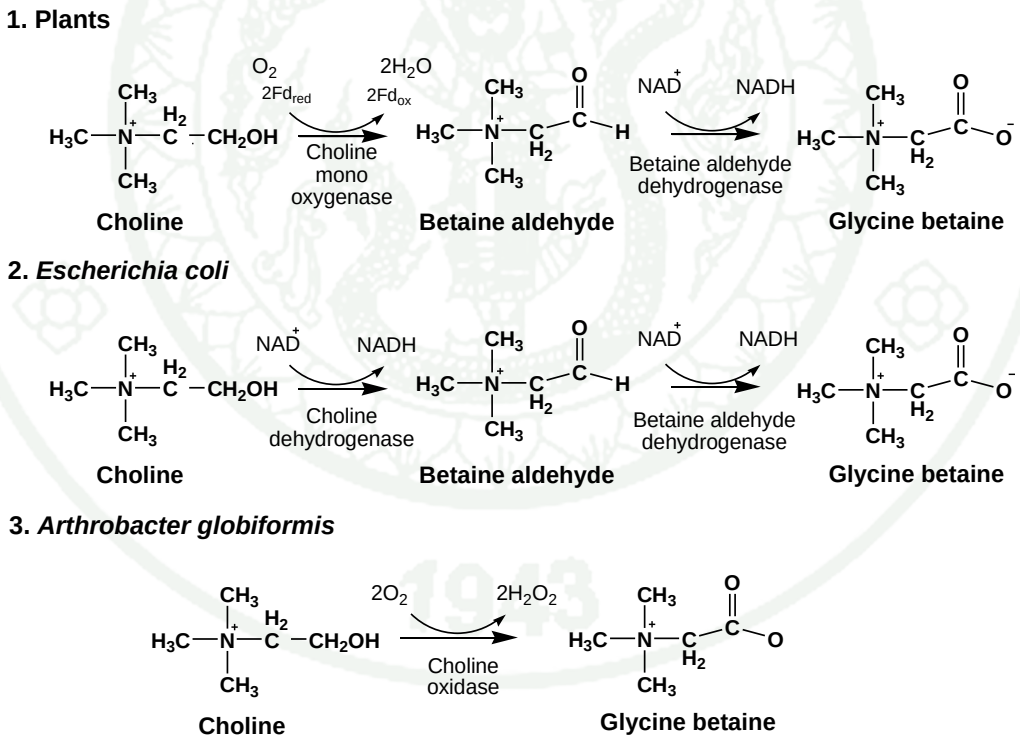

Figure 26 Pathway leading to the biosynthesis of glycine betaine in different species

Source: Sakamoto and Murata (2000)

Copyright by Kasetsart University All rights reserved

3.3 The structure of betaine aldehyde dehydrogenase

At the present, several crystal structures of BADH enzymes and two aminoaldehyde dehydrogenase (AMADH) (E.C. 1.2.1.19) enzymes from different species are available in Protein Data Bank (PDB). For instance, BADH from cod liver (codBADH) in apoenzyme form and complex with NAD^+ (PDB entries 1A4S and 1BPW, respectively) (Johansson *et al*., 1998), BADH from *E. coli* (eBADH) in apoenzyme form and complex with NADH and Bet-ald (PDB entries 1WND and 1WNB, respectively) (Gruez *et al*., 2004) and BADH from *P. aeruginosa* (PaBADH) in complex with $NADP^+$ and glycerol (PDB entry 2VE5) (González-Segura *et al*., 2009), and two AMADH isoforms from *P. sativum* (PsAMADH1 and PsAMADH2) in complex with NAD^+ and glycerol (PDB entries 3IWK and 3IWJ, respectively) (Tylichová *et al*., 2010). So far, the crystal structure of rice OsBADH2 has been solved at the lower resolution of 2.95 Å in the preliminary study (Kuaprasert *et al*., 2011). Most of the active form of BADH enzymes are tetrameric, except the plant AMADHs which are dimeric.

BADH subunits consist of the major three domains including substrate binding domain, oligomerization domain and coenzyme binding domain. The domain organization and the bound NAD^+ of the BADH monomer from cod liver is shown in Figure 27A (PDB entry 1BPW) (Johansson *et al*., 1998). Both coenzyme binding domain and substrate binding domain contain an α/β structure of a Rossmann type fold type like the other ALDH structures, while the oligomerization domain comprises the long extension of all β-strands at the C-terminus (Figure 27B). The N-terminal helix (α1 starts at residues 2-9) is unique for BADH and is not present in any of the other ALDH structures. The N-terminal helix is located at the surface and folded back onto the coenzyme binding domain. The central strand of the coenzyme binding domain (βA starts at residue 157-163) mainly forms a cap around the first mononucleotide binding unit of the domain (Johansson *et al*., 1998). The other side of βA is covered by long β-hairpin (β3 and β4 start at residues 37-53). The coenzyme binding domain has a similar fold as the central parts of the substrate binding domain containing five central strands (βA, βB, βC, βD and βE in coenzyme binding domain

Copyright by Kasetsart University All rights reserved

and βA′, βB′, βC′, βD′ and βE′ in substrate binding domain) and four helices (αB, αC, αD and αE in coenzyme binding domain and αB′, αC′, αD′ and αE′ in substrate binding domain). The substrate binding domain has a long insertion in the regular domain structure between βB′ and βC′ and contains long β-hairpin (β7, β8 and βC′) and long helices (αC′, α5, α6 and α7), together about 100 residues. These β-hairpins form most of the contact surface toward the coenzyme binding domain (Johansson *et al*., 1998).

Two connections between the coenzyme binding domain and the substrate binding domain are the one at residue 264-267 where the strand in the coenzyme binding domain (βE) continues until the strand of the substrate binding domain (βA′) starts, and the other at residues 456-471 where the last strand of the substrate binding domain (βE′) connects with the strand in the coenzyme binding domain (β9). The chain ends with the last strand at the C-terminus (β10 starts at residues 488-495) third component of the oligomerization domain. The subunits of BADH associate into dimers in which the last strand of the oligomerization domain (β10) is hydrogen bonded to the last strand of the substrate binding domain (βE′) in the second subunit leading to the formation of the ten-stranded pleated sheet (Johansson *et al*., 1998). The arrangement of the ten-stranded pleated sheet helps the domains to be tightly locked relative to each other. The coenzyme binding domain helix (αE) has numerous van der Waals interactions to each other in the dimer. The tetramer is formed by two dimers that interact back to back at the side opposite to where the coenzyme binds (Johansson *et al*., 1998).

Copyright by Kasetsart University All rights reserved

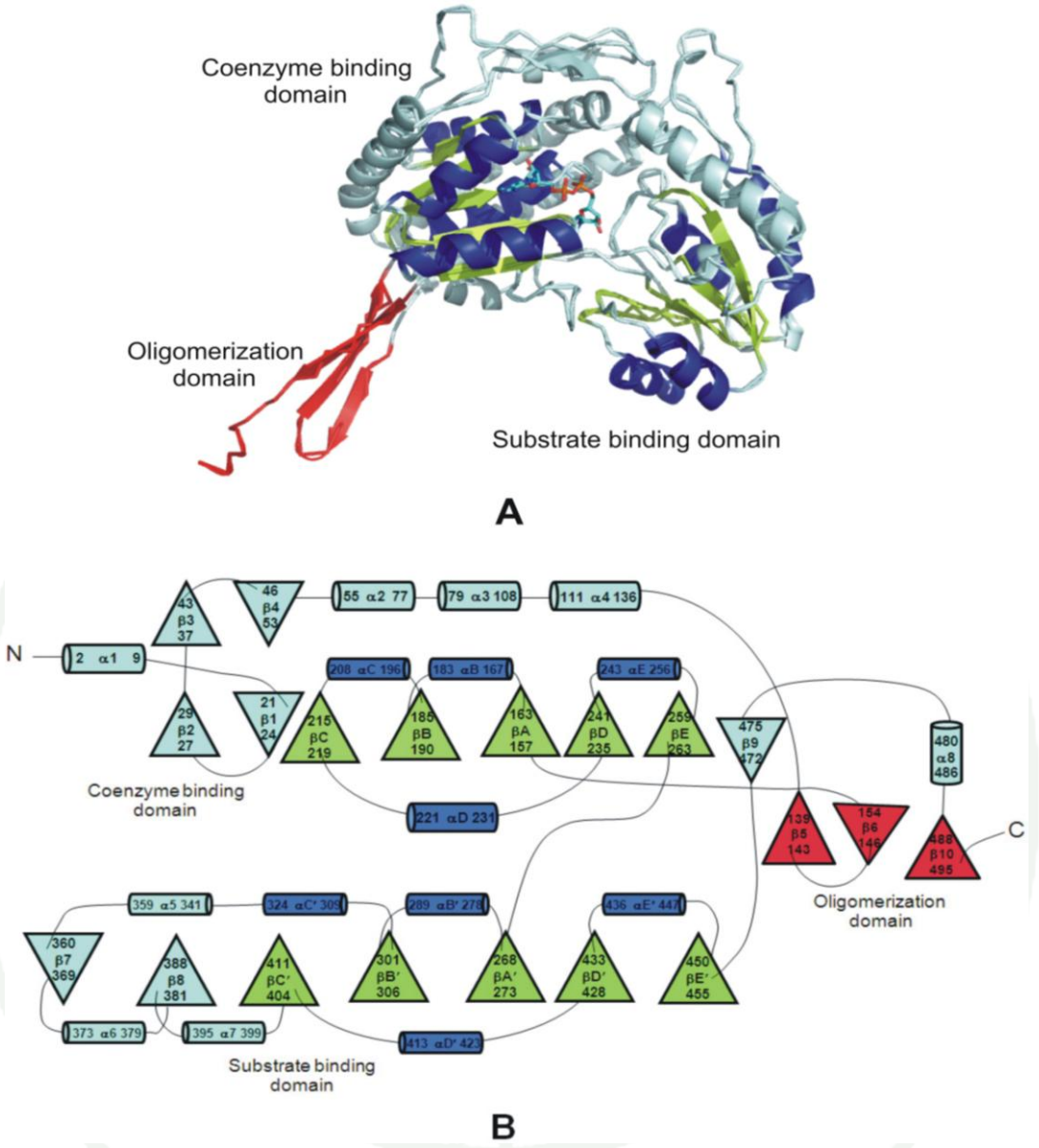

Figure 27 The structures of one monomer of BADH from cod liver. (A) The Rossmann type fold of BADH. (B) A topology diagram of an individual subunit of BADH. The α helices and β strands in Rossmann type fold are colored in blue and green, respectively whereas the remaining is colored in light blue. The oligomerization domain is colored in red and bound NAD^+ is shown in a ball and stick and colored by atoms (carbon, cyan).

Source: Johansson *et al*. (1998)

Copyright by Kasetsart University All rights reserved

3.4 Protein sequence alignment of OsBADHs and other BADHs

To identify the conserved regions and residues among OsBADHs and other BADHs, the amino acid sequence alignment among OsBADH1, OsBADH2, PsAMADH1 (PDB entry 3IWK), PsAMADH2 (PDB entry 3IWJ), human ALDH2, eBADH (PDB entry 1WNB) and codBADH (PDB entry 1A4S) are performed using ClustalW2 (Figure 28). According to Figure 28, the alignment of amino acid sequences of OsBADH1, OsBADH2, PsAMADH1, PsAMADH2, ALDH2, eBADH and codBADH displays some conserved regions among these BADHs. The identity and similarity of amino acid sequence are calculated using Discovery Studio 2.5 (Accelrys, Inc., CA, USA) (Table 6). The amino acid sequence of OsBADH1 and OsBADH2 shares 75.4 % for sequence identity and 89.5 % for sequence similarity.

Table 6 Amino acid sequence identity and similarity between OsBADHs and other BADHs

ALDH in other species	BADH in rice			
	OsBADH1		OsBADH2	
	% identity	% similarity	% identity	% similarity
PsAMADH1	71.5	85.9	71.6	86.9
PsAMADH2	73.7	87.7	76.5	88.9
ALDH2	43.1	61.6	43.1	61.6
eBADH	35.2	57.5	37.3	59.1
codBADH	37	59.1	36.9	59.6

The catalytic triad of BADH is conserved among various species such as N164, E262 and C296 in OsBADH1, N162, E260 and C294 in OsBADH2, N162, E260 and C294 in PsAMADH1, N162, E260 and C294 in PsAMADH2, N169, E268 and C302 in ALDH2, N166, E263 and C297 in codBADH and N149, E246 and C280 in eBADH.

Copyright by Kasetsart University All rights reserved

```
OsBADH1         -MAAPSAIPR---------RGLFIGGGWREPSLG--RRLPVVNPATEATIGDIPAATAED 48
OsBADH2         ---MATAIPQ---------RQLFVAGEWRAPALG--RRLPVVNPATESPIGEIPAGTAED 46
PsAMADH1        ---MAITVSS---------RQLFIDGEWRVPILN--KRIPNINPSTENIIGDIPAATKED 46
PsAMADH2        ---MDIPIPT---------RQLFINGDWKAPVLN--KRIPVINPATQNIIGDIPAATKED 46
ALDH2           SAAATQAVPAPNQQPEVFCNQIFINNEWHDAVSR--KTFPTVNPSTGEVICQVAEGDKED 58
codBADH         -AQLVDSMPSASTGSVVVTDDLNYWGGRRIKSKDGATTEPVFEPATGRVLCQMVPCGAEE 59
eBADH           ---MQH--------------KLLINGELVSGEGE---KQPVYNPATGDVLLEIAEASAEQ 40
                                     :   .            *  :*:*   : ::     *:

OsBADH1         VELAVSAARDAFGRDGGRHWSRAPGAVRAKYLKAIAAKIKDKKSYLALLETLDSGKP-LD 107
OsBADH2         VDAAVAAAREALKRNRGRDWARAPGAVRAKYLRAIAAKIIERKSELARLETLDCGKP-LD 105
PsAMADH1        VDLAVDAAKRAISRKNGRDWSAASGSLRARYLRAIAAKIKEKKDELGKLESIDCGKP-LE 105
PsAMADH2        VDVAVAAAKTALTRNKGADWATASGAVRARYLRAIAAKVTEKKPELAKLESIDCGKP-LD 105
ALDH2           VDKAVKAARAAFQ--LGSPWRRMDASHRGRLLNRLADLIERDRTYLAALETLDNGKPYVI 116
codBADH         VDQAVQSAQAAYLK-----WSKMAGIERSRVMLEAARIIRERRDNIAKLEVINNGKT-IT 113
eBADH           VDAAVRAADAAFA-----EWGQTTPKVRAECLLKLADVIEENGQVFAELESRNCGKPLHS 95
                *: ** :*  *        *       *.. :   *  :      :. **  : **.

OsBADH1         EAAGDMEDVAACFEYYADLAEALDGKQRAPISLPME-DFESYVLKEPIGVVGLITPWNYP 166
OsBADH2         EAAWDMDDVAGCFEYFADLAESLDKRQNAPVSLPME-NFKCYLRKEPIGVVGLITPWNYP 164
PsAMADH1        EALADLDDVVACFEYYAGLAEELDSKQKAPISLPMD-TFKSYILKEPIGVVALITPWNYP 164
PsAMADH2        EAAWDIDDVAGCFEYYADLAEKLDARQKAPVSLPMD-TFKSHVLREPIGVVGLITPWNYP 164
ALDH2           SYLVDLDMVLKCLRYYAGWADKYHGK-----TIPIDGDFFSYTRHEPVGVCGQIIPWNFP 171
codBADH         EAEYDIDAAWQCIEYYAGLAPTLSGQH---IQLPGG--AFAYTRREPLGVCAGILAWNYP 168
eBADH           AFNDEIPAIVDVFRFFAGAARCLNGLAAG--EYLEG--HTSMIRRDPLGVVASIAPWNYP 151
                    ::      :.::*. *                   .   ::*:** . * .**:*

OsBADH1         LLMATWKVAPALAAGCTAVLKPSELASLTCLELGGICAEIGLPPGVLNIITGLGTEAGAP 226
OsBADH2         LLMATWKVAPALAAGCTAVLKPSELASVTCLELADVCKEVGLPSGVLNIVTGLGSEAGAP 224
PsAMADH1        FLMATWKIAPALAAGCAAILKPSELASVTCLELGEICKEVGLPRGVLNIVTGLGHEAGAS 224
PsAMADH2        MLMATWKVAPALAAGCAAILKPSELASLTCLELGEICKEVGLPPGVLNILTGLGPEAGAP 224
ALDH2           LLMQAWKLGPALATGNVVVMKVAEQTPLTALYVANLIKEAGFPPGVVNIVPGFGPTAGAA 231
codBADH         FMIAAWKCAPALACGNAVVFKPSPMTPVTGVILAEIFHEAGVPVGLVNVVQG-GAETGSL 227
eBADH           LMMAAWKLAPALAAGNCVVLKPSEITPLTALKLAELAKDI-FPAGVVNILFGRGKTVGDP 210
                ::: :** .**** *  .::* :  :.:* : :. :  :  .* *::*:: * *  .*

OsBADH1         LASHPHVDKIAFTGSTETGKRIMITA-SQMVKPVSLELGGKSPLIVFDDVDIDKAVEWAM 285
OsBADH2         LSSHPGVDKVAFTGSYETGKKIMASA-APMVKPVSLELGGKSPIVVFDDVDVEKAVEWTL 283
PsAMADH1        LASHPDVDKISFTGSSATGSKIMTTA-AQLVKPVSLELGGKSPIVVFEDVDLDKVAEWTV 283
PsAMADH2        LATHPDVDKVAFTGSSATGSKIMTAA-AQLVKPVSLELGGKSPLVVFEDVDLDKAAEWAI 283
ALDH2           IASHEDVDKVAFTGSTEIGRVIQVAAGSSNLKRVTLELGGKSPNIIMSDADMDWAVEQAH 291
codBADH         LCHHPNVAKVSFTGSVPTGKKVMEMS-AKTVKHVTLELGGKSPLLIFKDCELENAVRGAL 286
eBADH           LTGHPKVRMVSLTGSIATGEHIISHT-ASSIKRTHMELGGKAPVIVFDDADIEAVVEGVR 269
                :  *  *  :::***   *  :   : :  :* . :*****:* :::.* ::: ... .

OsBADH1         FGCFANAGQVCSATSRLLLHEKIAKRFLDRLVAWAKSIKISDPLEEGCRLGSVVSEGQYQ 345
OsBADH2         FGCFWTNGQICSATSRLILHKKIAKEFQERMVAWAKNIKVSDPLEEGCRLGPVVSEGQYE 343
PsAMADH1        FGCFFTNGQICSATSRLIVHESIAVEFVDKLVKWAENIKISDPLEEGCRLGPIVSEAQYK 343
PsAMADH2        FGCFWTNGQICSATSRLILHESIATEFLNRIVKWIKNIKISDPLEEGCRLGPVVSEGQYE 343
ALDH2           FALFFNQGQCCCAGSRTFVQEDIYDEFVERSVARAKSRVVGNPFDSKTEQGPQVDETQFK 351
codBADH         MANFLTQGQVCTNGTRVFVQREIMPQFLEEVVKRTKAIVVGDPLLTETRMGGLISKPQLD 346
eBADH           TFGYYNAGQDCTAACRIYAQKGIYDTLVEKLGAAVATLKSGAPDDESTELGPLSSLAHLE 329
                   : . ** *    *   :. *   : :.          . *     . *   .  : .

OsBADH1         KIMKFISTARCEG-ATILYGGARP----QHLKRGFFIEPTIITNVSTSMQIWREEVFGPV 400
OsBADH2         KIKQFVSTAKSQG-ATILTGGVRP----KHLEKGFYIEPTIITDVDTSMQIWREEVFGPV 398
PsAMADH1        KVLNCISSAKSEG-ATILTGGRRP----EHLKKGYFVEPTIITDVTTSMQIWREEVFGPV 398
PsAMADH2        KILKFVSNAKSEG-ATILTGGSRP----EHLKKGFFIEPTIITDVTTNMQIWREEVFGPV 398
ALDH2           KILGYINTGKQEG-AKLLCGGG------IAADRGYFIQPTVFGDVQDGMTIAKEEIFGPV 404
codBADH         KVLGFVAQAKKEG-ARVLCGGEPLTPSDPKLKNGYFMSPCVLDNCRDDMTCVKEEIFGPV 405
eBADH           RVGKAVEEAKATGHIKVITGGEKR------KGNGYYYAPTLLAGALQDDAIVQKEVFGPV 383
                ::   :  .:  *   :: **           .*::  * :: .   .    ::*:****

OsBADH1         ICVKEFRTEREAVELANDTHYGLAGAVISNDLERCERISKAIQSGIVWINCSQPCFVQAP 460
OsBADH2         LCVKEFSTEEEAIELANDTHYGLAGAVLSGDRERCQRLTEEIDAGIIWVNCSQPCFCQAP 458
PsAMADH1        LAVKTFSTEEEAINLANDTHYGLGSAVMSNDLERCERLSKALQAGIVWINCAQPSFIQAP 458
PsAMADH2        LCVKTFSTEEEAIDLANDTVYGLGAAVISNDLERCERVTKAFKAGIVWVNCSQPCFTQAP 458
ALDH2           MQILKFKTIEEVVGRANNSTYGLAAAVFTKDLDKANYLSQALQAGTVWVNCYDVFGAQSP 464
codBADH         MSVLPFDTEEEVLQRANNTTFGLASGVFTRDISRAHRVAANLEAGTCYINTYSISPVEVP 465
eBADH           VSVTPFDNEEQVVNWANDSQYGLASSVWTKDVGRAHRVSARLQYGCTWVNTHFMLVSEMP 443
                : :  * . .:.:  **:: :**...* : *  :.. ::  :. *  ::*       : *
```

Copyright by Kasetsart University All rights reserved

```
OsBADH1          WGGNKRSGFGRELGQWGLDNYLSVKQVTKYCSDEPYGWYRPPSKL 505
OsBADH2          WGGNKRSGFGRELGEGGIDNYLSVKQVTEYASDEPWGWYKSPSKL 503
PsAMADH1         WGGIKRSGFGRELGEWGLENYLSVKQVTRYTSDEPWGWYQPPSKL 503
PsAMADH2         WGGVKRSGFGRELGEWGLDNYLSVKQVTQYISEEPWGWYQPPAKL 503
ALDH2            FGGYKMSGSGRELGEYGLQAYTEVKTVTVKVPQKNS--------- 500
codBADH          FGGYKMSGFGRENGQATVDYYSQLKTVIVEMGDVDSLF------- 503
eBADH            HGGQKLSGYGKDMSLYGLEDYTVVRHVMVKH-------------- 474
                  ** * ** *:: .   :: *  :: *
```

Figure 28 Amino acid sequence alignment of OsBADHs and other BADHs using ClustalW2. The underlined and bold letters represent the catalytic triad residues.

3.5 Substrate channel and substrate specificity of BADH

The amino acid sequence alignment revealed the highest sequence identity and similarity between OsBADHs and PsAMADHs compared to the others. Since both OsBADHs and PsAMADHs have found in plants while the others in different species. The structural analysis of PsAMADH1 (PDB entry 3IWK) revealed that the substrate channel is formed by residues A109 (W109 in PsAMADH2), D113, P452 and S453 (C453 in PsAMADH2) whereas the interior is formed by D110, N162, Y163, L166, M167, W170, E260, F284, F288 (W288 in PsAMADH2), I293, C294, S295, Q451 and W459 (Figure 29) (Tylichová *et al*., 2010; Kopečný *et al*., 2011). The PsAMADH1 structure contains bound NAD^+ and glycerol molecule (GOL). A glycerol molecule close to the catalytic cysteine mimics a substrate bound to the substrate binding site. The bound glycerol is surrounded by N162, Y163, W170, I293, C294, S295, S453 and W459 (Tylichová *et al*., 2010). Its O1 atom interacts with the main-chain NH of the catalytic C294 and the side chain ND2 of the catalytic N162 in PsAMADH1. Both carboxylate and aromatic residues at the entrance to the substrate channel are typically found in all plant BADHs, and almost all of the residues are highly conserved except for F288 (W288 in PsAMADH2), A109 (W109 in PsAMADH2) and S453 (C453 in PsAMADH2) (Kopečný *et al*., 2011).

Copyright by Kasetsart University All rights reserved

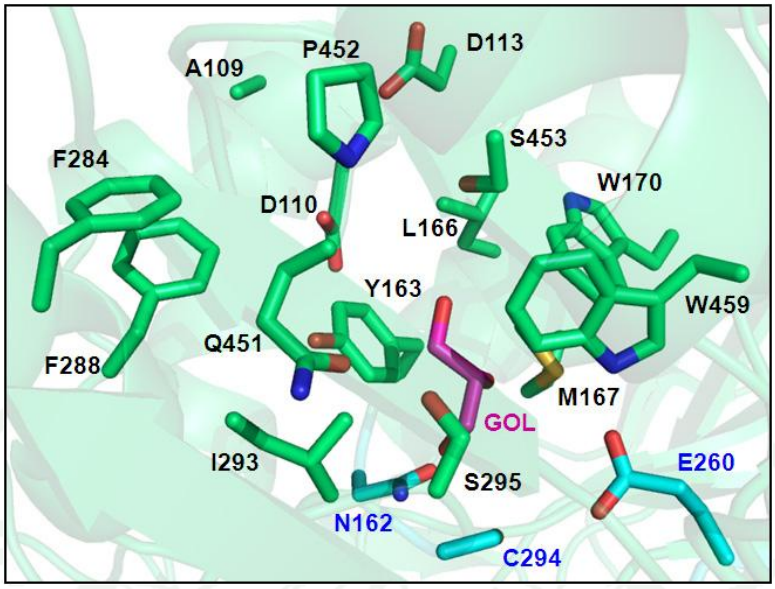

Figure 29 The substrate channel of PsAMADH1. The amino acid side chains around substrate channel are depicted in stick representation and colored by atoms (carbon, green lime). The catalytic triad is depicted in stick representation and colored by atoms (carbon, cyan). The glycerol molecule is shown in stick and colored by atoms (carbon, magenta).

The channel of PsAMADH1 is 14 Å in depth and about 5-8 Å in width from the entrance to the substrate channel (Tylichová *et al*., 2010) while the channel of eBADH is around 12 Å in depth and ~5-8 Å in width (Gruez *et al*., 2004). The cavity volume of PsAMADH1 is larger than the volume of betaine and can accommodate bulkier substrates such as valeraldehyde (C5), which is medium chain aldehyde (Gruez *et al*., 2004; Tylichová *et al*., 2010). On the other hand, the size of the binding site of eBADH is a rather narrow channel that is sufficient to accommodate molecules larger than Bet-ald such as n-alkyl aldehyde up to seven carbon atoms (Gruez *et al*., 2004). Regarding to the substrate specificity, BADHs from several species have been characterized with various aldehyde substrates such as C1-C11 n-alkyl aldehydes, branched n-alkyl aldehydes, aromatic aldehydes, ω-aminoaldehydes and trimethyl aminoaldehydes (Figure 30) (Gruez *et al*., 2004; Bradbury *et al*., 2008; Mitsuya *et al*., 2009; Tylichová *et al*., 2010; Kopečný *et al*., 2011).

Copyright by Kasetsart University All rights reserved

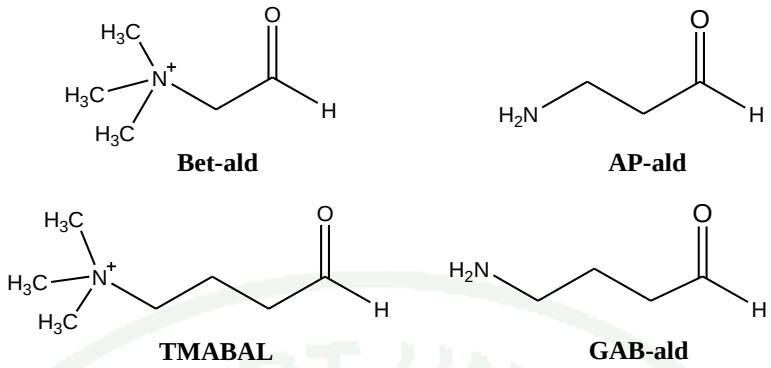

Figure 30 The structures of the basic aldehydes. Abbreviations used: Bet-ald, betaine aldehyde; AP-ald, 3-aminopropionaldehyde; GAB-ald, 4-aminobutyraldehyde; TMABAL, *N*,*N*,*N*-trimethyl-4-aminobutylraldehyde.

BADHs can oxidize a broad range aldehyde substrate better than betaine aldehyde, especially medium chain aldehyde such as AP-ald and GAB-ald which are ω-aminoaldehyde (Gruez *et al*., 2004; Bradbury *et al*., 2008; Mitsuya *et al*., 2009; Tylichová *et al*., 2010; Kopečný *et al*., 2011). The aromatic aldehydes, such as benzaldehyde and phenylacetaldehyde, are also less reactive and poor substrates whereas the branched n-alkyl aldehydes, iso-valeraldehyde, react slightly less than n-alkyl aldehydes, valeraldehyde (Gruez *et al*., 2004; Tylichová *et al*., 2010). Moreover, ω-aminoaldehydes are intermediates in the oxidation of polyamines such as Spermine (Spm), Spermidine (Spd) and Putrescine (Put), which are oxidized by diamine oxidase (E.C. 1.4.3.6, DAO) and polyamine oxidase (E.C. 1.5.3.3, PAO) (Moschou *et al*., 2008). Plant polyamines play important roles in plant growth, development, cell division and differentiation as well as adaptation to abiotic stress (Moschou *et al*., 2008).

Plant BADH enzymes can be classified into two subfamilies depending on their specificity. “True BADH” has Bet-ald as a substrate while “high BADH homology aminoaldehyde dehydrogenase (HBH-AMADH)” shows broader affinity for a range of aminoaldehyde substrates (Fitzgerald *et al*., 2009). Recently, rice BADHs have been classified as HBH-AMADH since they show only moderate to low activity on Bet-ald while strong activity on aminoaldehydes (Bradbury *et al*., 2008). Aminoaldehyde dehydrogenase (E.C. 1.2.1.19, AMADH) from *P. sativum*

Copyright by Kasetsart University All rights reserved

(PsAMADH1 and PsAMADH2) is an example of plant AMADH that catalyzes ω-aminoaldehydes to the corresponding ω-amino acids and shows broad aminoaldehydes substrate specificity (Šebela *et al*., 2000; Tylichová *et al*., 2010; Kopečný *et al*., 2011). BADH also oxidizes a wide range of ω-aminoaldehyde substrates in addition to its substrate, Bet-ald (Fujiwara *et al*., 2008; Bradbury *et al*., 2008; Mitsuya *et al*., 2009). Therefore, BADH can also be considered as AMADH (Fitzgerald *et al*., 2009). Since OsBADH1 and OsBADH2 are very similar in amino acid sequence but their function is likely to be different. Therefore, it is of our interest to elucidate and understand the substrate specificity of both OsBADHs. The catalytic asparagines, N164 of OsBADH1 and N162 of OsBADH2, and tryptophan residues, W172 of OsBADH1 and W170 of OsBADH2 (N162 and W170 of PsAMADH2), are considered in our study in term of substrate specificity. The asparagine involves in the stabilization of intermediate important for enzyme catalysis while tryptophan involves in the substrate recognition. It has been proposed that an entering substrate has a π-electron stacking interaction with surrounding aromatic residues (Y163, W170 (PsAMADH2 numbering)) (Kopečný *et al*., 2011). Both highly conserved aromatic residues constitute the middle section of the substrate channel and are only 3.5 Å apart from C3 and C4 atoms of the substrate when it binds in the active site (Kopečný *et al*., 2011).

4. Calculation of binding free energy

Recently, the computational chemistry has become a powerful method to study the function of proteins due to its ability to estimate energies of reactions in proteins such as activation, reaction and conformational energies (Kaukonen *et al*., 2008). The widely popular computational methods that combine molecular mechanics (MM) energy and implicit solvation models are Molecular Mechanics/Poisson Boltzmann Surface Area (MM/PBSA) and Molecular Mechanics/Generalized Born Surface Area (MM/GBSA) (Hou *et al*., 2011). In the MM/PBSA and MM/GBSA theory, the binding free energy ($\Delta G_{binding}$) of molecule is made up from the gas phase energy and the solvation free energy. The binding free energy ($\Delta G_{binding}$) between receptor and ligand to form a complex is calculated according to the thermodynamic

Copyright by Kasetsart University All rights reserved

cycle of complex formation (Figure 31) (Wang *et al*., 2006) with equations 1-7 (Figure 32) (Wang *et al*., 2006; Hou *et al*., 2011)

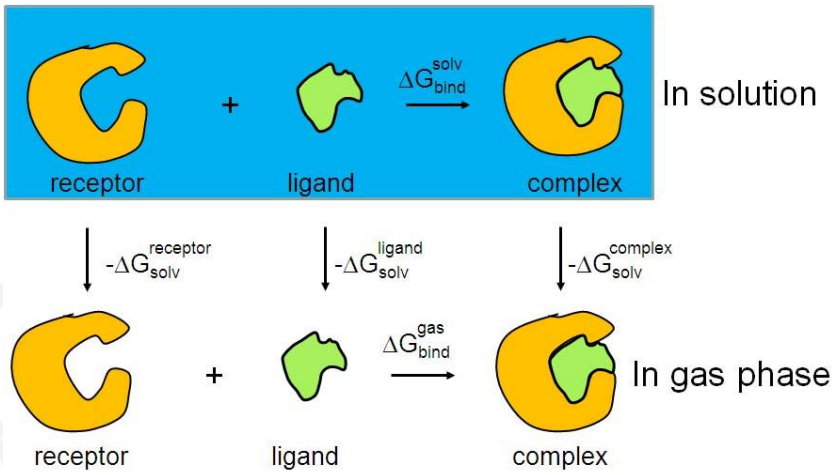

Figure 31 Thermodynamic cycle of a complex formation

Source: Wang *et al*. (2006)

$$\Delta G_{bind}^{solv} = \Delta G_{MM/PBSA,MM/GBSA} \quad (1)$$

$$\Delta G_{MM/PBSA,MM/GBSA} = \Delta H - T\Delta S \approx \Delta E_{gas} + \Delta G_{solv} - T\Delta S \quad (2)$$

$$\Delta E_{gas} = \Delta E_{vdw} + \Delta E_{ele} + \Delta E_{int} \quad (3)$$

$$\Delta G_{solv} = \Delta G_{PBSA/GBSA} = \Delta G_{PB/GB} + \Delta G_{SA} \quad (4)$$

$$\Delta\Delta G_{PB/GB} = \Delta G_{PB/GB}^{complex} - (\Delta G_{PB/GB}^{receptor} + \Delta G_{PB/GB}^{ligand}) \quad (5)$$

$$\Delta\Delta G_{SA} = \Delta G_{SA}^{complex} - (\Delta G_{SA}^{receptor} + \Delta G_{SA}^{ligand}) \quad (6)$$

$$\Delta\Delta G_{MM/PBSA,MM/GBSA} = \Delta G^{complex} - (\Delta G^{receptor} + \Delta G^{ligand}) \quad (7)$$

Figure 32 Equations for calculation of binding free energy

Source: Wang *et al*. (2006) and Hou *et al*. (2011)

Both $\Delta G_{MM/PBSA}$ and $\Delta G_{MM/GBSA}$ are the binding free energy in solution phase (ΔG_{solv}) (equation 1). $\Delta G_{MM/PBSA}$ and $\Delta G_{MM/GBSA}$ can calculate the relative free

Copyright by Kasetsart University All rights reserved

energy of molecule with equation 2 in combination of the gas phase energy (ΔE_{gas}) and the solvation free energy (ΔG_{solv}). ΔE_{gas} is calculated with equation 3 whereas ΔE_{vdw} and ΔE_{ele} are the van der Waals and the electrostatic interaction energies in gas phase, respectively. ΔE_{int} (bond, angle and dihedral energies) is typically neglected with an assumption that the intra-molecular energies of the receptor and ligand do not change upon binding (Wang *et al*., 2006). The solvation free energy (ΔG_{solv}) of a molecule is consisted of two parts, the electrostatic interaction energy (polarization energy), $\Delta G_{PB/GB}$, and the non-electrostatic component (non-polar energy), ΔG_{SA} (equation 4). The polarization energy is calculated with either a GB or PB model, whereas the non-polar energy is estimated by solvent accessible surface area (SAS) (Wang *et al*., 2006; Kaukonen *et al*., 2008). The equation 5, 6 and 7, are calculated from the difference in the binding free energy in $\Delta G_{PB/GB}$, ΔG_{SA} and $\Delta G_{MM/PBSA,MM/GBSA}$, respectively, between the complex, receptor and ligand.

Copyright by Kasetsart University All rights reserved

MATERIALS AND METHODS

Materials

1. *Escherichia coli* strains and plasmids

Escherichia coli strain XL-10 Gold was used as a bacterial cloning site-directed mutagenesis host, whereas strain BL21 (DE3) was used as a host for expressing OsBADHs wild-type and mutants. The plasmids pET28b containing *OsBADH1* and *OsBADH2*, were previously constructed as described in previous study (Wongpanya *et al*., 2011).

2. Media

2.1 LB Medium: 1% tryptone, 0.5% yeast extract and 0.5% NaCl. The pH of the solution was adjusted to 7.0 with NaOH.

2.2 LB agar plate: 1% tryptone, 0.5% yeast extract 0.5% NaCl and 2% agar. The pH of the solution was adjusted to 7.0 with NaOH.

3. Antibiotics

Kanamycin: stock solution (10 mg/ml) was prepared in milliQ water, filter sterilized and then stored at -20 ºC. Working concentration is at 50 µg/ml.

4. Chemical reagents

Table 7 Chemical reagents that used for this work

Reagent	Manufacturer, Country
β – mercaptoethanol (β-ME)	Acrōs Organic, USA
γ-Aminobutyraldehyde dimethyl acetal	Sigma, USA

Copyright by Kasetsart University All rights reserved

Table 7 (Continued)

Reagent	Manufacturer, Country
Acrylamide	Amersham Biosciences, Sweden
Agarose	ISCBioExpress, USA
Ammonium persulfate	USB, USA
Betaine aldehyde chloride (Bet-ald)	Sigma, USA
Boric acid	USB, USA
Calcium chloride	Univar, USA
Coomassie brilliant blue R-250	Bio Basic, Canada
EDTA	Bio Basic, Canada
Ethanol	Merck, Germany
Ethidium bromide	Bio Basic, Canada
GeneRuler 1kb DNA ladder	Fermentas, USA
Glycine	Amersham Biosciences, Sweden
HEPES	Acrōs Organic, USA
Imidazole	Fluka, Switzerland
IPTG	Sigma, USA
Methanol	Merck, Germany
NAD^+	Merck, Germany
PMSF	Thermo Scientific, USA
PageRuler prestained protein ladder	Fermentas, USA
Sodium chloride	Univar, USA
SDS	USB, USA
TEMED	USB, USA
Triton X-100	USB, USA
Tryptone Type – 1	Himedia, India
Yeast extract powder	Himedia, India

Copyright by Kasetsart University All rights reserved

5. Analytical equipments

Analytical equipments used in this research were listed in Table 8, along with their manufacturer.

Table 8 List of analytical equipments

Equipment	Manufacturer, Country
Fluorescence luminescence spectrometer	Perkin Elmer, USA
Fast protein liquid chromatography	GE Healthcare, Sweden
Gel documantation	DNr Bio-Imaging system, Israel
Hitrap Chelating HP column	GE Healthcare, Sweden
Microplate reader	Tecan, Switzerland
Nano Drop Spectrophotometer ND-100	Thermo Scientific, USA
Thermal Cycler	LabX, USA
UV-vis spectrophotometer	Shimazu, Japan

6. Computer resources and the software

The information regarding the crystal structure of OsBADH2 was obtained from Assist. Prof. Dr. Kiattawee Choowongkomon (Department of Biochemistry, Kasetsart University, Thailand) (Kuaprasert *et al*., 2011). The structure of Bet-ald was extracted from the crystal structure of *YdcW* gene in *E. coli* (PDB entry 1WNB) (Gruez *et al*., 2004), whereas the structure of GAB-ald was created by Discovery Studio 2.5 (Accelrys, Inc., CA, USA). The program for preparation of the protein and ligand was Discovery Studio 2.5 in which the water molecules were removed and hydrogen molecules were added prior to the interaction study. The AutoDock 4.0 and AMBER 10 simulations package were used for the docking and the energy minimization of the complexes. The simulations based on UNIX system (SUSE 10.3) were performed with Quad Core, 2.4 GHz processor and the results from the simulations were viewed and analyzed by VMD - Visual Molecular Dynamics, Swiss-PDB Viewer 4.0, Discovery Studio 2.5 and PyMol (Delano, 2002).

Copyright by Kasetsart University All rights reserved

Methods

1. Site-directed mutagenesis of OsBADH1 and OsBADH2

Mutations in the wild-type *OsBADH1* and *OsBADH2* gene were generated using site-directed mutagenesis which was used to make a point mutation. The mutants were N164A, W172A and W172F of OsBADH1 and N162A, W170A and W170F of OsBADH2. The mutagenic primers were designed by Quikchange® Primer Design Program from Stratagene (USA). The sense and antisense primers were purchased from Pacific Science (USA). All primer sequences were shown in Table 9. The appropriate length of each primer is 25-45 nucleotides, with a melting temperature (T_m) of ≥78 °C. The primers have the desired mutation in the middle of each primer with 10-15 bases of correct sequence on both sides. The mutagenic primers have a minimum GC content of 40% and terminate with one or more C or G base. Polymerase chain reaction (PCR) was performed using QuikChange® Lightning Site-Directed Mutagenesis kit (Stratagene, USA) according to the manufacturer's instruction. The reaction mixtures contained 1x reaction buffer, 100 ng of dsDNA template, 125 ng of each oligonucleotide sense and antisense primer, 1 µl of dNTP mix, 1.5 µl of QuikSolution reagent, 1 µl of QuikChange Lightning enzyme and milliQ water to final volume 50 µl. The PCR condition was shown in Table 10. After PCR cycle, 2 µl of *Dpn*I (target sequence: 5′-Gm6ATC-3′) was added to digest parental DNA template and the reaction was incubated at 37 °C for 30 min. Finally, the *Dpn*I-treated DNA was analyzed on 0.8% agarose gel.

Table 9 Primer sequences for site-directed mutagenesis. Bold and underlined sequences show corresponding triplets and mutated codon, respectively.

Set of primer	Sequence 5′-3′
N164A	
Sense	GGA CTT ATC ACT CCC TGG **GCT** TAT CCT CTG ATG GC
Antisense	GCC ATC AGA GGA TA**A** **GC**C CAG GGA GTG ATA AGT CC

Copyright by Kasetsart University All rights reserved

Table 9 (Continued)

Set of primer	Sequence 5′-3′
W172A	
Sense	TCT GCT GAT GGC TAC T**GC G**AA GGT TGC ACC TGC C
Antisense	GGC AGG TGC AAC CTT **C**GC AGT AGC CAT CAG CAG A
W172F	
Sense	CCT CTG CTG ATG GCT ACT **TTC** AAG GTT GCA CCT GC
Antisense	GCA GGT GCA ACC TT**G AA**A GTA GCC ATC AGC AGA GG
N162A	
Sense	GGT TGA TCA CAC CTT GG**G C**CT ATC CTC TCC TGA TGG C
Antisense	GCC ATC AGG AGA GGA TA**G GC**C CAA GGT GTG ATC AAC C
W170A	
Sense	TCT CCT GAT GGC AAC A**GC G**AA GGT AGC TCC TGC C
Antisense	GGC AGG AGC TAC CTT **C**GC TGT TGC CAT CAG GAG A
W170F	
Sense	CCT CTC CTG ATG GCA ACA **TTC** AAG GTA GCT CCT GC
Antisense	GCA GGA GCT ACC TT**G AA**T GTT GCC ATC AGG AGA GG

Table 10 PCR condition for site-directed mutagenesis

Segment	Temperature	Time	Cycle
Pre-denaturation	95 °C	2 min	1
Denaturation	95 °C	20 sec	18
Annealing	60 °C	10 sec	
Extension	68 °C	3.5 min (30 sec / 1 kb)	
Final extension	68 °C	5 min	1

2. Agarose gel electrophoresis

Agarose gel electrophoresis was used for separation of DNA fragment. The GeneRuler 1kb DNA ladder (Fermentas, USA) was used as a standard marker. Afterward, the DNA samples were mixed with 6x loading dye and then loaded into

Copyright by Kasetsart University All rights reserved

0.8 % agarose gel in 1x TBE buffer. The gel was run at 150 volts for 20 min, until the dye front migrated to the end of the gel. Subsequently, the gel was stained with ethidium bromide and washed with water before visualized under UV light and photographed using gel documentation.

3. Transformation of mutated plasmids into XL10-Gold ultracompetent cells

XL10-Gold ultracompetent cells were gently thawed on ice**.** After that, 2 µl of XL10-Gold β-mercaptoethanol mix (β-ME) was added into XL10-Gold ultracompetent cells and the cells were incubated on ice for 2 min. Subsequently, 10 µl of *Dpn*I-treated DNA was added into 45 µl of competent cells and the cells were incubated on ice for 30 min. After incubation, the cells were transferred to a heating block at 42 °C for 90 sec and then immediately put on ice for 2 min. The transformed cells were mixed with 800 µl of fresh LB and incubated with shaking at 220 rpm for 45 min at 37 °C. After incubation, the cells were harvested by centrifugation at 4,000 rpm for 5 min and supernatant was discarded. The cell pellet was resuspened in 200 µl of LB and spread on LB plate containing kanamycin and incubated at 37 °C for 16 hours. After transformation, the mutated plasmids were verified using restriction enzyme analysis, colony PCR screening and DNA sequencing.

4. Colony PCR screening of mutated plasmids

PCR screening was used to identify the desired mutation of *OsBADH1* and *OsBADH2*. A single colony of mutated plasmid was used as a template. The reaction mixtures were prepared containing 1x reaction buffer, 0.5 µM of each screening primer and reverse primer (as shown in Table 11), 0.2 mM of dNTP mix, 2 mM $MgCl_2$, 2.5 U *Taq* DNA polymerase (Fermentas, USA) and milliQ water to final volume 25 µl. The PCR condition was shown in Table 12. Afterward, the PCR screening products were visualized using 0.8% agarose gel electrophoresis and photographed by gel documentation.

Copyright by Kasetsart University All rights reserved

Table 11 Primer sequences for screening the mutant plasmid. The underlined represent the mutated codon. The bold letters represent the restriction site.

Set of primer	Sequence 5′-3′
Screening N164A OsBADH1	GGA CTT ATC ACT CCC TGG GC
Screening W172A OsBADH1	TCT GCT GAT GGC TAC TGC
Screening W172F OsBADH1	CCT CTG CTG ATG GCT ACT TTC
*Xho*I –Reverse OsBADH1	CCG **CTC GAG** CTA CAG CTT GGA TGG AGG C
Screening N162A OsBADH2	GGT TGA TCA CAC CTT GGG C
Screening W170A OsBADH2	TCT CCT GAT GGC AAC AGC
Screening W170F OsBADH2	CCT CTC CTG ATG GCA ACA TTC
*Xho*I –Reverse OsBADH2	CCG **CTC GAG** TTA CAG CTT GGA AGG GGA TT

Table 12 PCR condition for colony PCR screening of mutant plasmid

Segment	Temperature	Time	Cycle
Pre-denaturation	95 °C	5 min	1
Denaturation	95 °C	1 min	30
Annealing	50 °C	30 sec	
Extension	72 °C	1 min	
Final extension	72 °C	10 min	1

5. Plasmid extraction by GeneJET Plasmid Miniprep kit

A single colony of *E. coli* containing mutated plasmids which presented the corrected size from the colony PCR screening was inoculated into 5 ml LB broth containing kanamycin. The cultures were grown with shaking at 220 rpm at 37 °C for 16 hours. After 16 hours incubation, the cultures were centrifuged at 5,000 rpm in a benchtop centrifuge. Then, the plasmid DNA was extracted from the cell pellets using the GeneJET plasmid miniprep kit (Fermentas, USA) according to the manufacturer's instruction. Finally, DNA was eluted in sterile milliQ water. Subsequently, the

Copyright by Kasetsart University All rights reserved

concentration of DNA was analyzed using Nano Drop Spectrophotometer. Finally, the purified DNA was stored at -20 °C.

6. Restriction enzyme analysis

The mutated plasmids were verified using restriction enzyme analysis. The mutated plasmids of OsBADH1 and OsBADH2 were digested by two restriction enzymes, *Nde*I and *Xho*I. The restriction site and their reaction buffers were shown in Table 13. The restriction enzyme analysis was performed with reaction mixtures containing 100 ng of mutated plasmids, 10 U of *Xho*I, 10 U of *Nde*I, 1 µl of 10x buffer and milliQ water to final volume 10 µl. Afterward, the reaction mixtures were incubated in a water bath at 37 °C for 3 hour. The digestion products were verified by 0.8% agarose gel electrophoresis. After electrophoresis, the gels were stained with ethidium bromide and photographed by gel documentation. The plasmid from colony PCR screening and restriction analysis is also confirmed by DNA sequencing.

Table 13 List of restriction enzymes

Enzyme	Recognition site	Recommended Fermentas buffer for 100% enzyme activity	Temperature
*Nde*I	CA$^{\downarrow}$TATG	50 mM Tris-HCl (pH 7.5) 10 $MgCl_2$, 100 mM NaCl, 0.1 mg/ml BSA	37 °C
*Xho*I	C$^{\downarrow}$TCGAG	10 mM Tris-HCl (pH 8.5) 10 $MgCl_2$, 100 mM KCl, 0.1 mg/ml BSA	37 °C

Copyright by Kasetsart University All rights reserved

7. Preparation of $CaCl_2$ *E. coli* BL21 (DE3) competent cells

A single colony of *E. coli* BL21 (DE3) was inoculated into 5 ml LB broth and grown at 37 °C for 16 hours with shaking at 220 rpm. After incubation, 200 µl of starter culture was added into 100 ml LB broth and incubated at 37 °C with shaking at 220 rpm until O.D. at 600 nm reaches 0.6. Subsequently, cell culture was placed on ice for 10 min and centrifuged at 4,000 rpm at 4 °C for 15 min. The supernatant was discarded and then cell pellet was resuspended in 0.1 M $CaCl_2$. The *E. coli* BL21 (DE3) treated with $CaCl_2$ was placed on iced for 30 min and centrifuged at 4,000 rpm at 4 °C for 15 min. The supernatant was discarded and cell pellet was resuspended in 0.1 M $CaCl_2$ containing 15% glycerol. *E. coli* BL21 (DE3) competent cell was kept at -80 °C until used.

8. Transformation, protein expression and purification

The plasmids containing either wild-type or mutant *OsBADH* genes were transformed into *E. coli* BL21 (DE3) competent cells using heat shock method. The transformant colonies were selected in LB agar containing 50 µg/ml kanamycin. After that, a single transformant colony was picked and inoculated in 2.5 ml LB medium containing 50 µg/ml kanamycin as a starter cell. The starter cell culture was added into 250 ml LB medium containing 50 µg/ml kanamycin. The cell culture was grown in shaking incubator at 37 °C until OD at 600 nm reached 0.4-0.6. The cell containing either wild-type or mutant OsBADHs plasmids was induced by adding isopropyl-1-thio-β-D-galactopyranoside (IPTG) to a concentration of 0.4 mM. Subsequently, the cell culture was incubated at 22 °C in shaking incubator for overnight. The protein expression level was then analyzed by 12% SDS-PAGE. After the expression of protein, cells were harvested by centrifugation at 4,000 rpm for 30 min at 4 ºC. The cell pellet was resuspended in the extraction buffer (50 mM Tris-Cl pH 8, 0.5 mM NaCl and 0.5 mM imidazole), 1 mM PMSF, 2 mM β-mercaptoethanol (β-ME) and 1% triton X-100. Then, cells were sonicated using pulse amplitude (on 10 sec, off 5 sec) for 15 min. After the sonication, the cell lysate was centrifuged at 10,000 rpm for 30 min at 4 ºC. The supernatants were applied to HiTrap Chelating HP column (GE

Copyright by Kasetsart University All rights reserved

Healthcare Bioscience, Canada) previously equilibrated with washing buffer (50 mM Tris-Cl pH 8, 0.5 M NaCl, 0.03 M imidazole). Then, the column was washed with washing buffer to remove non-specific proteins. Either wild-type or mutant OsBADH proteins were eluted by an increasing imidazole gradient of elution buffer (50 mM Tris-Cl pH 8, 0.5 M NaCl, 0.5 M imidazole). Protein fractions containing the recombinant protein were pooled and analyzed by 12% SDS-PAGE. The expected molecular weight of monomer OsBADH1 and OsBADH2 were 56 kDa and 58 kDa, respectively. The protein of interest fractions was pooled and imidazole was then removed by dialysis overnight against dialysis buffer (50 mM HEPES-KOH, pH 8.0). The proteins were quickly frozen and stored in -80 °C.

9. SDS-PAGE analysis

Analysis of protein expression and purification were monitored by SDS-PAGE. 20 µl of loading samples consisting of a 1:1 ratio of protein sample and 2x loading buffer (100 mM Tris-Cl, pH 6.8, 4% (w/v) SDS, 0.2% (w/v) bromophenol blue, 20% (v/v) glycerol, 200 mM DTT) were boiled at 100 °C for 15 min and run to electrophoresis using running buffer (25 mM Tris pH 8.3, 250 mM glycine, 0.1% SDS). SDS-PAGE was run at 200 volts for 1 hour and 20 minutes at room temperature. After electrophoresis, protein bands were visualized by coomassie brilliant blue stain.

10. Estimation of protein concentration

Concentration of protein was measured using Beer-lambert law, $A = \varepsilon bc$ where ε was the molar extinction coefficient, c was the molar concentration and b, the path length which was measured in centimeters. The molar extinction coefficients of either OsBADH1 or OsBADH2 were calculated using Protparam (Gasteiger *et al*., 2005). Protparam computes various physicochemical properties that were deduced from a protein sequence including the molecular weight, theoretical pI, amino acid composition, atomic composition and extinction coefficient. Extinction coefficient of OsBADH1 and OsBADH2 were 80620 $M^{-1}cm^{-1}$ and 88765 $M^{-1}cm^{-1}$, respectively.

Copyright by Kasetsart University. All rights reserved

11. Intrinsic fluorescence of OsBADH wild-type and mutants

Fluorescence measurements were carried out according to the method described in a previous paper with some modifications (Gruez *et al*., 2004). The measurements were performed to investigate the binding of NAD^+ to OsBADH proteins by monitoring the intrinsic fluorescent intensity of Tryptophan residues. Fluorescence titration method was performed by adding microliter amounts of 5 mM NAD^+ to 400 µl of 1.5 µM OsBADH proteins in 50 mM HEPES-KOH buffer (pH 8.0). Excitation wavelength was 295 nm (slit 5 nm) and emission spectra were recorded between 300 nm and 450 nm (slit 5 nm). After addition of the cofactor, the sample was mixed and the spectrum was recorded. Titration results were corrected to account for ligand dilution. The apparent K_d for NAD^+ binding was obtained by fitting the fluorescence changes against the concentration of NAD^+ using the following equation:

$$\%\triangle F_{obs} = \frac{\triangle F_{max}[L]_0}{K_d + [L]_0}$$

where $\%\Delta F_{obs}$ is the enhancement of fluorescence upon binding to proteins, ΔF_{max} is the maximum attainable change in fluorescence intensity, $[L]_0$ is the total molar concentration of the ligand, and K_d is the dissociation constant for NAD^+ binding. Data were plotted as ΔF_{max} (the maximum attainable change in fluorescence intensity) at 350 nm versus the concentration of cofactors. The data were fitted and standard errors were calculated by non-linear regression analysis using the Microcal Origin 6.0 program.

Copyright by Kasetsart University All rights reserved

12. Enzyme kinetic of OsBADH wild-type and mutants

Enzyme kinetic assays of OsBADH were measured spectrophotometrically by monitoring the formation of NADH, using betaine aldehyde (Bet-ald) and γ-aminobutyraldehyde (GAB-ald) as substrate (Bradbury *et al*., 2008). Betaine aldehyde chloride was dissolved in d.H_2O and directly used in the enzymatic assay. γ-Aminobutyraldehyde dimethyl acetal was used for GAB-ald. The diethylacetals of γ-aminobutyraldehyde were hydrolyzed with of 1M HCl and heated at 80 °C for 1 h. The hydrolyzate was neutralized by adding an equivalent volume of 1N NaOH. Both Bet-ald and GAB-ald were stored at -20 °C while the 100 mM stock solution of acetaldehyde was prepared and kept at 4 °C until required. The enzyme activities were determined at 30 °C using a reaction mixture containing 5 mM NAD^+, 50 mM HEPES-KOH buffer (pH 8.0) and various concentration of each substrate (between 8–1000 μM). The absorbance was measured at 340 nm every 9 sec up to over 2 min. The linear interval of the reaction was determined using the Magellan 6 program. One unit of enzyme activity was defined as the amount of enzyme that catalyzes the formation of 1 μmol of NADH per minute at 30 °C. Reactions was monitored by following the change in absorbance at 340 nm corresponding to the formation of NADH (ε = 6220 M^{-1} cm^{-1}) (Bradbury *et al*., 2008). The K_m and V_{max} values were obtained by fitting the initial rates against the concentration of each substrate to the Michaelis-Menten equation:

$$V = \frac{V_{max}[S]}{K_m + [S]}$$

where V is the initial rate, [S] is the substrate concentrations, V_{max} is the initial rate achieved as [S] approach ∞, K_m is Michaelis-Menten constant or the value of [S] giving $V_{max}/2$. The data were fitted and standard errors were calculated by non-linear regression using Microcal Origin 6 program.

Copyright by Kasetsart University All rights reserved

13. Homology modeling and molecular docking of OsBADH1 and OsBADH2

The crystal structure of OsBADH2 was obtained from Assist. Prof. Dr. Kiattawee Choowongkomon (Department of Biochemistry, Kasetsart University, Thailand) (Kuaprasert *et al*., 2011). Since the sequence identity between OsBADH1 and OsBADH2 is about 75%**.** The protein structure of OsBADH1 was modeled with residues ranging from 8 to 504 amino acids by SWISS-MODEL using the crystal structures of OsBADH2 as a template. The structures of both OsBADH proteins were superimposed in order to compare the structural conformations using the program PyMol (Delano, 2002). The mutation in the protein was generated using Discovery Studio 2.5. Regarding for ligand**,** Bet-ald was taken from the crystal structure of *YdcW* (PDB entry 1WNB) (Gruez *et al*., 2004) whereas GAB-ald was built using Discovery Studio 2.5**.** After both proteins and ligands were successfully constructed, docking analyses were performed on AutoDock 4.0 (Morris *et al*., 1998). For docking ligand, the rotational bonds of the side chain were treated as flexible whereas those of main chain were regarded as rigid. All hydrogen atoms were added into the OsBADH1 and OsBADH2 proteins and water molecules were removed from the structure. The grid boxes were created to cover substrate-binding domain of the protein. The size of grid box was set at 60 × 60 × 60 $Å^3$ and the center of grid box was set at 7.545 Å (*x*), 3.238 Å (*y*), and 33.596 Å (*z*). The search parameter used was Lamarckian Genetic Algorithm (LGA) with 100 runs. Three-dimensional structures of OsBADHs–Bet-ald or OsBADHs–GAB-ald with the best docked conformation were observed. From the 100 running structure, one structure was chosen based on the lowest energy and the high population. The lowest energy and highest populations were visualized and analyzed by PyMol (Delano, 2002) and Discovery Studio 2.5. Therefore, the structures from the molecular docking analysis were used as an initial model for molecular dynamic (MD) simulations.

14. Molecular dynamic simulation of OsBADH1 and OsBADH2

The complexes from molecular docking analysis including OsBADH1-Bet-ald model run63, OsBADH1-GAB-ald model run96, OsBADH2-Bet-ald model run60 and OsBADH2-GAB-ald model run11 were applied for molecular dynamic (MD)

Copyright by Kasetsart University All rights reserved

simulations. The MD simulations were achieved by using the AMBER 10 simulation package. The number of amino acids in OsBADH1-Bet-ald and OsBADH1-GAB-ald complex was 505 residues while 503 residues in OsBADH2-Bet-ald and OsBADH2-GAB-ald complex. All complexes were solvated with octahedral box of 10 Å from solute surface using TIP3P water model (Jorgensen *et al*., 1983). The solvation in model OsBADH1-Bet-ald, OsBADH1-GAB-ald, OsBADH2-Bet-ald and OsBADH2-GAB-ald contained 32004, 32004, 32395 and 32395 water molecules, respectively. The complexes were neutralized with the counter ions of 6 Na^+ atoms for OsBADH1-Bet-ald system and 7 Na^+ atoms for OsBADH1-GAB-ald system while 13 Na^+ atoms for OsBADH2-Bet-ald system and 14 Na^+ atoms for OsBADH2-GAB-ald system. The energy minimization was achieved by using Cornell force field from the SANDER module of AMBER 10 (Cornell *et al.*, 1995). The stepwise minimizations were performed as following: 2000 steps for hydrogen atoms, 2000 steps for solvent water molecules and 5000 steps for all atoms of the complexes. The equilibration was perfomed in carononical ensemble (NVE) at 300 K; the steps included the first 100 ps in which all atoms in protein were restrained and the following 100 ps in which all atoms were set free. The MD simulations were carried out under an isobaric–isothermal ensemble (NPT), at 1 atm and 300 K. The equilibration was accomplished when the system was stable; then, the production phases were harvested during the last 500 ps of the trajectory. The trajectory analysis of the products included root-mean-square displacement (RMSD) versus time (ps) was plotted by Microcal Origin 6 program. The analysis included the distances of amino acid interaction, hydrogen bonds and binding free energies.

Copyright by Kasetsart University All rights reserved

RESULTS AND DISCUSSIONS

1. Site-directed mutagenesis of OsBADH1 and OsBADH2

The amino acids, either N164 and W172 of OsBADH1 or N162 and W170 of OsBADH2 were mutated to Alanine (A). Additionally, W172 and W170 of OsBADH1 and OsBADH2, respectively were mutated to Phenylalanine (F). The plasmids containing the desired mutation were transformed into *E. coli* strain XL-10 Gold and the transformant colonies were selected by kanamycin. The colony contained the mutated plasmid were verified by restriction enzyme analysis, colony PCR screening and DNA sequencing.

1.1 Construction of OsBADH1 and OsBADH2 mutants

The PCR products of OsBADH1 and OsBADH2 mutants were ran on 0.8% agarose gel electrophoresis and transformed into *E. coli*. The size of PCR product was about 6.8 kb and 7.1 kb for OsBADH1 and OsBADH2 mutants, respectively (Figure 33).

1.2 PCR screening of OsBADH1 and OsBADH2 mutants

PCR screening was firstly used to check the presence of the mutants prior to DNA sequencing. To confirm mutated plasmid, the screening primers specific for mutated sequence were designed as shown in Table 11 in methodology section. The mutated plasmid containing the desired mutation ought to be amplified using the designed primers while non-mutated plasmids could not be amplified. The PCR screening products of either OsBADH1 or OsBADH2 mutants were checked by 0.8% agarose gel electrophoresis as shown in Figure 34 and Figure 35, respectively. The strong band of 1008 bp could be seen in N164A and N162A whereas the band of 948 bp could be seen in W172A, W172F, W170A and W170F. This indicated that all mutated plasmids contained the expected mutation. The colony containing the mutated plasmids were subsequently extracted and digested with *Xho*I and *Nde*I.

Copyright by Kasetsart University All rights reserved

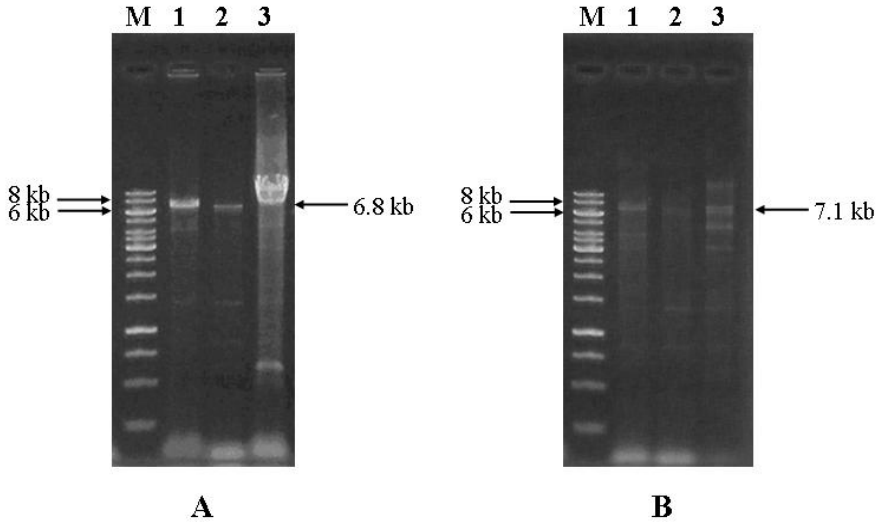

Figure 33 PCR products obtained from site-directed mutagenesis. (A) PCR amplification of OsBADH1 mutants; Lane M, GeneRuler DNA Ladder; Lane 1, N164A; Lane 2, W172A; Lane 3, W172F; (B) PCR amplification of OsBADH2 mutants; Lane 1, N162A; Lane 2, W170A; Lane 3, W170F.

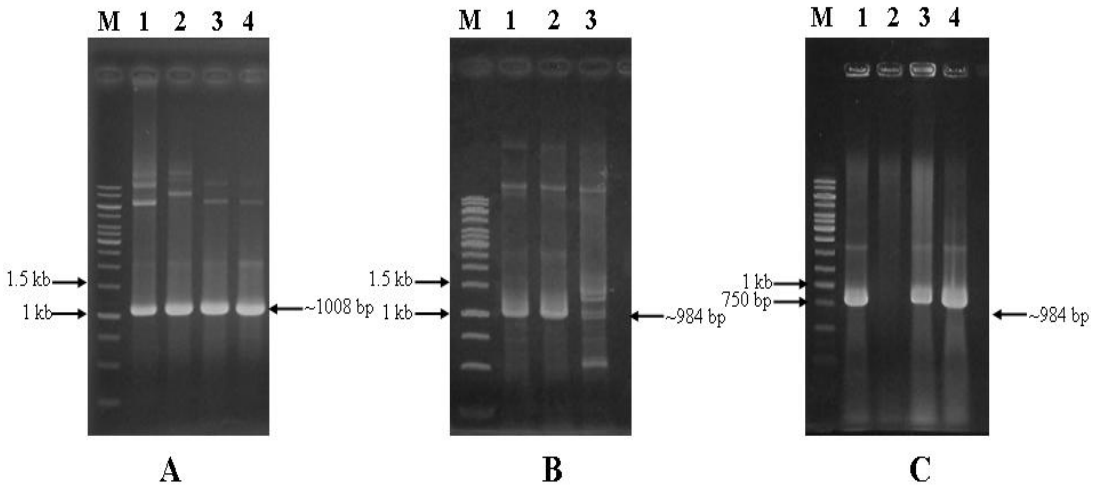

Figure 34 PCR screening of OsBADH1 mutants. (A) N164A; Lane M, GeneRuler DNA Ladder; Lanes 1-4, clones 1-4; (B) W172A; Lanes 1-3, clones 1-3; (C) W172F; Lanes 1-4, clones 1-4.

Copyright by Kasetsart University All rights reserved

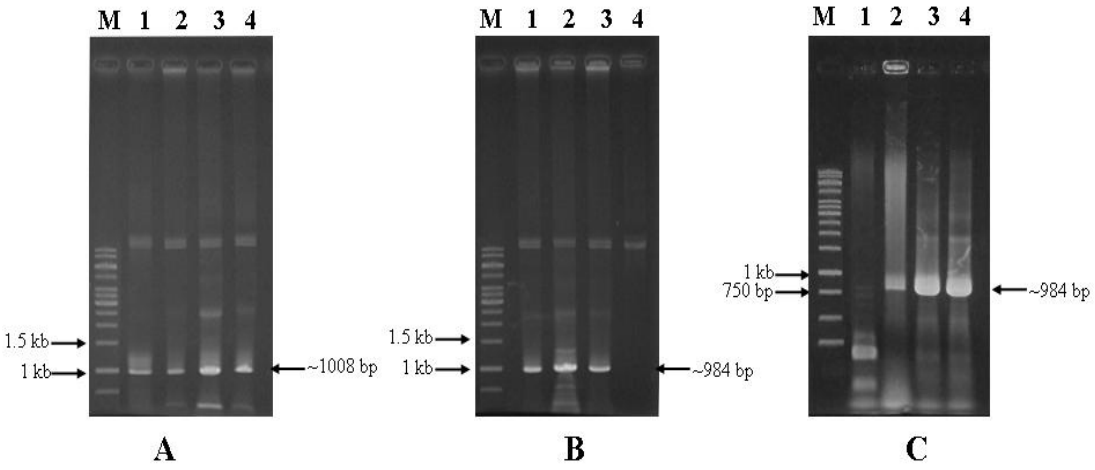

Figure 35 PCR screening of OsBADH2 mutants. (A) N162A; Lane M, GeneRuler DNA Ladder; Lanes 1-4, clones 1-4; (B) W170A; Lanes 1-4, clones 1-4; (C) W170F; Lanes 1-4, clones 1-4.

1.3 Restriction enzyme analysis of OsBADH1 and OsBADH2 mutants

To confirm whether the mutated plasmids contained the correct size of *OsBADH1* and *OsBADH2*, the restriction enzyme digestion with *Xho*I and *Nde*I of the chosen mutated plasmids were carried out. The digestion of the mutated plasmids generated two bands at 5.3 kb (represented size of plasmid pET28b) and 1.5 kb (represented size of *OsBADH1*) or 1.8 kb (represented size of *OsBADH2*) as shown in Figure 36 and Figure 37, respectively. In lane 2 of Figure 36A, the mutated plasmid was incompletely digested by *Xho*I and *Nde*I therefore giving the band of linearized pET28b-OsBADH1 above pET28b plasmid. In order to confirm the correction of the mutated gene, the mutated plasmids were sequenced. The sequence alignment of either OsBADH1 or OsBADH2 wide-type and mutants is shown in Figure 38 and Figure 39, respectively. DNA sequencing was used to confirm the mutation on the *OsBADH1* and *OsBADH2*. The sequencing result of N164A, W172A, N162A and W170A showed the codon GCT, GCG, GCC and GCG which codes for alanine, respectively. Likewise, the sequencing result of both W172F and W170F showed the codon TTC which codes for phenylalanine.

Copyright by Kasetsart University All rights reserved

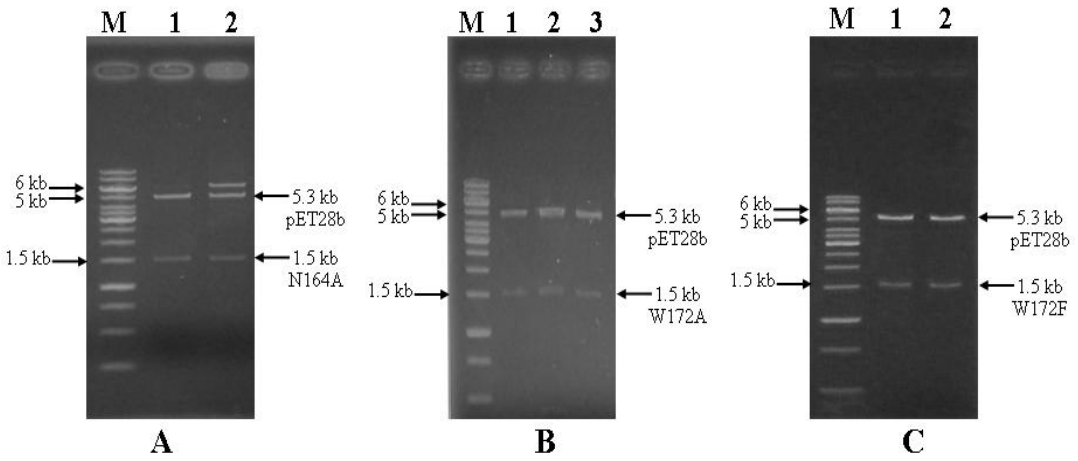

Figure 36 Restriction enzyme analysis of OsBADH1 mutants with *Xho*I and *Nde*I. (A) pET28b-N164A plasmids; Lane M, GeneRuler DNA Ladder; Lanes 1 and 2, pET28b-N164A clones 1 and 2 ; (B) pET28b-W172A plasmids; Lanes 1-3, pET28b-W172A clones 1-3; (C) pET28b-W172F plasmids; Lanes 1 and 2, pET28b-W172F clones 1 and 2.

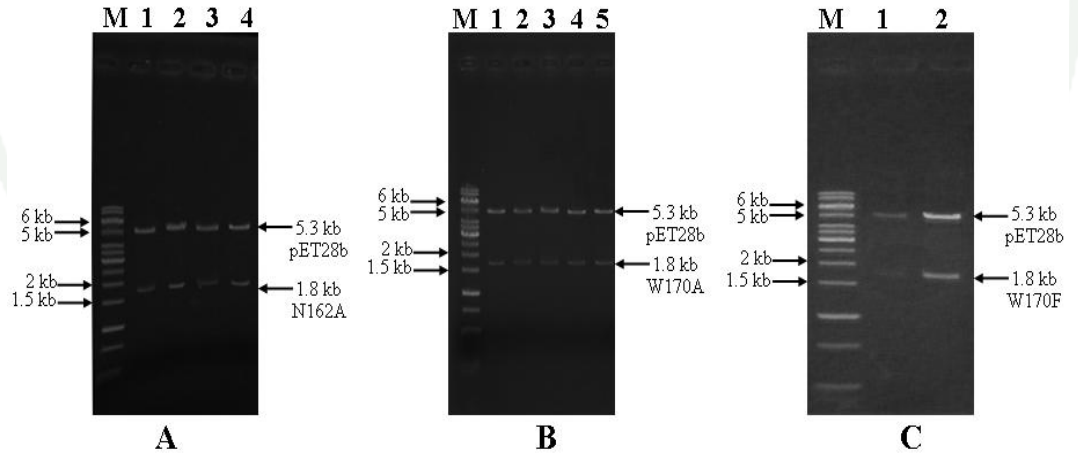

Figure 37 Restriction enzyme analysis of OsBADH2 mutants with *Xho*I and *Nde*I. (A) pET28b-N162A plasmids; Lane M, GeneRuler DNA Ladder; Lanes 1-4, pET28b-N162A clones 1-4 ; (B) pET28b-W170A plasmids; Lanes 1-5, pET28b-W170A clones 1-5 ; (C) pET28b-W170F plasmids; Lanes 1 and 2, pET28b-W170F clones 1 and 2.

Copyright by Kasetsart University All rights reserved

```
Wildtype_OsBADH1      ACTCCCTGGAATTATCCTCTGCTGATGGCTACTTGGAAGGTTGCACCTGCCCTGGCTGCT 540
N164A                 ACTCCCTGGGCTTATCCTCTGCTGATGGCTACTTGGAAGGTTGCACCTGCCCTGGCTGCT 540
W172A                 ACTCCCTGGAATTATCCTCTGCTGATGGCTACTGCGAAGGTTGCACCTGCCCTGGCTGCT 540
W172F                 ACTCCCTGGAATTATCCTCTGCTGATGGCTACTTTCAAGGTTGCACCTGCCCTGGCTGCT 540
                      ********* ********************** ************************
```

Figure 38 Pairwise alignment of partial DNA sequencing of wild-type and mutant of OsBADH1 using ClustalW2. The mutation sites for the N164A, W172A and W172F are shown in bold and underlined.

```
Wildtype_OsBADH2      TGGAACTATCCTCTCCTGATGGCAACATGGAAGGTAGCTCCTGCCCTGGCTGCTGGCTGT 540
N162A                 TGGGCCTATCCTCTCCTGATGGCAACATGGAAGGTAGCTCCTGCCCTGGCTGCTGGCTGT 540
W170A                 TGGAACTATCCTCTCCTGATGGCAACAGCGAAGGTAGCTCCTGCCCTGGCTGCTGGCTGT 540
W170F                 TGGAACTATCCTCTCCTGATGGCAACATTCAAGGTAGCTCCTGCCCTGGCTGCTGGCTGT 540
                      +++  ********************** ****************************
```

Figure 39 Pairwise alignment of partial DNA sequencing of wild-type and mutant of OsBADH2 using ClustalW2. The mutation sites for the N162A, W170A and W170F are shown in bold and underlined.

2. Protein expression and purification of OsBADH1 and OsBADH2

After the DNA sequence of the mutated *OsBADH1* and *OsBADH2* was confirmed, the chosen mutated plasmids were transformed into *E. coli* BL21 (DE3). All mutants were expressed and purified as described in methodology section. In small scale expression, cells were harvested before and after the induction with IPTG and then applied to 12% SDS-PAGE. It was found that the protein could be well expressed at 22 ºC with the induction of 0.4 mM IPTG. Then the large scale expression of OsBADH1 and OsBADH2 was performed in 500 ml LB medium. The expected size of either OsBADH1 or OsBADH2 was 56 kDa and 58 kDa as shown in Figure 40 and Figure 41, respectively.

Copyright by Kasetsart University All rights reserved

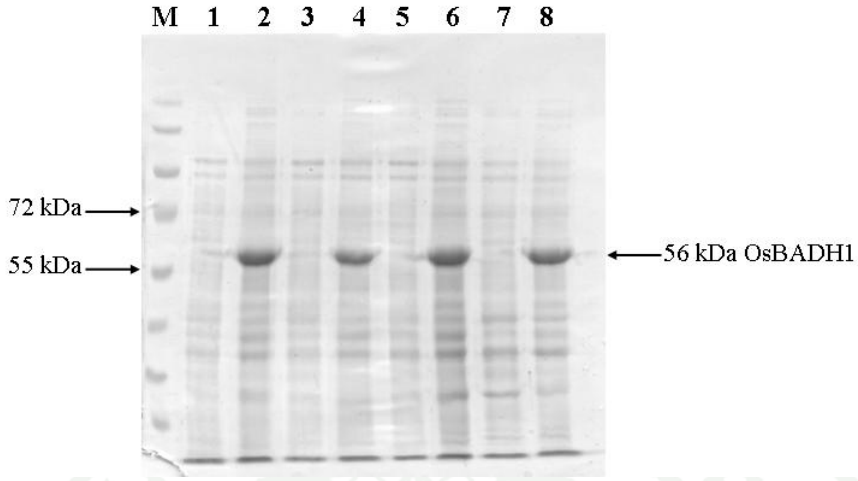

Figure 40 Expression analysis of OsBADH1 wild-type and mutants. Lane M, PageRuler prestained protein ladder; Lane 1-2, OsBADH1 wild-type; Lane 3-4, N164A ; Lane 5-6, W172A ; Lane 7-8, W172F . Odd number lanes represent for 0 hr, while even number lanes represent for overnight induction.

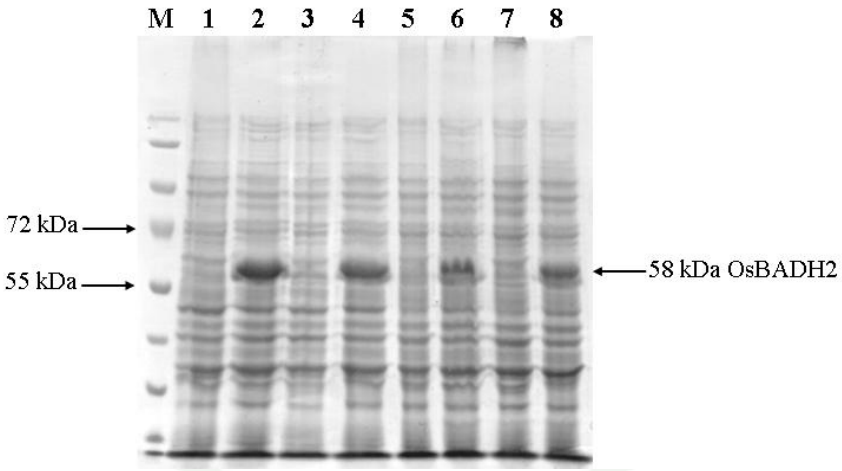

Figure 41 Expression analysis of OsBADH2 wild-type and mutants. Lane M, PageRuler prestained protein ladder; Lane 1-2, OsBADH2 wild-type; Lane 3-4, N162A ; Lane 5-6, W170A ; Lane 7-8, W170F . Odd number lanes represent for 0 hr, while even number lanes represent for overnight induction.

Copyright by Kasetsart University All rights reserved

The result indicated that OsBADH1 and OsBADH2 were vastly expressed as a soluble form but a few were expressed as an insoluble inclusion bodies. To purify the proteins, the harvested cells were lysed by extraction buffer and the soluble protein was centrifuged to separate the cell debris. The clarified supernatant was applied to HiTrap affinity column. The 6xHis proteins were eluted by an increasing imidazole gradient of elution buffer. The cell pellets, unbound and bound fractions from the purification were subjected to 12% SDS-PAGE as shown in Figure 42 and Figure 43. The result indicated that all OsBADH1 and OsBADH2 wild-type and mutants were purified to high yield and have an apparent molecular weight of 56 kDa and 58 kDa, respectively.

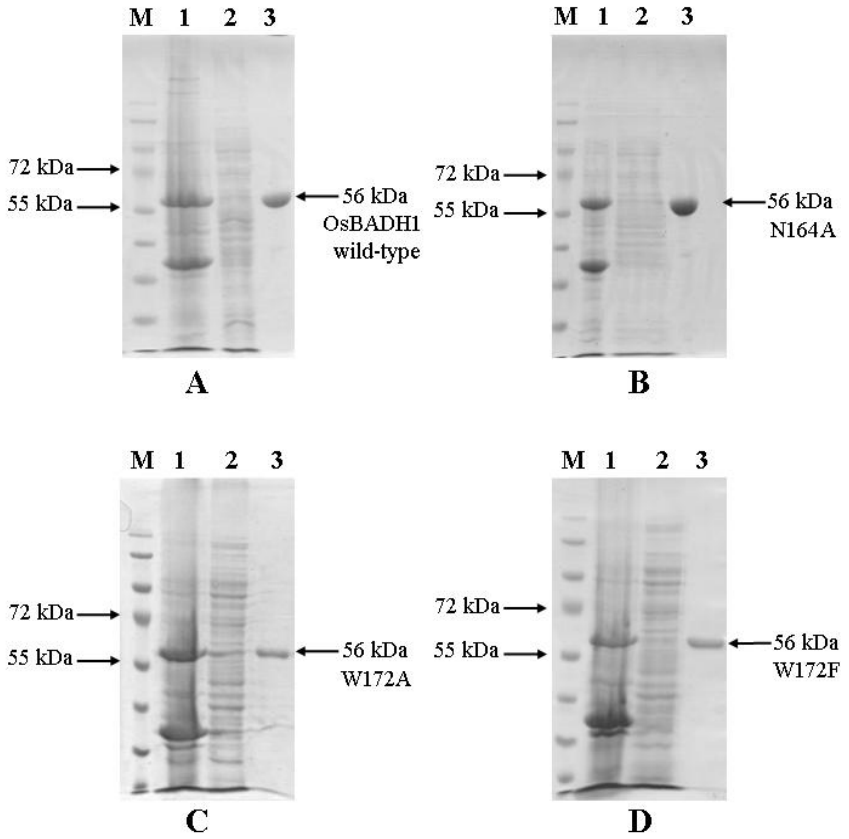

Figure 42 SDS-PAGE analysis of OsBADH1 purification. (A) OsBADH1 wild-type; (B) N164A; (C) W172A; (D) W172F; Lane M, PageRuler prestained protein ladder; Lane 1, insoluble fraction; Lane 2, unbound fraction; Lane 3, the eluted protein.

Copyright by Kasetsart University All rights reserved

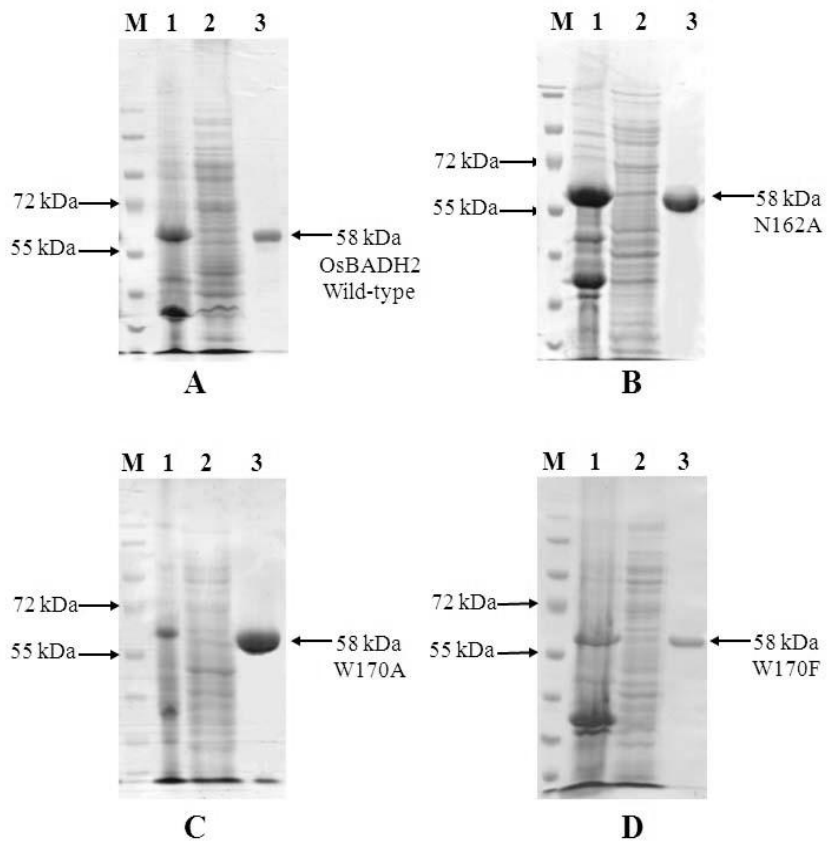

Figure 43 SDS-PAGE analysis of OsBADH2 purification. (A) OsBADH2 wild-type; (B) N162A; (C) W170A; (D) W170F; Lane M, PageRuler prestained protein ladder; Lane 1, insoluble fraction ; Lane 2, unbound fraction; Lane 3, the eluted protein.

3. NAD^+ binding study of OsBADH1 and OsBADH2

To investigate whether the mutation affected the overall folding of the protein, the NAD^+ binding study was carried out. The affinity between the enzymes and NAD^+ was investigated by the intrinsic tryptophan fluorescence study. The intrinsic tryptophan fluorescence of OsBADHs was recorded on the free enzyme and on the addition of NAD^+. The fluorescence properties of tryptophan amino acid residues can be altered upon co-factor binding. The conformation changes in the presence of ligand can result in fluorescence enhancement which can be examined protein-ligand interaction. Figure 44 reveals the modeled structure of OsBADH1 and OsBADH2 with tryptophan side chains and NAD^+.

Copyright by Kasetsart University All rights reserved

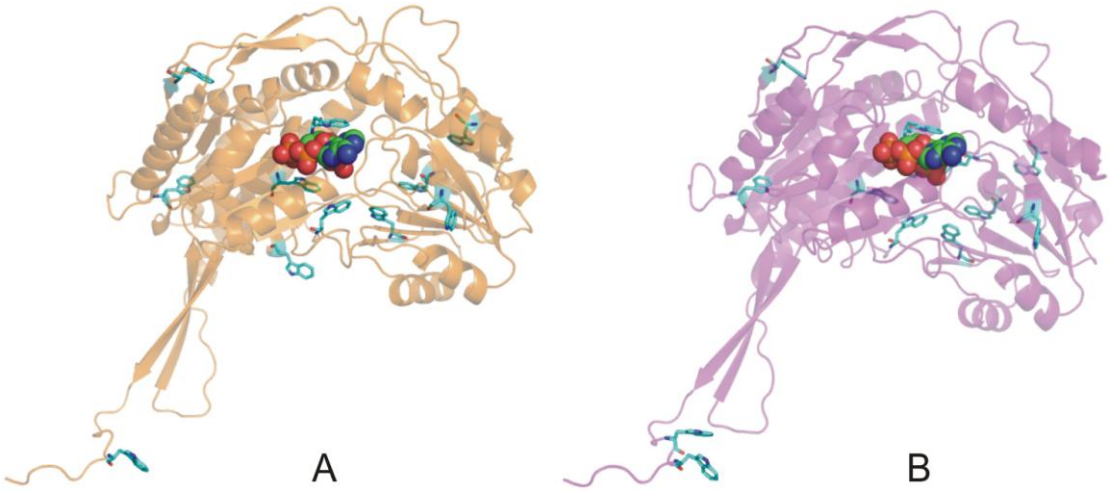

Figure 44 Structure of OsBADH1 and OsBADH2. OsBADH1 and OsBADH2 are shown in ribbon (orange and magenta, respectively). The tryptophan side chains are shown in stick and colored by atoms (carbon, cyan). The ADP moiety of NAD^+ are depicted in sphere representation and colored by atoms (carbon, green slate).

From Figure 44, OsBADH1 contains 11 tryptophan residues including W18, W68, W163, W172, W283, W319, W392, W448, W461, W476 and W498 whereas OsBADH2 contains 13 tryptophan residues including W16, W66, W109, W161, W170, W281, W288, W317, W390, W446, W459, W494 and W496. The structure of OsBADH2 was obtained from Assist. Prof. Dr. Kiattawee Choowongkomon (Department of Biochemistry, Kasetsart University, Thailand) (Kuaprasert *et al*., 2011) and that of OsBADH1 was gained from the homology modeling using OsBADH2 as a template. More details regarding the homology modeling are described in section 5 of this chapter. According to the crystal structure of OsBADH2, only the ADP moiety of the NAD^+ coenzyme is well defined in density. Several reports have previously shown that BADHs from several species can bind either NAD^+ or $NADP^+$ (Gruez *et al*., 2004; Fujiwara *et al*., 2008; Tylichová *et al*., 2010; Wongpanya *et al*., 2011). YdcW, a BADH from *E. coli*, has much better affinity for NAD^+ than for $NADP^+$ (Gruez *et al*., 2004) while BADHs in barley, BBD1 and BBD2, can also bind NAD^+ better than $NADP^+$ (Fujiwara *et al*., 2008). Likewise,

Copyright by Kasetsart University All rights reserved

BADHs in rice, OsBADH1 and OsBADH2, can also bind NAD^+ better than $NADP^+$ (Wongpanya *et al*., 2011). According to BADHs in *Pisum sativum*, PsAMADH1 and PsAMADH2, were tested with several NAD^+ analogs (Tylichová *et al*., 2010). The result shows that $NADP^+$ is a poor electron acceptor, reducing the activity of both enzymes by 85% comparing to NAD^+. Using the purified recombinant OsBADHs, the affinity of the enzymes and NAD^+ was investigated using the intrinsic tryptophan fluorescence study. The intrinsic tryptophan fluorescence of OsBADHs was recorded on the free enzyme and on the addition of NAD^+ to determine the direct affinity of NAD^+ and enzymes. The fluorescence properties of tryptophan amino acid residues can be altered upon co-factor binding. The conformation changes in the presence of ligand can result in either fluorescence quenching or enhancement, which can examine protein-ligand interaction. For BADH proteins, it has been reported that the binding of NAD^+ usually takes place prior to the binding of aldehyde substrate (Perez-Miller *et al*., 2003). When the wavelength at 295 nm was used to excite the tryptophan residues within the protein, the emission spectrum of OsBADHs exhibited a maximum wavelength at 350 nm. The decrease of the intensity of tryptophan fluorescence of OsBADHs can be observed upon the addition of NAD^+ (0–0.55 mM). This phenomenon is clearly associated to the binding of NAD^+, which can imply that the overall folding of the enzyme was correct and the mutations to the OsBADH active site do not induce considerable conformational changes. Since the same phenomenon was also observed in YdcW, a BADH from *E. coli* (Gruez *et al*., 2004) and BADH2 from rice (Wongpanya *et al*., 2011). The dissociation constant (K_d) values of OsBADH1 and OsBADH2 wild-type and mutants were determined for NAD^+ as shown in Table 14.

The K_d values of all mutants were increased less than 2-fold, indicating that the mutation did not cause a dramatic effect to the protein folding as well as the co-factor binding. The result of K_d values reported here is in agreement with the previously study (Wongpanya *et al*., 2011). However, the K_d value of OsBADH2 for NAD^+ (9 μM) suggest that OsBADH2 can bind to NAD^+ with higher affinity compared to OsBADH1 (K_d of 34 μM). Collectively, the results showed that mutants could bind NAD^+, indicating the correct folding of the enzyme. The K_d values of

Copyright by Kasetsart University All rights reserved

BBD1 and BBD2 for NAD^+ (25.9 μM and 23.6 μM) have been reported (Fujiwara *et al*., 2008) while the K_d values of PsAMADH1 and PsAMADH2 for NAD^+ were 40 μM and 55 μM, respectively (Tylichová *et al*., 2010). Their K_d values were not largely different from the corresponding K_d values in this study. Having determined the co-factor binding affinity, the kinetic parameters K_m, k_{cat} and k_{cat}/K_m for OsBADHs wild-type and mutants were also characterized using Bet-ald and GAB-ald as substrates.

Table 14 Dissociation constant (K_d) of NAD^+ and OsBADHs

K_d (μM)			
OsBADH1		OsBADH2	
Wild-type	34 ± 3	Wild-type	9 ± 1
N164A	51 ± 3	N162A	19 ± 4
W172A	56 ± 3	W170A	16 ± 3
W172F	50 ± 3	W170F	14 ± 2

4. Enzymatic characterization of OsBADH1 and OsBADH2

Using the purified OsBADHs, Michaelis constants (K_m values), k_{cat} values and k_{cat}/K_m values for Bet-ald and GAB-ald can be obtained. All OsBADH1 and OsBADH2 wild-type and mutants can catalyze the oxidation of Bet-ald and GAB-ald as shown in Table 15 and Table 16. The K_m value of OsBADH1 wild-type for Bet-ald was 3-fold higher than GAB-ald, suggesting that OsBADH1 can bind GAB-ald with a higher affinity than Bet-ald. The K_m values of the OsBADH1 mutants, N164A, W172A and W172F for Bet-ald were observed with 7.8-fold, 10-fold and 9.2-fold lower than that of the wild-type OsBADH1, respectively, while K_m values of N164A, W172A and W172F for GAB-ald were 5.5-fold, 1.5-fold and 6.6-fold lower than wild-type.

Copyright by Kasetsart University All rights reserved

Table 15 Kinetic parameters for wild type and mutant OsBADH1 with Bet-ald and GAB-ald

	OsBADH1					
	Bet-ald			GAB-ald		
	K_m (μM)	k_{cat} (s^{-1})	k_{cat}/K_m (M^{-1} s^{-1})	K_m (μM)	k_{cat} (s^{-1})	k_{cat}/K_m (M^{-1} s^{-1})
Wild-type	1288 ± 192	0.52 ± 0.0502	405 ± 0.0000719	432 ± 57	0.31 ± 0.01252	718 ± 0.000099
N164A	165 ± 35	0.032 ± 0.0023	194 ± 0.0000434	78 ± 5	0.023 ± 0.000353	295 ± 0.0000194
W172A	129 ± 23	0.0022 ± 0.00013	17 ± 0.00000321	291 ±18	0.22 ± 0.00376	756 ± 0.0000484
W172F	140 ± 51	0.0102 ± 0.00123	73 ± 0.0000279	65 ± 11	0.09 ± 0.0034	1385 ± 0.000239

Table 16 Kinetic parameters for wild type and mutant OsBADH2 with Bet-ald and GAB-ald

	OsBADH2					
	Bet-ald			GAB-ald		
	K_m (μM)	k_{cat} (s^{-1})	k_{cat}/K_m (M^{-1} s^{-1})	K_m (μM)	k_{cat} (s^{-1})	k_{cat}/K_m (M^{-1} s^{-1})
Wild-type	251 ± 62	0.057 ± 0.00546	228 ± 0.0000602	38 ± 11	0.032 ± 0.00222	842 ± 0.000251
N162A	66 ± 10	0.0093 ± 0.000368	141 ± 0.0000221	107 ± 12	0.012 ± 0.000404	112 ± 0.0000131
W170A	77 ± 7	0.0072 ± 0.00018	94 ± 0.00000882	58 ± 8	0.01 ± 0.000394	172 ± 0.0000247
W170F	57 ± 10	0.015 ± 0.000693	263 ± 0.0000476	105 ± 10	0.14 ± 0.00395	1333 ± 0.000132

These results showed that all OsBADH1 mutants seemed to bind both Bet-ald and GAB-ald tighter than wild-type OsBADH1. Similarly to OsBADH1, K_m value of OsBADH2 wild-type for Bet-ald was 6.6-fold higher than GAB-ald while those of N162A, W170A and W170F for Bet-ald were observed with 3.8-fold, 3.3-fold and 4.4-fold lower, respectively compared to OsBADH2 wild-type. In contrast, K_m values of N162A, W170A and W170F for GAB-ald were 2.8-fold, 1.5-fold and 2.8-fold increase, respectively compared to OsBADH2 wild-type. These results indicated that the mutants of OsBADH2 can bind Bet-ald tighter than wild-type but bind GAB-ald slightly less than wild-type. When comparing the K_m values of OsBADH1 and OsBADH2 for Bet-ald and GAB-ald to those previously reported (Bradbury *et al*., 2008; Mitsuya *et al*., 2009; Wongpanya *et al*., 2011), our results are in comparable in that the enzymes can bind GAB-ald better than Bet-ald.

For catalytic activity, the k_{cat} values of the N164A, W172A and W172F for Bet-ald were found to be 16-fold, 236-fold and 51-fold lower, respectively while those of N164A, W172A and W172F for GAB-ald were 13.5-fold, 1.4-fold and 3.4-fold lower, respectively compared to OsBADH1 wild-type. For OsBADH2 mutants, the k_{cat} values for Bet-ald of N162A, W170A and W170F were a 6-fold, 8-fold and 3.8-fold lower, respectively, compared to wild type OsBADH2. Likewise, the k_{cat} values of N162A and W170A for GAB-ald were 2.7-fold and 3.2-fold lower compared to the wild-type, respectively, but the W170F mutant had k_{cat} values 4.4-fold larger compared to that of the wild-type. Collectively, the results revealed that the substitution of N164 and W172 of OsBADH1 and N162 and W170 of OsBADH2 by alanine reduced the catalytic activity towards Bet-ald and GAB-ald. However, W170F of OsBADH2 exhibited slightly higher k_{cat} value for GAB-ald than the wild-type while W172F of OsBADH1 showed the reduced k_{cat} value.

For the catalytic efficiency (k_{cat}/K_m), the k_{cat}/K_m values of the OsBADH1 mutants, N164A, W172A and W172F, for Bet-ald were reduced by 2.1-fold, 23.8-fold and 5.5-fold, respectively, while the k_{cat}/K_m value of N164A for GAB-ald were 2.4-fold lower but the k_{cat}/K_m values of W172A and W172F for GAB-ald were 1.05-fold and 2-fold higher, respectively compared to OsBADH1 wild-type. For OsBADH2 mutants, the k_{cat}/K_m values of N162A and W170A for Bet-ald were 1.6-fold and 2.4-

Copyright by Kasetsart University All rights reserved

fold lower, respectively but the k_{cat}/K_m value of W170F for Bet-ald was 1.1-fold higher. Similarly, the k_{cat}/K_m values of N162A and W170A for GAB-ald were 7.5-fold and 4.9-fold lower, respectively while the k_{cat}/K_m value of W170F for GAB-ald was 1.6-fold higher. Out of six mutants, only two mutants (W172F of OsBADH1 and W170F of OsBADH2) showed a higher catalytic efficiency towards GAB-ald. This implied that either W172 or W170 in each protein may be a key residue for determining substrate specificity towards GAB-ald. In addition to Bet-ald and GAB-ald, acetaldehyde was also used as a substrate since it was previously reported (Mitsuya *et al*., 2009) that both OsBADH1 and OsBADH2 catalyzed the oxidation of acetaldehyde (Table 17). Accroding to Table 19, the result is in agreement with the previously report that with the higher k_{cat} and k_{cat}/K_m value, indicating that OsBADH1 is a better candidate enzyme for acetaldehyde than OsBADH2.

Table 17 Kinetic parameters for wild type OsBADHs with acetaldehyde

	Acetaldehyde		
	K_m (μM)	k_{cat} (s^{-1})	k_{cat}/K_m (M^{-1} s^{-1})
OsBADH1	99 ± 29	0.14 ± 0.00000001259	1425 ± 0.000414
OsBADH2	146 ± 34	0.08 ± 0.00000008862	607 ± 0.000128

BADH enzyme from *E. coli* was reported to be able to catalyze GAB-ald better than Bet-ald in general because of the shape of its active site (Gruez *et al*., 2004). The size of the binding site is sufficient to accommodate molecules larger than Bet-ald such as n-alkyl medium chain aldehydes. Both Pea AMADH and OsBADHs also showed a broad substrate specificity utilizing various aminoaldehydes (C3-C6) as substrates (Šebela *et al*., 2000; Tylichová *et al*., 2010; Mitsuya *et al*., 2009). It has also been reported that the residues C286, E252 and N153 make up the catalytic triad of the PaBADH active site in *Pseudomonas aeruginosa* (González-Segura1 *et al*., 2009). In the active site, the hydroxyl oxygen of a bound glycerol molecule, which mimics the thiohemiacetal intermediate, is hydrogen bonded to the side chain of N153 and the main chain of C286 forming the oxyanion hole that stabilizes the intermediate (González-Segura1 *et al*., 2009). In addition, the mutagenesis of the highly conserved

Copyright by Kasetsart University All rights reserved

N162 of PsAMADH2 confirmed that the mutation of N162 to alanine resulted in about a 200-fold reduction in dehydrogenase activity, indicating that the residue is involved in the catalytic efficiency of PsAMADH2 (Tylichová *et al*., 2010). Therefore, the mutation on the catalytic Asn residue would definitely affect k_{cat}/K_m value. Besides the catalytic triad, the Trp residues around the substrate binding pocket was proposed to be involved in the substrate binding pocket (Johansson *et al*., 1998), and hence the mutation on the Trp residues should also affect k_{cat}/K_m value when Trp residue was mutated. From overall results, most of the mutants exhibited lower or equal catalytic efficiency towards Bet-ald, while some mutants showed an increased catalytic efficiency towards GAB-ald than the wild type did. Additionally, changing Trp to Phe had a tremendous effect on k_{cat}/K_m towards GAB-ald but not towards Bet-ald. According to the kinetic results, Trp may be one of the recognition residues for Bet-ald but not for GAB-ald. Our result is well correlated with the study of aromatic active-site residues in PsAMADH2 (Kopečný *et al*., 2011) in that aromatic residues in the substrate cavity, such as W170, W288 and Y163 (PsAMADH2 numbering), are important for the overall geometry of the substrate channel allowing for the appropriate orientation of the substrate towards the catalytic C294. These residues are also essential for π-electron stacking interaction with an entering substrate. Alanine scanning of aromatic residues in the substrate channel resulted in a change in substrate specificity of PsAMADH2 (Kopečný *et al*., 2011). Since the crystal structure of complex between protein and aldehyde substrate is hard to come by and no structure of OsBADH is available**;** therefore, to gain a better understanding of the substrate specificity, molecular docking and molecular dynamics simulation were carried out.

5. Molecular docking analysis of OsBADH1 and OsBADH2

In order to visualize the spatial arrangement of the substrate in the substrate binding pocket, molecular modeling of wild-type and mutants was carried out. To date, the crystal structure of BADH in rice has not been reported in PDB database. However, the condition to obtain the crystal of OsBADH in complex with NAD^+ was reported and the crystal structure of OsBADH2 was solved at 2.95 Å (Kuaprasert *et al*., 2011). In order to validate this crystal structure, the comparison between the

Copyright by Kasetsart University All rights reserved

crystal structure and the modeled structure was carried out. Therefore, the crystal structure of OsBADH2 can be used as a template to create OsBADH1. The structure of OsBADH1 containing 498 residues (residues 8–504) was then modeled by SWISS-MODEL. The quality of the modeled OsBADH1 was evaluated using the program PROCHECK (Laskowski *et al*., 1993). A ramachandran plot is a plot of the torsional angles, phi (φ) and psi (ψ), of the amino acid residues in a peptide. Phi (φ) and psi (ψ) angles represent the rotation of the main chain N-C_α and C_α-C bonds in a polypeptide, respectively. There are four regions in Ramachandran plot, including red for most favored regions, yellow for additional allowed regions, cream for generously allowed regions, and white for disallowed regions, respectively (Laskowski *et al*., 1993). The red regions, corresponding to the possible conformation without the steric clashes between atoms, represent the alpha-helical and beta-sheet conformations. The yellow regions show that the atoms are allowed to be a little closer together while the cream regions correspond to the atoms being closer together than those in the yellow regions. The white regions represent the steric clash which is not allowed for all amino acids except glycine.

The OsBADH1 model possesses good geometry, with 85% of all residues in the most favored and 14.6% in the allowed regions of the Ramachandran plot as indicated in Figure 45. The RMSD value between OsBADH1 and PsAMADH2 was 0.57 Å. Subsequently, the molecular docking of either OsBADH1 or OsBADH2 wild-type and mutants was performed as described in methodology section.

Copyright by Kasetsart University All rights reserved

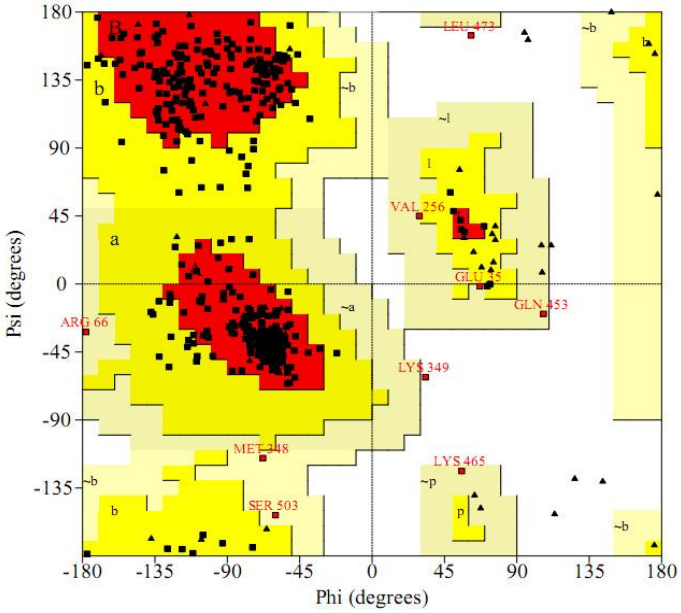

Figure 45 Ramachadran plot of OsBADH1 model. The red, yellow, cream and white regions represent the residues in most favored regions, additional allowed regions, generously allowed regions and disallowed regions, respectively.

To confirm the reliable of the result from molecular docking, the structure of OsBADH-substrate complexes from docking was superimposed with the structure of PsAMADH1 (PDB entry 3IWK) (Tylichová *et al*., 2010) using PyMol (Delano, 2002). As can be seen in Figure 46, the position of both Bet-ald and GAB-ald overlaps well with a glycerol molecule in PsAMADH1, which is close to the catalytic cysteine and mimics a substrate bound to the substrate binding site. Moreover, the carbonyl aldehyde in both substrates is aligned closely to the catalytic cysteine. According to the binding energy, GAB-ald displayed the lowest binding energy of the OsBADH-substrate complexes than Bet-ald, indicating that GAB-ald is likely to bind both OsBADH1 and OsBADH2 with high affinity (Table 18).

Copyright by Kasetsart University All rights reserved

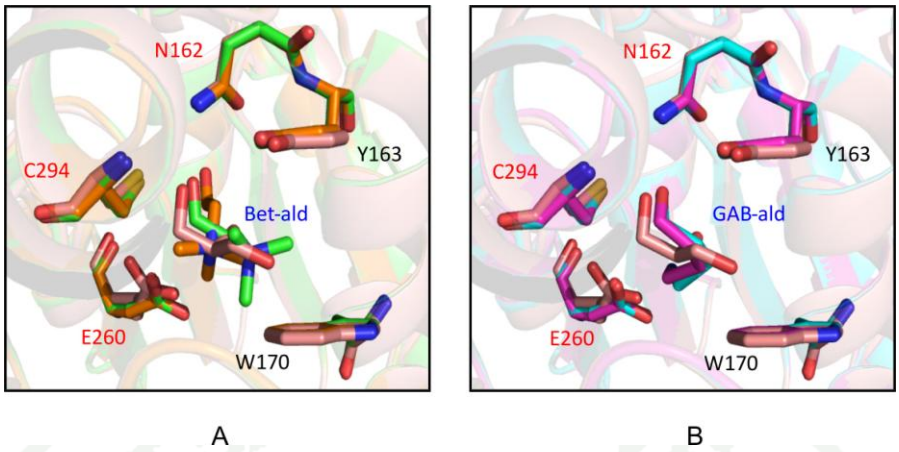

Figure 46 Superposition of OsBADH complexes from docking and PsAMADH1. (A) PsAMADH1 and OsBADHs with Bet-ald (B) PsAMADH1 and OsBADHs with GAB-ald. The amino acid residues of PsAMADH1 and glycerol are depicted in stick representation and colored by atoms (carbon, salmon). The color of OsBADH1-Bet-ald complex, OsBADH2-Bet-ald complex, OsBADH1-GAB-ald complex and OsBADH2-GAB-ald complex is shown in green, orange, cyan and magenta, respectively for carbon atoms. The red letter represents the catalytic triad residue of PsAMADH1 including C294, E260 and N162; the blue letter represents the aldehyde substrates whereas the black letter represents W170 and Y163 involved in the substrate recognition (*P. sativum* numbering).

Table 18 The lowest binding energy of wild-type and mutant OsBADHs from docking

Binding energy (kcal/mol)					
OsBADH1			OsBADH2		
	Bet-ald	GAB-ald		Bet-ald	GAB-ald
Wild-type	-3.66	-5.15	Wild-type	-4.03	-5.40
N164A	-3.78	-4.99	N162A	-4.07	-5.30
W172A	-3.68	-5.00	W170A	-3.83	-5.17
W172F	-3.81	-5.15	W170F	-4.00	-5.35

Copyright by Kasetsart University All rights reserved

The binding pockets of OsBADH1 and OsBADH2 in complex with Bet-ald and GAB-ald are shown in Figure 47 and Figure 48 with the hydrogen bonding analysis. It can be seen that the carbonyl group of Bet-ald can form two moderate to strong hydrogen bonds between the N-H main chain of C296 and the N-H side chain of N164 in OsBADH1-Bet-ald complex (Figure 47A) with a distance of 1.9 Å for C296 and 2.3 Å for N164. In N164A-OsBADH1-Bet-ald complex, the hydrogen bond between the N-H side chain of N164 and the carbonyl group of Bet-ald was abolished when residue N164 was replaced with alanine (Figure 47B). In W172A and W172F-OsBADH1-Bet-ald complexes, two strong hydrogen bonds were also observed as the same manner as those in wild-type OsBADH1 (Figure 47C). However, the distances of hydrogen bonds formed in all mutants were slightly longer than those observed wild-type. It is important to note that the tertiary amine group of Bet-ald was positioned away from the mutated residue whereas the oxygen was positioned toward the catalytic cysteine. Unlike OsBADH1-Bet-ald complex, four hydrogen bonds can be determined in wild-type OsBADH1-GAB-ald (Figure 47D) and W172A-OsBADH1-GAB-ald. Five hydrogen bonds are observed in W172F in complex with GAB-ald (Figure 47F). In OsBADH1 mutants – GAB-ald complex, the hydrogen bond between the N-H side chain of N164 and the carbonyl group of GAB-ald was also disturbed when residue N164 was changed to alanine (Figure 47E). Higher numbers of hydrogen bonds in GAB-ald complex collaborate well with the kinetic results in which the K_m values for GAB-ald are slightly lower than those for Bet-ald (Table 15). It is also noted that the amino group in GAB-ald is pointed toward E262 instead of W172. This therefore revealed the difference in the substrate recognition of OsBADH1.

In comparison to the OsBADH1-Bet-ald complex, similar patterns of hydrogen bond network were observed in the OsBADH2-Bet-ald complex. The N-H main chain of C294 and the N-H side chain of N162 can form hydrogen bonds with the oxygen carbonyl group of Bet-ald as seen in the OsBADH1 complex (Figure 48A). Similar to OsBADH1, the N162A mutation caused the loss of hydrogen bond (Figure 48B) but the same pattern of hydrogen bonds is observed in the W170A and W170F complexes (Figure 48C).

Copyright by Kasetsart University All rights reserved

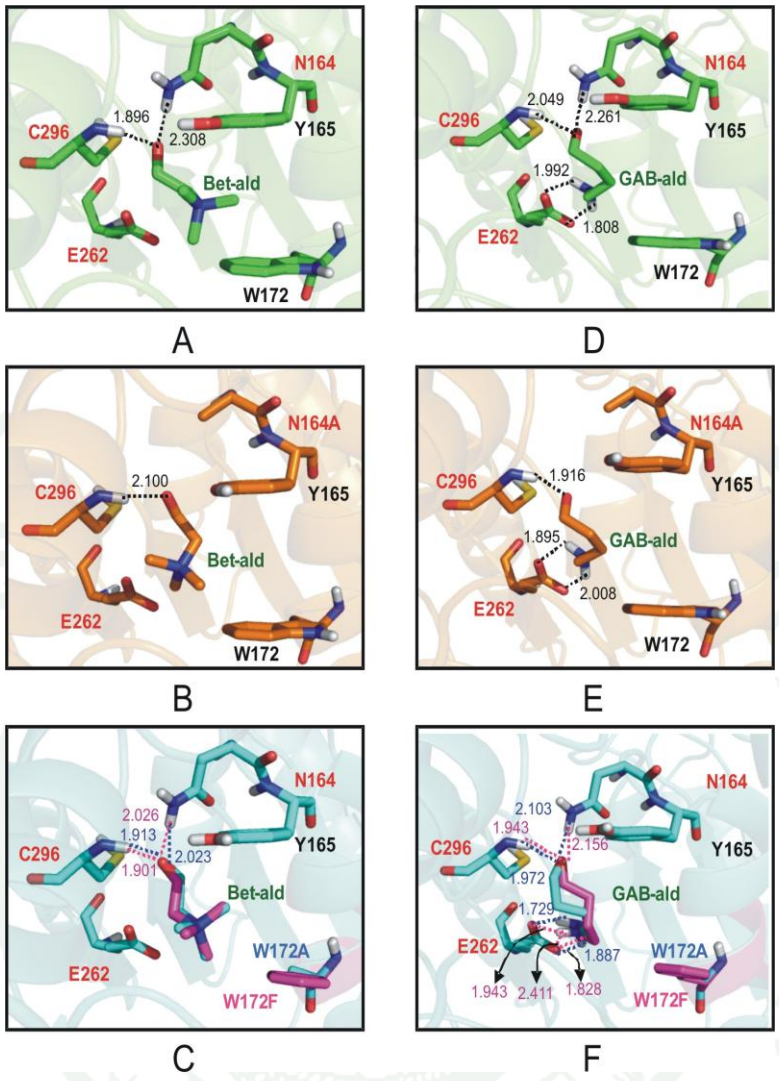

Figure 47 Molecular docking analysis of OsBADH1 complex. (A) OsBADH1 with Bet-ald (B) N164A with Bet-ald (C) W172A and W172F with Bet-ald (D) OsBADH1 with GAB-ald (E) N164A with GAB-ald (F) W172A and W172F with GAB-ald. The H-bonds are shown in dot line. The color of OsBADH1, N164A, W172A and W172F is shown in green, orange, cyan and magenta, respectively for carbon atoms. The red letter represents the catalytic triad residue of OsBADH1 including C296, E262 and N164. The green letter represents the aldehyde substrates, Bet-ald and GAB-ald. Distances are in angstrom.

Copyright by Kasetsart University All rights reserved

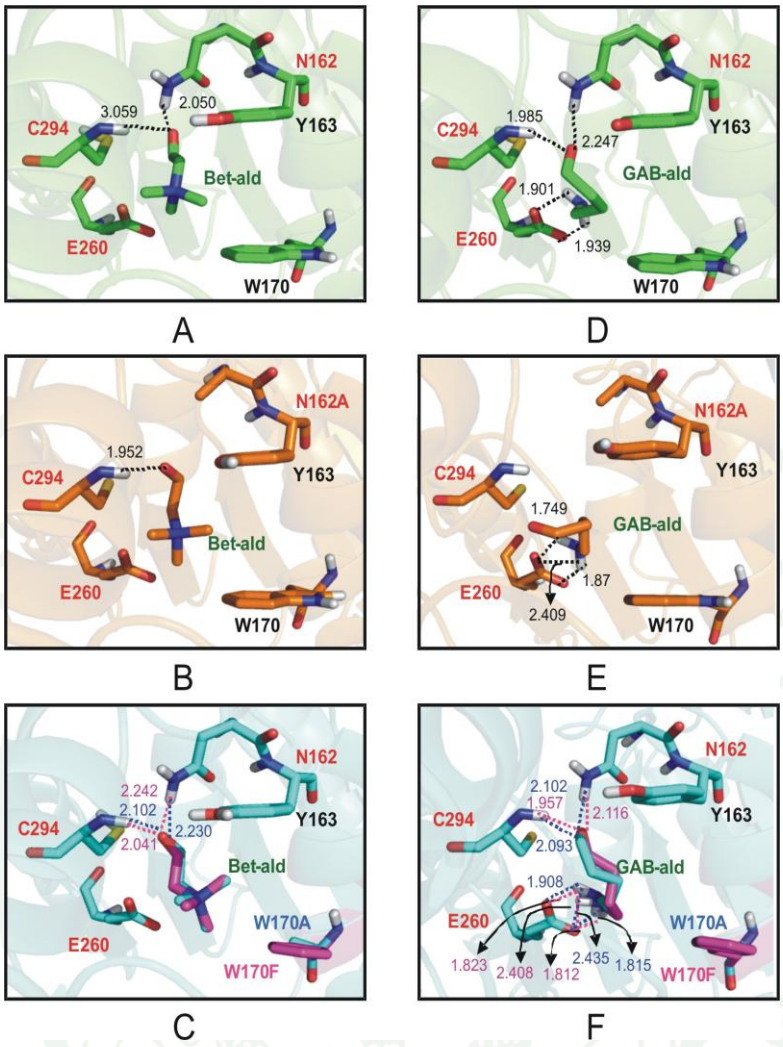

Figure 48 Molecular docking analysis of OsBADH2 complex. (A) OsBADH2 with Bet-ald (B) N162A with Bet-ald (C) W170A and W170F with Bet-ald (D) OsBADH2 with GAB-ald (E) N162A with GAB-ald (F) W170A and W170F with GAB-ald. The H-bond was shown in dot line. The color of OsBADH2, N162A, W170A and W170F is shown in green, orange, cyan and magenta, respectively for carbon atoms. The red letter represents the catalytic triad residue of OsBADH2 including C294, E260 and N162. The green letter represents the aldehyde substrates, Bet-ald and GAB-ald. Distances are in angstrom.

Copyright by Kasetsart University All rights reserved

For the OsBADH2-GAB-ald complex, four hydrogen bonds can be found between GAB-ald and residues C294, N162 and E260 (Figure 48D). It is noteworthy that two hydrogen bonds between N-H of GAB-ald and the carboxyl group of E260 are only detected in the complex with GAB-ald. However, in N162A- GAB-ald complex, only hydrogen bonds between the side chain of E260 and Bet-ald are observed (Figure 48E). On the other hand, five hydrogen bonds are observed in both W170A-GAB-ald and W170F-GAB-ald complex (Figure 48F). To further study the binding mode of both Bet-ald and GAB-ald to wild-type OsBADHs as well as to determine the interactions involving in the protein–ligand complex, four complexes of the wild-type enzymes (OsBADH1-Bet-ald, OsBADH1-GAB-ald, OsBADH2-Bet-ald and OsBADH2-GAB-ald) obtained from the docking experiment were used for molecular dynamics (MD) simulations.

6. Molecular dynamics (MD) simulations of OsBADH1 and OsBADH2

6.1 The RMSD of OsBADH1 and OsBADH2 complexes

Structural and dynamics studies of both OsBADHs with the ligand aldehyde substrates were carried out by MD simulations. The OsBADH complex contained the OsBADH proteins, NAD^+, and the aldehyde substrates. The trajectories of four simulation systems: OsBADH1-Bet-NAD^+, OsBADH1-GAB-NAD^+, OsBADH2-Bet-NAD^+ and OsBADH2-GAB-NAD^+, were analyzed for the last 500 ps after the models reached equilibrium. The RMSD fluctuations of the OsBADH complexes were observed to determine the structural equilibrium (Figure 49). In the OsBADH1 and OsBADH2 complexes, the RMSD of the complex and the OsBADH receptors are similar. The RMSD of OsBADH1-Bet-ald and OsBADH1-GAB-ald complex was obtained with average values of 2.75 Å (Figure 49A) and 3.8 Å (Figure 49B) with fluctuations of 0.25 and 0.5 Å, respectively. These low fluctuations indicated that both complexes and receptors were stable in the equilibrium. For the OsBADH2 complex, RMSD fluctuations of the OsBADH2-Bet-ald complex was around 2.7 ± 0.2 Å (Figure 49C) whereas that of the OsBADH2-GAB-ald complex was 3.2 ± 0.3 Å (Figure 49D); this indicates both complexes and the receptors reached the equilibrium.

Copyright by Kasetsart University All rights reserved

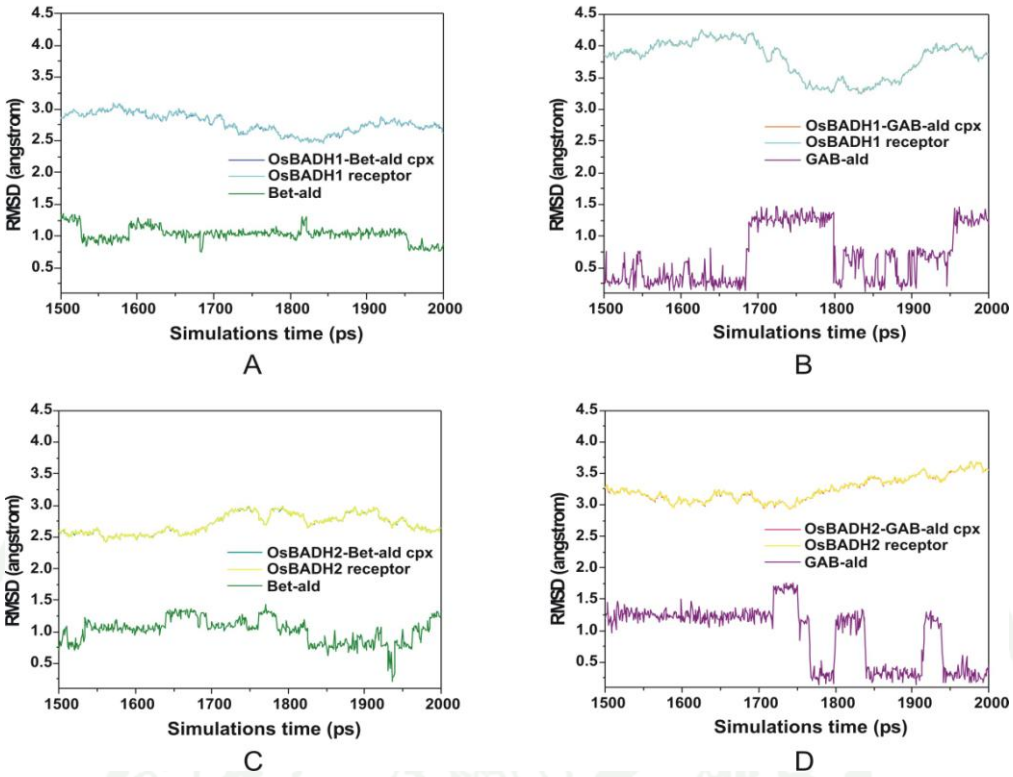

Figure 49 RMSD of OsBADH complexes. (A) OsBADH1-Bet-ald (B) OsBADH1-GAB-ald (C) OsBADH2-Bet-ald and (D) OsBADH2-GAB-ald.

For the ligands in the complexes, their equilibrium RMSDs show different characteristics in dynamics in that GAB-ald in both complexes displays RMSD fluctuation with a value around 0.5-1.5 Å whereas Bet-ald has a slightly constant RMSD fluctuation than GAB-ald with a value around 1 Å. Overall, the results confirmed that all components were well in equilibration state throughout the analysis range; therefore, the next sections are focused on the binding energy of the complex as well as the preferable binding sites of each substrate.

6.2 Binding energy of OsBADH1 and OsBADH2 complexes

The thermodynamic properties in the binding process between OsBADHs-Bet-ald and OsBADHs-GAB-ald are presented in Table 19. Considering the energy components involved in the binding, the simulation models can be separated into two sets by the ligand driven force for the interaction. Set I was the binding of OsBADHs

Copyright by Kasetsart University All rights reserved

with Bet-ald. The important interactions for these models were electrostatic interactions (ΔE_{ELE}), which played a major role as the main attractive force (-239.51 kcal/mol for OsBADH1 and -224.06 kcal/mol for OsBADH2). The *van der Waal* interactions in the gas phase (ΔE_{VDW}) were the second most important energy component for this binding (-20.53 kcal/mol for OsBADH1 and -17.66 kcal/mol for OsBADH2). Set II contained the binding of OsBADHs with GAB-ald. Unlike OsBADHs-Bet-ald, the electrostatic interaction was not the main interaction. The electrostatic interactions for OsBADH1 and OsBADH2 were -22.62 and -22.67 kcal/mol, respectively while the *van der Waal* interaction was -17.74 kcal/mol for OsBADH1 and -19.05 kcal/mol for OsBADH2. It is noted that the nonpolar interaction of solvation ($\Delta\Delta G_{SA}$) of four complexes is lower than the *van der Waal* interaction in gas phase (ΔE_{VDW}). This perhaps may be caused by the hydrogen bonding interactions during complex formation, resulting in the reduction of the polar surface exposed to water solvent. Additionally, the unfavorable energy component might have resulted from the electrostatic contributions of solvation ($\Delta\Delta G_{PB}$), which are 246.01, 24.66, 227.09 and 28.64 kcal/mol for OsBADH1-Bet-ald, OsBADH1-GAB-ald, OsBADH2-Bet-ald and OsBADH2-GAB-ald, respectively. The positive solvation energy suggested that the individual components interacted with water molecules more than their complex form. Thus, these hinder the binding between OsBADHs and the substrates. According to the total binding energy of OsBADH1-ligand complexes, GAB-ald was represented as a higher potential ligand for OsBADH1 than Bet-ald with $\Delta\Delta G_{MM/PBSA}$ of -18.34 kcal/mol, which agreed well with the kinetic result. However the binding energy of OsBADH2-Bet-ald (-17.65 kcal/mol) was stronger than OsBADH2-GAB-ald (-15.78 kcal/mol), which slightly dissented with the kinetic data.

Copyright by Kasetsart University. All rights reserved

Table 19 The binding free energy of four trajectories from OsBADH1-Bet-ald, OsBADH1-GAB-ald, OsBADH2-Bet-ald and OsBADH2-GAB-ald systems.

Energy (kcal/mol)	OsBADH1		OsBADH2	
	Bet-ald	GAB-ald	Bet-ald	GAB-ald
ΔE_{ELE}[a]	-239.51	-22.62	-224.06	-22.67
ΔE_{VDW}[b]	-20.53	-17.74	-17.82	-19.05
$\Delta\Delta G_{SA}$[c]	-2.85	-2.65	-2.85	-2.70
$\Delta\Delta G_{PB}$[d]	246.01	24.66	227.09	28.64
$\Delta\Delta G_{MM/PBSA}$[e]	-16.88	-18.34	-17.65	-15.78

[a] Electrostatic energy.

[b] van der Waals energy.

[c] Nonpolar contribution to solvation.

[d] Electrostatic contribution to solvation.

[e] Total binding energy.

To confirm our result, the simulation experiments were carried out three times and the similar results were obtained. While the binding energy from docking in which the conformation of receptors is rigid correlated well with the kinetic result, MD simulations providing flexibility of both receptors and ligands revealed a slightly different binding energy. This suggested that the dynamics of OsBADHs and the aldehyde substrates significantly affected the binding event. The conformational changes of the amino acid residues around the binding site of OsBADH2 are discussed in the next section. However, it seems that relative energy between OsBADH-Bet-ald and OsBADH-GAB-ald from molecular docking and molecular dynamics simulations were comparable. The binding energy difference between OsBADH1-Bet-ald and OsBADH1-GAB-ald complex obtained from molecular docking was 1.49 kcal/mol and from MD simulation was 1.46 kcal/mol, whereas that between OsBADH2-Bet-ald and OsBADH2-GAB-ald complex was 1.37 and 1.87 kcal/mol from molecular docking and MD simulation, respectively.

Copyright by Kasetsart University All rights reserved

According to the docking analysis, the arrangement of the ligand in the complex was initially revealed; however, the binding free energy was still not accurate due to the fact that the backbone of the protein was fixed in the docking resulting in the higher binding energy. Unlike molecular docking, MD simulation allows the protein-ligand complex to be fully relaxed in the solvent environment, therefore generating more reliable binding properties. In the OsBADH1 system, the OsBADH1-GAB-ald complex showed the lowest binding energy from docking and exhibited the best binding from molecular dynamics simulation. However, in the OsBADH2 system, the OsBADH2-GAB-ald complex gave the lowest binding energy from docking but not from MD simulation. In order to understand this difference, hydrogen bonding interactions and MMGBSA decomposition of the binding energy were considered.

6.3 Protein-ligand interactions of OsBADH1 and OsBADH2 complexes

According to MD simulation, the statistical analysis was applied to observe the equilibrium distance and hydrogen bonding interactions. Some atoms of the ligands and the receptors moved closer to or further from each other in equilibrium due to the dynamics in the binding process. The conformation of either Bet-ald or GAB-ald upon binding to both OsBADH complexes was examined (Figure 50). In OsBADH1-Bet-ald, only one hydrogen bond was observed (Figure 50A) between the main chain of C296 (N) and the oxygen atom (O) of Bet-ald with an average distance of 2.91 Å. In OsBADH1-GAB-ald, four hydrogen bonds observed are the following (Figure 50B): E262 (O) and GAB-ald (H1), GAB-ald (N1) and W454 (HE1), GAB-ald (O1) and C296 (H) and L263 (O) and GAB-ald (H2) with average distances of 2.88, 2.90, 2.89 and 2.89 Å, respectively. In OsBADH2, no hydrogen bonds were observed for Bet-ald (Figure 50C) but five hydrogen bonds were observed for GAB-ald (Figure 50D). The five hydrogen bonds in the OsBADH2-GAB-ald complex contained GAB-ald (O1) and C294 (H), L261 (O) and GAB-ald (H2), GAB-ald (O1) and N162 (HD21), GAB-ald (N1) and W456 (HE1) and E260 (O) and GAB-ald (H1) with average distances of 2.87, 2.89, 2.91, 2.92 and 2.91 Å, respectively. In the light of the MD simulation, it was revealed that GAB-ald formed stronger hydrogen bonds than Bet-ald with the OsBADH1. As for OsBADH2,

Copyright by Kasetsart University All rights reserved

five hydrogen bonds were formed in the OsBADH2-GAB-ald complex while none was observed in OsBADH2-Bet-ald complex.

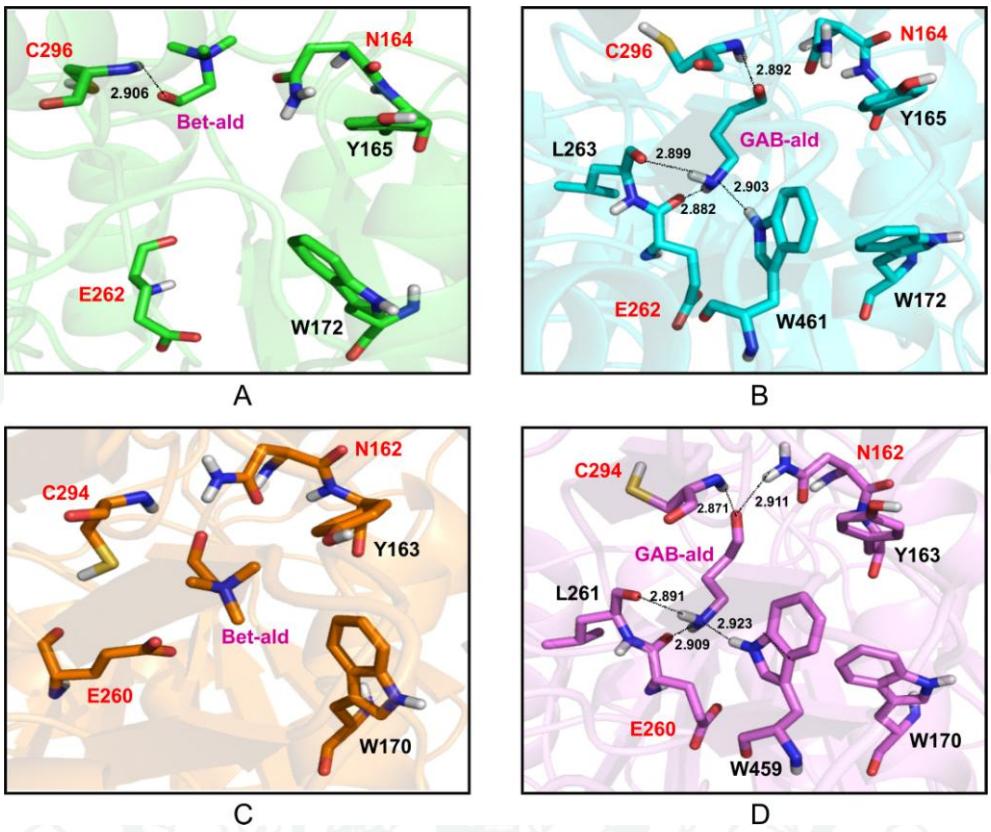

Figure 50 Active site of OsBADH-ligand complexes from MD simulations. (A) OsBADH1-Bet-ald (B) OsBADH1-GAB-ald (C) OsBADH2-Bet-ald (D) OsBADH2-GAB-ald. The hydrogen bonds are shown in dot line. The color of OsBADH1-Bet-ald, OsBADH1-GAB-ald, OsBADH2-Bet-ald and OsBADH2-GAB-ald is shown in green, cyan, orange and magenta, respectively for carbon atoms. The red letter represents the catalytic triad residues of OsBADH1 including C296, E262 and N164 whereas OsBADH2 including C294, E260 and N162. The pink letter represents the aldehyde substrates, Bet-ald and GAB-ald. Distances are in angstrom.

Copyright by Kasetsart University All rights reserved

In addition to hydrogen bond formation, relationships between the orientation of the Bet-ald and GAB-ald in the complex were different. First, Bet-ald in OsBADH1 complex was far away from the catalytic triad compared with that in OsBADH2 complex. It is important to note that the position of Bet-ald observed in the crystal structure of BADH in *E. coli* was also different from that in PaBADH (Gruez *et al*., 2004; González-Segura *et al*., 2009). Secondly, when looking at the two substrates, GAB-ald was located closer to the catalytic residue, E262 compared to Bet-ald. This finding here was in agreement with the previous work, reporting that BADH catalyzes GAB-ald (C3-C6 aminoaldehydes) better than Bet-ald (Mitsuya *et al*., 2009; Tylichová *et al*., 2010).

6.4 Energy decomposition of the binding energy

To gain more details in the energy of binding, interactions between ligand and surrounding residues within 5 Å were observed through decomposition energy using MMGBSA (Molecular Mechanics-Generalized Born Surface Area) method as implemented in AMBER10. Eighteen residues within 5 Å radius of each OsBADH complexes interacting with the substrate aldehydes were observed (Table 20 and 21) and the interaction energies were shown in Table 22. When amino acid sequences of both OsBADHs were aligned (Figure 28), most of these residues are conserved except for two following residues: residue 290 (Ala in OsBADH1 and Trp in OsBADH2) and residue 295 (Val in OsBADH1 and Ile in OsBADH2). It is interesting to note that a change from aliphatic to aromatic amino acids was seen at position 290 while at position 295 a change is within the same group of amino acids (Val to Ile). The interactions between ligand and the selection of eighteen residues were calculated as shown in Figure 51. It can be seen that three residues (W163, N164 and C296) mainly interact with Bet-ald in OsBADH1 complex in which the interaction energy of W163 and N164 was higher than those in the other complexes with values of -3.88 and -4.28 kcal/mol, respectively (Figure 51A). Additionally, interaction with Q294 and F397 (-1.42 and -1.27 kcal/mol) were also important for OsBADH1-Bet-ald interaction. However, in OsBADH1-GAB-ald, E262, L263, C296 and W461 are the main residues for the attractive interaction with GAB-ald, with interaction energies of -2.8, -2.16, -2.87 and -4.34 kcal/mol, respectively. Remarkably, N164, one of the catalytic

Copyright by Kasetsart University All rights reserved

triad, is also important for OsBADH1-GAB-ald (-1.17 kcal/mol); this was not observed from docking experiments.

In the case of OsBADH2-Bet-ald, decomposition energy provided an interesting result. Six residues showing strong attractive interactions with Bet-ald include Y163, M167, W170, E260, S295 and C453 with interaction energies of -2.46, -3.29, -2.46, -14.21, -3.06 and -2.64 kcal/mol, respectively (Figure 51B). It is noteworthy that E260 becomes the main residue having strong interactions with Bet-ald in this complex, suggesting the negative charge side chain of E260 interacts with the positive charge of the quaternary ammonium of Bet-ald. For OsBADH2-GAB-ald, four residues interact with GAB-ald including E260, L261, C294 and W459, with energies of -2.07, -2.4, -2.99 and -3.17 kcal/mol, respectively. This observation is in agreement with the result that four residues can form hydrogen bonds in the structure and that N162 is important for OsBADH2-GAB-ald (-1.93 kcal/mol).

Taken together, the data from Figure 51 indicates that the interactions involving both OsBADH1-GAB-ald and OsBADH2-GAB-ald complexes are relatively similar. GAB-ald usually interacts with amino acid residues, N164, M169, E262, L263, V295, C296 and W461 in OsBADH1 and N162, M167, E260, L261, I293, C294 and W459 in OsBADH2, with the same position of the amino acid but a different spatial arrangement of GAB-ald. In contrast with GAB-ald, the interaction of Bet-ald in the complex is varied and a different spatial arrangement of Bet-ald was observed both in our MD and in the crystal structure of BADH in *E. coli* (Gruez *et al*., 2004). This discrepancy may have stemmed from the fact that Bet-ald carries a positive charge and less hydrogen bond are observed in the complex, leading to the large movement of the molecule, whereas GAB-ald can form several hydrogen bond networks to the enzyme thus generating a more rigid position in the substrate binding site.

Copyright by Kasetsart University All rights reserved

Table 20 Amino acid residues within 5 Å radius of OsBADH1-substrate complexes

Substrate	OsBADH1																	
	W163	N164	Y165	M169	W172	G240	E262	L263	G264	A290	Q294	V295	C296	S297	F397	L423	C455	W461
Bet-ald	+	+	-	+	-	+	-	-	+	-	+	+	+	-	+	-	-	-
GAB-ald	-	+	+	+	-	+	+	+	+	-	-	+	+	+	+	+	-	+

Table 21 Amino acid residues within 5 Å radius of OsBADH2-substrate complexes

Substrate	OsBADH2																	
	W161	N162	Y163	M167	W170	G238	E260	L261	G262	W288	Q292	I293	C294	S295	F395	L421	C453	W459
Bet-ald	-	+	+	+	+	-	+	-	-	+	-	+	+	+	-	+	+	+
GAB-ald	-	+	-	+	-	+	+	+	+	-	-	+	+	-	+	+	-	+

Presence (+) or absence (-) of residue within 5 Å radius of OsBADH complexes is shown in each indicated structure.

Copyright by Kasetsart University All rights reserved

Table 22 The interaction energy of amino acid residues within 5 Å radius of OsBADH-substrate complexes

Interaction energy (kcal/mol)					
Residue	OsBADH1-Bet-ald	OsBADH1-GAB-ald	Residue	OsBADH2-Bet-ald	OsBADH2-GAB-ald
W163	-3.88	-0.12	W161	-0.09	-0.13
N164	-4.28	-1.17	N162	-0.3	-1.93
Y165	-0.24	-0.37	Y163	-2.46	-0.78
M169	-0.93	-1.6	M167	-3.29	-1.5
W172	-0.06	-0.1	W170	-2.46	-0.06
G240	0	-0.8	G238	-0.15	-1.88
E262	-0.13	-2.8	E260	-14.21	-2.07
L263	0	-2.16	L261	-0.35	-2.4
G264	-0.59	-1.08	G262	0	-0.4
A290	-0.03	0	W288	-0.59	-0.02
Q294	-1.42	-0.11	Q292	-0.07	-0.05
V295	-0.76	-1.51	I293	-1.56	-2.29
C296	-2.75	-2.87	C294	-1.76	-2.99
S297	-0.21	-0.28	S295	-3.06	-0.34
F397	-1.27	-1.06	F395	-0.14	-0.51
L423	-0.03	-1.21	L421	-0.14	-1.14
C455	0	-0.01	C453	-2.64	-0.01
W461	-0.07	-4.34	W459	-1.4	-3.17

Copyright by Kasetsart University All rights reserved

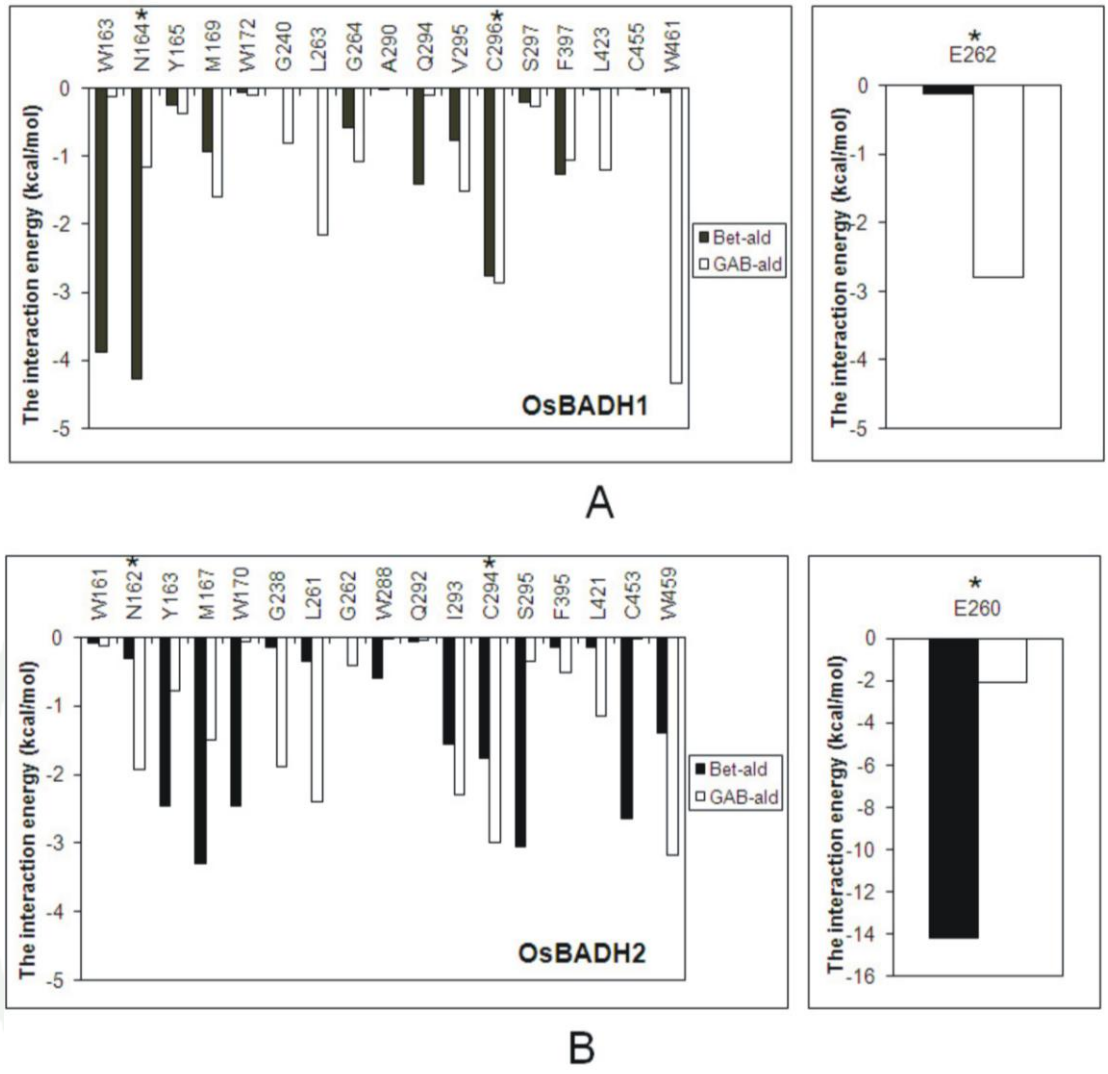

Figure 51 The decomposition of binding free energy between ligand aldehyde and amino acid residues within 5 Å radius of OsBADH active site. (A) OsBADH1 (B) OsBADH2. The asterisk represents the catalytic triad residues.

According to our result, the difference in amino acid residues of OsBADH1 (A290) and OsBADH2 (W288) may account for the substrate recognition between both OsBADHs. W288 of OsBADH2 can interact well with Bet-ald (-0.59 kcal/mol) but not GAB-ald. It has been proposed that W288 in PsAMADH2 affects the affinity of the enzyme without affecting the reaction rate (Kopečný *et al*., 2011). However, this residue is also different between PsAMADH1 and PsAMADH2 (F288 for PsAMADH1 and W288 for PsAMADH2) (Tylichová *et al*., 2010). The W288 side

Copyright by Kasetsart University All rights reserved

chain of PsAMADH2 reduces the volume of the substrate channel compared to F288 of PsAMADH1 (Tylichová *et al*., 2010). Therefore, this residue may be key to the differences in substrate specificity observed among plant AMADH isoforms (Kopečný *et al*., 2011). In the comparison of W288 of OsBADH2 and A290 of OsBADH1, W288 reduces the volume of the substrate channel compared to A290 of OsBADH1. Bet-ald in OsBADH2 complex can interact with W288 through π electron interactions between the positive charge of the quaternary ammonium and the negative charge of the W288 indole ring while in OsBADH1, this position is replaced by A290, which cannot form any interaction with Bet-ald (Kopečný *et al*., 2011). Consistent with the results from PsAMADHs, W288 is the key residue in the recognition and importance for the substrate specificity in OsBADH isoforms in rice.

6.5 Relationship between kinetics and MD results

This section described the comparison between the kinetics results and the interaction energies of OsBADHs-complexes obtained from MD. For OsBADH1-Bet-ald complex, Bet-ald was far away from the active site, N164 and W172 residues, compared with the position of glycerol in PsAMADH so it was impossible to compare the results between kinetics and MD. For OsBADH1-GAB-ald complex, the interaction energies of N164 and W172 for GAB-ald were -1.17 and -0.1 kcal/mol, respectively (Table 21). According to kinetics results, the change of N164 to alanine affected k_{cat} and k_{cat}/K_m value for GAB-ald by 13.5 and 2.1-fold, respectively less than that of wild-type, whereas the mutation at W172 did show the same effect on k_{cat} and k_{cat}/K_m value for GAB-ald. Therefore, the kinetics results were in well agreement with the MD results that GAB-ald formed less interactions with W172, but much stronger with N164.

In OsBADH2-Bet-ald complex, the interaction energies of N162 and W170 for Bet-ald were -0.3 and -1.93 kcal/mol, respectively (Table 21). The mutation at N162 to alanine brought about the reduction in k_{cat} and k_{cat}/K_m value with 6 and 1.6-fold less compared to wild-type, while the mutation in W170 reduced k_{cat} and k_{cat}/K_m value by 8 and 2.4-fold compared to wild-type. These kinetics results correlated well with MD results in that Bet-ald formed slightly interactions with N162, but strong

Copyright by Kasetsart University All rights reserved

interaction with W170. The W172A mutation had more effect on k_{cat} and k_{cat}/K_m value than the N164 mutation. For OsBADH2-GAB-ald, the interaction energies of N162 and W170 for GAB-ald were -2.46 and -0.06 kcal/mol, respectively (Table 21). The k_{cat}/K_m values of N162A and W170A mutant reduced with 7.5 and 4.9-fold, respectively, compared to wild-type. These kinetics results again agreed with the MD results in that GAB-ald in OsBADH2 showed strong interactions to N162, but fewer interactions to W170.

Collectively, the kinetics results revealed that the mutation at both N164 and W172 of OsBADH1 and N162 and W170 of OsBADH2 exhibited a marked effect to k_{cat} than K_m values. The mutants can catalyze the oxidation of substrate aldehyde lower than the wild-type, indicating that these residues may be important for enzyme catalysis. The kinetics results from our study are in agreement with the MD results in that the residues with strong interaction energies may be vital for enzyme catalysis. According to our results, mutations of residues with strong interaction energies can result in the greater reduction in the catalytic efficiency of the enzyme compared to the mutation of the residues with less interaction energies.

6.6 Conformation of the catalytic Cysteine and Glutamate

The conformation of catalytic Cys and Glu was observed from MD simulations of the OsBADH-ligand complexes. According to the previous study, the catalytic Cys residue can adopt two conformations: the “resting” conformation in which the Cys residue is far from the carbonyl carbon of the bound aldehyde (González-Segura *et al*., 2009), and the “attacking” conformation in which the Cys residue is close to this carbon in the correct position to perform the nucleophilic attack (Perez-Miller and Hurley, 2003). In the case of the catalytic Glu residue, three possible conformations have been observed: the “inside” conformation in which the Glu residue can activate the catalytic Cys residue for nucleophilic attack, since its carboxyl group is close to the thiol (Perez-Miller and Hurley, 2003; Gruez *et al*., 2004), the “intermediate” conformation in which the Glu residue is suited for the activation of the hydrolytic water molecule (Perez-Miller and Hurley, 2003; González-Segura *et al*., 2009), and the “outside” conformation in which the catalytic

Copyright by Kasetsart University All rights reserved

Glu releases the proton that was previously taken from either the catalytic Cys or a hydrolytic water involved in the proton relay mechanism (Perez-Miller and Hurley, 2003; González-Segura *et al*., 2009). The conformations of both catalytic residues from PaBADH (PDB codes 2WME) (González-Segura *et al*., 2009) and ALDH2 (PDB codes 1O02) (Perez-Miller and Hurley, 2003) are shown in Figure 52.

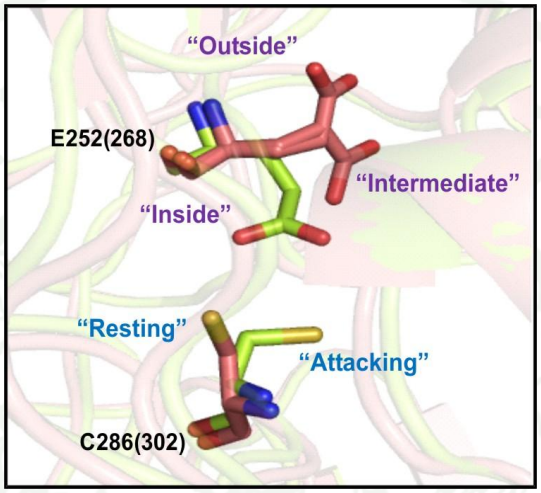

Figure 52 ALDH active sites. The distinct conformations of the catalytic Cys (resting and attacking) and catalytic Glu (inside, intermediate and outside) are displayed. The numbers of the residues correspond to PaBADH (2WME) and those within parenthesis to ALDH2 (1O02). Side chain atoms of residues are shown in stick and colored by atoms (PaBADH carbon: salmon pink, and ALDH2 carbon: lemon green).

The catalytic Cys (C286) in PaBADH is in the "resting" conformation and the catalytic Glu (E252) is found in both "outside" and "intermediate" conformations whereas in ALDH2 the catalytic Cys (C302) is found in the "attacking" conformation and the catalytic Glu (E268) is in "inside" conformation. When the structure of PaBADH is compared with the structure of ALDH2 and with OsBADH complexes from MD (Figure 53), it is revealed that the catalytic Glu residue in all structures exists in the "outside" conformation whereas the catalytic Cys residue is found in the "resting" conformation with the exception of the catalytic Glu residue of OsBADH2-Bet-ald complex that exists in an "inside" conformation.

Copyright by Kasetsart University All rights reserved

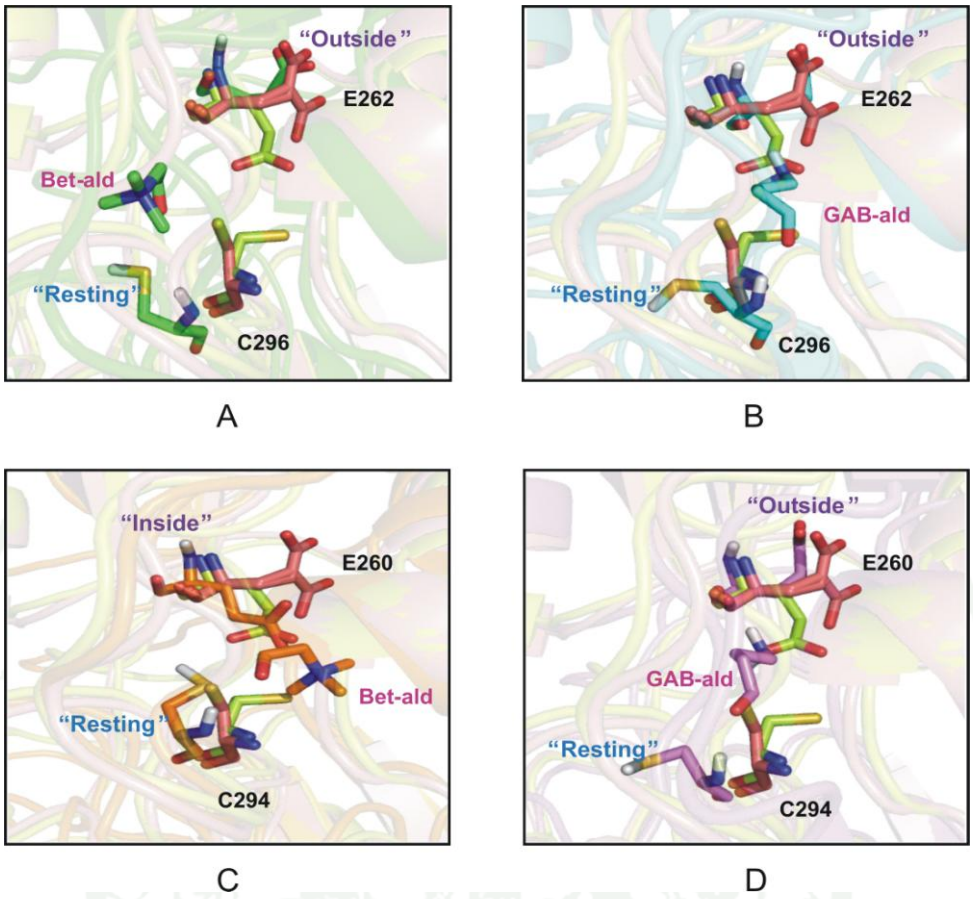

Figure 53 The conformations of active site residue in OsBADH-substrate complexes from MD simulations compared to PaBADH (2WME) and ALDH2 (1O02). (A) OsBADH1 with Bet-ald (B) OsBADH1 with GAB-ald (C) OsBADH2 with Bet-ald (D) OsBADH2 with GAB-ald. The black letter represents the catalytic residues of OsBADH1 including C296, E262 while OsBADH2 including C294, E260. The pink letter represents the aldehyde substrates, Bet-ald and GAB-ald. Side chain atoms of residue are shown in stick and colored by atoms (PaBADH carbon: salmon pink, ALDH2 carbon: lemon green, OsBADH1-Bet-ald carbon: green, OsBADH1-GAB-ald carbon: cyan, OsBADH2-Bet-ald carbon: orange, OsBADH2-GAB-ald carbon: magenta).

Copyright by Kasetsart University All rights reserved

The negatively charged side chain of the catalytic Glu residue is positioned towards the positive quaternary ammonium of Bet-ald, suggesting it may have strong electrostatic interactions, consistent with the binding energy from MMGBSA decomposition. Additionally, the difference in the conformation of the catalytic Glu residue of OsBADH1 and OsBADH2 observed from MD simulations may also bring about the substrate specificity between the two substrates and the enzymes. Collectively, the work presented here for the first time provides the structure of OsBADH in complex with the substrates generated by MD. Further studies on other residues in the substrate binding pocket to better understand the substrate specificity are in progress.

Copyright by Kasetsart University All rights reserved

CONCLUSION

In this study, we describe the kinetic analysis of OsBADH1 and OsBADH2 wild-type and mutant enzymes using Bet-ald and GAB-ald as substrates. The kinetic results indicated that the enzymes would prefer GAB-ald to Bet-ald, which is in agreement with previous studies (Bradbury *et al*., 2008; Mitsuya *et al*., 2009; Wongpanya *et al*., 2011). Out of the six mutants (N164A, W172A, W172F for OsBADH1 and N162A, W170A, W170F for OsBADH2), only W172F of OsBADH1 and W170F of OsBADH2 mutants showed a higher catalytic efficiency towards GAB-ald, indicating that this position may be important for substrate specificity towards GAB-ald. In addition to the enzyme kinetics, the binding mode between the enzymes and substrates was carried out by molecular docking followed by MD simulations of the protein–ligand complexes of wild-type OsBADHs bound with Bet-ald and GAB-ald. It is noteworthy that this is the first report to show the structure of a protein–ligand complex of OsBADHs generated by MD. MD simulations suggested that GAB-ald forms hydrogen bonds with C296, E262, L263, and W461 in OsBADH1 and C294, E260, L261, and W459 in OsBADH2 better than Bet-ald. The decomposition energy was also carried out to determine the interaction energy of the important residues within a 5 Å radius that interact with the substrates. The decomposition energy revealed that W163, N164, Q294, C296 and F397 mainly interacted with Bet-ald in the OsBADH1-Bet-ald complex while E262, L263, C296 and W461 mainly interacted with GAB-ald in the OsBADH1-GAB-ald complex. In the case of the OsBADH2-Bet-ald complex, Y163, M167, W170, E260, S295 and C453 displayed strong interactions and the strongest was with E260, suggesting that the negatively charged side chain of E260 interacts with the positively charged group of Bet-ald. For the OsBADH2-GAB-ald complex, E260, L261, C294 and W459 are shown to interact with GAB-ald, which is consistent with the hydrogen bonding analysis.

According to our data, the interactions of Bet-ald in the complex are varied in comparison with GAB-ald. This may be accounted for by a positive charge in the molecule and less hydrogen bond formation, leading to movement at various positions

Copyright by Kasetsart University All rights reserved

which can be observed in our MD result and the crystal structure of BADH in *E. coli* (Gruez *et al*., 2004). In contrast, GAB-ald can form several hydrogen bonds, leading to a fixed position in the substrate binding site. One interesting point for the substrate recognition of OsBADHs is the difference in the amino acid residues position 290 of OsBADH1 (A290) and position 288 of OsBADH2 (W288). W288 in OsBADH1 interacts with Bet-ald through π electron interactions but not with GAB-ald while A290 in OsBADH1 cannot form any interaction with the substrates. In plant PsAMADHs, the position 288 has been proposed to be the key to the differences in substrate specificity in both PsAMADHs isoforms (F288 for PsAMADH1 and W288 for PsAMADH2) (Tylichová *et al*., 2010). Therefore, W288 is also the key residue in recognition and substrate specificity in OsBADH isoforms.

Additionally, the conformation of the catalytic residues, Cys and Glu was investigated in comparison to that of PaBADH (PDB codes 2WME) (González-Segura *et al*., 2009) and ALDH2 (PDB codes 1O02) (Perez-Miller and Hurley, 2003). The result revealed that the catalytic Cys residue exists in the "resting" conformation in all structures whereas the catalytic Glu residue exists in the "outside" conformation except for Glu in OsBADH2-Bet-ald, which was found to adopt an "inside" conformation. It is suggested that the negatively charged side chain of catalytic Glu has strong electrostatic interactions with the positive quaternary ammonium of Bet-ald. This difference in the conformation of catalytic Glu residue of OsBADH1 and OsBADH2 may account for the substrate specificity between the two substrates and the enzymes.

Copyright by Kasetsart University. All rights reserved

LITERATURE CITED

Arikit, S., T. Yoshihashi , S. Wanchana, T. T. Uyen ,N. T. T. Huong, S. Wongpornchai and A. Vanavichit. 2010. Deficiency in the amino aldehyde dehydrogenase encoded by *GmAMADH2*, the homologue of rice Os2AP, enhances 2-acetyl-1-pyrroline biosynthesis in soybeans (*Glycine max* L.). **Plant Biotechnol. J.** : 1–13.

Ashraf, M. and M. R. Foolad. 2007. Roles of glycine betaine and proline in improving plant abiotic stress resistance. **Environ. Exp. Bot**. 59: 206–216.

Bouché, N. and H. Fromm. 2004. GABA in plants: just a metabolite? **Trends Plant Sci**. 9:110-115.

Boyd, L. A., L. Adam, L. E. Pelcher, A. McHughen, R. Hirji and G. Selvaraj. 1991. Characterization of *Escherichia coli* gene encoding betaine aldehyde dehydrogenase (BADH): structural similarity to mammalian ALDHs and a plant BADH. **Gene.** 103: 45-52.

Bradbury, L. M. T., T. L. Fitzgerald, R. J. Henry, Q. Jin and D. L. E. Waters. 2005. The gene for fragrance in rice. **Plant Biotechnol. J.** 3:363–370.

_____, S. Gillies, D. Brushett, D. Waters and R. Henry. 2008. Inactivation of an aminoaldehyde dehydrogenase is responsible for fragrance in rice. **Plant Mol. Biol.** 68: 439-449.

Buttery, R. G., L. C. Ling, B. O. Juliano and J. G. Turnbaugh. 1983. Cooked rice aroma and 2-acetyl-1-pyrroline. **J. Agric. Food Chem.** 31: 823–826.

Copyright by Kasetsart University All rights reserved

Chen, S., Y. Yang, W. Shi, Q. Ji, F. He, Z. Zhang, Z. Cheng, X. Liu and M. Xu. 2008. *Badh2*, encoding betaine aldehyde dehydrogenase, inhibits the biosynthesis of 2-acetyl-1-pyrroline, a major component in rice fragrance. **Plant Cell** 20: 1850-1861.

Coleman, S. T., T. K. Fang, S. A. Rovinsky, F. J. Turano and W. S. Moye-Rowley. 2001. Expression of a glutamate decarboxylase homologue is required for normal oxidative stress tolerance in *Saccharomyces cerevisiae*. **J. Biol. Chem.** 276: 244–250.

Cornell, W., P. Cieplak, C. Bayly, I. Gould, K. Merz, D. Ferguson, D. Spellmeyer, T. Fox, J. Caldwell and P. Kollman. 1995. A second generation force field for the simulation of proteins, nucleic acids, and organic molecules. **J. Am. Chem. Soc.** 117: 5179-5197.

Delano, W. L. 2002. **The PyMOL Molecular Graphics System**, Available Source: http://www.pymol.org, December 15, 2010.

Erdo, S. L. and J. R. Wolff, 1990. γ-Aminobutyric acid outside the mammalian brain. **J. Neurochem**. 54: 363-372.

Fitzgerald, T. L., D. L. E. Waters and R. J. Henry. 2009. Betaine aldehyde dehydrogenase in plants. **Plant Biology** 11: 119–130.

Foster, A. C. and J. A. Kemp. 2006. Glutamate- and GABA-based CNS therapeutics. **Pharmacology** 6: 7–17.

Fujiwara, T., K. Hori, K. Ozaki, Y. Yokota, S. Mitsuya, T. Ichiyanagi, T. Hattori and T. Takabe. 2008. Enzymatic characterization of peroxisomal and cytosolic betaine aldehyde dehydrogenases in barley. **Physiol. Plant** 134: 22-30.

Copyright by Kasetsart University All rights reserved

Gao, C. and B. Han. 2009. Evolutionary and expression study of the aldehyde dehydrogenase (ALDH) gene superfamily in rice (*Oryza sativa*). **Gene** 431: 86–94.

Gasteiger, E., Hoogland, C., Gattiker, A., Duvaud, S., Wilkins, M. R., Appel, R. D. and Bairoch, A. 2005. Protein identification and analysis tools on the expasy server. **Humana Press.** 571-607.

González-Segura, L., E. Rudiño-Piñera, R.A. Muñoz-Clares and E. Horjales. 2009. The crystal structure of a ternary complex of betaine aldehyde dehydrogenase from *Pseudomonas aeruginosa* provides new insight into the reaction mechanism and shows a novel binding mode of the 2'-Phosphate of $NADP^+$ and a novel cation binding site. **J. Mol. Biol.** 385: 542–557.

Gruez, A., V. Roig-Zamboni, S. Grisel, A. Salomoni, C. Valencia, V. Campanacci, M. Tegoni and C. Cambillau. 2004. Crystal structure and kinetics identify *Escherichia coli* YdcW gene product as a medium-chain aldehyde dehydrogenase. **J. Mol. Biol.** 343: 29-41.

Holmström, K. O., B. Welin, A. Mandal, I. Kristiansdottir, T. H. Teeri, T. Lamark, A. R. Strom and T.E. Palva. 1994. Production of the *Escherichia coli* betaine-aldehyde dehydrogenase, an enzyme required for the synthesis of the osmoprotectant glycine betaine, in transgenic plants. **Plant J.** 6: 749-758.

Hou, T., J. Wang, Y. Li and W. Wang. 2011. Assessing the performance of the MM/PBSA and MM/GBSA methods. 1. the accuracy of binding free energy calculations based on molecular dynamics simulations. **J. Chem. Inf. Model.** 51: 69–82.

Copyright by Kasetsart University All rights reserved

Huang, T-C., C-S. Teng, J-L. Chang, H-S. Chuang, C-T. HO and M-L. Wu. 2008. Biosynthetic mechanism of 2-acetyl-1-pyrroline and its relationship with Δ^1-pyrroline-5-carboxylic acid and methylglyoxal in aromatic rice (*Oryza sativa* L.) callus. **J. Agric. Food Chem.** 56: 7399–7404.

Ishitani, M., T. Nakamura, S. Y. Han and T. Takabe. 1995. Expression of the betaine aldehyde dehydrogenase gene in barley in response to osmotic stress and abscisic acid. **Plant Mol. Biol.** 27: 307–315.

Jimenez-Lopez, J. C., E. W. Gachomo, M. J. Seufferheld and S. O. Kotchoni. 2010. The maize ALDH protein superfamily: linking structural features to functional specificities. **BMC Struct. Biol**. 10: 43-57.

Johansson, K., M. El-Ahmad, S. Ramaswamy, L. Hjelmqvist, H. Jornvall and H. Eklund. 1998. Structure of betaine aldehyde dehydrogenase at 2.1 Å resolution. **Protein Sci.** 7: 2106-2117.

Jorgensen, W. L., J. Chandrasekhar, J. D. Madura, R. W. Impey, and M. L. Klein. 1983. Comparison of simple potential functions for simulating liquid water. **J. Chem. Phys.** 79: 926-935.

Kakkar, R. K., P. K. Nagar, P. S. Ahuja and V. K Rai. 2000. Polyamines and plant morphogenesis. **Biol. Plant** 43: 1–11.

Kaukonen, M., P. Söderhjelm, J. Heimdal and U. Ryde. 2008. QM/MM-PBSA method to estimate free energies for reactions in proteins. **J. Phys. Chem. B** 112: 12537–12548.

Kinnersley, A.M. and F.J. Turano. 2000. Gamma aminobutyric acid (GABA) and plant responses to stress. **Crit. Rev. Plant Sci.** 19: 479–509.

Kirch, H. H., D. Bartels, Y. Wei, P. S. Schnable and A. J. Wood. 2004. The *ALDH* gene superfamily of *arabidopsis*. **Trends Plant Sci.** 9: 371–377.

Copyright by Kasetsart University All rights reserved

Kopečný, D., M. Tylichová, J. Snegaroff, H. Popelková and M. Šebela. 2011. Carboxylate and aromatic active-site residues are determinants of high-affinity binding of ω-aminoaldehydes to plant aminoaldehyde dehydrogenases. **FEBS J.** 278: 3130-3139.

Kotchoni, S. O. and D. Bartels. 2003. Water stress induces the up-regulation of a specific set of genes in plants: aldehyde dehydrogenases as an example. **Bulg. J. Plant physiol.** Special: 37–51.

_____, J. C. Jimenez-Lopez, D. Gao, V. Edwards, E. W. Gachomo, V. M. Margam and M. J. Seufferheld. 2010. Modeling-dependent protein characterization of the rice aldehyde dehydrogenase (ALDH) superfamily reveals distinct functional and structural features. **PLoS One** 5: e11516.

Kovacha, M. J., M. N. Calingacionb, M. A. Fitzgeraldb, and S. R. McCouch. 2009. The origin and evolution of fragrance in rice (*Oryza sativa* L.). **PNAS** 106: 14444–14449.

Kuaprasert, B., K. Silprasit, N. Horata, P. Khunrae, R. Wongpanya, N. Boonyalai, A. Vanavichit and K. Choowongkomon. 2011. Purification, crystallization and preliminary X-ray analysis of recombinant betaine aldehyde dehydrogenase 2 (OsBADH2), a protein involved in jasmine aroma, from Thai fragrant rice (*Oryza sativa* L.). **Acta Crystallogr. Sect. F** 67: 1221-1223.

Laskowski, R. A., MacArthur, M. W., Moss, D. S. and Thornton, J. M. 1993. PROCHECK - a program to check the stereochemical quality of protein structures. **J. Appl. Crystallogr.** 26: 283-291.

Liu, Z. J., Y. J. Sun, J. Rose, Y. J. Chung, C. D. Hsiao, W. R. Chang, I. Kuo, J. Perozich, R. Lindahl, J. Hempel, B.C. Wang. 1997. The first structure of an aldehyde dehydrogenase reveals novel interactions between NAD and the Rossmann fold, **Nat. Struct. Biol.** 4: 317-326.

Copyright by Kasetsart University All rights reserved

Lorieux, M., M. Petrov, N. Huang, E. Guiderdoni and A. Ghesquière. 1996. Aroma in rice: genetic analysis of a quantitative trait. **Theor. Appl. Genet.** 93: 1145-1151.

Nakamura, T., S. Yokota, Y. Muramoto, K. Tsutsui, Y. Oguri, K. Fukui and T. Takabe. 1997. Expression of a betaine aldehyde dehydrogenase gene in rice, a glycinebetaine non accumulator, and possible localization of its protein in peroxisomes. **Plant J.** 11: 1115–1120**.**

Nuccio, M. L., D. Rhodes, S. D. McNeil and A. D. Hanson.1999. Metabolic engineering of plants for osmotic stress resistance. **Curr. Opin. Plant Biol.** 2:128-134.

Mitsuya, S., Y. Yokota, T. Fujiwara, N. Mori and T. Takabe. 2009. OsBADH1 is possibly involved in acetaldehyde oxidation in rice plant peroxisomes. **FEBS Lett.** 583: 3625–3629.

Moore, S. A., H. M. Baker, T. J. Blythe, K. E. Kitson, T. M. Kitson and E. N. Baker.1998. Sheep liver cytosolic aldehyde dehydrogenase: the structure reveals the basis for the retinal specificity of class 1 aldehyde dehydrogenases. **Structure** 6: 1541-1551.

Mori, N., N. Yoshida and Y. Kitamoto. 1992. Purification and properties of betaine aldehyde dehydrogenase from *Xanthomonas translucens*. **J. Ferment. Bioeng.** 73: 352-356.

Morris, G. M., D. S. Goodsell, R. S. Halliday, R. Huey, W. E. Hart, R. K. Belew, and A. J. Olson.1998. Automated docking using a lamarckian genetic algorithm and an empirical binding free energy function. **J. Com. Chem.** 19: 1662-1998.

Moschou, P. N., K. A. Paschalidis and K. A. Roubelakis-Angelakis. 2008. Plant polyamine catabolism: The state of the art. **Plant Signal Behav.** 3: 1061-1066.

Copyright by Kasetsart University All rights reserved

Muñoz-Clares, R. A., A. G. Díaz-Sánchez, L. González-Segura and C. Montiel. 2010. Kinetic and structural features of betaine aldehyde dehydrogenases: mechanistic and regulatory implications. **Arch. Biochem. Biophys.** 493: 71–81.

_____, L González-Segura and A. G. Díaz-Sánchez. 2011. Crystallographic evidence for active-site dynamics in the hydrolytic aldehyde dehydrogenases. Implications for the deacylation step of the catalyzed reaction. **Chem. Biol. Interact.** 191: 137–146.

Muntz, J. A. 1950. The inability of choline to transfer a methyl group directly to homocysteine for methionine formation. **J. Biol. Chem**. 182: 489–499.

Muzio, G., R. A. Canuto, A. Trombetta and M. Maggiora. 2001. Inhibition of cytosolic class 3 aldehyde dehydrogenase by antisense oligonucleotides in rat hepatoma cells. **Chem. Biol. Interact.** 130–132: 219–225.

Perez-Miller, J. S and T. D. Hurley. 2003. Coenzyme isomerization is integral to catalysis in aldehyde dehydrogenase. **Biochemistry** 42: 7100-7109.

Perozich, J., H. Nicholas, B-C. Wang, R. Lindahl and J. Hempel. 1999. Relationships within the aldehyde dehydrogeanse extended family. **Protein Sci.** 8: 137-146.

Sage, A. E., A. I. Vasil and M. L. Vasil. 1997. Molecular characterization of mutants affected in the osmoprotectant-dependent induction of phospholipase C in *Pseudomonas aeruginosa* PAO1. **Mol. Microbiol**. 23: 43-56.

Sakamoto, A. and N. Murata. 2000. Genetic engineering of glycine betaine synthesis in plants: current status and implications for enhancement of stress tolerance. **J. Exp. Bot**. 51: 81–88.

Copyright by Kasetsart University All rights reserved

Sakthivel, K., R. M. Sundaram, N. Shobha Rani, S. M. Balachandran and C. N. Neeraja. 2009. Genetic and molecular basis of fragrance in rice. **Biotechnol. Adv.** 27: 468–473.

Šebela, M., F. Brauner, A. Radová, S. Jacobsen, J. Havliš, P. Galuszka and P. Peč. 2000. Characterisation of a homogeneous plant aminoaldehyde dehydrogenase. **Biochim. Biophys. Acta** 1480: 329-341.

Shelp, B. J., A. W. Bown and M. D. McLean. 1999. Metabolism and functions of gamma-aminobutyric acid. **Trends Plant Sci.** 4: 446–452.

Sophos, N. A. and V. Vasiliou. 2003. Aldehyde dehydrogenase gene superfamily: the 2002 update. **Chem. Biol. Interact.** 143: 5-22.

Steinmetz, C. G., P. Xie, H. Weiner and T. D. Hurley. 1997. Structure of mitochondrial aldehyde dehydrogenase: the genetic component of ethanol aversion. **Structure** 5: 701-711.

Struve, C. and C. Christophersen. 2003. Structural equilibrium and ringchain tautomerism of aqueous solutions of 4-aminobutyraldehyde. **Heterocycles** 60: 1907–1914.

Tsuji, H., N. Meguroa, Y. Suzuki, N. Tsutsumi, A. Hirai and M. Nakazonoa. 2003. Induction of mitochondrial aldehyde dehydrogenase by submergence facilitates oxidation of acetaldehyde during re-aeration in rice. **FEBS Lett.** 546: 369-373.

Tyagi, A. K., J. P. Khurana, P. Khurana, S. Raghuvanshi, A. Gaur, A. Kapur, V. Gupta, D. Kumar, V. Ravi, S. Vij, P. Khurana and S. Sharma. 2004. Structural and functional analysis of rice genome. **J. Genet.** 83: 79-99.

Copyright by Kasetsart University All rights reserved

Tylichová, M., D. Kopecný, S. Moréra, P. Briozzo, R. Lenobel, J. Snégaroff and M. Šebela. 2010. Structural and functional characterization of plant aminoaldehyde dehydrogenase from *Pisum sativum* with a broad specificity for natural and synthetic aminoaldehydes. **J. Mol. Biol.** 396: 870-882.

Velasco-García, R., C. Mújica-Jiménez, G. Mendoza-Hernández and R. A. Muñoz-Clares. 1999. Rapid purification and properties of betaine aldehyde dehydrogenase from *Pseudomonas aeruginosa*. **J. Bact**. 181: 1292-1300.

_____, M. A. Villalobos, M. A. Ramírez-Romero, C. Mújica-Jiménez, G. Iturriaga and R. A. Muñoz-Clares. 2006. Betaine aldehyde dehydrogenase from *Pseudomonas aeruginosa*: cloning, over-expression in *Escherichia coli*, and regulation by choline and salt. **Arch. Microbiol.** 185: 14–22.

Wang, J., T. Hou and X. Xu. 2006. Recent advances in free energy calculations with a combination of molecular mechanics and continuum models. **Curr. Comput. Aided Drug Des.** 2: 95-103.

Weigel, P., E. A. Weretilnyk and A. D. Hanson. 1986. Betaine aldehyde oxidation by spinach chloroplasts. **Plant Physiol**. 82: 753-759.

Widjaja, R., J. D. Craske and M. Wootton. 1996. Comparative studies on volatile components of non-fragrant and fragrant rices**. J. Sci. Food Agric.** 70: 151-161.

Wolins, N. E. and R. P. Donaldson. 1997. Binding of the peroxisomal targeting sequence SKL is specified by a low-affinity site in castor bean glyoxysomal membranes. **Plant Physiol**. 113: 943-949.

Wongpanya, R., N. Boonyalai, N. Thammachuchourat, N. Horata, S. Arikit, K. Myint, A. Vanavichit and K. Choowongkomon. 2011. Biochemical and enzymatic study of rice BADH wild-type and mutants: an insight into fragrance in rice. **Protein J.** 30: 529-538.

Copyright by Kasetsart University All rights reserved

Yoshida, A., A. Rzhetsky, L. C. Hsu and C. Chang, 1998. Human aldehyde dehydrogenase gene family. **Eur. J. Biochem.** 251: 549-557.

Yoshihashi, T., N. T. T. Huong and H. Inatomi. 2002. Precursors of 2-acetyl-1-pyrroline, a potent flavor compound of an aromatic rice variety. **J. Agric. Food Chem.** 50: 2001–2004.

Copyright by Kasetsart University All rights reserved

APPENDICES

Copyright by Kasetsart University All rights reserved

Appendix A

Pairwise alignment of DNA sequencing results of the OsBADH1 and OsBADH2

Copyright by Kasetsart University All rights reserved

Appendix A1 Pairwise alignment of DNA sequencing results of the OsBADH1

```
Wildtype_OsBADH1     ATGGCCGCGCCGTCGGCGATCCCCCGCCGCGGCCTGTTCATCGGCGGCGGGTGGCGGGAG 60
N164A                ATGGCCGCGCCGTCGGCGATCCCCCGCCGCGGCCTGTTCATCGGCGGCGGGTGGCGGGAG 60
W172A                ATGGCCGCGCCGTCGGCGATCCCCCGCCGCGGCCTGTTCATCGGCGGCGGGTGGCGGGAG 60
W172F                ATGGCCGCGCCGTCGGCGATCCCCCGCCGCGGCCTGTTCATCGGCGGCGGGTGGCGGGAG 60
                     ************************************************************

Wildtype_OsBADH1     CCGTCCCTCGGCCGCCGCCTCCCCGTCGTCAACCCGGCCACGGAGGCAACCATCGGTGAC 120
N164A                CCGTCCCTCGGCCGCCGCCTCCCCGTCGTCAACCCGGCCACGGAGGCAACCATCGGTGAC 120
W172A                CCGTCCCTCGGCCGCCGCCTCCCCGTCGTCAACCCGGCCACGGAGGCAACCATCGGTGAC 120
W172F                CCGTCCCTCGGCCGCCGCCTCCCCGTCGTCAACCCGGCCACGGAGGCAACCATCGGTGAC 120
                     ************************************************************

Wildtype_OsBADH1     ATCCCGGCGGCCACGGCGGAGGACGTCGAGCTCGCGGTGTCGGCGGCGAGGGATGCGTTC 180
N164A                ATCCCGGCGGCCACGGCGGAGGACGTCGAGCTCGCGGTGTCGGCGGCGAGGGATGCGTTC 180
W172A                ATCCCGGCGGCCACGGCGGAGGACGTCGAGCTCGCGGTGTCGGCGGCGAGGGATGCGTTC 180
W172F                ATCCCGGCGGCCACGGCGGAGGACGTCGAGCTCGCGGTGTCGGCGGCGAGGGATGCGTTC 180
                     ************************************************************

Wildtype_OsBADH1     GGCCGCGACGGTGGGAGACACTGGTCGCGCGCGCCTGGGGCCGTGCGGGCCAAGTACCTC 240
N164A                GGCCGCGACGGTGGGAGACACTGGTCGCGCGCGCCTGGGGCCGTGCGGGCCAAGTACCTC 240
W172A                GGCCGCGACGGTGGGAGACACTGGTCGCGCGCGCCTGGGGCCGTGCGGGCCAAGTACCTC 240
W172F                GGCCGCGACGGTGGGAGACACTGGTCGCGCGCGCCTGGGGCCGTGCGGGCCAAGTACCTC 240
                     ************************************************************

Wildtype_OsBADH1     AAGGCGATCGCCGCTAAGATTAAAGATAAGAAATCTTATCTAGCTTTGTTGGAGACTCTT 300
N164A                AAGGCGATCGCCGCTAAGATTAAAGATAAGAAATCTTATCTAGCTTTGTTGGAGACTCTT 300
W172A                AAGGCGATCGCCGCTAAGATTAAAGATAAGAAATCTTATCTAGCTTTGTTGGAGACTCTT 300
W172F                AAGGCGATCGCCGCTAAGATTAAAGATAAGAAATCTTATCTAGCTTTGTTGGAGACTCTT 300
                     ************************************************************

Wildtype_OsBADH1     GATTCTGGGAAGCCTCTGGATGAAGCAGCTGGGGACATGGAGGATGTCGCTGCATGCTTT 360
N164A                GATTCTGGGAAGCCTCTGGATGAAGCAGCTGGGGACATGGAGGATGTCGCTGCATGCTTT 360
W172A                GATTCTGGGAAGCCTCTGGATGAAGCAGCTGGGGACATGGAGGATGTCGCTGCATGCTTT 360
W172F                GATTCTGGGAAGCCTCTGGATGAAGCAGCTGGGGACATGGAGGATGTCGCTGCATGCTTT 360
                     ************************************************************

Wildtype_OsBADH1     GAGTATTATGCTGATCTGGCAGAAGCTTTAGATGGGAAACAACGGGCACCAATCTCTCTA 420
N164A                GAGTATTATGCTGATCTGGCAGAAGCTTTAGATGGGAAACAACGGGCACCAATCTCTCTA 420
W172A                GAGTATTATGCTGATCTGGCAGAAGCTTTAGATGGGAAACAACGGGCACCAATCTCTCTA 420
W172F                GAGTATTATGCTGATCTGGCAGAAGCTTTAGATGGGAAACAACGGGCACCAATCTCTCTA 420
                     ************************************************************

Wildtype_OsBADH1     CCCATGGAAGATTTTGAGTCCTATGTACTCAAAGAACCCATTGGGGTTGTCGGACTTATC 480
N164A                CCCATGGAAGATTTTGAGTCCTATGTACTCAAAGAACCCATTGGGGTTGTCGGACTTATC 480
W172A                CCCATGGAAGATTTTGAGTCCTATGTACTCAAAGAACCCATTGGGGTTGTCGGACTTATC 480
W172F                CCCATGGAAGATTTTGAGTCCTATGTACTCAAAGAACCCATTGGGGTTGTCGGACTTATC 480
                     ************************************************************

Wildtype_OsBADH1     ACTCCCTGGAATTATCCTCTGCTGATGGCTACTTGGAAGGTTGCACCTGCCCTGGCTGCT 540
N164A                ACTCCCTGGGCTTATCCTCTGCTGATGGCTACTTGGAAGGTTGCACCTGCCCTGGCTGCT 540
W172A                ACTCCCTGGAATTATCCTCTGCTGATGGCTACTGCGAAGGTTGCACCTGCCCTGGCTGCT 540
W172F                ACTCCCTGGAATTATCCTCTGCTGATGGCTACTTTCAAGGTTGCACCTGCCCTGGCTGCT 540
                     *********  **********************  ************************

Wildtype_OsBADH1     GGGTGTACAGCTGTATTAAAGCCATCTGAGCTTGCTTCCCTGACATGTTTAGAGCTTGGT 600
N164A                GGGTGTACAGCTGTATTAAAGCCATCTGAGCTTGCTTCCCTGACATGTTTAGAGCTTGGT 600
W172A                GGGTGTACAGCTGTATTAAAGCCATCTGAGCTTGCTTCCCTGACATGTTTAGAGCTTGGT 600
W172F                GGGTGTACAGCTGTATTAAAGCCATCTGAGCTTGCTTCCCTGACATGTTTAGAGCTTGGT 600
                     ************************************************************

Wildtype_OsBADH1     GGAATATGTGCAGAAATTGGATTACCTCCAGGAGTCTTGAACATAATTACTGGTCTGGGC 660
N164A                GGAATATGTGCAGAAATTGGATTACCTCCAGGAGTCTTGAACATAATTACTGGTCTGGGC 660
W172A                GGAATATGTGCAGAAATTGGATTACCTCCAGGAGTCTTGAACATAATTACTGGTCTGGGC 660
W172F                GGAATATGTGCAGAAATTGGATTACCTCCAGGAGTCTTGAACATAATTACTGGTCTGGGC 660
                     ************************************************************
```

Copyright by Kasetsart University All rights reserved

```
Wildtype_OsBADH1     ACTGAAGCTGGTGCTCCATTAGCTTCACATCCCCATGTGGATAAGATTGCTTTTACTGGA 720
N164A                ACTGAAGCTGGTGCTCCATTAGCTTCACATCCCCATGTGGATAAGATTGCTTTTACTGGA 720
W172A                ACTGAAGCTGGTGCTCCATTAGCTTCACATCCCCATGTGGATAAGATTGCTTTTACTGGA 720
W172F                ACTGAAGCTGGTGCTCCATTAGCTTCACATCCCCATGTGGATAAGATTGCTTTTACTGGA 720
                     ************************************************************

Wildtype_OsBADH1     AGCACAGAAACTGGTAAGAGGATAATGATTACTGCTTCCCAAATGGTCAAGCCTGTTTCG 780
N164A                AGCACAGAAACTGGTAAGAGGATAATGATTACTGCTTCCCAAATGGTCAAGCCTGTTTCG 780
W172A                AGCACAGAAACTGGTAAGAGGATAATGATTACTGCTTCCCAAATGGTCAAGCCTGTTTCG 780
W172F                AGCACAGAAACTGGTAAGAGGATAATGATTACTGCTTCCCAAATGGTCAAGCCTGTTTCG 780
                     ************************************************************

Wildtype_OsBADH1     TTAGAGCTTGGTGGCAAAAGTCCTCTTATTGTCTTTGATGATGTTGATATTGATAAAGCT 840
N164A                TTAGAGCTTGGTGGCAAAAGTCCTCTTATTGTCTTTGATGATGTTGATATTGATAAAGCT 840
W172A                TTAGAGCTTGGTGGCAAAAGTCCTCTTATTGTCTTTGATGATGTTGATATTGATAAAGCT 840
W172F                TTAGAGCTTGGTGGCAAAAGTCCTCTTATTGTCTTTGATGATGTTGATATTGATAAAGCT 840
                     ************************************************************

Wildtype_OsBADH1     GTTGAGTGGGCCATGTTTGGGTGTTTTGCGAACGCTGGTCAAGTCTGCAGTGCTACTTCT 900
N164A                GTTGAGTGGGCCATGTTTGGGTGTTTTGCGAACGCTGGTCAAGTCTGCAGTGCTACTTCT 900
W172A                GTTGAGTGGGCCATGTTTGGGTGTTTTGCGAACGCTGGTCAAGTCTGCAGTGCTACTTCT 900
W172F                GTTGAGTGGGCCATGTTTGGGTGTTTTGCGAACGCTGGTCAAGTCTGCAGTGCTACTTCT 900
                     ************************************************************

Wildtype_OsBADH1     CGTCTACTTTTGCATGAGAAAATTGCAAAGCGATTCTTGGATAGGTTGGTTGCATGGGCA 960
N164A                CGTCTACTTTTGCATGAGAAAATTGCAAAGCGATTCTTGGATAGGTTGGTTGCATGGGCA 960
W172A                CGTCTACTTTTGCATGAGAAAATTGCAAAGCGATTCTTGGATAGGTTGGTTGCATGGGCA 960
W172F                CGTCTACTTTTGCATGAGAAAATTGCAAAGCGATTCTTGGATAGGTTGGTTGCATGGGCA 960
                     ************************************************************

Wildtype_OsBADH1     AAGAGTATCAAAATCTCAGATCCACTAGAAGAAGGTTGCAGGCTGGGGTCAGTCGTTAGT 1020
N164A                AAGAGTATCAAAATCTCAGATCCACTAGAAGAAGGTTGCAGGCTGGGGTCAGTCGTTAGT 1020
W172A                AAGAGTATCAAAATCTCAGATCCACTAGAAGAAGGTTGCAGGCTGGGGTCAGTCGTTAGT 1020
W172F                AAGAGTATCAAAATCTCAGATCCACTAGAAGAAGGTTGCAGGCTGGGGTCAGTCGTTAGT 1020
                     ************************************************************

Wildtype_OsBADH1     GAAGGGCAGTATCAAAAAATAATGAAGTTCATCTCAACAGCAAGATGTGAAGGTGCCACA 1080
N164A                GAAGGGCAGTATCAAAAAATAATGAAGTTCATCTCAACAGCAAGATGTGAAGGTGCCACA 1080
W172A                GAAGGGCAGTATCAAAAAATAATGAAGTTCATCTCAACAGCAAGATGTGAAGGTGCCACA 1080
W172F                GAAGGGCAGTATCAAAAAATAATGAAGTTCATCTCAACAGCAAGATGTGAAGGTGCCACA 1080
                     ************************************************************

Wildtype_OsBADH1     ATTCTATATGGGGGTGCCCGACCACAACACCTCAAAAGGGGGTTCTTTATTGAGCCTACT 1140
N164A                ATTCTATATGGGGGTGCCCGACCACAACACCTCAAAAGGGGGTTCTTTATTGAGCCTACT 1140
W172A                ATTCTATATGGGGGTGCCCGACCACAACACCTCAAAAGGGGGTTCTTTATTGAGCCTACT 1140
W172F                ATTCTATATGGGGGTGCCCGACCACAACACCTCAAAAGGGGGTTCTTTATTGAGCCTACT 1140
                     ************************************************************

Wildtype_OsBADH1     ATTATAACAAATGTTAGCACATCAATGCAAATTTGGCGAGAGGAAGTCTTTGGACCGGTT 1200
N164A                ATTATAACAAATGTTAGCACATCAATGCAAATTTGGCGAGAGGAAGTCTTTGGACCGGTT 1200
W172A                ATTATAACAAATGTTAGCACATCAATGCAAATTTGGCGAGAGGAAGTCTTTGGACCGGTT 1200
W172F                ATTATAACAAATGTTAGCACATCAATGCAAATTTGGCGAGAGGAAGTCTTTGGACCGGTT 1200
                     ************************************************************

Wildtype_OsBADH1     ATCTGCGTTAAAGAATTTAGGACAGAGCGTGAAGCAGTAGAACTTGCAAATGATACTCAC 1260
N164A                ATCTGCGTTAAAGAATTTAGGACAGAGCGTGAAGCAGTAGAACTTGCAAATGATACTCAC 1260
W172A                ATCTGCGTTAAAGAATTTAGGACAGAGCGTGAAGCAGTAGAACTTGCAAATGATACTCAC 1260
W172F                ATCTGCGTTAAAGAATTTAGGACAGAGCGTGAAGCAGTAGAACTTGCAAATGATACTCAC 1260
                     ************************************************************

Wildtype_OsBADH1     TATGGTCTAGCTGGCGCTGTGATTTCCAATGATCTAGAGAGGTGCGAGCGCATTTCAAAG 1320
N164A                TATGGTCTAGCTGGCGCTGTGATTTCCAATGATCTAGAGAGGTGCGAGCGCATTTCAAAG 1320
W172A                TATGGTCTAGCTGGCGCTGTGATTTCCAATGATCTAGAGAGGTGCGAGCGCATTTCAAAG 1320
W172F                TATGGTCTAGCTGGCGCTGTGATTTCCAATGATCTAGAGAGGTGCGAGCGCATTTCAAAG 1320
                     ************************************************************

Wildtype_OsBADH1     GCTATCCAGTCAGGTATCGTTTGGATAAATTGCTCGCAACCATGCTTTGTTCAAGCTCCA 1380
N164A                GCTATCCAGTCAGGTATCGTTTGGATAAATTGCTCGCAACCATGCTTTGTTCAAGCTCCA 1380
W172A                GCTATCCAGTCAGGTATCGTTTGGATAAATTGCTCGCAACCATGCTTTGTTCAAGCTCCA 1380
W172F                GCTATCCAGTCAGGTATCGTTTGGATAAATTGCTCGCAACCATGCTTTGTTCAAGCTCCA 1380
                     ************************************************************
```

Copyright by Kasetsart University All rights reserved

```
Wildtype_OsBADH1     TGGGGAGGGAACAAGCGGAGTGGTTTTGGCCGGGAGCTAGGACAGTGGGGCCTCGATAAC 1440
N164A                TGGGGAGGGAACAAGCGGAGTGGTTTTGGCCGGGAGCTAGGACAGTGGGGCCTCGATAAC 1440
W172A                TGGGGAGGGAACAAGCGGAGTGGTTTTGGCCGGGAGCTAGGACAGTGGGGCCTCGATAAC 1440
W172F                TGGGGAGGGAACAAGCGGAGTGGTTTTGGCCGGGAGCTAGGACAGTGGGGCCTCGATAAC 1440
                     ************************************************************

Wildtype_OsBADH1     TACTTGAGCGTGAAGCAAGTCACCAAGTACTGCTCAGATGAACCATACGGATGGTACCGG 1500
N164A                TACTTGAGCGTGAAGCAAGTCACCAAGTACTGCTCAGATGAACCATACGGATGGTACCGG 1500
W172A                TACTTGAGCGTGAAGCAAGTCACCAAGTACTGCTCAGATGAACCATACGGATGGTACCGG 1500
W172F                TACTTGAGCGTGAAGCAAGTCACCAAGTACTGCTCAGATGAACCATACGGATGGTACCGG 1500
                     ************************************************************

Wildtype_OsBADH1     CCTCCATCCAAGCTGTAG 1518
N164A                CCTCCATCCAAGCTGTAG 1518
W172A                CCTCCATCCAAGCTGTAG 1518
W172F                CCTCCATCCAAGCTGTAG 1518
                     ******************
```

Appendix A2 Pairwise alignment of DNA sequencing results of the OsBADH2

```
Wildtype_OsBADH2     ATGGCCACGGCGATCCCGCAGCGGCAGCTCTTCGTCGCCGGCGAGTGGCGCGCCCCCGCG 60
N162A                ATGGCCACGGCGATCCCGCAGCGGCAGCTCTTCGTCGCCGGCGAGTGGCGCGCCCCCGCG 60
W170A                ATGGCCACGGCGATCCCGCAGCGGCAGCTCTTCGTCGCCGGCGAGTGGCGCGCCCCCGCG 60
W170F                ATGGCCACGGCGATCCCGCAGCGGCAGCTCTTCGTCGCCGGCGAGTGGCGCGCCCCCGCG 60
                     ************************************************************

Wildtype_OsBADH2     CTCGGCCGCCGCCTCCCCGTCGTCAACCCCGCCACCGAGTCCCCCATCGGCGAGATCCCG 120
N162A                CTCGGCCGCCGCCTCCCCGTCGTCAACCCCGCCACCGAGTCCCCCATCGGCGAGATCCCG 120
W170A                CTCGGCCGCCGCCTCCCCGTCGTCAACCCCGCCACCGAGTCCCCCATCGGCGAGATCCCG 120
W170F                CTCGGCCGCCGCCTCCCCGTCGTCAACCCCGCCACCGAGTCCCCCATCGGCGAGATCCCG 120
                     ************************************************************

Wildtype_OsBADH2     GCGGGCACGGCGGAGGACGTGGACGCGGCGGTGGCGGCGGCGCGGGAGGCGCTGAAGAGG 180
N162A                GCGGGCACGGCGGAGGACGTGGACGCGGCGGTGGCGGCGGCGCGGGAGGCGCTGAAGAGG 180
W170A                GCGGGCACGGCGGAGGACGTGGACGCGGCGGTGGCGGCGGCGCGGGAGGCGCTGAAGAGG 180
W170F                GCGGGCACGGCGGAGGACGTGGACGCGGCGGTGGCGGCGGCGCGGGAGGCGCTGAAGAGG 180
                     ************************************************************

Wildtype_OsBADH2     AACCGGGGCCGCGACTGGGCGCGCGCGCCGGGCGCCGTCCGGGCCAAGTACCTCCGCGCA 240
N162A                AACCGGGGCCGCGACTGGGCGCGCGCGCCGGGCGCCGTCCGGGCCAAGTACCTCCGCGCA 240
W170A                AACCGGGGCCGCGACTGGGCGCGCGCGCCGGGCGCCGTCCGGGCCAAGTACCTCCGCGCA 240
W170F                AACCGGGGCCGCGACTGGGCGCGCGCGCCGGGCGCCGTCCGGGCCAAGTACCTCCGCGCA 240
                     ************************************************************

Wildtype_OsBADH2     ATCGCGGCCAAGATAATCGAGAGGAAATCTGAGCTGGCTAGACTAGAGACGCTTGATTGT 300
N162A                ATCGCGGCCAAGATAATCGAGAGGAAATCTGAGCTGGCTAGACTAGAGACGCTTGATTGT 300
W170A                ATCGCGGCCAAGATAATCGAGAGGAAATCTGAGCTGGCTAGACTAGAGACGCTTGATTGT 300
W170F                ATCGCGGCCAAGATAATCGAGAGGAAATCTGAGCTGGCTAGACTAGAGACGCTTGATTGT 300
                     ************************************************************

Wildtype_OsBADH2     GGGAAGCCTCTTGATGAAGCAGCATGGGACATGGACGATGTTGCTGGATGCTTTGAGTAC 360
N162A                GGGAAGCCTCTTGATGAAGCAGCATGGGACATGGACGATGTTGCTGGATGCTTTGAGTAC 360
W170A                GGGAAGCCTCTTGATGAAGCAGCATGGGACATGGACGATGTTGCTGGATGCTTTGAGTAC 360
W170F                GGGAAGCCTCTTGATGAAGCAGCATGGGACATGGACGATGTTGCTGGATGCTTTGAGTAC 360
                     ************************************************************

Wildtype_OsBADH2     TTTGCAGATCTTGCAGAATCCTTGGACAAAAGGCAAAATGCACCTGTCTCTCTTCCAATG 420
N162A                TTTGCAGATCTTGCAGAATCCTTGGACAAAAGGCAAAATGCACCTGTCTCTCTTCCAATG 420
W170A                TTTGCAGATCTTGCAGAATCCTTGGACAAAAGGCAAAATGCACCTGTCTCTCTTCCAATG 420
W170F                TTTGCAGATCTTGCAGAATCCTTGGACAAAAGGCAAAATGCACCTGTCTCTCTTCCAATG 420
                     ************************************************************

Wildtype_OsBADH2     GAAAACTTTAAATGCTATCTTCGGAAAGAGCCTATCGGTGTAGTTGGGTTGATCACACCT 480
N162A                GAAAACTTTAAATGCTATCTTCGGAAAGAGCCTATCGGTGTAGTTGGGTTGATCACACCT 480
W170A                GAAAACTTTAAATGCTATCTTCGGAAAGAGCCTATCGGTGTAGTTGGGTTGATCACACCT 480
W170F                GAAAACTTTAAATGCTATCTTCGGAAAGAGCCTATCGGTGTAGTTGGGTTGATCACACCT 480
                     ************************************************************
```

Copyright by Kasetsart University All rights reserved

```
Wildtype_OsBADH2     TGGAACTATCCTCTCCTGATGGCAACATGGAAGGTAGCTCCTGCCCTGGCTGCTGGCTGT 540
N162A                TGGGCCTATCCTCTCCTGATGGCAACATGGAAGGTAGCTCCTGCCCTGGCTGCTGGCTGT 540
W170A                TGGAACTATCCTCTCCTGATGGCAACAGCGAAGGTAGCTCCTGCCCTGGCTGCTGGCTGT 540
W170F                TGGAACTATCCTCTCCTGATGGCAACATTCAAGGTAGCTCCTGCCCTGGCTGCTGGCTGT 540
                     ***  ********************  ******************************

Wildtype_OsBADH2     ACAGCTGTACTAAAACCATCTGAATTGGCTTCCGTGACTTGTTTGGAGCTTGCTGATGTG 600
N162A                ACAGCTGTACTAAAACCATCTGAATTGGCTTCCGTGACTTGTTTGGAGCTTGCTGATGTG 600
W170A                ACAGCTGTACTAAAACCATCTGAATTGGCTTCCGTGACTTGTTTGGAGCTTGCTGATGTG 600
W170F                ACAGCTGTACTAAAACCATCTGAATTGGCTTCCGTGACTTGTTTGGAGCTTGCTGATGTG 600
                     ************************************************************

Wildtype_OsBADH2     TGTAAAGAGGTTGGTCTTCCTTCAGGTGTGCTAAACATAGTGACTGGATTAGGTTCTGAA 660
N162A                TGTAAAGAGGTTGGTCTTCCTTCAGGTGTGCTAAACATAGTGACTGGATTAGGTTCTGAA 660
W170A                TGTAAAGAGGTTGGTCTTCCTTCAGGTGTGCTAAACATAGTGACTGGATTAGGTTCTGAA 660
W170F                TGTAAAGAGGTTGGTCTTCCTTCAGGTGTGCTAAACATAGTGACTGGATTAGGTTCTGAA 660
                     ************************************************************

Wildtype_OsBADH2     GCCGGTGCTCCTTTGTCATCACACCCTGGTGTAGACAAGGTTGCATTTACTGGGAGTTAT 720
N162A                GCCGGTGCTCCTTTGTCATCACACCCTGGTGTAGACAAGGTTGCATTTACTGGGAGTTAT 720
W170A                GCCGGTGCTCCTTTGTCATCACACCCTGGTGTAGACAAGGTTGCATTTACTGGGAGTTAT 720
W170F                GCCGGTGCTCCTTTGTCATCACACCCTGGTGTAGACAAGGTTGCATTTACTGGGAGTTAT 720
                     ************************************************************

Wildtype_OsBADH2     GAAACTGGTAAAAAGATTATGGCTTCAGCTGCTCCTATGGTTAAGCCTGTTTCACTGGAA 780
N162A                GAAACTGGTAAAAAGATTATGGCTTCAGCTGCTCCTATGGTTAAGCCTGTTTCACTGGAA 780
W170A                GAAACTGGTAAAAAGATTATGGCTTCAGCTGCTCCTATGGTTAAGCCTGTTTCACTGGAA 780
W170F                GAAACTGGTAAAAAGATTATGGCTTCAGCTGCTCCTATGGTTAAGCCTGTTTCACTGGAA 780
                     ************************************************************

Wildtype_OsBADH2     CTTGGTGGAAAAAGTCCTATAGTGGTGTTTGATGATGTTGATGTTGAAAAAGCTGTTGAG 840
N162A                CTTGGTGGAAAAAGTCCTATAGTGGTGTTTGATGATGTTGATGTTGAAAAAGCTGTTGAG 840
W170A                CTTGGTGGAAAAAGTCCTATAGTGGTGTTTGATGATGTTGATGTTGAAAAAGCTGTTGAG 840
W170F                CTTGGTGGAAAAAGTCCTATAGTGGTGTTTGATGATGTTGATGTTGAAAAAGCTGTTGAG 840
                     ************************************************************

Wildtype_OsBADH2     TGGACTCTCTTTGGTTGCTTTTGGACCAATGGCCAGATTTGCAGTGCAACATCGCGTCTT 900
N162A                TGGACTCTCTTTGGTTGCTTTTGGACCAATGGCCAGATTTGCAGTGCAACATCGCGTCTT 900
W170A                TGGACTCTCTTTGGTTGCTTTTGGACCAATGGCCAGATTTGCAGTGCAACATCGCGTCTT 900
W170F                TGGACTCTCTTTGGTTGCTTTTGGACCAATGGCCAGATTTGCAGTGCAACATCGCGTCTT 900
                     ************************************************************

Wildtype_OsBADH2     ATTCTTCATAAAAAAATCGCTAAAGAATTTCAAGAAAGGATGGTTGCATGGGCCAAAAAT 960
N162A                ATTCTTCATAAAAAAATCGCTAAAGAATTTCAAGAAAGGATGGTTGCATGGGCCAAAAAT 960
W170A                ATTCTTCATAAAAAAATCGCTAAAGAATTTCAAGAAAGGATGGTTGCATGGGCCAAAAAT 960
W170F                ATTCTTCATAAAAAAATCGCTAAAGAATTTCAAGAAAGGATGGTTGCATGGGCCAAAAAT 960
                     ************************************************************

Wildtype_OsBADH2     ATTAAGGTGTCAGATCCACTTGAAGAGGGTTGCAGGCTTGGGCCCGTTGTTAGTGAAGGA 1020
N162A                ATTAAGGTGTCAGATCCACTTGAAGAGGGTTGCAGGCTTGGGCCCGTTGTTAGTGAAGGA 1020
W170A                ATTAAGGTGTCAGATCCACTTGAAGAGGGTTGCAGGCTTGGGCCCGTTGTTAGTGAAGGA 1020
W170F                ATTAAGGTGTCAGATCCACTTGAAGAGGGTTGCAGGCTTGGGCCCGTTGTTAGTGAAGGA 1020
                     ************************************************************

Wildtype_OsBADH2     CAGTATGAGAAGATTAAGCAATTTGTATCTACCGCCAAAAGCCAAGGTGCTACCATTCTG 1080
N162A                CAGTATGAGAAGATTAAGCAATTTGTATCTACCGCCAAAAGCCAAGGTGCTACCATTCTG 1080
W170A                CAGTATGAGAAGATTAAGCAATTTGTATCTACCGCCAAAAGCCAAGGTGCTACCATTCTG 1080
W170F                CAGTATGAGAAGATTAAGCAATTTGTATCTACCGCCAAAAGCCAAGGTGCTACCATTCTG 1080
                     ************************************************************

Wildtype_OsBADH2     ACTGGTGGGGTTAGACCCAAGCATCTGGAGAAAGGTTTCTATATTGAACCCACAATCATT 1140
N162A                ACTGGTGGGGTTAGACCCAAGCATCTGGAGAAAGGTTTCTATATTGAACCCACAATCATT 1140
W170A                ACTGGTGGGGTTAGACCCAAGCATCTGGAGAAAGGTTTCTATATTGAACCCACAATCATT 1140
W170F                ACTGGTGGGGTTAGACCCAAGCATCTGGAGAAAGGTTTCTATATTGAACCCACAATCATT 1140
                     ************************************************************

Wildtype_OsBADH2     ACTGATGTCGATACATCAATGCAAATTTGGAGGGAAGAAGTTTTTGGTCCAGTGCTCTGT 1200
N162A                ACTGATGTCGATACATCAATGCAAATTTGGAGGGAAGAAGTTTTTGGTCCAGTGCTCTGT 1200
W170A                ACTGATGTCGATACATCAATGCAAATTTGGAGGGAAGAAGTTTTTGGTCCAGTGCTCTGT 1200
W170F                ACTGATGTCGATACATCAATGCAAATTTGGAGGGAAGAAGTTTTTGGTCCAGTGCTCTGT 1200
                     ************************************************************
```

Copyright by Kasetsart University All rights reserved

```
Wildtype_OsBADH2     GTGAAAGAATTTAGCACTGAAGAAGAAGCCATTGAATTGGCCAACGATACTCATTATGGT 1260
N162A                GTGAAAGAATTTAGCACTGAAGAAGAAGCCATTGAATTGGCCAACGATACTCATTATGGT 1260
W170A                GTGAAAGAATTTAGCACTGAAGAAGAAGCCATTGAATTGGCCAACGATACTCATTATGGT 1260
W170F                GTGAAAGAATTTAGCACTGAAGAAGAAGCCATTGAATTGGCCAACGATACTCATTATGGT 1260
                     ************************************************************

Wildtype_OsBADH2     CTGGCTGGTGCTGTGCTTTCCGGTGACCGCGAGCGATGCCAGAGATTAACTGAGGAGATC 1320
N162A                CTGGCTGGTGCTGTGCTTTCCGGTGACCGCGAGCGATGCCAGAGATTAACTGAGGAGATC 1320
W170A                CTGGCTGGTGCTGTGCTTTCCGGTGACCGCGAGCGATGCCAGAGATTAACTGAGGAGATC 1320
W170F                CTGGCTGGTGCTGTGCTTTCCGGTGACCGCGAGCGATGCCAGAGATTAACTGAGGAGATC 1320
                     ************************************************************

Wildtype_OsBADH2     GATGCCGGAATTATCTGGGTGAACTGCTCGCAACCCTGCTTCTGCCAAGCTCCATGGGGC 1380
N162A                GATGCCGGAATTATCTGGGTGAACTGCTCGCAACCCTGCTTCTGCCAAGCTCCATGGGGC 1380
W170A                GATGCCGGAATTATCTGGGTGAACTGCTCGCAACCCTGCTTCTGCCAAGCTCCATGGGGC 1380
W170F                GATGCCGGAATTATCTGGGTGAACTGCTCGCAACCCTGCTTCTGCCAAGCTCCATGGGGC 1380
                     ************************************************************

Wildtype_OsBADH2     GGGAACAAGCGCAGCGGCTTTGGACGCGAGCTCGGAGAAGGGGGCATTGACAACTACCTA 1440
N162A                GGGAACAAGCGCAGCGGCTTTGGACGCGAGCTCGGAGAAGGGGGCATTGACAACTACCTA 1440
W170A                GGGAACAAGCGCAGCGGCTTTGGACGCGAGCTCGGAGAAGGGGGCATTGACAACTACCTA 1440
W170F                GGGAACAAGCGCAGCGGCTTTGGACGCGAGCTCGGAGAAGGGGGCATTGACAACTACCTA 1440
                     ************************************************************

Wildtype_OsBADH2     AGCGTCAAGCAAGTGACGGAGTACGCCTCCGATGAGCCGTGGGGATGGTACAAATCCCCT 1500
N162A                AGCGTCAAGCAAGTGACGGAGTACGCCTCCGATGAGCCGTGGGGATGGTACAAATCCCCT 1500
W170A                AGCGTCAAGCAAGTGACGGAGTACGCCTCCGATGAGCCGTGGGGATGGTACAAATCCCCT 1500
W170F                AGCGTCAAGCAAGTGACGGAGTACGCCTCCGATGAGCCGTGGGGATGGTACAAATCCCCT 1500
                     ************************************************************

Wildtype_OsBADH2     TCCAAGCTGTAA 1512
N162A                TCCAAGCTGTAA 1512
W170A                TCCAAGCTGTAA 1512
W170F                TCCAAGCTGTAA 1512
                     ************
```

Copyright by Kasetsart University All rights reserved

Appendix B

Fluorescence binding studies

Copyright by Kasetsart University All rights reserved

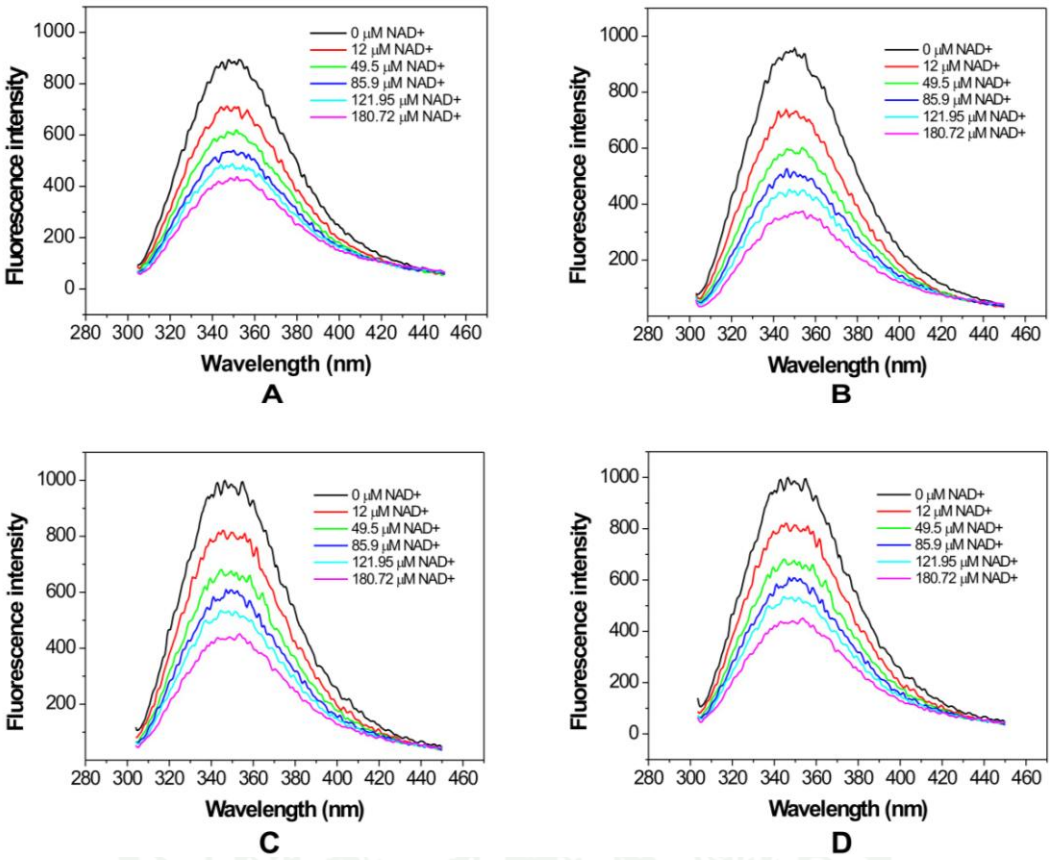

Appendix Figure B1 Fluorescence spectra of OsBADH1 upon the addition of NAD^+. (A) wild-type, (B) N164A, (C) W172A and (D) W172F.

.

Copyright by Kasetsart University All rights reserved

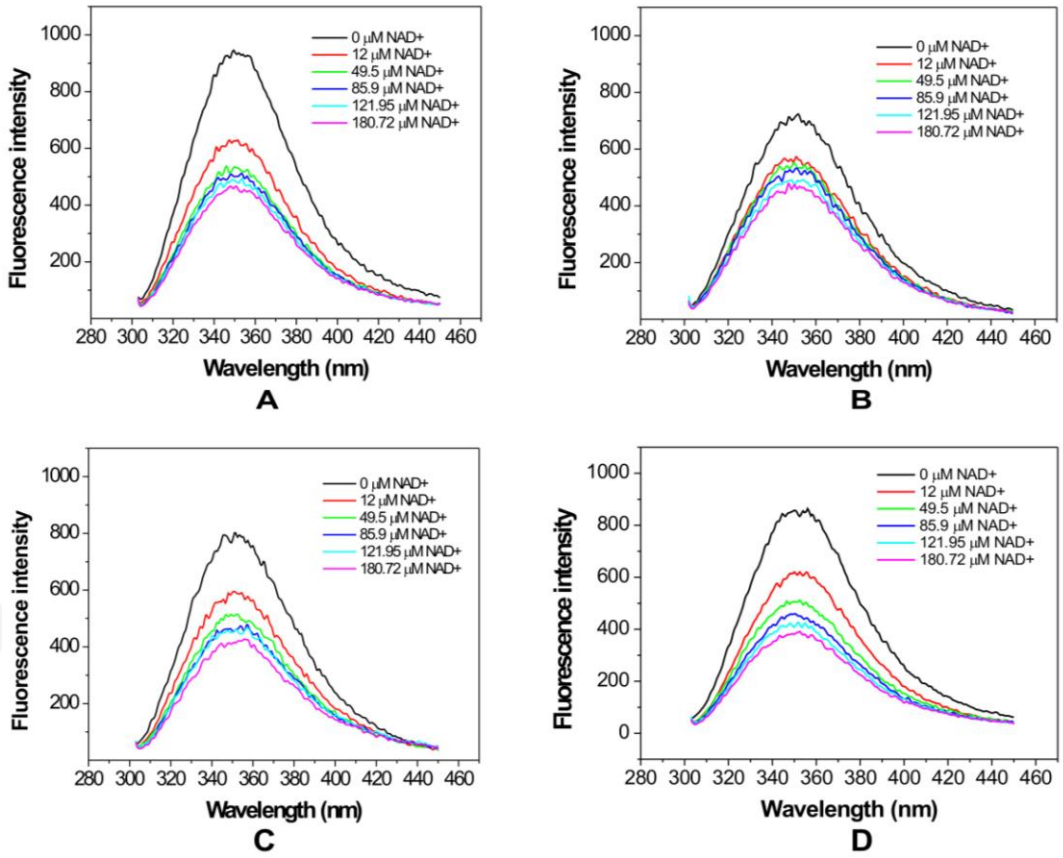

Appendix Figure B2 Fluorescence spectra of OsBADH2 upon the addition of NAD^+. (A) wild-type, (B) N162A, (C) W170A and (D) W170F.

Copyright by Kasetsart University All rights reserved

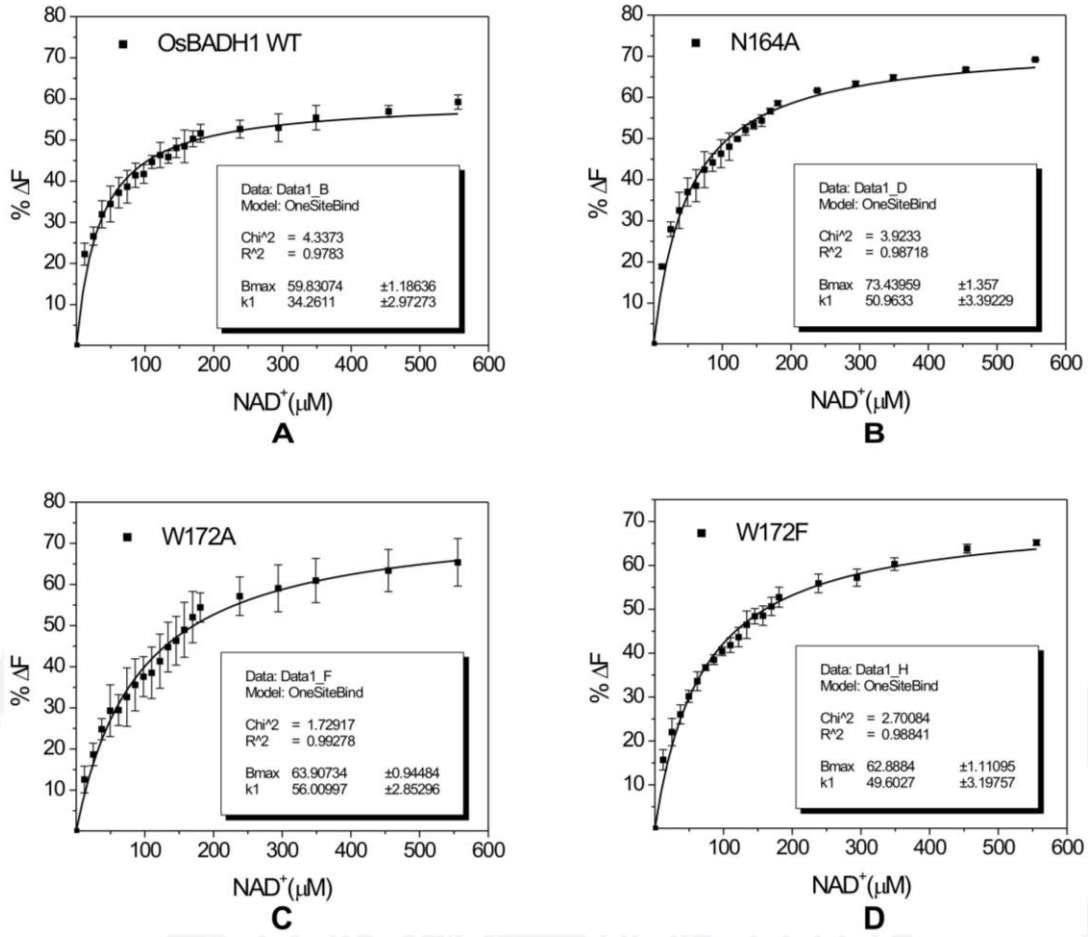

Appendix Figure B3 Binding isotherm of OsBADH1 in the presence of 5 mM NAD^+. (A) wild-type, (B) N164A, (C) W172A and (D) W172F.

Copyright by Kasetsart University All rights reserved

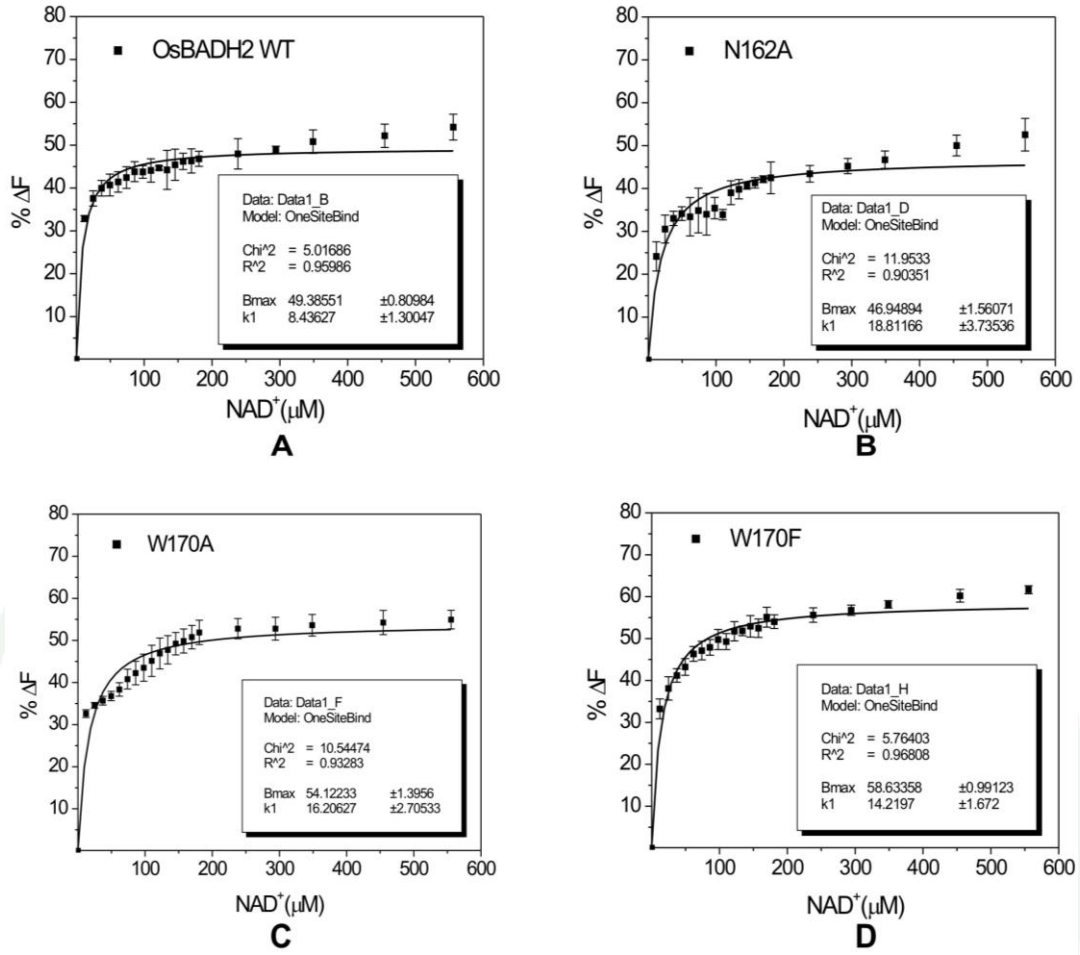

Appendix Figure B4 Binding isotherm of OsBADH2 in the presence of 5 mM NAD^+. (A) wild-type, (B) N162A, (C) W170A and (D) W170F.

Copyright by Kasetsart University All rights reserved

Appendix C

Enzymatic characterization

Copyright by Kasetsart University All rights reserved

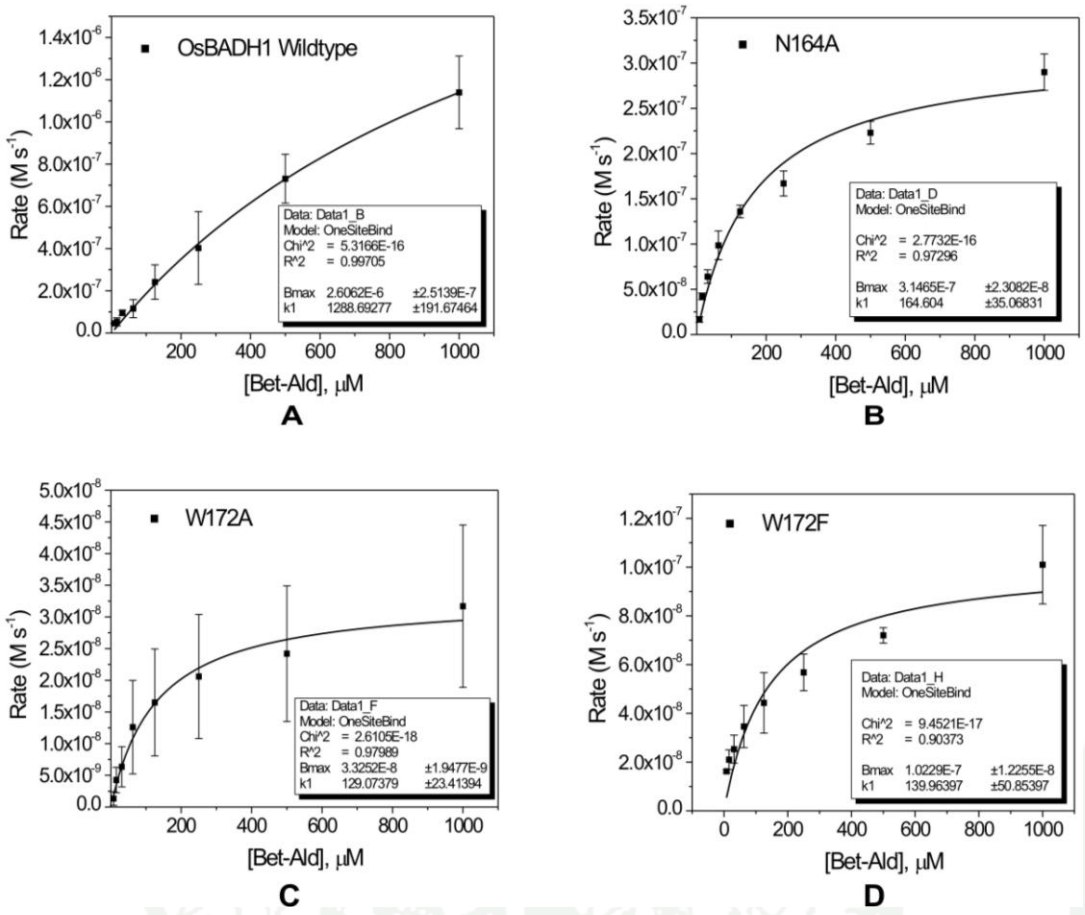

Appendix Figure C1 Effect of Betaine aldehyde (Bet-Ald) on the rate of aldehyde oxidation by OsBADH1. (A) wild-type, (B) N164A, (C) W172A and (D) W172F.

Copyright by Kasetsart University All rights reserved

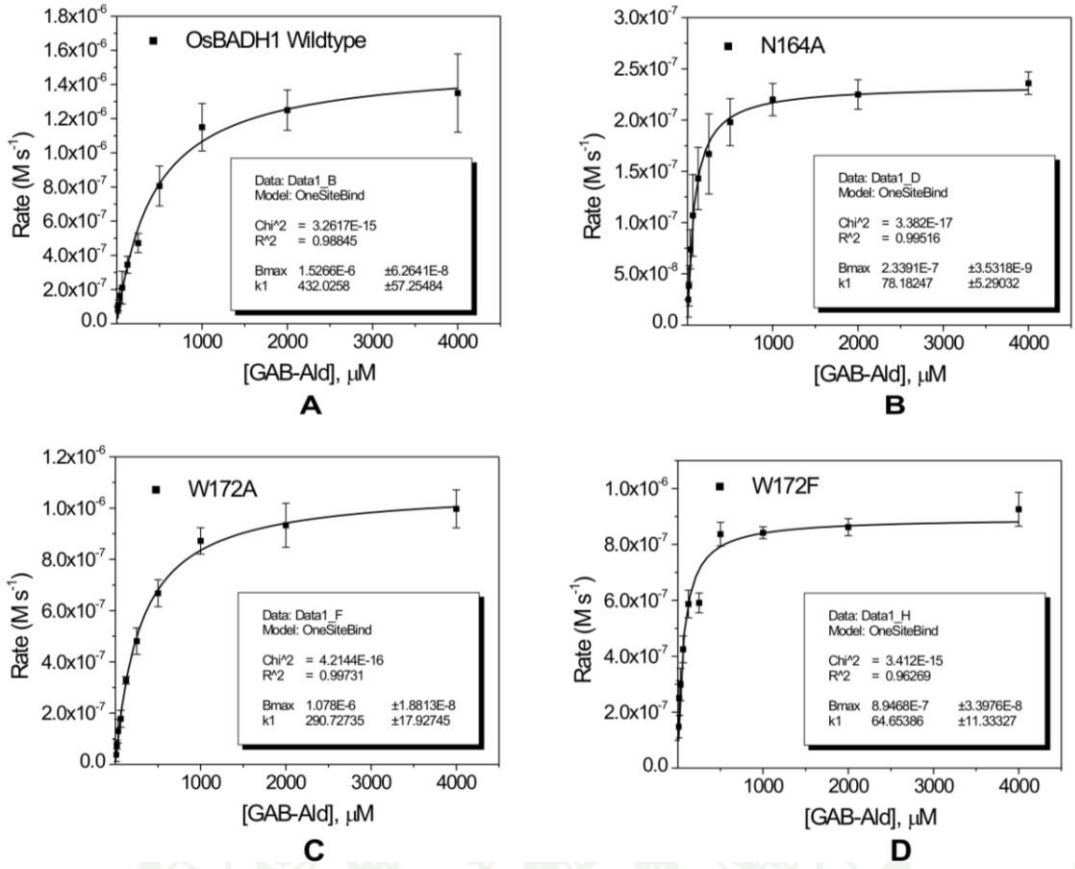

Appendix Figure C2 Effect of γ-aminobutyraldehyde (GAB-Ald) on the rate of aldehyde oxidation by OsBADH1. (A) wild-type, (B) N164A, (C) W172A and (D) W172F.

Copyright by Kasetsart University All rights reserved

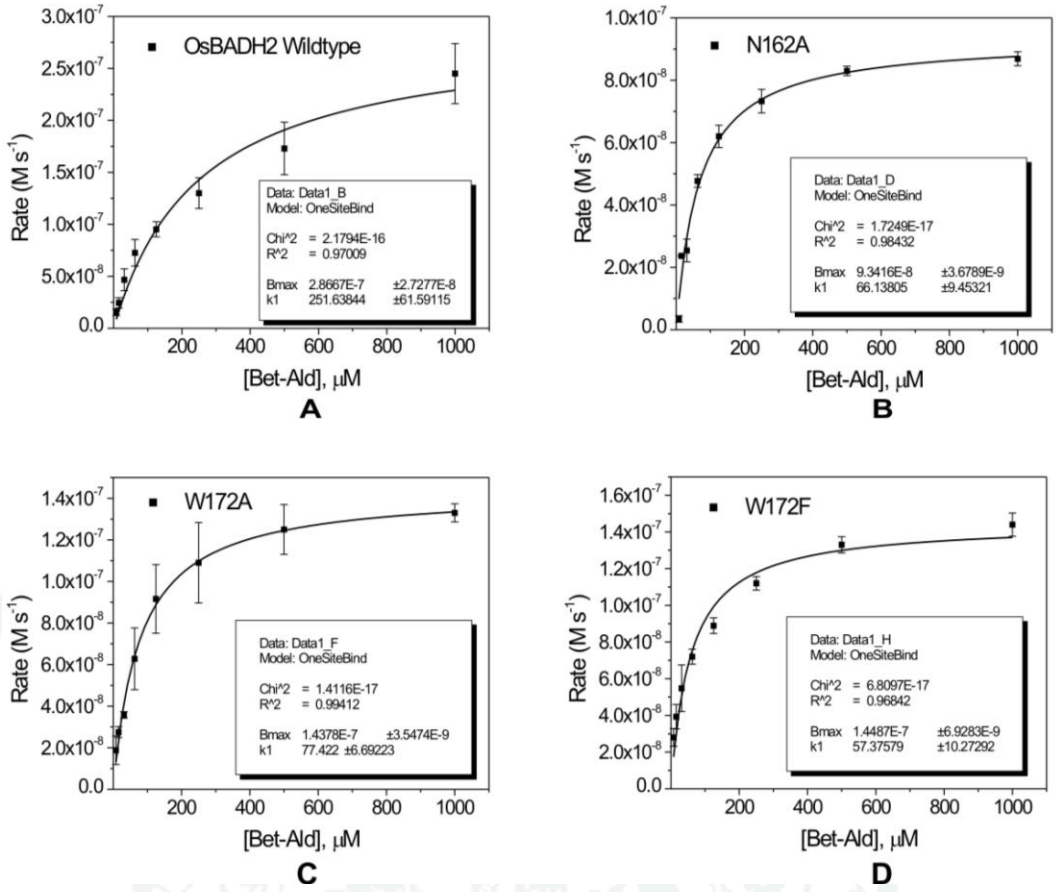

Appendix Figure C3 Effect of Betaine aldehyde (Bet-Ald) on the rate of aldehyde oxidation by OsBADH2. (A) wild-type, (B) N162A, (C) W170A and (D) W170F.

Copyright by Kasetsart University All rights reserved

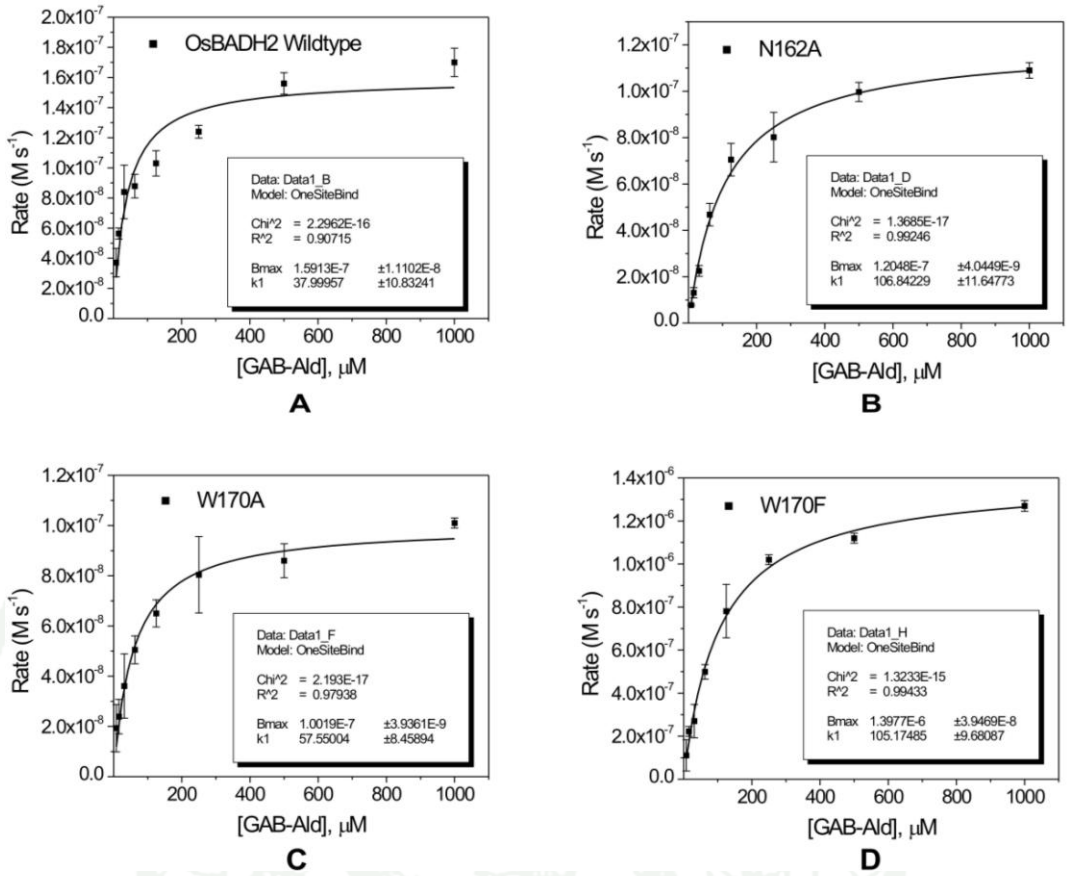

Appendix Figure C4 Effect of γ-aminobutyraldehyde (GAB-Ald) on the rate of aldehyde oxidation by OsBADH2. (A) wild-type, (B) N162A, (C) W170A and (D) W170F.

Copyright by Kasetsart University All rights reserved

CIRRICULUM VITAE

NAME : Ms. Kultida Jiamsomboon

BIRTH DATE : February 4, 1987

BIRTH PLACE : Phuket, Thailand

EDUCATION :

YEAR	INSTITUTE	DEGREE
2005-2008	Kasetsart University	B.S. (Biochemistry)
2009-present	Kasetsart University	M.S. (Biochemistry)

SCHOLARSHIPS:

YEAR	SCHOLARSHIPS
2009-2011	Center of excellence for the innovation in chemistry (PERCH-CIC) commission on higher education, ministry of education

AWARDS:

YEAR	AWARDS
2011	Outstanding poster presentation awards from the International Congress for Innovation in Chemistry (PERCH-CIC Congress VII)
2011	Thesis proposal award. Graduate School, Kasetsart University

POSTER PRESENTATIONS

1. Kultida Jiamsomboon and Nonlawat Boonyalai. 2011. The Dissection of OsBADH1 from Rice (*Oryza sativa*) for Substrate Specificity. The 3rd International Conference on Biochemistry and Molecular Biology conference. April 6th -8th 2011, the Empress Convention Centre, Chiang Mai, Thailand.

Copyright by Kasetsart University All rights reserved

2. Kultida Jiamsomboon and Nonlawat Boonyalai. 2011. Protein engineering of OsBADH1 from rice (*Oryza sativa*) for substrate specificity. The International Congress for Innovation in Chemistry (PERCH-CIC Congress VII). May 4th - 7th 2011, Jomtien Palm Beach Hotel & Resort, Pattaya, Thailand.

PUBLICATION

1. Kultida Jiamsomboon, Witcha Treesuwan and Nonlawat Boonyalai. 2012. Dissecting substrate specificity of two rice BADH isoforms: enzyme kinetics, docking and molecular dynamics simulation studies. **Biochimie**. doi: 10.1016/j.biochi.2012.04.009.

Copyright by Kasetsart University All rights reserved

ARTICLE IN PRESS BIOCHI3875_proof ■ 21 April 2012 ■ 1/11

Biochimie xxx (2012) 1–11

Contents lists available at SciVerse ScienceDirect

Biochimie

journal homepage: www.elsevier.com/locate/biochi

Research paper

Dissecting substrate specificity of two rice BADH isoforms: Enzyme kinetics, docking and molecular dynamics simulation studies

Kultida Jiamsomboon [a], Witcha Treesuwan [c], Nonlawat Boonyalai [a,b,*]

[a] Departmant of Biochemistry, Faculty of Science, Kasetsart University, Chatuchak, Bangkok 10900, Thailand
[b] Center of Excellence for Innovation in Chemistry, Faculty of Science, Kasetsart University, Chatuchak, Bangkok 10900, Thailand
[c] Institute of Food Research and Product Development, Kasetsart University, Chatuchak, Bangkok 10900, Thailand

ARTICLE INFO

Article history:
Received 16 December 2011
Accepted 7 April 2012
Available online xxx

Keywords:
Betaine aldehyde dehydrogenase
Molecular docking analysis
Molecular dynamics simulation
Site-directed mutagenesis

ABSTRACT

Fragrance rice (*Oryza sativa*) contains two isoforms of BADH, named OsBADH1 and OsBADH2. OsBADH1 is implicated in acetaldehyde oxidation in rice plant peroxisomes, while the non-functional OsBADH2 is believed to be involved in the accumulation of 2-acetyl-1-pyrroline, the major compound of aroma in fragrance rice. In the present study, site-directed mutagenesis, molecular docking and molecular dynamics simulation studies were used to investigate the substrate specificity towards Bet-ald and GAB-ald. Consistent with our previous study, kinetics data indicated that the enzymes catalyze the oxidation of GAB-ald more efficiently than Bet-ald and the OsBADH1 W172F and OsBADH2 W170F mutants displayed a higher catalytic efficiency towards GAB-ald. Molecular docking analysis and molecular dynamics simulations for the first time provided models for aldehyde substrate-bound complexes of OsBADHs. The amino acid residues, E262, L263, C296 and W461 of OsBADH1 and E260, L261, C294 and W459 of OsBADH2 located within 5 Å of the OsBADH active site mainly interacted with GAB-ald forming strong hydrogen bonds in both OsBADH isoforms. Residues W163, N164, Q294, C296 and F397 of OsBADH1–Bet-ald and Y163, M167, W170, E260, S295 and C453 of OsBADH2–Bet-ald formed the main interaction sites while E260 showed an interaction energy of −14.21 kcal/mol. Unconserved A290 in OsBADH1 and W288 in OsBADH2 appeared to be important for substrate recognition similar to that observed in PsAMADHs. Overall, the results here help to explain how two homologous rice BADHs recognize the aldehyde substrate differently, a key property to their biological role.

© 2012 Published by Elsevier Masson SAS.

1. Introduction

Aldehyde dehydrogenases (ALDHs) (E.C. 1.2.1.3) are a superfamily of NAD(P)$^+$-dependent enzymes which metabolize many biologically important intermediate aldehydes [1]. These aldehyde compounds are ubiquitous in nature and quite toxic to cells. Therefore, the regulation of the level of aldehyde intermediates must be carefully controlled. ALDHs catalyze the irreversible oxidation of aldehyde to their corresponding carboxylic acid. Some ALDHs can catalyze a very limited range of substrates whereas the others recognize a broad range of substrates. ALDH enzymes require either NAD^+ or $NADP^+$ as a cofactor [2] and the classification of ALDH members is determined by their aldehyde substrates such as alcohol, lactaldehyde and aminoaldehyde dehydrogenases. Aminoaldehyde dehydrogenases (AMADHs, EC 1.2.1.19) belong to the aldehyde dehydrogenase 9 family (ALDH9) [3] and are NAD(P)$^+$-dependent enzymes which can catalyze the oxidation of a broad range of ω-aminoaldehydes to the corresponding ω-amino acids. The ω-aminoaldehydes are obtained from the oxidation of polyamines such as spermine (Spm), spermidine (Spd) and putrescine (Put) which are oxidized by amine oxidases [4]. AMADH from *Pisum sativum* is an example of a plant AMADH that exhibits broad aminoaldehyde substrate specificity [5,6]. Besides AMADHs, plant betaine aldehyde dehydrogenases (BADHs, EC 1.2.1.8) also oxidize a wide range of ω-aminoaldehyde substrates in addition to its natural substrate, Bet-ald [8–10]. BADH enzymes generally catalyze the last step in the synthesis of the osmoprotectant glycine betaine from choline [11]. Thus, BADHs can be classified into two

Abbreviations: ALDH, Aldehyde dehydrogenase; AMADH, Aminoaldehyde dehydrogenase; 2AP, 2-acetyl-1-pyrroline; AP-ald, 3-aminopropionaldehyde; BADH, Betaine aldehyde dehydrogenase; Bet-ald, Betaine aldehyde; GAB-ald, γ-aminobutyraldehyde; IPTG, Isopropyl-β-D-thio-galactoside; MD, Molecular dynamics; TMAB-ald, 4-*N*-trimethylaminobutyraldehyde; TMAP-ald, 3-*N*-trimethylaminopropionaldehyde.

* Corresponding author. Departmant of Biochemistry, Faculty of Science, Kasetsart University, 50 Phahonyothin Road, Chatuchak, Bangkok 10900, Thailand. Tel.: +662 562 5555x2048; fax : +662 561 4627.
E-mail address: nonlawat.b@ku.ac.th (N. Boonyalai).

0300-9084/$ – see front matter © 2012 Published by Elsevier Masson SAS.
doi:10.1016/j.biochi.2012.04.009

Please cite this article in press as: K. Jiamsomboon, et al., Dissecting substrate specificity of two rice BADH isoforms: Enzyme kinetics, docking and molecular dynamics simulation studies, Biochimie (2012), doi:10.1016/j.biochi.2012.04.009

Copyright by Kasetsart University All rights reserved

ARTICLE IN PRESS BIOCHI3875_proof ■ 21 April 2012 ■ 2/11

subfamilies. The first group is those with high specificity for, and activity toward the substrate Bet-ald (true BADH) while the second group exhibits broad affinity for a range of aminoaldehydes (high BADH homology aminoaldehyde dehydrogenase (HBH-AMADH)) [7]. BADHs from rice have been previously shown to be an HBH-AMADH since they showed only moderate to low activity toward Bet-ald but high activity for aminoaldehydes [9,10,17]. Therefore, BADHs from rice can also be considered AMADHs [7].

At present, five crystal structures of BADHs and two crystal structures of plant AMADHs are available [6,12–14]. Most of the known structures of BADH are in tetrameric form, except for the plant AMADH which is dimeric. Each subunit of BADH comprises a coenzyme binding domain, an oligomerization domain and a catalytic domain. The catalytic triad of AMADH from *P. sativum* contains C294, N162 and E260 which are conserved in BADH from different species [6]. In the catalytic cycle of BADH, the catalytic cysteine attacks the aldehyde substrate forming a thiohemiacetal intermediate whereas the glutamate, which is involved in the proton relay system, has been proposed to be the general base in the catalysis. The asparagine on the other hand has been implicated in stabilizing the thiohemiacetal intermediate forming the oxyanion hole [14].

Two BADH homologs in rice (*Oryza sativa*), *OsBADH1* and *OsBADH2*, are encoded on chromosome four and chromosome eight, respectively [15] and share 75% amino acid sequence identity. It has been speculated that OsBADH1 is localized in rice plant peroxisome [10] since its deduced primary structure contains a Ser–Lys–Leu (SKL) motif at the C-terminus, whereas an experiment in young panicles of rice plants used to identify the subcellular localization of OsBADH2 indicates that an OsBADH2 signal was only found in the cytoplasm and not in the nucleus [16]. Moreover, the eight base pair deletion in exon 7 of the *OsBADH2* gene results in a truncated non-functional OsBADH2 and the partial loss of OsBADH2 function is proposed to account for the accumulation of 2-acetyl-1-pyrroline (2AP), the major compound of aroma in fragrance rice [9,15]. Both OsBADHs have shown broad aminoaldehydes substrate specificity [9,10] and the enzymatic characterization of both OsBADHs showed that the enzymes can oxidize C3 and C4 aminoaldehydes or medium-chain aldehyde such as γ-aminobutyraldehyde (GAB-ald), 3-aminopropionaldehyde (AP-ald), 4-*N*-trimethylaminobutyraldehyde (TMAB-ald) and 3-*N*-trimethylaminopropionaldehyde (TMAP-ald) better than Bet-ald. Recently, it was reported that OsBADH2_Y420, containing a Y420 insertion similar to BADH2.8 from Myanmar fragrance rice, exhibited less catalytic efficiency towards GAB-ald but not for Bet-ald compared to the wild-type enzyme [17]. This mutant may bring about the accumulation of GAB-ald/Δ^1-pyrroline, which is subsequently converted to 2AP.

Although both OsBADHs are highly similar in amino acid sequence, their functions might be different. To elucidate and understand the substrate specificity of both OsBADHs, we first used site-directed mutagenesis of amino acids involved in catalysis and substrate recognition. Subsequently the cofactor NAD^+ binding to each enzyme was investigated to evaluate changes in enzyme conformation upon binding. The substrate specificity of the enzymes towards Bet-ald and GAB-ald was also investigated. In addition to biochemical experiments, molecular docking and molecular dynamics simulation were carried out to gain better understanding factors determining substrate specificity and catalysis.

2. Materials and methods

2.1. Materials

Betaine aldehyde chloride and γ-aminobutyraldehyde dimethyl acetal were obtained from Sigma–Aldrich Chemical Co. (St Louis, MO, USA) while acetaldehyde was purchased from Fluka A. G. (Buchs, Switzerland). Nicotinamide adenine dinucleotide (NAD^+) was obtained from Merck (Darmstadt, Germany). Ingredients for bacterial media and buffers were obtained from Himedia, USB and Acrös Organic. Molecular biology reagents, including restriction enzymes, PCR reagents, DNA polymerase, DNA ladders and protein molecular weight standards, were obtained from Fermentas (USA). Hitrap Chelating HP columns were purchased from GE Healthcare Bio-Sciences AB (Uppsala, Sweden).

2.2. Bacterial s1trains and plasmids

Escherichia coli strains XL10-Gold (Stratagene, La Jolla, CA, USA) were used for cloning and isolation of plasmids. The pET28b-OsBADH1 and pET28b-OsBADH2 plasmids, containing the *OsBADH1* and *OsBADH2* genes, respectively, were constructed as described in Wongpanya et al. [17]. The *E. coli* strain BL21 (DE3) was used for protein expression.

2.3. Site-directed mutagenesis

OsBADH1 or OsBADH2 mutants were generated by PCR with the Quikchange® lightning site-directed mutagenesis kit from Stratagene (La Jolla, CA, USA), using the pET28b–OsBADH1 or pET28b–OsBADH2 plasmid [17] as a template, respectively. The mutagenic primers include mutations (underlined) at the corresponding triplets (bold) (only direct constructions are shown in Table 1). The presence of each specific mutation was confirmed by DNA sequencing.

2.4. Expression and purification of OsBADH wild-type and mutants

OsBADH1 and OsBADH2 enzymes, either wild-type or mutants, were produced in *E. coli* BL21 (DE3) using the pET28b expression system. Expression and purification of the enzymes were performed essentially as previously described with some modifications [17]. Transformed *E. coli* cells were taken from an LB-kanamycin plate and inoculated into 5 ml of LB-broth-kanamycin medium as overnight cultures. These starter cultures were subsequently used to inoculate 250 ml of LB-broth-kanamycin medium. The cultures were grown in a shaking incubator at 37 °C until A_{600} reached 0.4–0.6 and then protein expression was induced by adding IPTG to a final concentration of 0.4 mM. Induction progressed for 16–24 h at 22 °C before the cells were harvested by centrifugation (1900× *g* for 15 min) and stored at −20 °C.

The cell pellet was thawed and resuspended in 15 ml of extraction buffer (50 mM Tris–HCl pH 8, 0.5 mM NaCl and 5 mM imidazole). Cells were then broken by sonication using pulse amplitude (on 10 s, off 5 s) for 15 min. Cell debris was removed by centrifugation (11950× *g* for 30 min). The supernatant was filtered through a 0.45 μm pore diameter filter and then applied to a HiTrap Chelating HP column previously equilibrated with washing buffer A (50 mM Tris–HCl pH 8, 0.5 M NaCl and 0.03 M imidazole). Retained proteins were eluted with buffer B (50 mM Tris–HCl pH 8, 0.5 M

Table 1
Oligonucleotides used as primers for PCR site-directed mutagenesis.

Mutations	Mutagenic primer sequences (5′ to 3′)
N164A_OsBADH1	GGA CTT ATC ACT CCC TGG GCT TAT CCT CTG ATG GC
W172A_OsBADH1	TCT GCT GAT GGC TAC T**GC** GAA GGT TGC ACC TGC C
W172F_OsBADH1	CCT CTG CTG ATG GCT ACT **TTC** AAG GTT GCA CCT GC
N162A_OsBADH2	GGT TGA TCA CAC CTT GG**G CC**T ATC CTC TCC TGA TGG C
W170A_OsBADH2	TCT CCT GAT GGC AAC A**GC** GAA GGT AGC TCC TGC C
W170F_OsBADH2	CCT CTC CTG ATG GCA ACA **TTC** AAG GTA GCT CCT GC

Please cite this article in press as: K. Jiamsomboon, et al., Dissecting substrate specificity of two rice BADH isoforms: Enzyme kinetics, docking and molecular dynamics simulation studies, Biochimie (2012), doi:10.1016/j.biochi.2012.04.009

Copyright by Kasetsart University All rights reserved

ARTICLE IN PRESS BIOCHI3875_proof ■ 21 April 2012 ■ 3/11

NaCl and 0.5 M imidazole). Protein fractions were analyzed by 12% SDS-PAGE. Fractions containing purified enzyme were pooled and the buffer was exchanged with 50 mM HEPES-KOH, pH 8 to remove imidazole. Subsequently, the purified enzyme was stored at 4 °C for immediate use or −80 °C until future use.

2.5. Intrinsic fluorescence of OsBADH wild-type and mutants

Fluorescence measurements were carried out as described previously with some modifications [13]. Measurements were performed to investigate the binding of NAD^+ to OsBADH proteins. Fluorescence binding between proteins and NAD^+ was carried out by monitoring the intrinsic fluorescent intensity of tryptophan residues. Fluorescence titration was performed by adding microliter amounts of NAD^+ to 400 μl of 1.5 μM OsBADH in 50 mM HEPES-KOH buffer (pH 8). Excitation wavelength was 295 nm (slit 5 nm) and emission spectra were recorded between 300 nm and 450 nm (slit 5 nm). After addition of the cofactor, the sample was mixed and the spectrum was recorded. Titration results were corrected to account for ligand dilution in buffer. Data were plotted as ΔF_{max} (the maximum attainable change in fluorescence intensity) at 350 nm versus the concentration of cofactor. The dissociation constant (K_d) for NAD^+ was obtained by fitting the change in fluorescence against the concentration of NAD^+ using the following equation:

$$\%\Delta F_{obs} = \frac{\Delta F_{max}[L]_0}{K_d + [L]_0}$$

where $\%\Delta F_{obs}$ is the enhancement of fluorescence upon binding to protein, ΔF_{max} is the maximum attainable change in fluorescence intensity, $[L]_0$ is the total molar concentration of the ligand, and K_d is the dissociation constant for NAD^+ binding. The data were fitted and standard errors were calculated by non-linear regression analysis using the Microcal Origin 6.0 program.

2.6. Enzymatic activity of OsBADH wild-type and mutants

Enzyme kinetic assays for wild-type and mutant OsBADHs were measured spectrophotometrically by monitoring the oxidation of Bet-ald and GAB-ald [9]. Betaine aldehyde chloride was dissolved in H_2O and directly used in the enzymatic assay. γ-amino-butyraldehyde dimethyl acetal was used for GAB-ald. The diethylacetals of γ-aminobutyraldehyde were hydrolyzed with 1 M HCl and heated at 80 °C for 1 h. The hydrolyzate was neutralized by adding an equivalent volume of 1 N NaOH. Bet-ald and GAB-ald were stored at −20 °C while the 100 mM stock solution of acetaldehyde was prepared and kept at 4 °C until required. Enzymatic activities were determined using a reaction mixture containing 50 mM HEPES-KOH buffer, pH 8, 5 mM NAD^+ and various concentration of each substrate (between 8 and 1000 μM). One unit of enzyme activity was defined as the amount of enzyme that catalyzed the formation of 1 μmol of NADH per minute at 30 °C. Reactions was monitored by following the change in absorbance at 340 nm corresponding to the formation of NADH (ε = 6220 M^{-1} cm^{-1}) [9]. K_m and V_{max} values were obtained by fitting the initial rates against the concentration of each substrate to the Michaelis–Menten equation. The data were fitted and standard errors were calculated by non-linear regression using the Microcal Origin 6 software.

2.7. Molecular docking analysis

The crystal structure of OsBADH2 was obtained from Assist. Prof. Dr. Kiattawee Choowongkomon (Department of Biochemistry, Kasetsart University, Thailand) [18]. Since the amino acid sequence identity between OsBADH1 and OsBADH2 is about 75%, a homology model of OsBADH1 was generated by SWISS-MODEL using the crystal structure of OsBADH2 as a template. The structures of both OsBADH proteins were superimposed using the program PyMOL [19]. Bet-ald was taken from the crystal structure of *YdcW* (PDB entry 1WNB) [13] whereas GAB-ald was built using Discovery Studio 2.5 (Accelrys, Inc., CA, USA). Mutant proteins were generated using Discovery Studio 2.5. After both proteins and ligands were successfully constructed, the docking was performed on Autodock 4.0 [20]. For docking ligand, the rotational bonds of the side chain were treated as flexible whereas those of main chain were regarded as rigid. Grid boxes were created to cover the substrate-binding domain of the protein. The size of the grid box was set at 60 × 60 × 60 $Å^3$ and the center of the grid box was set at 7.545 Å (x), 3.238 Å (y), and 33.596 Å (z). The Lamarckian Genetic Algorithm (LGA) with 100 runs was used as the search algorithm. The population size was set at 150. Three-dimensional structures of OsBADHs–Bet-ald or OsBADHs–GAB-ald with the lowest energy and highest populations were visualized and analyzed by PyMOL [19] and Discovery Studio 2.5.

2.8. Molecular dynamics simulations

The selected models of OsBADHs–Bet-ald or OsBADHs–GAB-ald complexes obtained from docking were used for MD simulations. MD simulations were performed using the AMBER10 simulation package with the Cornell force field [21]. OsBADH1 and OsBADH2 contained 505 and 503 amino acid residues, respectively. All complexes were immersed in an octahedral box of TIP3P water [22] with the distance between solute surface and the edge of the box set at 10 Å. Minimization was achieved stepwise as follows: 2000 steps for hydrogen atoms, 2000 steps for solvent water molecules and 5000 steps for all atoms in the system. The equilibration was perfomed in the carononical ensemble (NVE) at 300 K; during the initial 100 ps all atoms in the protein were restrained while in the following 100 ps all atoms were set free. MD simulations were carried out under an isobaric–isothermal ensemble (NPT), at 1 atm and 300 K. Equilibration was achieved when the system was stable and this was followed by a production phase which was harvested during the last 500 ps of the trajectory. Root-mean-square displacement (RMSD) values for distances between interacting amino acid residues, hydrogen bonds and binding free energies were also calculated.

3. Results and discussion

3.1. NAD^+ cofactor binding

Several reports have previously shown that BADHs from several species can bind either NAD^+ or $NADP^+$ [6,8,13,17]. BADHs from rice, OsBADH1 and OsBADH2, have greater affinity for NAD^+ than for $NADP^+$ [17]. The affinity of each enzyme for NAD^+ was investigated by monitoring changes in intrinsic tryptophan fluorescence upon binding. For BADHs, it has been reported that the binding of NAD^+ usually takes place prior to the binding of aldehyde substrate [23]. When the wavelength at 295 nm was used to excite the tryptophan residues within the protein, the emission spectrum of OsBADHs exhibited maxima at 350 nm. A decrease in the intensity of tryptophan fluorescence for OsBADHs was observed upon the addition of NAD^+. This phenomenon was clearly associated with the binding of NAD^+ implying that the overall structure of the enzyme was correct and that mutations to the OsBADH active site do not induce significant changes in conformation. Dissociation constant (K_d) values for OsBADH1 and OsBADH2 wild-type and mutants were determined for NAD^+ and are shown in Table 2. K_d

Please cite this article in press as: K. Jiamsomboon, et al., Dissecting substrate specificity of two rice BADH isoforms: Enzyme kinetics, docking and molecular dynamics simulation studies, Biochimie (2012), doi:10.1016/j.biochi.2012.04.009

Copyright by Kasetsart University All rights reserved

Table 2
Dissociation constant (K_d) of NAD^+ and OsBADHs.

K_d (μM)			
OsBADH1		OsBADH2	
Wild-type	34 ± 3	Wild-type	9 ± 1
N164A	51 ± 3	N162A	19 ± 4
W172A	56 ± 3	W170A	16 ± 3
W172F	50 ± 3	W170F	14 ± 2

values of all mutants increased by less than 2-fold, indicating that each mutation mentioned herein did not dramatically affect protein structure or cofactor binding. The K_d values reported here were in agreement with a previous study [17]. However, the K_d value of OsBADH2 for NAD^+ (9 μM) suggested that OsBADH2 can bind to NAD^+ with higher affinity compared to OsBADH1 (K_d of 34 μM). Collectively, the results showed that each mutant could bind NAD^+, indicating they are correctly folded. Having determined the cofactor binding affinity, the kinetic parameters K_m, k_{cat} and k_{cat}/K_m for OsBADH wild-type and mutants were also characterized using Bet-ald and GAB-ald as substrates.

3.2. Enzymatic characterization

All OsBADH1 and OsBADH2 wild-type and mutants can catalyze the oxidation of Bet-ald and GAB-ald as shown in Table 3. The K_m value of wild-type OsBADH1 for Bet-ald was 3-fold higher than GAB-ald, suggesting that OsBADH1 can bind GAB-ald with a higher affinity than Bet-ald. The K_m values for the OsBADH1 mutants were about 7–10-fold lower than that of the wild-type OsBADH1, respectively, while K_m values for the OsBADH1 mutants for GAB-ald were 1.5–6.6-fold lower. These results showed that all OsBADH1 mutants seemed to bind both Bet-ald and GAB-ald tighter than wild-type OsBADH1. Similar to OsBADH1, the K_m value of wild-type OsBADH2 for Bet-ald was 6.6-fold higher than GAB-ald while the K_m values of the OsBADH2 mutants for Bet-ald were observed to have a 3.3–4.4-fold lower, respectively compared to wild-type OsBADH2. In contrast, K_m values of the OsBADH2 mutants for GAB-ald showed a 1.5–2.8-fold increase, respectively compared to wild-type OsBADH2. These results indicated that mutants of OsBADH2 could bind Bet-ald tighter than wild-type but bind GAB-ald slightly less than wild-type. When comparing the K_m values of OsBADH1 and OsBADH2 for Bet-ald and GAB-ald to those previously reported [9,10,17], our results are comparable in that the enzymes can bind GAB-ald better than Bet-ald.

For catalytic activity, the k_{cat} values of the OsBADH1 mutants for Bet-ald were found to be between 16 and 236-fold lower, respectively, while those of the OsBADH1 mutants for GAB-ald were around 1.4–13.5-fold lower, respectively, compared to wild-type OsBADH1. For the OsBADH2 mutants, the k_{cat} values for Bet-ald were 3.8–8-fold lower compared to wild-type OsBADH2. Likewise, the k_{cat} values of N162A and W170A for GAB-ald were 2.7-fold and 3.2-fold lower compared to the wild-type, respectively, but the W170F mutant had k_{cat} values 4.4-fold larger compared to that of the wild-type. Collectively, the results revealed that substitution of N164 and W172 of OsBADH1 and N162 and W170 of OsBADH2 by alanine reduced the catalytic activity towards Bet-ald and GAB-ald. However, the OsBADH2 W170F mutant exhibited a slightly higher k_{cat} value than the wild-type while OsBADH1 W172F exhibited a reduced k_{cat} value. For the catalytic efficiency, the k_{cat}/K_m values of the OsBADH1 mutants for Bet-ald were reduced by 2.1–23.8-fold, while the k_{cat}/K_m value of N164A for GAB-ald were 2.4-fold lower but the k_{cat}/K_m values of W172A and W172F for GAB-ald were unchanged and 2-fold higher, respectively compared to OsBADH1 wild-type. For OsBADH2 mutants, the k_{cat}/K_m values of N162A and W170A for Bet-ald were 1.6-fold and 2.4-fold lower, respectively but the k_{cat}/K_m value of W170F for Bet-ald was 1.2-fold higher. Similarly, the k_{cat}/K_m values of N162A and W170A for GAB-ald were 7.5-fold and 4.9-fold lower, respectively while the k_{cat}/K_m value of W170F for GAB-ald was 1.6-fold higher. Out of six mutants, only two mutants (OsBADH1 W172F and OsBADH2 W170F) showed a higher catalytic efficiency towards GAB-ald. This implied that either W172 or W170 in each protein may be key residues determining substrate specificity towards GAB-ald. In addition to Bet-ald and GAB-ald, acetaldehyde was also used as a substrate since it was previously reported that both OsBADH1 and OsBADH2 catalyzed the oxidation of acetaldehyde [10]. Our results (Table 4) were in agreement with those previously reported indicating that OsBADH1 is a better candidate enzyme for acetaldehyde than OsBADH2.

Table 4
Kinetic parameters for wild-type OsBADHs with acetaldehyde.

Acetaldehyde			
	K_m (μM)	k_{cat} (s^{-1})	k_{cat}/K_m (M^{-1} s^{-1})
OsBADH1	99 ± 29	0.14	1425
OsBADH2	146 ± 34	0.08	607

BADH enzyme from *E. coli* was reported to be able to catalyze the oxidation of GAB-ald better than Bet-ald in general because of the shape of its active site [13]. Mutagenesis of the highly conserved N162 of PsAMADH2 to alanine resulted in about a 200-fold reduction in dehydrogenase activity, indicating that the residue is involved in the catalytic efficiency of PsAMADH2 [6]. Therefore, mutation of the catalytic Asn residue would definitely affect the k_{cat}/K_m value. Besides the catalytic triad, Trp residues lining the substrate binding pocket were proposed to be involved in substrate binding [12], and hence mutation of these Trp residues should also affect k_{cat}/K_m. Most of the mutants examined herein exhibited lower or equal catalytic efficiency towards Bet-ald, while some mutants showed an increased catalytic efficiency towards GAB-ald compared to the wild type. Additionally, changing Trp to Phe had a tremendous effect on k_{cat}/K_m towards GAB-ald but not towards Bet-ald indicating that Trp may be involved in the recognition of Bet-ald but not GAB-ald. Our result correlated well with a previous

Table 3
Kinetic parameters for wild type and mutant OsBADHs with Bet-ald and GAB-ald.

	OsBADH1							OsBADH2						
	Bet-ald			GAB-ald				Bet-ald			GAB-ald			
	K_m (μM)	k_{cat} (s^{-1})	k_{cat}/K_m (M^{-1} s^{-1})	K_m (μM)	k_{cat} (s^{-1})	k_{cat}/K_m (M^{-1} s^{-1})		K_m (μM)	k_{cat} (s^{-1})	k_{cat}/K_m (M^{-1} s^{-1})	K_m (μM)	k_{cat} (s^{-1})	k_{cat}/K_m (M^{-1} s^{-1})	
Wild-type	1288 ± 192	0.52	405	432 ± 57	0.31	718	Wild-type	251 ± 62	0.057	228	38 ± 11	0.032	842	
N164A	165 ± 35	0.032	194	78 ± 5	0.023	295	N162A	66 ± 10	0.0093	141	107 ± 12	0.012	112	
W172A	129 ± 23	0.0022	17	291 ± 18	0.22	756	W170A	77 ± 7	0.0072	94	58 ± 8	0.01	172	
W172F	140 ± 51	0.0102	73	65 ± 11	0.09	1385	W170F	57 ± 10	0.015	263	105 ± 10	0.14	1333	

Please cite this article in press as: K. Jiamsomboon, et al., Dissecting substrate specificity of two rice BADH isoforms: Enzyme kinetics, docking and molecular dynamics simulation studies, Biochimie (2012), doi:10.1016/j.biochi.2012.04.009

Copyright by Kasetsart University All rights reserved

ARTICLE IN PRESS BIOCHI3875_proof ■ 21 April 2012 ■ 5/11

study of aromatic active-site residues in PsAMADH2 [24] which showed that W170, W288 and Y163 (PsAMADH2 numbering), were important for the overall geometry of the substrate channel allowing for the appropriate orientation of the substrate towards the catalytic residue C294. These residues are also essential for π-electron stacking interaction with an entering substrate. Alanine scanning of aromatic residues in the substrate channel resulted in a change in the substrate specificity of PsAMADH2 [24]. Since no crystal structures of enzyme/aldehyde complexes or of OsBADH are currently available, we used molecular docking and molecular dynamics simulation to gain a better understanding of factors determining differences in substrate specificity.

3.3. Molecular docking analysis

The crystal structure of OsBADH2 [18] was used as a template to generate a homology model of OsBADH1 (residues 8–504) using SWISS-MODEL. The quality of the OsBADH1 model was evaluated using the program PROCHECK [25]. The model possessed good geometry, with 85% of all residues in the most favored and 14.6% in the allowed regions of the Ramachandran plot (Supplementary data Fig. S1). The RMSD value between OsBADH1 and PsAMADH2 was 0.57 Å. To confirm the reliability of the results from molecular docking, the structure of OsBADH-substrate complexes from docking were superimposed with the structure of PsAMADH1 (PDB

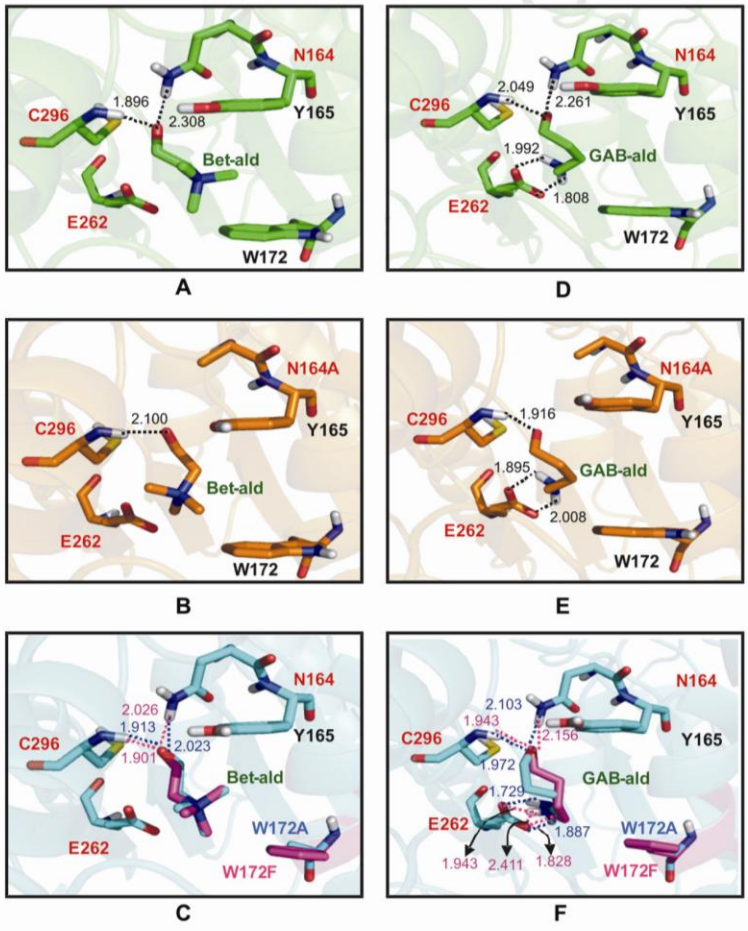

Fig. 1. Molecular docking analysis of (A) OsBADH1 with Bet-ald (B) N164A with Bet-ald (C) W172A and W172F with Bet-ald (D) OsBADH1 with GAB-ald (E) N164A with GAB-ald and (F) W172A and W172F with GAB-ald. Hydrogen bonds are shown as dotted lines. Carbon atoms of OsBADH1, N164A, W172A and W172F are colored green, orange, cyan and magenta, respectively. The names of catalytic triad residues for OsBADH1 including C296, E262 and N164 are colored red while the aldehyde substrates, Bet-ald and GAB-ald are green. Distances are in angstrom. (For interpretation of the references to color in this figure legend, the reader is referred to the web version of this article.)

Please cite this article in press as: K. Jiamsomboon, et al., Dissecting substrate specificity of two rice BADH isoforms: Enzyme kinetics, docking and molecular dynamics simulation studies, Biochimie (2012), doi:10.1016/j.biochi.2012.04.009

Copyright by Kasetsart University All rights reserved

entry 3IWK) [6] using PyMOL [19]. The position of both Bet-ald and GAB-ald overlapped well with the glycerol molecule in PsAMADH1 (Supplementary data Fig. S2). For the OsBADH-substrate complexes GAB-ald displayed a lower binding energy than Bet-ald, indicating that GAB-ald is likely to bind both OsBADH1 and OsBADH2 with high affinity (Supplementary data Table S1). The binding pockets of OsBADH1 and OsBADH2 in complex with Bet-ald and GAB-ald are shown in Figs. 1 and 2 with the hydrogen bonding analysis. It can be seen that the carbonyl group of Bet-ald can form two moderate to strong hydrogen bonds between the N–H main chain of C296 and the N–H side chain of N164 in the OsBADH1–Bet-ald complex (Fig. 1A). In the N164A–OsBADH1-Bet-ald complex, the hydrogen bond between the N–H side chain of N164 and the carbonyl group of Bet-ald was abolished when residue N164 was replaced with alanine (Fig. 1B). In the W172A- and W172F–OsBADH1-Bet-ald complexes, two strong hydrogen bonds were also observed similar to those in wild-type OsBADH1 (Fig. 1C). However, the hydrogen bond distances in all mutants were slightly longer than those observed in the wild-type enzyme. It is important to note that the tertiary amine group of Bet-ald was positioned away from the mutated residue whereas the oxygen was positioned toward the catalytic cysteine. Unlike the OsBADH1–Bet-ald complex, four hydrogen bonds were observed in wild-type OsBADH1–GAB-ald and W172A–OsBADH1-GAB-ald while five hydrogen bonds are

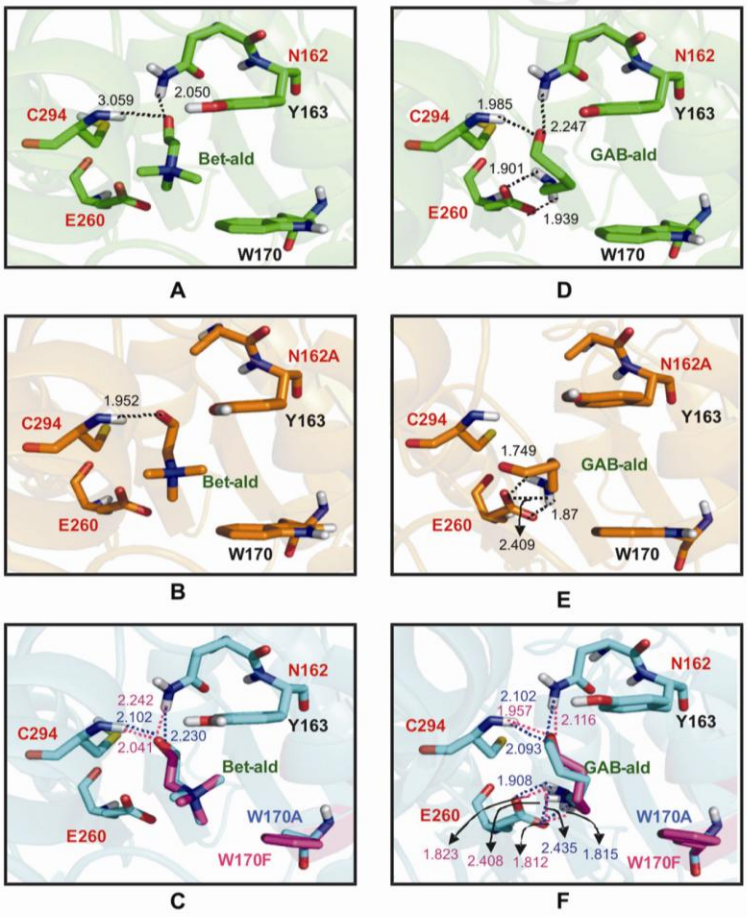

Fig. 2. Molecular docking analysis of (A) OsBADH2 with Bet-ald (B) N162A with Bet-ald (C) W170A and W170F with Bet-ald (D) OsBADH2 with GAB-ald (E) N162A with GAB-ald and (F) W170A and W170F with GAB-ald. Hydrogen bonds are shown as dotted lines. Carbon atoms of OsBADH2, N162A, W170A and W170F are colored green, orange, cyan and magenta, respectively. The names of the catalytic triad residues for OsBADH2 including C294, E260 and N162 are highlighted with red text. Bet-ald and GAB-ald are designated by green text. Distances are in angstrom. (For interpretation of the references to color in this figure legend, the reader is referred to the web version of this article.)

Please cite this article in press as: K. Jiamsomboon, et al., Dissecting substrate specificity of two rice BADH isoforms: Enzyme kinetics, docking and molecular dynamics simulation studies, Biochimie (2012), doi:10.1016/j.biochi.2012.04.009

Copyright by Kasetsart University All rights reserved

observed in W172F–OsBADH1-GAB-ald (Fig. 1F). In the OsBADH1 mutant – GAB-ald complexes, the hydrogen bond between the N–H side chain of N164 and the carbonyl group of GAB-ald was also disturbed when residue N164 was changed to alanine (Fig. 1E). Higher numbers of hydrogen bonds in the GAB-ald complex correlate well with the kinetic results in which K_m values for GAB-ald were slightly lower than those for Bet-ald. It was also noted that the amino group in GAB-ald was pointed toward E262 instead of W172. These results offer a possible explanation for the observed differences in substrate specificity for OsBADH1.

In comparison to the OsBADH1–Bet-ald complex, similar hydrogen bonding networks were observed in the OsBADH2–Bet-ald complex. The N–H main chain of C294 and the N–H side chain of N162 could form hydrogen bonds with the oxygen atom of the carbonyl group of Bet-ald as seen in the OsBADH1 complex (Fig. 2A). Similar to OsBADH1, the N162A mutation resulted in the loss of a hydrogen bond (Fig. 2B) but the same pattern of hydrogen bonds is observed in the W170A and W170F complexes (Fig. 2C). For the OsBADH2–GAB-ald complex, four hydrogen bonds can be found between GAB-ald and residues C294, N162 and E260 (Fig. 2D). It is noteworthy that two hydrogen bonds between N–H of GAB-ald and the carboxyl group of E260 are only detected in the complex with GAB-ald. However, in the N162A–GAB-ald complex, only hydrogen bonds between the side chain of E260 and Bet-ald are observed (Fig. 2E). On the other hand, five hydrogen bonds are observed in both the W170A–GAB-ald and W170F–GAB-ald complexes (Fig. 2F). To further examine the binding mode of both Bet-ald and GAB-ald to wild-type OsBADHs as well as to determine interactions involved in the protein–ligand complex, four complexes of the wild-type enzymes (OsBADH1–Bet-ald, OsBADH1–GAB-ald, OsBADH2–Bet-ald and OsBADH2–GAB-ald) obtained from the docking experiment were used for MD simulations.

3.4. MD simulations and binding energy of OsBADH complexes

Structural and dynamic studies of both OsBADHs with aldehyde substrates were carried out by MD simulations. The OsBADH complex comprised OsBADHs, NAD^+, and their aldehyde sub strates. The trajectories for four simulation systems: OsBADH1–Bet-NAD^+, OsBADH1–GAB-NAD^+, OsBADH2–Bet-NAD^+ and OsBADH2–GAB-NAD^+, were analyzed over the last 500 ps after reaching equilibrium. RMSD fluctuations for OsBADH complexes were monitored to determine the structural equilibrium (Supplementary data Fig. S3). Overall, the results confirmed that all components were well in equilibration throughout the analysis range thus allowing us to determine binding energies and preferred binding sites for each complex.

Thermodynamic parameters for OsBADHs–Bet-ald and OsBADHs–GAB-ald complexes are presented in Table 5. The energy component involved in binding indicated that the simulation models could be separated into two sets based on the ligand driving force for the interaction. Set I was the binding of OsBADHs to Bet-ald. The important interactions for these models were electrostatic interactions (ΔE_{ELE}), which played a major role as the main attractive force. The *van der Waal* interactions in the gas phase (ΔE_{VDW}) were the second most important energy component for this binding. Set II contained models of OsBADHs binding to GAB-ald in which, unlike OsBADHs–Bet-ald, the electrostatic interaction was not the main interaction. Electrostatic interactions for OsBADH1 and OsBADH2 were −22.62 and −22.67 kcal/mol, respectively, while the *van der Waal* interaction was −17.74 kcal/mol for OsBADH1 and −19.05 kcal/mol for OsBADH2. It is noted that the nonpolar interaction of solvation ($\Delta\Delta G_{SA}$) of the four complexes was lower than the *van der Waal* interaction in gas phase

Table 5
Binding free energies for four trajectories of the OsBADH1–Bet-ald, OsBADH1–GAB-ald, OsBADH2–Bet-ald and OsBADH2–GAB-ald complexes.

Energy (kcal/mol)	OsBADH1		OsBADH2	
	Bet-ald	GAB-ald	Bet-ald	GAB-ald
ΔE_{ELE}[a]	−239.51	−22.62	−224.06	−22.67
ΔE_{VDW}[b]	−20.53	−17.74	−17.82	−19.05
$\Delta\Delta G_{SA}$[c]	−2.85	−2.65	−2.85	−2.70
$\Delta\Delta G_{PB}$[d]	246.01	24.66	227.09	28.64
$\Delta\Delta G_{MM/PBSA}$[e]	−16.88	−18.34	−17.65	−15.78

[a] Electrostatic energy.
[b] van der Waals energy.
[c] Nonpolar contribution to solvation.
[d] Electrostatic contribution to solvation.
[e] Total binding energy.

(ΔE_{VDW}). This may be caused by hydrogen bonding interactions during complex formation, resulting in the reduction of the polar surface exposed to water solvent. Additionally, the unfavorable energy component might have resulted from the electrostatic contributions of solvation ($\Delta\Delta G_{PB}$), which are 246.01, 24.66, 227.09 and 28.64 kcal/mol for OsBADH1–Bet-ald, OsBADH1–GAB-ald, OsBADH2–Bet-ald and OsBADH2–GAB-ald, respectively. According to the total binding energy of OsBADH1–ligand complexes, GAB-ald was represented as a higher potential ligand for OsBADH1 than Bet-ald with $\Delta\Delta G_{MM/PBSA}$ of −18.34 kcal/mol, which agreed well with the kinetic result. However, in contrast to the kinetic data the binding energy of OsBADH2–Bet-ald (−17.65 kcal/mol) was stronger than OsBADH2–GAB-ald (−15.78 kcal/mol). To confirm our results, the simulation experiments were carried out in triplicate and the similar results were obtained. While the binding energy from docking in which the conformation of the enzyme was kept rigid correlated well with the kinetic results, MD simulations in which the enzyme and ligands were allow to be flexible revealed a slightly different binding energy. This suggested that the dynamics of OsBADHs and the aldehyde substrates significantly affected the binding event. Conformational changes of amino acid residues around the binding site of OsBADH2 are discussed in the next section.

Unlike molecular docking, MD simulations allowed the protein–ligand complex to be fully relaxed in the solvent environment, thereby generating more reliable binding properties. In the OsBADH1 system, the OsBADH1–GAB-ald complex showed the lowest binding energy from docking and exhibited the best binding from molecular dynamics simulation. However, in the OsBADH2 system, the OsBADH2–GAB-ald complex gave the lowest binding energy from docking but not from MD simulations. In order to understand this difference, hydrogen bonding interactions and MMGBSA decomposition of the binding energy were considered.

3.5. Protein–ligand interactions

A statistical analysis of the equilibrium distance and hydrogen bonding interactions during the course of the MD simulation revealed that some atoms of the ligands and the enzyme moved closer to or further from each other due to the dynamics in the binding process. The conformation of either Bet-ald or GAB-ald upon binding to both OsBADH complexes was examined as shown in Fig. 3. In OsBADH1–Bet-ald, only one hydrogen bond was observed (Fig. 3A) between the main chain of C296 (N) and the oxygen atom (O) of Bet-ald. In OsBADH1–GAB-ald, the four observed hydrogen bonds were between (Fig. 3B): E262 (O) and GAB-ald (H1), GAB-ald (N1) and W454 (HE1), GAB-ald (O1) and C296 (H) and L263 (O) and GAB-ald (H2). In OsBADH2, no hydrogen bonds were observed for Bet-ald (Fig. 3C) but five hydrogen bonds

Please cite this article in press as: K. Jiamsomboon, et al., Dissecting substrate specificity of two rice BADH isoforms: Enzyme kinetics, docking and molecular dynamics simulation studies, Biochimie (2012), doi:10.1016/j.biochi.2012.04.009

Copyright by Kasetsart University All rights reserved

ARTICLE IN PRESS BIOCHI3875_proof ■ 21 April 2012 ■ 8/11

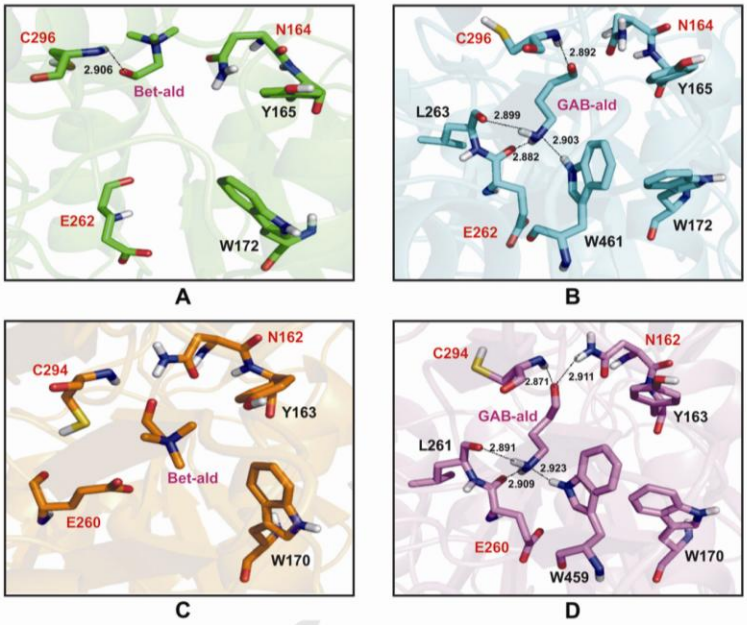

Fig. 3. MD simulations of the active site of (A) modeled OsBADH1 with Bet-ald (B) OsBADH1 with GAB-ald (C) OsBADH2 with Bet-ald and (D) OsBADH2 with GAB-ald. Hydrogen bonds are shown as dotted lines. Carbon atoms of OsBADH1–Bet-ald, OsBADH1–GAB-ald, OsBADH2–Bet-ald and OsBADH2–GAB-ald are colored green, cyan, orange and magenta, respectively. The names of catalytic triad residues for OsBADH1 including C296, E262 and N164 and OsBADH2 including C294, E260 and N162 are colored red. Bet-ald and GAB-ald are designated with green test. Distances are in angstrom. (For interpretation of the references to color in this figure legend, the reader is referred to the web version of this article.)

were observed for GAB-ald (Fig. 3D). The five hydrogen bonds in the OsBADH2–GAB-ald complex were between GAB-ald (O1) and C294 (H), L261 (O) and GAB-ald (H2), GAB-ald (O1) and N162 (HD21), GAB-ald (N1) and W456 (HE1) and E260 (O) and GAB-ald (H1).

In the light of the MD simulations, it was revealed that GAB-ald formed stronger hydrogen bonds than Bet-ald with OsBADH1. As for OsBADH2, five hydrogen bonds were formed in the OsBADH2–GAB-ald complex while none was observed in OsBADH2–Bet-ald complex. In addition to hydrogen bond formation, relationships between the orientation of the Bet-ald and GAB-ald in the complex were different. First, Bet-ald in the OsBADH1 complex was far away from the catalytic triad compared with that in the OsBADH2 complex. It is important to note that the position of Bet-ald observed in the crystal structure of BADH in *E. coli* was also different from that in PaBADH [13]. Secondly, when looking at the two substrates, GAB-ald was located closer to the catalytic residue, E262, compared to Bet-ald. This finding was in agreement with a previous work, which reported that BADH catalyzes the oxidation of GAB-ald (C3–C6 aminoaldehydes) better than Bet-ald [5,6,10].

3.6. Energy decomposition of the binding energy

To gain more details in the energy of binding, interactions between ligand and surrounding residues within 5 Å were observed through decomposition energy using the MMGBSA (Molecular Mechanics-Generalized Born Surface Area) method as implemented in AMBER10. Eighteen residues within 5 Å radius of each OsBADH active site interacting with the substrate aldehydes were observed (Supplementary data Table S2) and the interaction energies were shown in Supplementary data Table S3. Alignment of the amino acid sequences for the OsBADHs showed that most residues are identical (Supplementary data Fig. S4) except for the two following residues: residue 290 (Ala in OsBADH1 and Trp in OsBADH2) and residue 295 (Val in OsBADH1 and Ile in OsBADH2). It is interesting to note that a change from aliphatic to aromatic amino acids was seen at position 290 while at position 295 a change is conservative (Val to Ile). Interactions between ligand and a selection of eighteen different residues were calculated as shown in Fig. 4A and B. It can be seen that three residues (W163, N164 and C296) mainly interact with Bet-ald in the OsBADH1 complex in which the interaction energies of W163 and N164 were higher than those in the other complexes (Fig. 4A). Additionally, interactions with Q294 and F397 were also important for OsBADH1–Bet-ald interactions. However, in OsBADH1–GAB-ald, E262, L263, C296 and W461 are the main residues for the attractive interaction with GAB-ald. Remarkably, N164, one of the catalytic triad, is also important for OsBADH1–GAB-ald (−1.17 kcal/mol); this was not observed from docking experiments. In the case of OsBADH2–Bet-ald, decomposition energies showed that six residues had strong attractive interactions with Bet-ald including Y163, M167, W170, E260, S295 and C453 (Fig. 4B). It is noteworthy that E260 becomes the main residue having strong interactions with Bet-ald in this complex, suggesting that the negatively charge

Please cite this article in press as: K. Jiamsomboon, et al., Dissecting substrate specificity of two rice BADH isoforms: Enzyme kinetics, docking and molecular dynamics simulation studies, Biochimie (2012), doi:10.1016/j.biochi.2012.04.009

Copyright by Kasetsart University All rights reserved

ARTICLE IN PRESS BIOCHI3875_proof ■ 21 April 2012 ■ 9/11

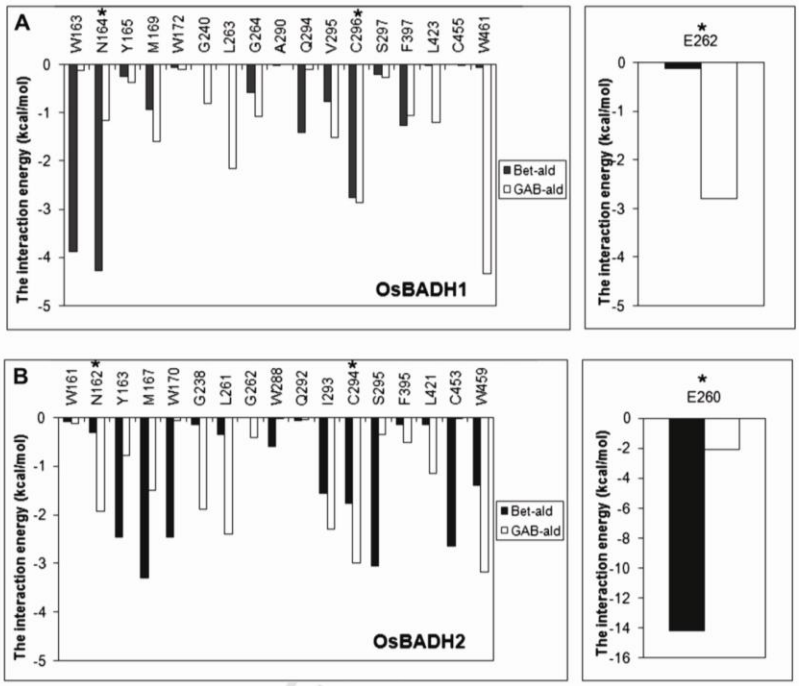

Fig. 4. Decomposition of binding free energies between aldehyde ligand and amino acid residues within 5 Å radius of this ligand within the OsBADH complexes (A) OsBADH1 (B) OsBADH2. The asterisk represents the catalytic triad residues.

side chain of E260 interacts with the positive charge of the quaternary ammonium of Bet-ald. For OsBADH2–GAB-ald, four residues interact with GAB-ald including E260, L261, C294 and W459. This observation is in agreement with the result that four residues can form hydrogen bonds in the structure and that N162 is important for OsBADH2–GAB-ald (−1.93 kcal/mol). Taken together, the data from Fig. 4 indicates that interactions involving both OsBADH1–GAB-ald and OsBADH2–GAB-ald complexes are relatively similar. GAB-ald usually interacts with amino acid residues, N164, M169, E262, L263, V295, C296 and W461 in OsBADH1 and N162, M167, E260, L261, I293, C294 and W459 in OsBADH2, with the same position of the amino acid but a different spatial arrangement of GAB-ald. In contrast with GAB-ald, the interaction of Bet-ald in the complex is varied and a different spatial arrangement of Bet-ald was observed both in our MD simulations and in the crystal structure of BADH from *E. coli* [13]. This discrepancy may have stemmed from the fact that Bet-ald carries a positive charge and less hydrogen bonds are observed in the complex, leading to a large movement of the molecule, whereas GAB-ald can form several hydrogen bond networks to the enzyme thus generating a more rigid position within the substrate binding site.

According to our result, difference in amino acid residues between OsBADH1 (A290) and OsBADH2 (W288) may account for differences in substrate specificity between both OsBADHs. W288 of OsBADH2 can interact well with Bet-ald (−0.59 kcal/mol) but not GAB-ald. It has been proposed that W288 in PsAMADH2 affects the affinity of the enzyme without affecting the reaction rate [24]. However, this residue is also different between PsAMADH1 and PsAMADH2 (F288 for PsAMADH1 and W288 for PsAMADH2) [6]. The W288 side chain of PsAMADH2 reduces the volume of the substrate channel compared to F288 of PsAMADH1 [6]. Therefore, this residue may be key to the differences in substrate specificity observed among plant AMADH isoforms [24]. W288 of OsBADH2 reduces the volume of the substrate channel compared to A290 of OsBADH1. Bet-ald in the OsBADH2 complex can interact with W288 through π electron interactions between the positive charge of the quaternary ammonium and the negative charge of the W288 indole ring while in OsBADH1 this position is replaced by A290 which cannot form any interaction with Bet-ald [24]. Consistent with the results from PsAMADHs, W288 is the key residue in determining the substrate specificity in OsBADH isoforms in rice.

3.7. Conformation of the catalytic cysteine and glutamate

The conformation of catalytic Cys and Glu was observed from MD simulations of the OsBADH–ligand complexes. According to the previous study, the catalytic Cys residue can adopt two conformations: the "resting" conformation in which the Cys residue is far from the carbonyl carbon of the bound aldehyde [14],

Please cite this article in press as: K. Jiamsomboon, et al., Dissecting substrate specificity of two rice BADH isoforms: Enzyme kinetics, docking and molecular dynamics simulation studies, Biochimie (2012), doi:10.1016/j.biochi.2012.04.009

Copyright by Kasetsart University All rights reserved

ARTICLE IN PRESS BIOCHI3875_proof ■ 21 April 2012 ■ 10/11

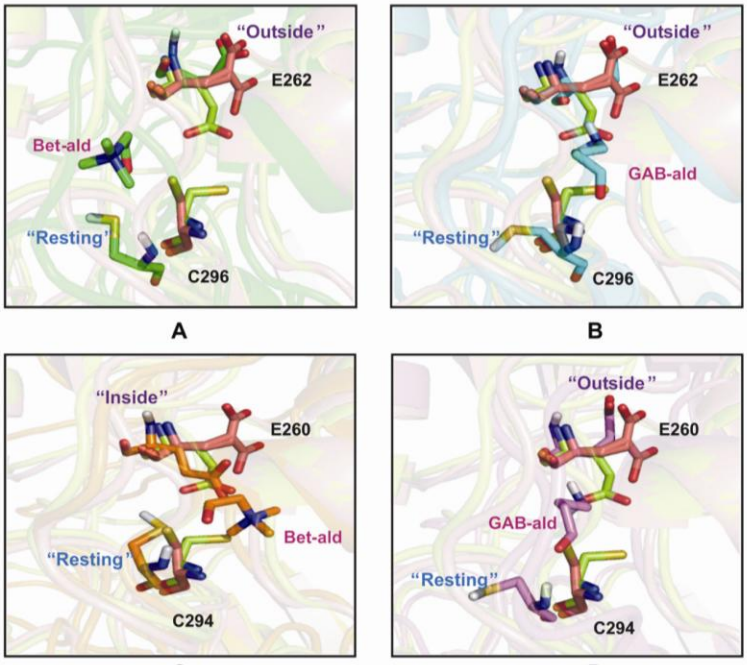

Fig. 5. The conformation of active site residues in OsBADH–substrate complexes from MD simulations compared to PaBADH (2WME) and ALDH2 (1O02). (A) OsBADH1 with Bet-ald (B) OsBADH1 with GAB-ald (C) OsBADH2 with Bet-ald (D) OsBADH2 with GAB-ald. The names of catalytic residues for OsBADH1 including C296, E262 while OsBADH2 including C294, E260 are shown in black text while the aldehyde substrates, Bet-ald and GAB-ald have pink text. Side chain atoms of residue are shown in stick and colored by atoms (PaBADH carbon: salmon pink, ALDH2 carbon: lemon green, OsBADH1–Bet-ald carbon: green, OsBADH1–GAB-ald carbon: cyan, OsBADH2–Bet-ald carbon: orange, OsBADH2–GAB-ald carbon: magenta). (For interpretation of the references to color in this figure legend, the reader is referred to the web version of this article.)

and the "attacking" conformation in which the Cys residue is close to this carbon in the correct position to perform the nucleophilic attack [23]. In the case of the catalytic Glu residue, three possible conformations have been observed: the "inside" conformation in which the Glu residue can activate the catalytic Cys residue for nucleophilic attack, since its carboxyl group is close to the thiol [13,23], the "intermediate" conformation in which the Glu residue is suited for the activation of the hydrolytic water molecule [1,14,23], and the "outside" conformation in which the catalytic Glu releases the proton that was previously taken from either the catalytic Cys or a hydrolytic water involved in the proton relay mechanism [14,23].

The conformations of both catalytic residues from PaBADH (PDB codes 2WME) [14] and ALDH2 (PDB codes 1O02) [23] are shown in Supplementary data Fig. S5. When the structure of PaBADH is compared with the structure of ALDH2 and with OsBADH complexes from MD simulations (Fig. 5), it is revealed that the catalytic Glu residue in all structures exists in the "outside" conformation whereas the catalytic Cys residue is found in the "resting" conformation with the exception of the catalytic Glu residue of OsBADH2–Bet-ald complex that exists in an "inside" conformation. The negatively charged side chain of the catalytic Glu residue is positioned towards the positive quaternary ammonium of Bet-ald, suggesting it may have strong electrostatic interactions, consistent with the binding energy from MMGBSA decomposition. Additionally, the difference in the conformation of the catalytic Glu residue of OsBADH1 and OsBADH2 observed from MD simulations may also bring about the substrate specificity between the two substrates and the enzymes. Collectively, the work presented here for the first time provides the structure of OsBADH in complex with the substrates generated by MD simulations. Further studies on other residues in the substrate binding pocket to better understand the substrate specificity are in progress.

4. Conclusion

In this study, we describe the kinetic analysis of OsBADH1 and OsBADH2 wild-type and mutant enzymes using Bet-ald and GAB-ald as substrates. Kinetic results indicated that these enzymes would prefer GAB-ald to Bet-ald, which is in agreement with previous studies [9,10,17]. Out of the six mutants (N164A, W172A, W172F for OsBADH1 and N162A, W170A, W170F for OsBADH2), only the W172F of OsBADH1 and W170F of OsBADH2 mutants showed a higher catalytic efficiency towards GAB-ald, indicating that this position may be important for substrate specificity

Please cite this article in press as: K. Jiamsomboon, et al., Dissecting substrate specificity of two rice BADH isoforms: Enzyme kinetics, docking and molecular dynamics simulation studies, Biochimie (2012), doi:10.1016/j.biochi.2012.04.009

Copyright by Kasetsart University All rights reserved

towards GAB-ald. MD simulations suggested that GAB-ald forms hydrogen bonds with C296, E262, L263, and W461 in OsBADH1 and C294, E260, L261, and W459 in OsBADH2 better than Bet-ald. Decomposition energies revealed that W163, N164, Q294, C296 and F397 mainly interacted with Bet-ald in the OsBADH1–Bet-ald complex while E262, L263, C296 and W461 mainly interacted with GAB-ald in the OsBADH1–GAB-ald complex. In the OsBADH2–Bet-ald complex, Y163, M167, W170, E260, S295 and C453 displayed strong interactions and the strongest was with E260, suggesting that the negatively charged side chain of E260 interacts with the positively charged group of Bet-ald. E260, L261, C294 and W459 were shown to interact with GAB-ald in the OsBADH2–GAB-ald complex, which is consistent with the hydrogen bonding analysis. Our data indicate that the interactions of Bet-ald in the complex are varied in comparison with GAB-ald. This may be accounted for by a positive charge in Bet-ald and less hydrogen bond formation, leading to movement at various positions which can be observed in the MD simulation and the crystal structure of *E. coli* BADH [13]. In contrast, GAB-ald can form several hydrogen bonds, leading to a fixed position in the substrate binding site. One interesting point for the substrate recognition of OsBADHs is the difference in the amino acid residues at position 290 of OsBADH1 (A290) and position 288 of OsBADH2 (W288). W288 in OsBADH1 interacts with Bet-ald through π electron interactions but not with GAB-ald while A290 in OsBADH1 cannot form any interaction with the substrates. In plant PsAMADHs, the amino acid residue at position 288 has been proposed to play a key role in the difference in substrate specificity between both PsAMADHs isoforms (F288 for PsAMADH1 and W288 for PsAMADH2) [6]. Therefore, W288 is also a key residue in recognition and substrate specificity in OsBADH isoforms. We also compared the conformation of the catalytic residues, Cys and Glu with that of PaBADH and ALDH2. Results revealed that the catalytic Cys residue existed in the "resting" conformation in all structures whereas the catalytic Glu residue existed in the "outside" conformation except for Glu in OsBADH2–Bet-ald, which was found to adopt an "inside" conformation. It is suggested that the negatively charged side chain of catalytic Glu has strong electrostatic interactions with the positive quaternary ammonium of Bet-ald. This difference in the conformation of catalytic Glu residue of OsBADH1 and OsBADH2 may account for differences in substrate specificity between the two enzymes.

Acknowledgments

We thank National Nanotechnology Center (NANOTEC) for generously providing the discovery studio software and the National Electronics and Computer Technology Center (NECTEC) for providing computational resources. This research was supported by Kasetsart University Research and Development Institute (grant: v-t(d)43.54), Faculty of Science (grant: ScRF-S10/2553), Graduate School Kasetsart University and Thailand Research Fund (grant: RTA5380010). Financial support from the Center of Excellence for Innovation in Chemistry (PERCH-CIC), Commission on Higher Education, Ministry of Education is also gratefully acknowledged.

Appendix A. Supplementary material

Supplementary material associated with this article can be found, in the online version, at doi:10.1016/j.biochi.2012.04.009.

References

[1] Z.J. Liu, Y.J. Sun, J. Rose, Y.J. Chung, C.D. Hsiao, W.R. Chang, I. Kuo, J. Perozich, R. Lindahl, J. Hempel, B.C. Wang, The first structure of an aldehyde dehydrogenase reveals novel interactions between NAD and the Rossmann fold, Nat. Struct. Biol. 4 (1997) 317–326.
[2] A. Yoshida, A. Rzhetsky, L.C. Hsu, C. Chang, Human aldehyde dehydrogenase gene family, Eur. J. Biochem. 251 (1998) 549–557.
[3] J. Perozich, H. Nicholas, B.-C. Wang, R. Lindahl, J. Hempel, Relationships within the aldehyde dehydrogeanse extended family, Protein Sci. 8 (1999) 137–146.
[4] P.N. Moschou, K.A. Paschalidis, K.A. Roubelakis-Angelakis, Plant polyamine catabolism: the state of the art, Plant Signal. Behav. 3 (2008) 1061–1066.
[5] M. Šebela, F. Brauner, A. Radová, S. Jacobsen, J. Havliš, P. Galuszka, P. Pe&ccaron, Characterisation of a homogeneous plant aminoaldehyde dehydrogenase, Biochim. Biophys. Acta 1480 (2000) 329–341.
[6] M. Tylichová, D. Kopecný, S. Moréra, P. Briozzo, R. Lenobel, J. Snégaroff, M. Šebela, Structural and functional characterization of plant aminoaldehyde dehydrogenase from *Pisum sativum* with a broad specificity for natural and synthetic aminoaldehydes, J. Mol. Biol. 396 (2010) 870–882.
[7] T.L. Fitzgerald, D.L.E. Waters, R.J. Henry, Betaine aldehyde dehydrogenase in plants, Plant Biol. 11 (2009) 119–130.
[8] T. Fujiwara, K. Hori, K. Ozaki, Y. Yokota, S. Mitsuya, T. Ichiyanagi, T. Hattori, T. Takabe, Enzymatic characterization of peroxisomal and cytosolic betaine aldehyde dehydrogenases in barley, Physiol. Plant 134 (2008) 22–30.
[9] L. Bradbury, S. Gillies, D. Brushett, D. Waters, R. Henry, Inactivation of an aminoaldehyde dehydrogenase is responsible for fragrance in rice, Plant Mol. Biol. 68 (2008) 439–449.
[10] S. Mitsuya, Y. Yokota, T. Fujiwara, N. Mori, T. Takabe, OsBADH1 is possibly involved in acetaldehyde oxidation in rice plant peroxisomes, FEBS Lett. 583 (2009) 3625–3629.
[11] P. Weigel, E.A. Weretilnyk, A.D. Hanson, Betaine aldehyde oxidation by spinach chloroplasts, Plant Physiol. 82 (1986) 753–759.
[12] K. Johansson, M. El-Ahmad, S. Ramaswamy, L. Hjelmqvist, H. Jornvall, H. Eklund, Structure of betaine aldehyde dehydrogenase at 2.1 A resolution, Protein Sci. 7 (1998) 2106–2117.
[13] A. Gruez, V. Roig-Zamboni, S. Grisel, A. Salomoni, C. Valencia, V. Campanacci, M. Tegoni, C. Cambillau, Crystal structure and kinetics identify *Escherichia coli* YdcW gene product as a medium-chain aldehyde dehydrogenase, J. Mol. Biol. 343 (2004) 29–41.
[14] L. González-Segura, E. Rudiño-Piñera, R.A. Muñoz-Clares, E. Horjales, The crystal structure of a ternary complex of betaine aldehyde dehydrogenase from *Pseudomonas aeruginosa* provides new insight into the reaction mechanism and shows a novel binding mode of the 2'-phosphate of $NADP^+$ and a novel cation binding site, J. Mol. Biol. 385 (2009) 542–557.
[15] L.M.T. Bradbury, T.L. Fitzgerald, R.J. Henry, Q. Jin, D.L.E. Waters, The gene for fragrance in rice, Plant Biotechnol. J. 3 (2005) 363–370.
[16] S. Chen, Y. Yang, W. Shi, Q. Ji, F. He, Z. Zhang, Z. Cheng, X. Liu, M. Xu, Badh2, encoding betaine aldehyde dehydrogenase, inhibits the biosynthesis of 2-acetyl-1-pyrroline, a major component in rice fragrance, Plant Cell 20 (2008) 1850–1861.
[17] R. Wongpanya, N. Boonyalai, N. Thammachuchourat, N. Horata, S. Arikit, K. Myint, A. Vanavichit, K. Choowongkomon, Biochemical and enzymatic study of rice BADH wild-type and mutants: an insight into fragrance in rice, Protein J. 30 (2011) 529–538.
[18] B. Kuaprasert, K. Silprasit, N. Horata, P. Khunrae, R. Wongpanya, N. Boonyalai, A. Vanavichit, K. Choowongkomon, Purification, crystallization and preliminary X-ray analysis of recombinant betaine aldehyde dehydrogenase 2 (OsBADH2), a protein involved in jasmine aroma, from Thai fragrant rice (*Oryza sativa* L.), Acta Crystallog. Sect. F 67 (2011) 1221–1223.
[19] W.L. Delano, The PyMOL molecular graphics system, DeLano Scientific (2002).
[20] G.M. Morris, D.S. Goodsell, R.S. Halliday, R. Huey, W.E. Hart, R.K. Belew, A.J. Olson, Automated docking using a Lamarckian genetic algorithm and an empirical binding free energy function, J. Comput. Chem. 19 (1998) 1639–1662.
[21] W. Cornell, P. Cieplak, C. Bayly, I. Gould, K. Merz, D. Ferguson, D. Spellmeyer, T. Fox, J. Caldwell, P. Kollman, A second generation force field for the simulation of proteins, nucleic acids, and organic molecules, J. Am. Chem. Soc. 117 (1995) 5179–5197.
[22] W.L. Jorgensen, J. Chandrasekhar, J.D. Madura, R.W. Impey, M.L. Klein, Comparison of simple potential functions for simulating liquid water, J. Chem. Phys. 79 (1983) 926–935.
[23] S.J. Perez-Miller, T.D. Hurley, Coenzyme isomerization is integral to catalysis in aldehyde dehydrogenase, Biochemistry 42 (2003) 7100–7109.
[24] D. Kopečný, M. Tylichová, J. Snegaroff, H. Popelková, M. Šebela, Carboxylate and aromatic active-site residues are determinants of high-affinity binding of ω-aminoaldehydes to plant aminoaldehyde dehydrogenases, FEBS J. 278 (2011) 3130–3139.
[25] R.A. Laskowski, M.W. MacArthur, D.S. Moss, J.M. Thornton, PROCHECK: a program to check the stereochemical quality of protein structures, J. Appl. Crystallogr. 26 (1993) 283–291.

Please cite this article in press as: K. Jiamsomboon, et al., Dissecting substrate specificity of two rice BADH isoforms: Enzyme kinetics, docking and molecular dynamics simulation studies, Biochimie (2012), doi:10.1016/j.biochi.2012.04.009

Copyright by Kasetsart University All rights reserved